

INFORMATION TO USERS

While the most advanced technology has been used to photograph and reproduce this manuscript, the quality of the reproduction is heavily dependent upon the quality of the material submitted. For example:

- Manuscript pages may have indistinct print. In such cases, the best available copy has been filmed.
- Manuscripts may not always be complete. In such cases, a note will indicate that it is not possible to obtain missing pages.
- Copyrighted material may have been removed from the manuscript. In such cases, a note will indicate the deletion.

Oversize materials (e.g., maps, drawings, and charts) are photographed by sectioning the original, beginning at the upper left-hand corner and continuing from left to right in equal sections with small overlaps. Each oversize page is also filmed as one exposure and is available, for an additional charge, as a standard 35mm slide or as a 17"x 23" black and white photographic print.

Most photographs reproduce acceptably on positive microfilm or microfiche but lack the clarity on xerographic copies made from the microfilm. For an additional charge, 35mm slides of 6"x 9" black and white photographic prints are available for any photographs or illustrations that cannot be reproduced satisfactorily by xerography.

Order Number 8726660

**Urethane-based IPNs and polyureas in reactive polymer
processing**

Hsu, Tzu-Chien Jeffrey, Ph.D.

The Ohio State University, 1987

U·M·I
300 N. Zeeb Rd.
Ann Arbor, MI 48106

PLEASE NOTE:

In all cases this material has been filmed in the best possible way from the available copy. Problems encountered with this document have been identified here with a check mark .

1. Glossy photographs or pages _____
2. Colored illustrations, paper or print _____
3. Photographs with dark background
4. Illustrations are poor copy _____
5. Pages with black marks, not original copy _____
6. Print shows through as there is text on both sides of page _____
7. Indistinct, broken or small print on several pages
8. Print exceeds margin requirements _____
9. Tightly bound copy with print lost in spine _____
10. Computer printout pages with indistinct print _____
11. Page(s) _____ lacking when material received, and not available from school or author.
12. Page(s) _____ seem to be missing in numbering only as text follows.
13. Two pages numbered _____. Text follows.
14. Curling and wrinkled pages _____
15. Dissertation contains pages with print at a slant, filmed as received
16. Other _____

University
Microfilms
International

URETHANE-BASED IPNS AND POLYUREAS

IN

REACTIVE POLYMER PROCESSING

DISSERTATION

Presented in Partial Fulfillment of the Requirements for
the Degree Doctor of Philosophy in the Graduate
School of the Ohio State University

By

Tzu-Chien Jeffrey Hsu, B.S., M.S.

* * * * *

The Ohio State University

1987

Dissertation Committee:

Dr. L. James Lee

Dr. Edwin E. Smith

Dr. Shang-Tian Yang

Approved by



Advisor

Department of Chemical Engineering

In Memory of My Father

Hsu, Ching-Sung

ACKNOWLEDGEMENTS

It is with the greatest pleasure that I acknowledge professor L. James Lee, my research advisor, for his inspiring suggestions, generous support, and enthusiasm throughout this work. His help and guidance were instrumental in the completion of this work. Thanks go to the other members of my dissertation committee, Drs. Edward E. Smith, Shang-Tian Yang, and Richard Firestone, for their suggestions and comments. Mr. Martin Nelson, whom I have worked with in the RIM project, deserves special thanks. Experiments in RIM could never be materialized without his input on machine design and construction. I also appreciate the efforts of Mr. K.J. Wang, who made dynamic mechanical analysis possible. The contributions of design engineer Mike Kukla to this project will always be remembered. Thanks also go to members of our research group for their kind assistance; to Y.J. Chen and J.J. Wang of Chemistry Department for their encouragement and warm friendship.

Financial support from General Motors Corporation is gratefully appreciated. In particular, Mr. George Ferber of GM Technical Center in Detroit, have provided suggestions and constructive guidance in this study.

Many thanks are due to Sing-Ling Yu. Her regular doses of encouragement, compassion, and support would always mercifully relieve me of the tension that accompanied this endeavor. Finally, I would like to thank my parents and members of my family, who have been a continual source of inspiration and whose sacrifices made my education possible. The completion of this work is as much their accomplishment as it is mine.

VITA

September 28, 1956 ----- Born, Taipei, Taiwan
Republic of China.

June, 1979 ----- B.S. Chemistry
National Taiwan University
Taipei, Taiwan, ROC

1979 - 1981 ----- Military Service

June, 1984 ----- M.S., Chemical Engineering
The Ohio State University

1982 - 1987 ----- Research Associate and
Teaching Associate
The Ohio Stat University

PUBLICATIONS

1. "A Feasibility Study of Polyurethane-Polyester Interpenetrating Polymer Network (IPN) and Its Potential Applications to Reinforced Reaction Injection Molding (RRIM)." M.S. Thesis, The Ohio State University (1984).
2. "Reaction Kinetics of Polyurethane-Polyester Interpenetrating Polymer Network in the Bulk Polymerization." Co-authored with L. James Lee, Polym, Eng. Sci., 25(15), 951 (1985).
3. "Effect of Compound Composition on Fast Reactions of Polyurethane and Unsaturated Polyester in the Bulk State." Co-authored with Y.J. Huang and L. James Lee, Polymer. 26, 1247 (1985).
4. "Physical Properties of Transfer-Molded Polyurethane-Polyester Interpenetrating Polymer Network." Co-authored with L. James Lee, J. Appl. Polym. Sci., 33, 793 (1987).
5. "Processing of Polyurethane-Polyester Interpenetrating Polymer Network." Co-authored with L. James Lee, 42nd Annual Conference,

Composite Institute, The Society of Plastics Industry, Inc.
Session 18-C, February 2-6, Cincinnati, Ohio (1987).

FIELDS OF STUDY

1. Polymeric Composites.
2. Reactive Polymer Processing
3. Polymer Chemistry and Physics

TABLE OF CONTENTS

	DEDICATION.....	ii
	ACKNOWLEDGEMENTS.....	iii
	VITA.....	v
	LIST OF TABLES.....	x
	LIST OF FIGURES.....	xi
	NOMENCLATURES.....	xviii
	ABSTRACT.....	xxii
		PAGE
<u>Chapter 1</u>	INTRODUCTION.....	1
1.1	Reactive Polymer Processing.....	1
1.2	Problem Statement.....	8
<u>Chapter 2</u>	REACTIVE POLYMER PROCESSING.....	15
2.1	Reactive Polymer Processing.....	15
2.1.1	Reaction Injection Molding.....	16
2.2.2	Transfer Molding.....	26
2.2.3	Casting.....	31
2.2	Materials.....	36
2.2.1	Polyurethanes.....	36
2.2.2	Modifications of Polyurethanes.....	42
2.2.3	IPNs.....	47
2.2.4	Polyureas.....	55
<u>Chapter 3</u>	PROCESSING OF IPN.....	60
3.1	Previous Work on IPN Processing.....	60
3.1.1	Kinetic Studies of Polyurethane Reactions.....	60
3.1.2	Heat Transfer Studies of Polyurethane Formation in Reactive Processing.....	64
3.1.3	Kinetic Studies of Unsaturated Polyester Reaction.....	66

3.1.4	Heat Transfer Studies of Styrene-Unsaturated Polyester Reaction in Reactive Processing.....	69
3.1.5	Interpenetrating Polymer Networks.....	71
3.2	Experimental.....	72
3.2.1	Materials.....	72
3.2.2	Instrumentation and Experimental Procedure....	76
3.3	Results and Discussions.....	84
3.3.1	Moldability Test.....	86
3.3.2	Kinetic Measurement of IPN by DSC.....	88
3.3.3	Adiabatic Temperature Rise.....	94
3.3.4	Reaction Injection Molding.....	94
3.3.5	Casting.....	97
3.3.6	FTIR Analysis of Cast IPNs.....	100
3.4	Kinetic and Heat Transfer Modelling of IPN Reaction..	111
3.4.1	Theoretical Model.....	111
3.4.2	Parameter Estimation.....	119
3.4.3	Model Prediction.....	122
<u>Chapter 4</u>	<u>PROPERTY-STRUCTURE-PROCESSING RELATIONSHIPS OF IPN...</u>	<u>129</u>
4.1	Previous Work on Morphology and Mechanical Properties of IPNs.....	129
4.1.1	Survey of Morphological Studies.....	129
4.1.2	Survey of Mechanical and Thermal Studies.....	135
4.2	Experimental.....	140
4.2.1	Materials.....	140
4.2.2	Sample Preparation.....	140
4.2.3	Methods of Measurement.....	143
4.3	Morphology and Dynamic Mechanical Properties.....	146
4.3.1	A Comparison of Morphology of IPNs Prepared by Transfer Molding and RIM Processes.....	148
4.3.2	Effect of Molding Temperature.....	153
4.3.3	Effect of Compound Composition.....	155
4.3.4	Effect of Reaction Sequence.....	160
4.3.5	Crosslinking Effect.....	162

4.4	Tensile Properties.....	164
4.4.1	Compositional and Temperature Effects.....	164
4.4.2	Sequential Effect.....	176
4.4.3	Crosslinking Effect.....	180
<u>Chapter 5</u>	PROCESSING OF POLYUREA.....	186
5.1	Previous Work on Polyurea RIM.....	186
5.1.1	Materials.....	186
5.1.2	Polyurea RIM.....	189
5.2	Experimental.....	192
5.2.1	Materials.....	192
5.2.2	Instrumentation and Experimental Procedure....	195
5.3	Results and Discussion.....	201
5.3.1	Reaction Injection Molding of Polyurea.....	201
5.3.2	Solution Polymerization.....	205
5.4	Kinetic and Heat Transfer Models for Polyurea Reactions.....	231
5.4.1	Models.....	231
5.4.2	Parameter Estimation.....	235
5.4.3	Model Prediction.....	245
<u>Chapter 6</u>	CONCLUSIONS AND RECOMMENDATIONS.....	255
6.1	Conclusions.....	255
6.2	Recommendations.....	263
	REFERENCES.....	266
	APPENDICES.....	279
A.	ACSL Program for polyurea Reaction.....	280
B.	ACSL Program for PU/PES IPN reaction.....	282

LIST OF TABLES

TABLE	PAGE
1.1 Reactive polymer processing.....	3
2.1 Market of RIM and RRIM.....	18
2.2 Major RIM machine manufacturers.....	20
2.3 Reactions of isocyanate with various functional groups....	36
2.4 A review of PU-based IPNs.....	54
2.5 Current suppliers of polyureas.....	59
3.1 Materials used in IPNs' study.....	73
3.2 IR peaks for different functional groups of PU/PES IPN....	107
3.3 Parameters used in modeling of IPN.....	120
4.1 Recipe used in Property-Structure-Processing Relationships Study of IPN.....	141
4.2 Tensile strength and ultimate elongation of 80 °C-transfer molded and 120 °C-postcured L/C samples tested at three different temperatures.....	169
4.3 Tensile strength, ultimate elongation, and limiting conversion of 80 °C-transfer molded L/C samples with different initiator concentrations (PU/PES = 50/50, testing temperature was 25 °C.....	179
4.4 Effect of crosslinking on tensile strength and limiting conversion of 80 °C-transfer molded samples before and after postcure treatment (PU/PES = 50/50, testing temperature was 25 °C.....	183
5.1 Recipe of polyurea systems used.....	194
5.2 Variations of soft segment/hard segment ratios.....	217
5.3 Parameters used for modelling of polyurea reaction.....	243

LIST OF FIGURES

FIGURE	PAGE
1.1	A schematic diagram of the reactive polymer processing..... 5
1.2	Research scheme of reactive polymer processing in this study.. 11
2.1	Schematic diagram of the reaction injection molding process... 17
2.2	<p>(A) Krauss-Maffei and American E.M.B. use this mixing head design. The left side of the drawing shows the head in the recycle position, the right side shows the shot position. Numbered items are as follows: 1. Hydraulic piston in shot position; 2. Hydraulic piston in recycle position; 3. Clean-out piston in shot position; 4. Clean-out piston in recycle position; 5. Polyol feed; 6. Isocyanate feed; 7. Return line, no flow; 8. Return line, recycling; 9. Nozzle needle adjustment; 10. Nozzle and needle (E.M.B. machines substitute orifice plates for nozzle and needles.); 11. Polyol and isocyanate impinge and flow to mold. (B) Henneke uses this mixing head design. The left side of the drawing shows the head in the recycle position, the right shows the shot position. Numbered components are as follows: 1. Hydraulic piston in shot position; 2. Hydraulic piston in recycle position; 3. Clean-out piston in shot position; 4. Clean-out piston in recycle position; 5. Polyol feed; 6. Isocyanate feed; 7. Return line, no flow; 8. Return line, recycling; 9. By-pass piston system in shot position; 10. By-pass piston system in recycle position; 11. Impingement nozzles; 12. Polyol and isocyanate impinge and flow to the mold. (C) Battenfield (Schloemen-Siemag) uses a mixing head of this design. The recycle position is shown on the left, and the shot position on the right. This cross-sectional schematic is shown in a plane perpendicular to the axis of the shot piston. Numbered parts are as follows: 1. Mixer housing hydraulic piston in by-pass position; 2. Mixer housing hydraulic piston in shot position; 3. Mixer housing in by-pass position; 4. Mixer housing in shot position; 5. Feed port "A"; 6. Feed port "B"; 7. Needle valve adjustment "A"; 8. Needle valve adjustment "B"; 9. By-pass channel of mixer housing in recycle position; 10. Return port "B", no flow; 11. Return port "A", recycling; 12. Mixing chamber (Sweeney, 1979)..... 22</p>

2.3	True, or pot-type, transfer molding. (a) Mold open, pot loaded; (b) mold closed; and (c) mold open, parts ejected, sprue on force plug (Hull, 1984).....	28
2.4	Plunger mold configurations. (a) Mold closed, pot loaded; (b) mold closed, plunger down; and (c) mold open, molded part, cull, and runners ejected (Hull, 1984).....	29
2.5	(A) Conventional cell casting mold configuration. (a) Face view and (b) edge view (Harbison, 1984). (B) Continuous casting apparatus.....	33
2.6	Domain formation of polyurethanes.....	38
2.7	Schematic diagram showing two possible routes for reinforced reaction injection molding (RRIM).....	44
2.8	Synthesis of IPNs.....	49
	(A) sequential-IPN	
	(B) semi-IPN (sequential)	
	(C) simultaneous IPN (SIN)	
	(D) semi-SIN	
2.9	A comparison of various polymeric composites.....	51
3.1	Procedure for DSC experiment, (A) isothermal run to determine the reaction rate, (B) 1st scanning to determine the residual activity, and (C) 2nd scanning run to determine the base line.	78
3.2	Schematic diagram showing the laboratory scale RIM machine. (1) control panel, (2) 7-1/2 Hp motor, (3) hydraulic pump, (4) directional solenoid, (5) hydraulic reservoir, (6) flow control valves, (7) drive cylinders, (8) material cylinders (9) mixhead, (10) material storage tanks.....	80
3.3	Schematic diagram of casting set-up.....	83
3.4	Schematic diagram showing the reaction mechanism of PU/PES IPN.....	85
3.5	Adiabatic temperature rise vs. time of two polyurethanes and one polyester resin.....	87
3.6	Adiabatic temperature rises of PU/PES IPNs using different initiators for polyester resin.....	89
3.7	Chain growth and step growth polymerization measured by DSC isothermal mode.....	90

3.8	Compositional effect of PU/PES IPNs reacted at 353 °C.....	92
3.9	Adiabatic temperature rise of linear polyurethane. The solid line is curve fitted by multiple linear regression.....	95
3.10	Adiabatic temperature rises of IPNs at two compositions. Model predictions are presented by solid lines.....	96
3.11	Casting of polyurethane at 353.5 °K.....	98
3.12	Casting of unsaturated polyester resin at 353.5 °K.....	99
3.13	Casting of 75/25 IPN at 353.5 °K.....	101
3.14	Casting of 50/50 IPN at 353.5 °K.....	102
3.15	Casting of 25/75 IPN at 353.5 °K.....	103
3.16	Casting of 50/50 IPN at 393.5 °K.....	104
3.17	FTIR spectrum of 50/50 IPN before reaction (Yang and Lee, 1987).....	105
3.18	FTIR spectra of 393.5 °K-cast 50/50 IPN sampled (A) at wall and (B) at center of glasstube.....	109
3.19	Predicted reaction rate vs. time of polyurethane and polyester at 353.5 °K.....	123
3.20	Predicted reaction rate vs. time of IPNs at three compositions (353.5 °K).....	124
3.21	Predicted conversion profiles of 50/50 IPN cast at 353.5 °K....	127
4.1	Tensile at break vs. polyurethane concentration for polyurethane/epoxy S/INs (Frisch et al., 1974).....	136
4.2	Schematic of the transfer mold. (A) before molding, (B) after molding.....	142
4.3	Transmission electron microscopies of 50/50 IPNs by (A) RIM, (B) transfer molding.....	149
4.4	Dependence of storage modulus G' on temperature of 50/50 IPN by transfer molding and RIM. Individual networks molded by transfer molding.....	151

4.5	Dependence of $\tan\delta$ on temperature of 50/50 IPNs by transfer molding and RIM at 120 °C. Individual networks of IPN prepared by transfer molding.....	152
4.6	Transmission electron microscopies of 50/50 IPNs transfer molded at (A) 80 °C, and (B) 120 °C.....	154
4.7	Transmission electron microscopies of 80 °C-transfer molded IPN samples with compositions of (A) 75/25, (B) 50/50, and (C) 25/75.....	156
4.8	Dependence of storage modulus G' on temperature of 80 °C-transfer molded IPNs with three compositions.....	158
4.9	Dependence of $\tan\delta$ on temperature of 80 °C-transfer molded IPNs with three compositions.....	159
4.10	Transmission electron microscopy of 120 °C-transfer molded IPN samples with compositions of (A) 75/25, (B) 50/50, and (C) 25/75.....	161
4.11	Transmission electron microscopies of 80 °C-transfer molded MEKP/amine/Co-8-initiated 50/50 IPNs at (A) 2.0% MEKP, 0.67% amine, and 0.67% Co-8, (B) 0.67% MEKP, 0.22% amine, and 0.22% Co-8.....	163
4.12	Transmission electron microscopies showing the crosslinking effect of 120 °C-molded 50/50 IPNs, (A) with linear polyurethane, (B) with crosslinked polyurethane.....	165
4.13	Typical stress-strain curves of linear polyurethane, polyester, and IPN (L/C sample, 50/50) tested at 25 °C. Samples were molded at 80 °C and postcured at 120 °C for 6 hours.....	166
4.14	Tensile strength and limiting conversion of 80 °C-transfer molded L/C samples before (Δ) and after (\circ) postcure. Test temperature is 25 °C.	167
4.15	Scanning DSC results of 80 °C-transfer molded L/C samples.....	170
4.16	Scanning DSC results of 80 °C-transfer molded L/C samples after postcure treatment.....	171
4.17	Comparison of tensile strength of 80 °C- (Δ) and 120 °C (\bullet) transfer molded L/C samples. Test temperature at 25 °C.....	172
4.18	Scanning DSC results of 120 °C-transfer molded L/C samples.....	175

4.19	Tensile strength of 80 °C-transfer molded, 120 °C-postcured L/C samples tested at -2 °C (■), 25 °C (o), and 93 °C (Δ).....	177
4.20	Scanning DSC results of 80 °C-transfer molded L/C samples with different initiator combination (PU/PES = 50/50).....	181
4.21	Scanning DSC results of 80 °C-transfer molded L/L samples. (A) molding, and (b) after postcure.....	185
5.1	Experimental set-up for rheological measurements (Lae, 1986)..	197
5.2	Reaction injection molding of polyurea III at 35 °C and 55 °C...	202
5.3	Reaction injection molding of polyurea III in bulk and in 15% nitrobenzene.....	203
5.4	Maximum adiabatic temperature rises of three different isocyanate/amine ratios of polyurea III.....	204
5.5	Comparison of three material systems currently developed for RIM process.....	206
5.6	Chain extender effect of T5000/1305/X using Brookfield viscometer, where X stands for different diamine chain extenders studied at 80% nitrobenzene solution at 25 °C.....	208
5.7	Chemical structures of various diamine chain extenders.....	209
5.8	Viscosity vs. time plot of polyurea III at three concentrations by Haake viscometer at 25 °C.....	210
5.9	Effect of soft segment/hard segment ratios on viscosity rise in 80% nitrobenzene solution of T5000/MDI/TBTDA using Haake viscometer at 25 °C.....	211
5.10	Viscosity rise vs.time plot of polyurea I and II in 80% nitrobenzene.	213
5.11	Effect of soft segment/hard segment ratios on viscosity rise in 85% nitrobenzene solution of T5000/MDI/TBTDA using Haake viscometer at 25 °C.....	214
5.12	Viscosity rise vs. time plot of polyurea I and II in 85% nitrobenzene.....	215
5.13	Gel time vs. the amount of soft segment.....	218
5.14	Schematic diagram showing the formation of polyurea.....	220

5.15 FTIR spectra of polyurea III in 80% nitrobenzene solution recorded at several reaction times. Reaction temperature = 25 °C.....	223
5.16 Conversion vs. time plot of polyurea III in 95% nitrobenzene with two different chain extenders.....	224
5.17 Conversion vs. time plot of polyurea III in 90% nitrobenzene at three temperatures. Data were obtained according to the NCO peak at 2273.4 cm ⁻¹ and the NH stretching peak at 3312.5 cm ⁻¹ from FTIR spectra.....	225
5.18 Conversion vs. time plot of polyurea III at three concentrations from FTIR measurements. Reaction temperature = 25 °C.....	226
5.19 Viscosity vs. conversion plot of polyurea III at three concentrations measured at 25 °C.....	228
5.20 Viscosity vs. conversion plot of polyurea III at three compositions in 85% nitrobenzene measured at 25 °C.....	229
5.21 Curve fitting of conversion vs. time of polyurea II in 90% nitrobenzene at three temperatures.....	236
5.22 Plot of $\log(d\alpha_{II}/dt)$ vs. $\log(1-\alpha_{II})$ of polyurea II.....	238
5.23 Plot of G_{II} vs. $1/T$ of polyurea II.	239
5.24 Curve fitting of conversion vs. time of polyurea I in 92.5% nitrobenzene at three temperatures.....	240
5.25 Plot of $\log(d\alpha_I/dt)$ vs. $\log(1-\alpha_I)$ of polyurea I.....	241
5.26 Plot of G_I vs. $1/T$ of polyurea I.	242
5.27 Comparisons of predicted and observed conversion profiles of polyurea I in 92.5% nitrobenzene solution.....	244
5.28 Model predictions of temperature profile for polyurea III by RIM in bulk and 15% nitrobenzene.....	246
5.29 Model predictions of temperature profile for polyurea III by RIM at 35 and 55 °C.....	247
5.30 Predicted conversion profiles of 70/30 polyurea III in bulk in adiabatic condition.....	249

5.31 Predicted adiabatic temperature profiles of polyurea III in bulk with various compositions (100/0 ~ 70/30).....	250
5.32 Predicted adiabatic temperature profiles of polyurea III in bulk with various compositions (80/20 ~ 0/100).....	251
5.33 Predicted adiabatic conversion profiles of polyurea III in bulk with various compositions (100/0 ~ 20/80).....	252
5.34 Predicted adiabatic conversion profiles of polyurea III in bulk with various compositions (85/15 ~ 0/100).....	253

NOMENCLATURES

- \bar{A} = normalized absorbance in FTIR
- \tilde{A} = frequency coefficient (app. unit)
- A = frequency coefficient (app. unit)
- A_0 = rate constant in eq. (3.5)
- A_d = frequency coefficient in initiation of polyester (app. unit)
- A_i = absorbance of species i in FTIR
- A_p = frequency coefficient in propagation of polyester (app. unit)
- $\bar{A}_p = 2fI_0 A_p$
- A = frequency coefficient (app. unit)
- C = concentration of monomer (gm/cm^3)
- C_i = parameters used in eq. (3.35), $i = 1 \sim 3$
- C_p = heat capacity ($\text{cal/gm/}^\circ\text{C}$)
- d_1 = inner diameter of glass tube (cm)
- d_2 = outer diameter of glass tube (cm)
- D = parameter used in eq. (3.38)
- D_2 = "sphere" domain diameter of polymer (cm)
- DSC = differential scanning calorimetry
- E_d = activation energy in initiation of polyester (kcal/mole)
- E_p = activation energy in propagation of polyester (kcal/mole)
- E = activation energy (kcal/mole)
- f = initiator efficiency in eq. (3.14), $0 \sim 1$,
functionality in eq. (5.4).

FTIR = Fourier transform infrared spectroscopy

G = shear modulus in eq. (4.5),
parameters used in eqs. (5.17) and (5.18).

ΔH = heat of reaction (kcal/mole)

h_w = overall heat transfer coefficient (cal/sec/cm² / °C)

I = concentration of initiator (mole/cc.)

I = concentration of initiator after all inhibitor has been
consumed (mole/cc.)

IPN = interpenetrating polymer network

K = rate constant

k = thermal conductivity (cal/sec/cm / °C)

k_i = rate constants in eqs. (3.1), (3.2), and (3.3), $i = 1, 1', 2, 2'$

l = sample length (mm)

M = concentration of monomer (mole/cc.)

p = extent of reaction in eq. (5.4) (dimensionless)

PES = polyester

PU = polyurethane

q = inhibitor efficiency, $0 \sim 1$

r = reaction rate (mole/sec)

R = gas constant

R = concentration of free radical (mole/cc.)

SIN = simultaneous interpenetrating network

T = temperature

T_{ad} = maximum temperature rise

t = reaction time

t_d = induction time for polyester reaction
 t_m = time to reach maximum exotherm in polyester reaction
 V = crosslink density
 X = parameter used in eq. (4.9)
 Y = parameter used in eq. (4.10)
 Z = concentration of inhibitor (mole/cc.)

Greek Letters

α = extent of reaction of polyurethane or polyurea, 0.0 - 1.0
 β = extent of reaction of polyester, 0.0 - 1.0
 β_i = absorptivity of absorbing species in FTIR
 $\lambda = k/\rho/C_p$ (cm^2/sec),
 parameter used in eqs. (4.7) and (4.8)
 ρ = density (gm/cc)
 η = viscosity (cp)
 ϕ = volume fraction
 π_i = parameters used in eq. (3.7), $i = 1 \sim 4$
 ε = ratio of A group on branch units to all A groups in eq. (5.4)
 γ = interfacial tension in eq. (4.1),
 N_A/N_B , molar ratio in eq. (5.4)

Subscripts

e = polyester phase
 u = polyurethane phase

g = glass phase
I = IPN phase,
polyurea with soft segment only
II = polyurea with hard segment only
III = polyurea with soft and hard segments
o = condition before reaction (initial condition)
ad = adiabatic condition
d = inhibition step in polyester polymerization
p = propagation step in polyester polymerization
z = induction time

Superscript

l = reaction order (dimensionless)
m = reaction order (dimensionless)
n = reaction order (dimensionless)

ABSTRACT

The processing characteristics of polyurethane/polyester IPNs and polyureas in reactive polymer processing have been studied. The kinetics and heat transfer were investigated experimentally and theoretically. For IPNs, the model gave a reasonably good prediction of temperature profiles for adiabatic reactions and cast IPNs, but not for isothermal reactions. The discrepancy might largely result from component interactions, both physically and chemically. Physical interactions mainly came from the "cage effect" of polyurethane on polyester and the "solvent effect" of polyester on polyurethane. Chemical interaction might happen between the isocyanate group of polyurethane and the hydroxyl and carboxylic groups of unsaturated polyester. The property-structure-processing relationships of polyurethane/polyester IPNs were characterized. The RIM processed IPN had a more homogeneous morphology than the transfer-molded IPN, indicating that phase interpenetration was better achieved in RIM process. Two-phase morphology was observed in transfer molded IPNs. Better mechanical properties was obtained at high molding temperatures. For polyureas, the rheological and kinetic information was obtained from solution polymerizations. There existed a critical soft segment concentration at 8.2%. Above this point, increasing the

amount of soft segment in polyurea decreased the gelation time. Below this point, gelation time increased with increasing amount of soft segment. The kinetic model assumed no interaction between soft and hard segments in reaction. The kinetic parameters used were determined using data from solution polymerizations. The reaction rate of soft segment was much faster than that of hard segment. Increasing the hard segment content increased the maximum adiabatic temperature rise. The predictions of the adiabatic temperature rises of polyurea reaction in RIM were reasonably good.

CHAPTER I

INTRODUCTION

SYNOPSIS

The rationale of this study is stated in this chapter. Introduction to the reactive polymer processing is first described followed by the problem statement, the research objectives, and the outline of the research scheme.

1.1 REACTIVE POLYMER PROCESSING

Over the last two decades, research and development of polymers have focused less on the development of new polymers than on the improvement of processing technology and the modifications of existing polymers. Among the newly developed processes, reactive polymer processing has been proved to be an efficient, productive, and energy-saving process. It is one of the fastest growing areas in the plastics industry. On the other hand, modifications of existing polymers have attracted a great deal of research attention since the existing polymers do not seem to possess all the desired properties.

The advent of polymeric composite materials such as fiber-reinforced plastics (FRP) and interpenetrating polymer networks (IPNs) are among the recent developments in polymer industry.

The reactive polymer processing operations innovatively involve polymerization and fabrication in a single step. In other words, the polymer is formed after the monomer mixture is in the desired shape. Today, a large amount of polymer products are produced by reactive polymer processing. Sheet molding compound (SMC) and bulk molding compound (BMC), in which unsaturated polyester and styrene are usually the primary components, are two of the well-known products which are processed by this technology. Other examples include compression molding of rubber and reaction injection molding (RIM) of polyurethane. The former is a popular process in the rubber industry; the latter is a relatively new area with continuously growing potential. One of the new applications of reactive polymer processing is in the electronic industry where electric charge plates are encapsulated by thermosetting polymers like epoxies and polyurethanes. The applications of reactive polymer processing in various areas are summarized in Table 1.1.

The characteristics of reaction in reactive polymer processing can usually be described as:

Table 1.1 Reactive polymer processing

<u>Process</u>	<u>Resin</u>
Reaction injection molding (RIM)	Polyurethane, Epoxy Nylon, Polyester
Transfer molding	Thermosets
Compression molding	Sheet molding compound Bulk molding compound
Injection molding	Bulk molding compound
Electric encapsulation	Thermosets
Casting Potting Embedding	PMMA, Acrylate Epoxy, Nylon

- a. Bulk state.
- b. High reaction rate.
- c. High exotherm.
- d. Fast cycle time.

In most cases, physical properties of the finished products depend not only on raw materials used and the product morphology, but also on the operating conditions. In each process, raw materials go through a series of unit operations such as mixing, mold filling, and curing (Figure 1.1). The performance of each unit operation is governed by the microscopic changes of the reactive materials, which include flow pattern, rheological changes, molecular diffusion, and reaction kinetics as shown in Figure 1.1. For example, viscosity rise can affect the flow pattern in the mixing step and the mold filling step. Flow pattern and molecular diffusion may determine the reaction rate and the final conversion in the curing stage.

The reaction kinetics usually involves both chemical reactions and physical changes. The chemical reactions involved can be classified as:

REACTIVE PROCESSING OF POLYMERS

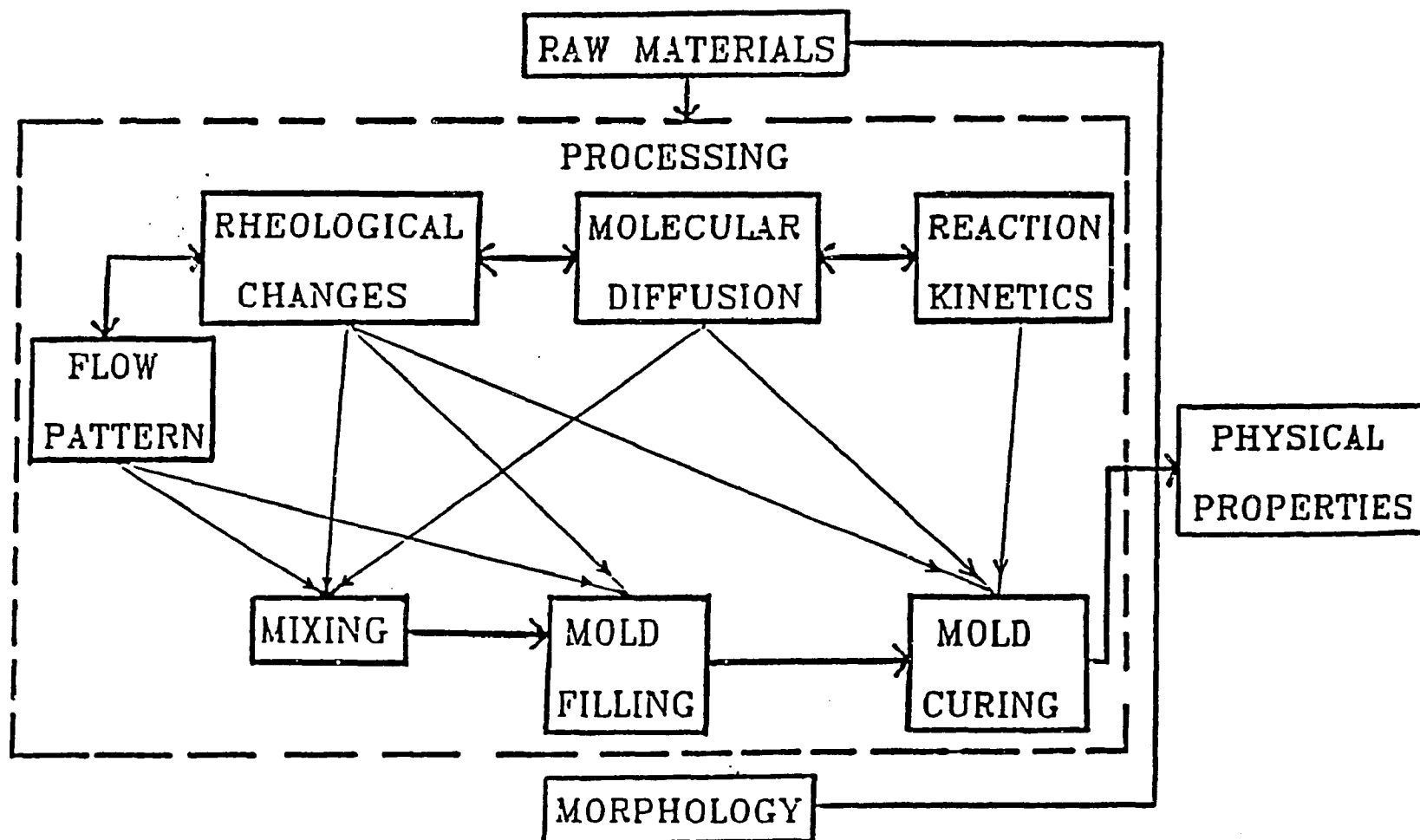


Figure 1.1 A schematic diagram of the reactive processing of polymers

- A. Chain growth polymerization.
(unsaturated polyesters, styrenes, etc.)
- B. Step growth polymerization.
(polyurethanes, epoxies, etc.)

The physical changes involved play influential roles in determining the properties of the finished product. These changes include:

- a. Gelation.
- b. Phase separation.
- c. Crystallization.
- d. Glass transition.

Gelation occurs when polymer changes from a viscous fluid to a network structure with chemical crosslinking. Phase separation results from domain formation due to thermodynamic incompatibility of the constituents of resins. Crystallization takes place when components of resins are arranged in a patterned order. Glass transition occurs when polymer changes from the rubbery state to the glassy state.

The chemical reactions, which are mainly kinetics controlled and which may influence each other, are further complicated by the

physical changes. These interactions will definitely affect the properties of the finished products. For example, the glass transition effect can make polymerization incomplete because molecular diffusion is much more difficult in the glassy state than in the rubbery or liquid state. As a result, only limited conversion can be expected. Phase separation, on the other hand, may affect the mechanical properties of urethane elastomers. Although crystallization makes polymers stronger, it may also impose processing problems such as in reaction injection molding (RIM) of nylon. In the chain growth polymerization, gel effect can cause thermal runaway problem due to excessive temperature rise from rapid conversion.

Various ingredients are used in reactive polymer processing. The selection depends on the product specifications and the process applied. The primary components are resins such as polyurethanes, polyesters, and epoxies. Catalysts, initiators and inhibitors are added to control the reaction rate. To increase the mechanical properties, fillers like mica, glass fiber, and calcium carbonate are also added to the reaction system. Other ingredients like low profile agent (e.g., PMMA for sheet molding compound), and foaming agent (e.g., water and methylene chloride for polyurethane) are added for different purposes. This complicated material system makes reactive polymer processing much more complicated than the conventional polymerization technique. In developing reactive

polymer processing technologies, research efforts in polymeric materials have paralleled the efforts in process design and modifications.

1.2 PROBLEM STATEMENT

The goals of this study are two-folded:

1. To explore novel resins as the materials for reactive polymer processing.
2. To study the processibility of these novel resins in reactive polymer processing.

To achieve the first goal, two polyurethane-based resins are chosen. One of them is an interpenetrating polymer network (IPN) based on a polyurethane (PU) and an unsaturated polyester (PES); the other is polyurea which is a modification of polyurethane. Traditionally, polyurethanes have been the most popular resins for RIM in the production of car bumpers. The addition of glassy polyester to polyurethane can reinforce the elastomeric properties of polyurethane so that structural applications in automobile are possible.

Many IPNs have been developed in the past (Sperling, 1985). Typically, an IPN consists of two polymeric resins, one step growth and one chain growth polymerizations. For instance, epoxy resins (step growth type) can be added to acrylic solutions (chain growth type) (Touhsaent et al., 1974) while polyesters, acrylates, styrenic monomers, and other vinyl systems (chain growth type) can be blended into urethane resins (step growth type) (Frisch et al., 1974; Kircher et al., 1984). Two step-growth polymerizations can also be combined to form an IPN (Frisch et al., 1982; Pernice et al., 1982).

Most IPNs are developed for slow processes like casting and coating. For applications of IPNs in reactive polymer processing such as RIM, there are only a few commercially available IPN compounds. Ashland Chemical developed an acrylamate polymer (Wilkinson et al., 1983; Kelly, 1986) which is basically a polyurethane with a high level of unsaturation on the polyol chain. When combining with a crosslinking agent (i.e, acrylic monomer), a second network is formed. Amoco Chemical developed a series of polyester-polyurethane hybrides which can be used in the reactive polymer processing (Edwards, 1986). Similar polyester-polyurethane IPNs have also been studied by others (Hsu and Lee, 1985; Nguyen and Suh, 1986). They found that the morphology, and subsequently the physical properties of IPNs can be affected by the processing conditions in RIM. These processing conditions include impingement pressure and stream Reynolds number.

Another resin, polyurea, which is a modification of polyurethane, is chosen for reactive polymer processing in this study. The main difference between polyurea and polyurethane is that the former uses a low molecular weight diamine as a chain extender instead of butanediol or ethylene glycol. With flexural modulus up to 25,000 - 100,000 psi, polyurea is a desirable RIM material for structural and other applications in automobile industry (Ewen 1985; Vespoli, 1986). One major problem of polyurea RIM is that the reaction is so fast (sometimes solidified upon mixing) that, in many cases, it exhibits processing difficulty and may result in poor final properties due to insufficient mixing and low conversion. Since it is impossible to follow the entire reaction course with available analytical tools (e.g., FTIR, DSC, Brookfield viscometer), one often needs to study polyurea reaction in the solution state, since the reaction rate is reduced in solution polymerization.

To achieve the second goal, it is important to know property-process-structure relationship of polyurethane-polyester IPN and polyurea. In this study, a comprehensive research scheme is designed in an effort to have a complete understanding of the PU/PES IPN in reactive polymer processing. Major areas to be studied and their interactive relationships among these factors are shown in Figure 1.2. Relationships among reaction kinetics, morphology, compound composition, rheology, and moldability are investigated. The reaction kinetics are followed by differential scanning

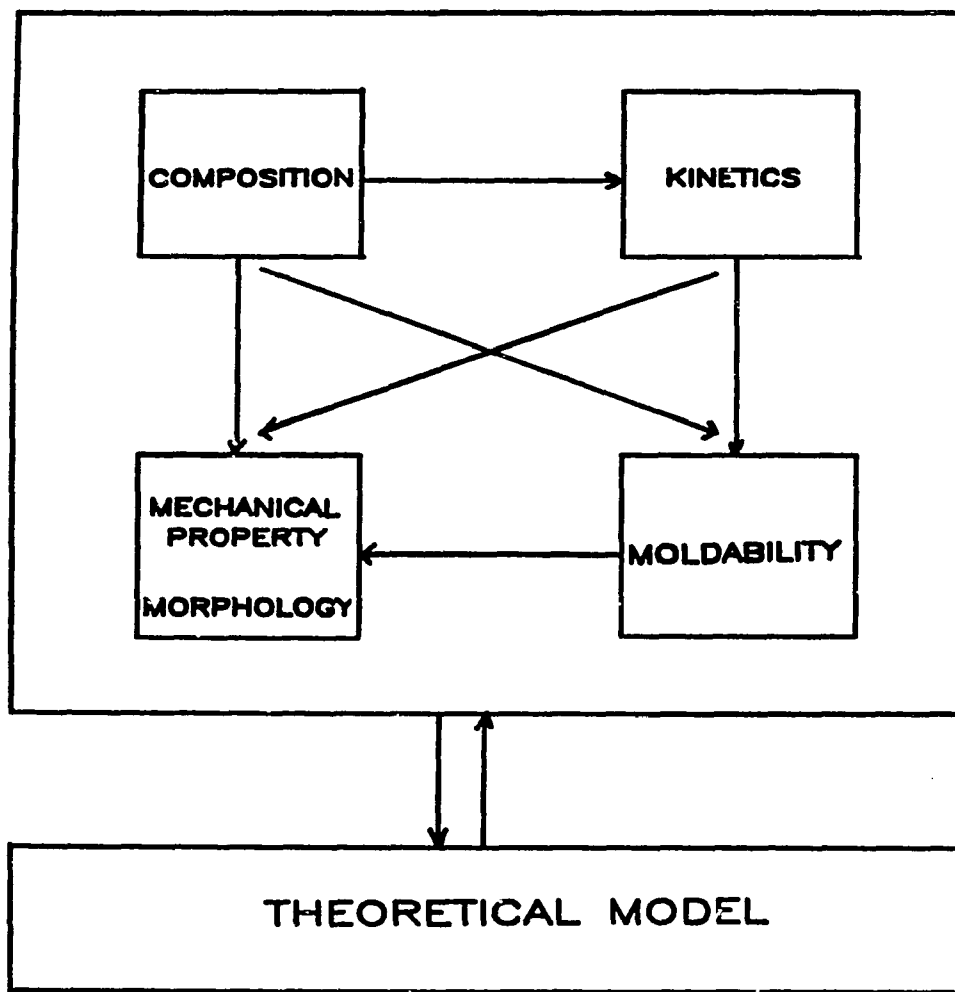


Figure 1.2 Research scheme of reactive polymer processing in this study.

calorimetry and Fourier transform infrared spectroscopy. The dynamic mechanical properties and morphology are studied using a Weissenberg Rheogoniometer and transmission electron microscopy. The rheology is investigated using Haake and Brookfield viscometers. The moldability is studied using RIM and a transfer mold of laboratory size.

Experimental results are compared with theoretical studies through numerical simulations of kinetics and heat transfer effect. Research scheme of each resin is outlined separately as follows:

A. INTERPENETRATING POLYMER NETWORK

Research of IPN was conducted in four sequential and interactive steps:

1. Material characterization
2. Processing of IPNs by reactive polymer processing (RIM and transfer molding).
3. Theoretical modelling of IPN's reaction kinetics and heat transfer
4. Characterization of IPNs produced by reactive polymer processing.

B. POLYUREA

The objectives of research on polyurea in reactive polymer processing are:

1. To explore polyurea RIM experimentally.
2. To evaluate the processibility of polyurea by solution polymerization.
3. To predict polyurea reaction in RIM by the data from solution polymerization.

Based on the above research scheme, this thesis is organized into six chapters. The rationale and objectives of this study are outlined in Chapter I. Chapter II introduces the basics of reactive polymer processing, including process equipment and polymeric systems which have been used or are currently being developed. Chapter III is designed to study the kinetic and heat transfer of polyurethane-polyester IPNs experimentally and theoretically. Also included in this chapter is the rheological and kinetic characterization of polyurethane-polyester IPNs by various analytical instruments. Chapter IV addresses several aspects of solid state characterization of IPNs in morphology, thermal and mechanical behavior, and phase interpenetration in RIM and transfer molding processes. Studies of polyurea are presented in Chapter V

where emphasis are placed on the material characterization, processing of polyurea by RIM, solution polymerization, and data extrapolation from solution to bulk polymerization. Finally, conclusions and recommendations are given in Chapter VI.

CHAPTER II

REACTIVE POLYMER PROCESSING

SYNOPSIS

Related literature of three processes in reactive polymer processing, i.e., reaction injection molding, transfer molding, and casting, are reviewed in this chapter, with emphasis on the machine designs and operational principles. Following an introduction to polyurethanes, the review also covers two polyurethane-based resins, namely, polyurethane-polyester IPNs and polyureas as materials in reactive polymer processing.

2.1 REACTIVE POLYMER PROCESSING

There are many types of processes in reactive polymer processing. Examples are reaction injection molding of polyurethane, epoxy, and polyester, transfer molding of thermosetting polymers, compression molding of bulk molding compound, casting of acrylate sheet, and electronic encapsulation of thermosetting polymers. They can be divided into two types: fast processes such as RIM and the slow processes such as transfer molding and casting. The following sections will review these three processes.

2.1.1 REACTION INJECTION MOLDING

Reaction injection molding is one of the fastest growing processing technologies in reactive polymer processing. A complete review of the RIM process can be found in the literature (Sweeney, 1979; Lee, 1980; Macosko, 1983). Figure 2.1 shows a schematic diagram of the RIM process. Two precisely controlled reactive streams, either monomer or prepolymer, are forced to impinge. This impingement takes place at very high speed and balanced stoichiometry in order to achieve thorough mixing. This highly turbulent flow is then pushed from the mixhead to the mold, where chemical reactions start in only a few seconds to produce a solid part. The mixing chamber also has a capacity of self-cleaning. The reaction in a typical polyurethane RIM can be characterized as fast and highly exothermic. Because of the relatively low viscosity of the liquid monomer, low process pressure and temperature are required. With all these merits, application of RIM process is expected to grow in the future. A study showed that about 30 - 90 million pounds per year of RIM polyurethanes are in the automotive and non-automotive markets. Table 2.1 indicates the statistics (Alberino, et al., 1983).

The United States automobile industry has successfully developed polyurethane elastomer front end fascias by using the RIM process. Here, lightweight, high impact resistance, and a class A

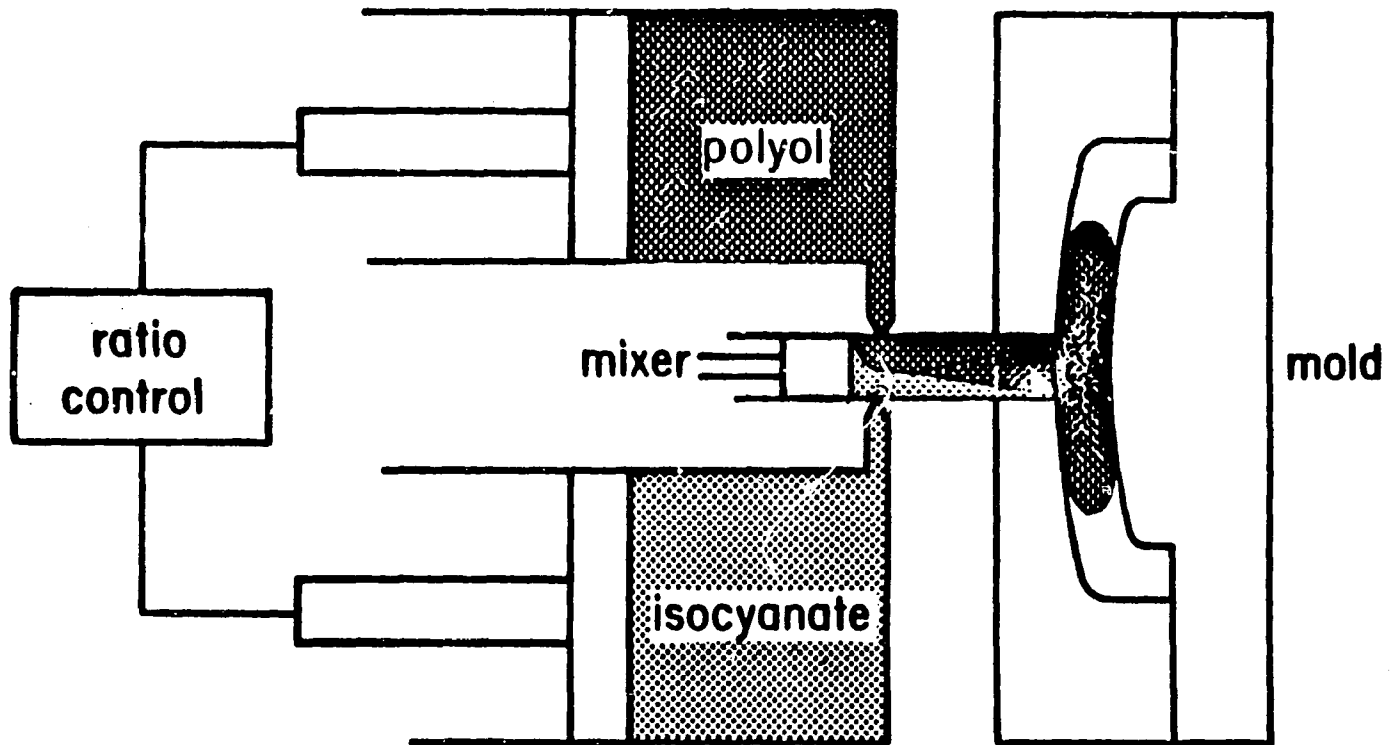


Figure 2.1 Schematic diagram of the reaction injection molding process.

Table 2.1 Market of RIM and RRIM

<u>I. Automotive</u>	<u>Million Pounds Per Year</u>	
<u>Model Year</u>	<u>1982</u>	<u>1984</u>
RIM Elastomer	32	53
RRIM	0.1	8.6
Interior Trim Foam	13 -15	17 -19
<u>II. Non-Automotive</u>	<u>Millions of Pounds</u>	
<u>Model Year</u>	<u>1982</u>	<u>1985</u>
Elastomer	1	5
Urethane Structural Foam	6 - 9.9 (est.)	12 - 15

Reference: Alberino et al., 1983.

RRIM: Reinforced reaction injection molding.

surface are the most important design criteria (Mikhail and Girgis, 1983; Sneller, 1986; Wigotsky, 1986). Front and rear bumper fascia covers were first produced in model year 1975 for General Motors' Monza, Skyhawk, and Starfire series. Later, the Corvette and Firebird were introduced with full front and rear fascias which were also molded in RIM urethanes. In 1978, the Monte Carlo, Lemans, and Camero were produced with flexible front and rear bumper fascias. Since then, the applications of RIM have been extended to other parts of automobile such as the steering station, fenders, truck lids, doors, and even hoods.

Since the first commercialization of RIM in 1975, the major development of RIM technology has been in the automotive industry. However, applications have also been extended to non-automotive markets recently such as aerospace industry and toward the production of furniture, housing appliances, and sporting goods. In addition to PU-RIM, nylon RIM has been commercially developed (Sibal, et al., 1984; Lin et al., 1985). Other chemical systems such as epoxies and unsaturated polyesters are potentially new RIM markets. There has been a steady growth of RIM not only in the market volume, but also in the applications.

There are two types of RIM machines -- the displacement piston RIM and the metering pump RIM. Manufacturers along with classification of their machines are summarized in Table 2.2. Among the RIM-manufacturers, Cincinnati Milacron of USA and Krauss-Maffei

Table 2.2 Major RIM machine manufacturers

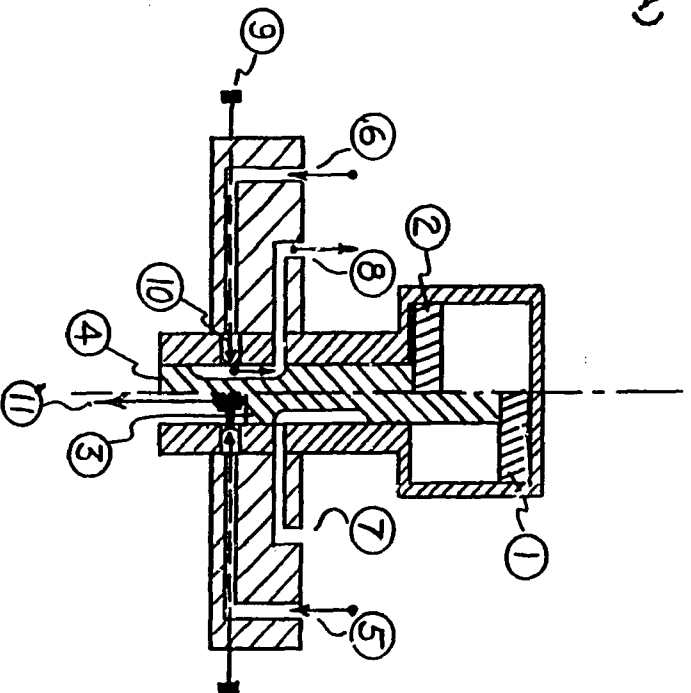
<u>Machine</u>	<u>Type of Machine</u>
Accuratio (U.S.)	Displacement Piston
Cannon (U.S./Italy)	Metering Pumps & Displacement Piston
Cincinnati-Milacron (U.S.)	Displacement Piston
Desma (Germany)	Metering Pumps
Elastogran-EMB (Germany) (U.S. EMB)	Metering Pumps
Mobay/Henneke (U.S./Germany)	Metering Pumps
Impianti (Italy)	Metering Pumps
Krauss-Maffei (Germany/U.S.)	Metering Pumps
Battenfeld/ Schloemann-Siemag (U.S./Germany)	Metering Pumps

Reference: Sweeney, 1979

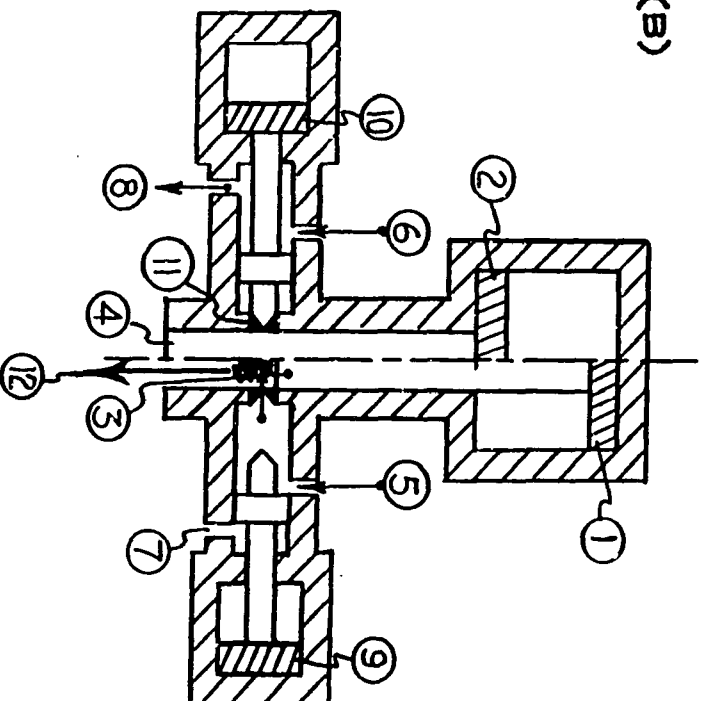
of West Germany are the two major suppliers. There are also several other companies like Accuratio and Martin Sweet, which make pilot-plant scale RIM machines.

The major feature of RIM process is the mixing by impingement of jets of liquid reactants against one another, using positive displacement pumps or cylinders. The mixhead design in today's commercial RIM is reviewed by Lee (1980). Figure 2.2 illustrates various designs of mixhead by several RIM manufacturers. For uniform temperature control, reactants are usually allowed to circulate through the mixhead using low pressure circulation pump. By simultaneously uncovering the impingement nozzles, the mixhead can easily switch from recycle-mode to injection-mode. This is accomplished through either the action of a centrally located hydraulic piston (the designs of Admiral, Battenfeld, Krauss Maffei, and Cincinnati Milacron) or the action of a hydraulically driven valve (the designs of Cannon, Accuratio, and Henneke). The rapid mechanical shift of both reactant streams from recycle to injection mode allows accurate control of material metering. All mixhead designs have a capability of self-cleaning once the impingement process is completed. The mixture is pushed out from the mixhead when the piston returns to its recycle mode at the end of each shot. To permit easy change of fluid flow rate, the Cincinnati Milacron mixhead uses slits for the impinging streams rather than circular nozzles. This allows mixhead to uncover different portions of the

(A)



(B)



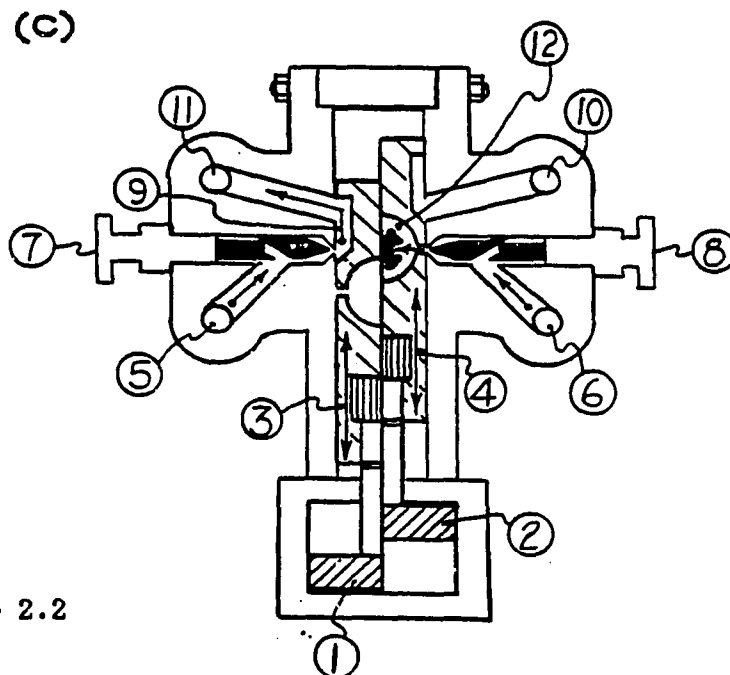


Figure 2.2

(A) Krauss-Maffei and American E.M.B. use this mixing head design. The left side of the drawing shows the head in the recycle position, the right side shows the shot position. Numbered items are as follows: 1. Hydraulic piston in shot position; 2. Hydraulic piston in recycle position; 3. Clean-out piston in shot position; 4. Clean-out piston in recycle position; 5. Polyol feed; 6. Isocyanate feed; 7. Return line, no flow; 8. Return line, recycling; 9. Nozzle needle adjustment; 10. Nozzle and needle (E.M.B. machines substitute orifice plates for nozzle and needles.); 11. Polyol and isocyanate impinge and flow to mold. (B) Henneke uses this mixing head design. The left side of the drawing shows the head in the recycle position, the right shows the shot position. Numbered components are as follows: 1. Hydraulic piston in shot position; 2. Hydraulic piston in recycle position; 3. Clean-out piston in shot position; 4. Clean-out piston in recycle position; 5. Polyol feed; 6. Isocyanate feed; 7. Return line, no flow; 8. Return line, recycling; 9. By-pass piston system in shot position; 10. By-pass piston system in recycle position; 11. Impingement nozzles; 12. Polyol and isocyanate impinge and flow to the mold. (C) Battenfield (Schloemen-Siemag) uses a mixing head of this design. The recycle position is shown on the left, and the shot position on the right. This cross-sectional schematic is shown in a plane perpendicular to the axis of the shot piston. Numbered parts are as follows: 1. Mixer housing hydraulic piston in by-pass position; 2. Mixer housing hydraulic piston in shot position; 3. Mixer housing in by-pass position; 4. Mixer housing in shot position; 5. Feed port "A"; 6. Feed port "B"; 7. Needle valve adjustment "A"; 8. Needle valve adjustment "B"; 9. By-pass channel of mixer housing in recycle position; 10. Return port "B", no flow; 11. Return port "A", recycling; 12. Mixing chamber (Sweeney, 1979).

slits when it switches from recycle to injection mode. Others (i.e., Admiral, Henneke) have tapered annular nozzles.

Metering control is achieved through several designs. The control devices can be classified as:

- a. Piston type hydraulic cylinder
(Accuratio, Martin Sweet).
- b. Lance type hydraulic cylinder
(Cincinnati Milacron).
- c. Axial/radial piston pump
(Krauss-Maffei).

High speed mixing is the main challenge in RIM design. The impingement is designed to provide turbulent mixing of a large amount (greater than 5 kg) of viscous liquid (100 to 600 cp) in a very short period of time (few seconds). The flow of the mixture should be in the laminar state when it is flowing in the mold. The transition from turbulent to laminar flow has to take place in a very short period of time. This requires a proper design of aftermixer, runner, and mold. The review of mold design can be found in a review article (Lee, 1980).

Since RIM is originally designed as a very fast process, the development of RIM materials has to meet certain criteria which include:

- a. Rapid chemical reaction within few seconds.
- b. Low viscosity of reactive monomers for
 - i. energy saving.
 - ii. complete mixing in mixhead.
- c. Stable storage conditions.
- d. Efficient catalyst to control reaction rate.
- e. Effective demoldability after molding.

In addition to the criteria listed above, the finished RIM products also have to meet Federal Regulations for economic and safety reasons. However, the major driving force is the sky-rocketing fuel cost in the early 1970s. As a result, gradual replacement of iron and steel by plastics and aluminum should continue in the foreseeable future. Although different parts of an automobile require various thermal and mechanical standards, in general, the replacement of metals by plastics should meet the following requirements:

- a. Tensile strength greater than 2,000 psi.
- b. Class A surface quality.
- c. Good paintability at elevated temperatures of
250 - 350 °F.
- d. Flexural modulus greater than 20,000 psi.
- e. Good weatherability --- Temperature insensitivity.

2.1.2 Transfer Molding

Transfer molding is one of the conventional methods in rubber industry and electronic industry for molding parts from thermosetting plastics. The development of transfer molding is parallel to that of compression molding. First commercial application of transfer molding was carried out in the mid-1930s (O'Brien and Lenosky, 1986). In transfer molding, a charge of thermosetting compound is heated at high temperature to soften it in order to flow into the mold and for the material to polymerize and become crosslinked. Pressure range can be as high as 10,000 psi for a period of time.

Different from compression molding where materials are charged into the mold before closing the mold, in transfer molding, the mold is closed before the molding compound is introduced in its fluid state. The fluid goes through a small opening or gate leading to the mold cavity. Two types of transfer molding processes are generally practiced in the plastic industry: the pot-type transfer molding and the plunger-type transfer molding. These will be described respectively as follows (Tadmor and Gogos, 1979; Schwartz and Goodman, 1982; Hull, 1984; O'Brien and Lenosky, 1986) .

Pot-type transfer molding. In this design, the mold is closed before the charge is introduced. Placed in an open air, the mold has an open pot at the top of it where the plunger is to be placed when

the press is closed. As the press closes, it pushes the plunger, and consequently exerts pressure on the charge, and forces the charge down through a vertical sprue (in some cases, multi-sprues), runners, and gates into the cavities, where chemical reaction, i.e., polymerization or curing, takes place. Figure 2.3 schematically describes this procedure. To ensure the mold remains closed during pressing and curing period, the area of the pot requires about 15% more than the projected area of the molded part and runners. After the cure, the plunger is withdrawn, the mold and subsequently, the press, are opened, and the solid parts are ejected. Some portions of the charge is wasted in the pot. For this reason, the pot-type transfer mold is not very economical.

Plunger-type transfer molding. In this process, the plunger is a part of the mold rather than a part of the press. A cylinder (the plunger) is attached to the head of the press. Smaller projected area is required than the pot-type molding. The mold is closed before the material is charged into the mold. The clamping action of the press keeps the plunger movement independent of the action of mold closing. The process is described schematically in Figure 2.4. The plunger-molding is the most common type of transfer molding in plastic industry.

Whether or not to use pot-type or plunger-type transfer molding depends on the price of molding material, the cost of the

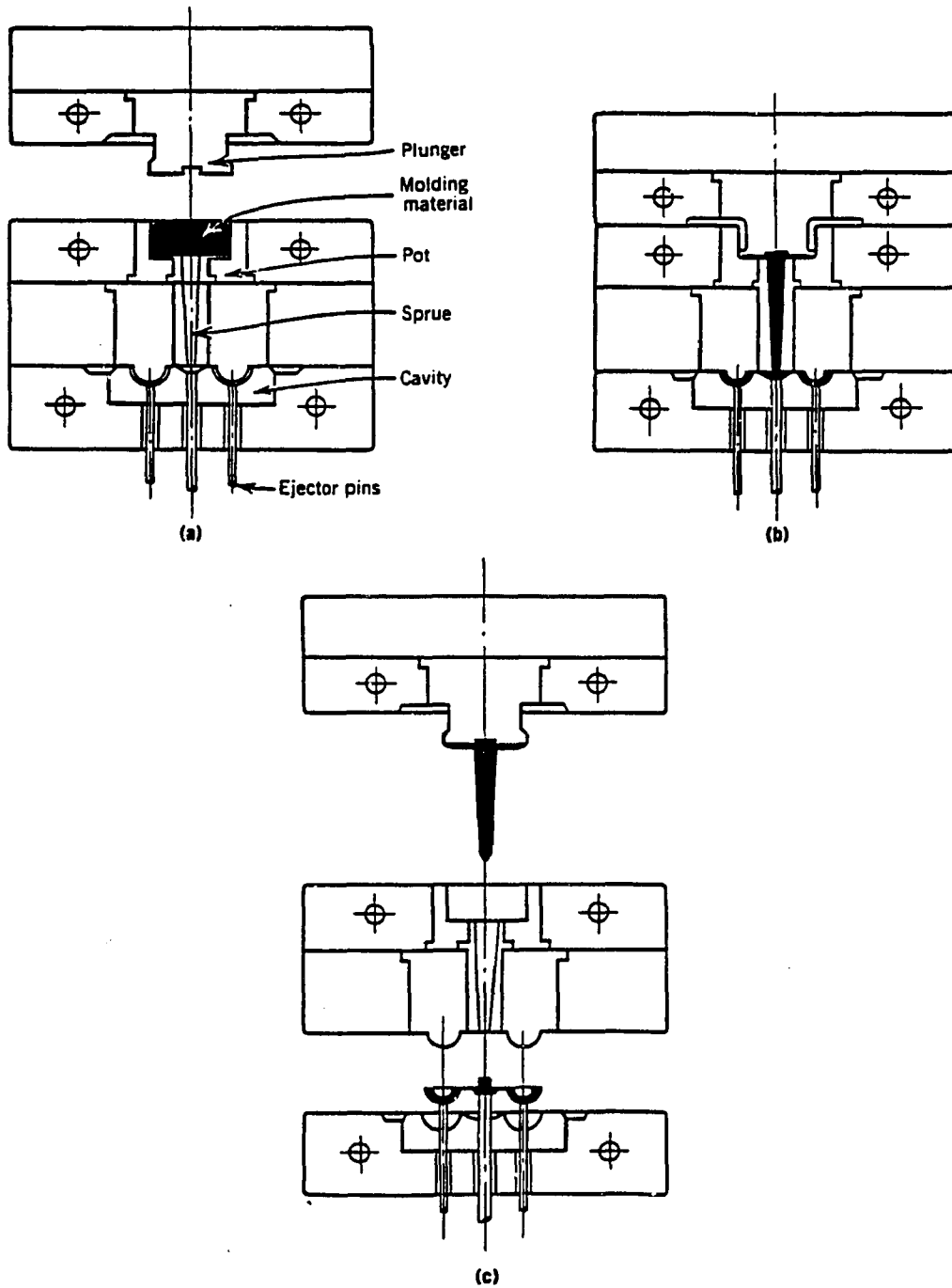


Figure 2.3 True, or pot-type, transfer molding. (a) Mold open, pot loaded; (b) mold closed; and (c) mold open, parts ejected, sprue on force plug (Hull, 1984).

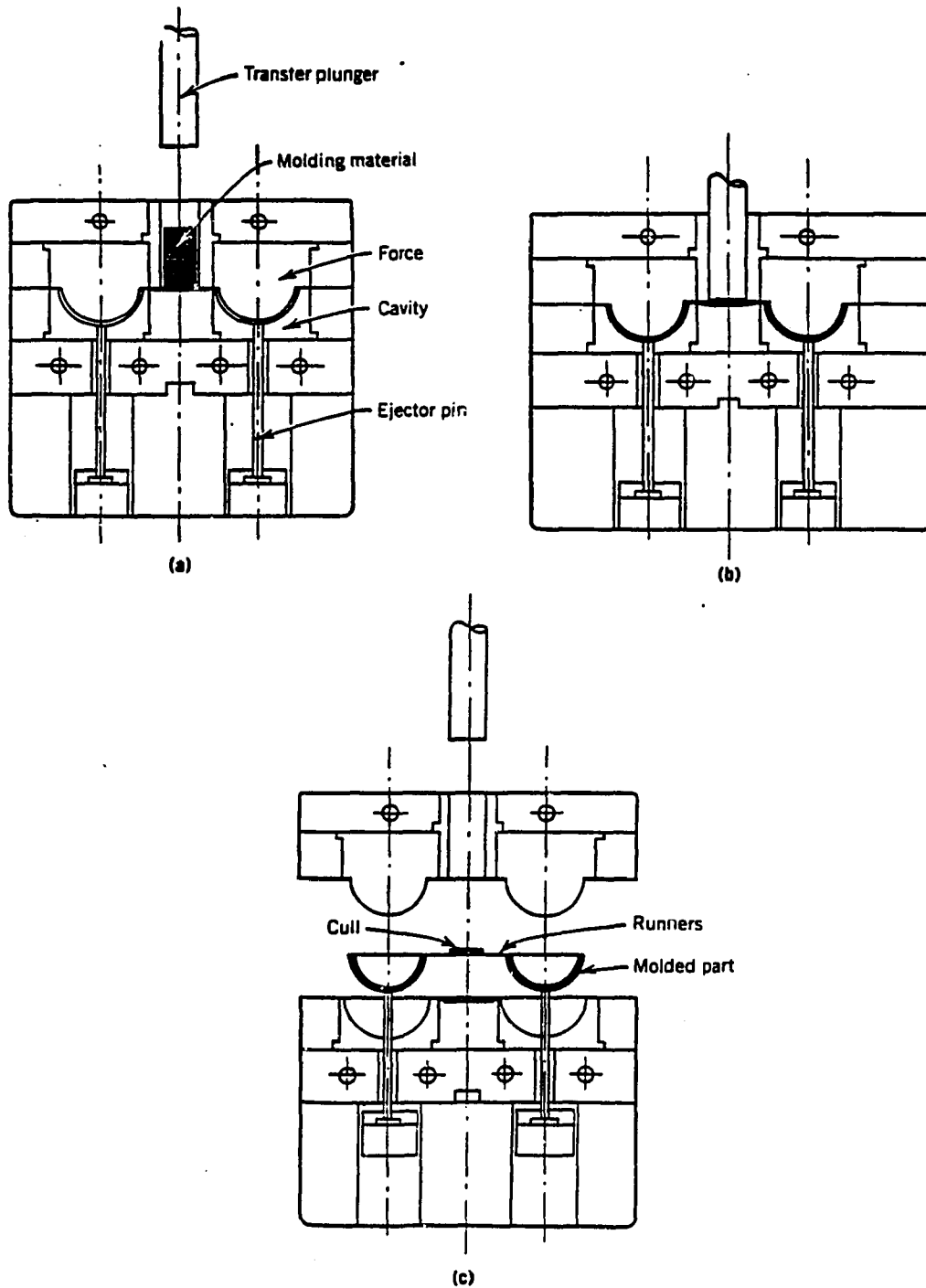


Figure 2.4 Plunger mold configurations. (a) Mold closed, pot loaded; (b) mold closed, plunger down; and (c) mold open, molded part, cull, and runners ejected (Hull, 1984).

mold and press, the type of die required (the shape of the finished products), and the equipment available.

Transfer Process. For optimum cure, most thermosetting compounds must be heated at high temperature (e.g., 150 °C for unsaturated polyester resin). Higher temperature may cause earlier solidification before the cavity is completely filled. However, low temperature requires longer curing time. There is always an optimum molding temperature at which the best flow characteristics of the particular molding compound are achieved. To shorten the cycle time, quite often the charge is preheated. Common preheating temperature ranges from 65 to 95 °C. Again, excessive preheating may cause premature polymerization. The frictional heat generated during the closing of the mold may also contribute heat input to the process. The amount of frictional heat depends on the speed of the plunger, the surface finish of the mold, and the size and configuration of the runners and the gates. After molding, the materials generally require postcure, typically 2 hours at or slightly higher than the molding temperature. The pressure needed to mold thermosetting polymers generally ranges from 3,000 to 10,000 psi, since the charges are quite often of highly viscous fluids. The viscosity-time curve of the thermosetting compound is the most important processing variable in this process.

In some cases, the thermosetting compounds give off gaseous products such as water vapor and carbon dioxide during

polymerization. The trapped gases may cause blisters and ruptures of the finished products because the resin has not crosslinked sufficiently to retain its shape. To release these gaseous products, the mold is designed with venting lines. For more effective degassing, the mold is opened for a short period of time to allow it to "breathe.". The duration of opening is called "dwell."

Molding Compounds. Most applications of transfer molding involve thermosetting plastics such as unsaturated polyesters, alkyd resins, melamine-formaldehydes, epoxies, phenol-ureas, and rubbers.

2.1.3 Casting

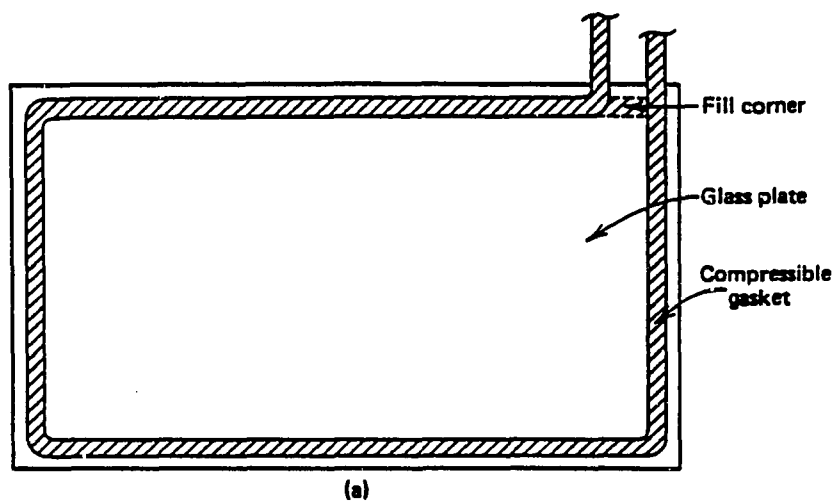
Casting represents another slow process in reactive polymer processing. It is a process in which liquid monomer is poured into a mold where polymerization takes place. A rigid object which reproduces the mold cavity is formed at the end of casting. By far the most frequently practiced casting process is the manufacturing of acrylic sheet. Methyl methacrylate is the principal monomer used in acrylic sheet casting. Other resins such as diethyl glycol, styrene, epoxy, and silicone may also be utilized in this process.

The primary articles manufactured by casting process in plastic industries are the high molecular weight cast acrylic sheets (Tadmor and Gogos, 1979; Schwartz and Goodman, 1982; Harbison et al., 1984; Jans, 1986). Other articles of complicated shapes, tubes,

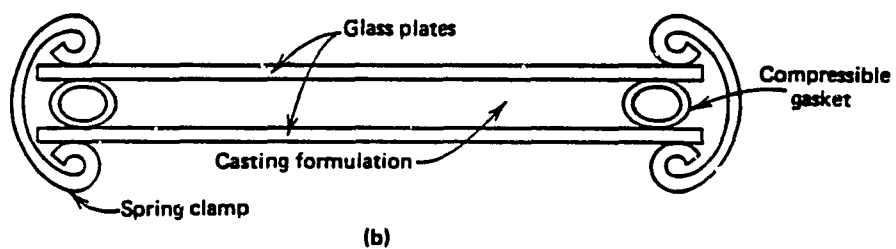
rods, can also be produced by cast acrylate. Other resins such as casting of nylon (Nichols, 1986) and PVC film (Knoop, 1986) have been commercially available. The development of casting can be dated as far back to the 1930's. Casting of methyl methacrylate monomer into slabs of organic glass, known as Plexiglas, was developed by Rohm and Haas Co. in 1930. Since then, similar processes were also developed by Du Pont and Imperial Chemical Industries. In the United States, an estimated 8.6×10^4 metric tons of cast acrylic sheets were produced in 1982. The sheets have been used for various applications such as furniture, displays, signs, and glazing (for automotive, aircraft, mass transit, and architecture). The operational principle of casting process is similar to potting, encapsulating, and embedding. In potting, the mold itself becomes the permanent part of the finished assembly. In encapsulating, the electronic component is protected with an external coating of polymer. In embedding, the embedded material is encased with some uniform external shape. On the other hand, the mold in casting process is removed from the finished product. Two processes of casting are commonly practiced in the plastic industries: the cell casting and the continuous casting.

Cell Casting. Shown in Figure 2.5A is the standard cell casting operations which consist of two flat glass plates separated by an elastomeric gasket. The assembled glass-gasket-glass mold is clamped together to form a tight seal around the periphery. For complete

(A)



(a)



(b)

(B)

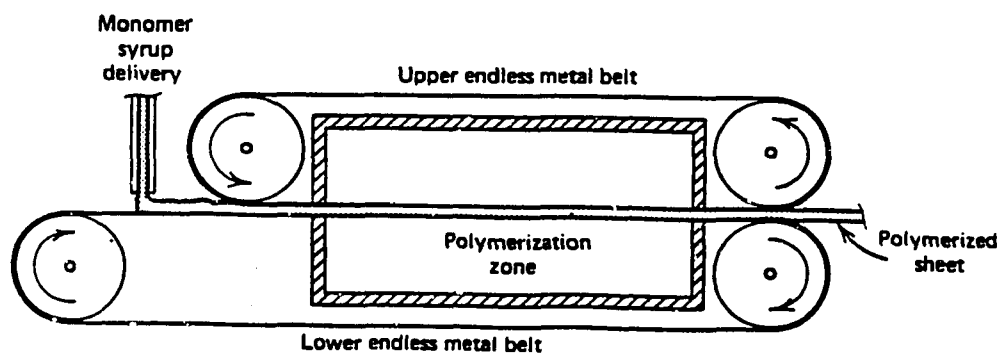


Figure 2.5 (A) Conventional cell casting mold configuration. (a) Face view and (b) edge view (Harbison, 1984).

(B) Continuous casting apparatus.

filling, the mold is placed in a slightly to fully vertical position. Once the mold is filled, it is heated to initiate the polymerization. With methyl methacrylate monomer, the total shrinkage is about 20% and occurs almost entirely in thickness. After demolding, the product may be annealed or postcured and then slowly cooled to release internal stress due to different thermal history. Sheet thickness up to 2.5 cm can be produced by this process.

Continuous Casting. A more popular way to produce acrylic sheet is the continuous casting. This process was developed by Swedlow, Inc. in the early 1960s. It is a faster and an inexpensive process compared to the cell casting. However, sheet thickness is limited to only 2 -12 mm due to design limitation. In continuous casting, the expensive breakage of glass and cell handling are eliminated. As shown in Figure 2.5B, the process utilizes two parallel, continuously conveying stainless metal belts. A syrup or prepolymer dissolved in monomer is delivered onto the top surface of the lower belt, which conveys the syrup forward to meet the upper belt. The lower and upper belts move together with entrapped syrup and the flexible gasket along the edge to prevent breakage. Heating is provided along the belt to control polymerization effectively.

2.2 MATERIALS

2.2.1 Polyurethanes

A. Chemistry and Kinetics

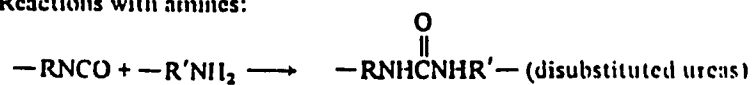
The reaction kinetics of polyurethane is a typical step-growth polymerization. Detailed urethane chemistry can be found in several review (Saunders and Frisch, 1962, Sweeney, 1979; Lee, 1980). Basically, there are three ingredients in a segmented polyurethane: diisocyanate, a low molecular weight chain extender (usually a diol or diamine), and a long chain polyester or polyether diol (molecular weight of about 2,000 to 3,000). For a crosslinked polyurethane, the chain extender and the long chain diol are replaced by a triol with molecular weight about 500. The primary reaction that occurs during urethane polymerization is



where a hydroxyl group -OH reacts with an isocyanate group -NCO. The reaction mechanism is usually expressed as an nth order reaction. An organometallic compound is usually used as the catalyst. Side reactions such as dimer and trimer formation of isocyanate may also occur. These side reactions are summarized in Table 2.3. It is well known that thermoplastic urethane elastomers are segmented copolymers containing both hard and soft domains. The hard domains

Table 2.3 Reactions of isocyanate with various functional groups

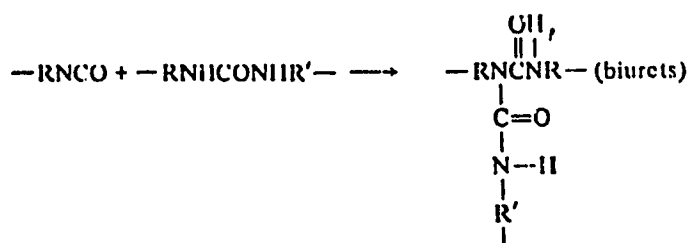
1. Reactions with amines:



2. Reactions with amides:



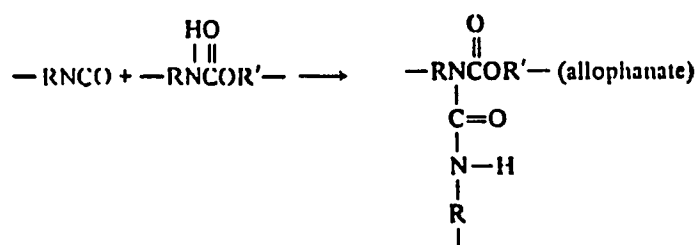
3. Reactions with ureas:



4. Reactions with alcohols:



5. Reactions with urethanes:



6. Reactions with carboxylic acids:

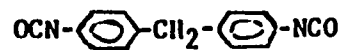


7. Reaction with water:



are composed of diisocyanate and chain extender; while the soft domains are formed from the long chain ingredient. Figure 2.6 shows a schematic diagram of domain formation (Lee, 1979). Phase separation due to the incompatibility of these domains has been the interest of several studies (Castro et al., 1981; Camargo, et al., 1982; Blackwell and Lee, 1983; Camargo et al., 1983). Recently, Huang et al. (1985), studied the effect of compound composition on the reaction kinetics of polyurethane RIM by using a differential scanning calorimeter (DSC). By varying the ratio of the hard and soft segments, they were able to observe the effects of phase separation and crystallization on the polyurethane residual activity (i.e., limiting conversion) and on the shifting of the melting peaks of polyurethane.

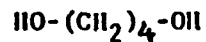
Camargo et al. (1982) studied the phase separation of the catalyzed and the uncatalyzed polyurethane polymerization by using a mini-RIM machine. For the highly catalyzed samples, a high degree of phase intermixing, low crystallinity, low number average molecular weight were obtained. In an effort to find the reaction mechanism, Richter and Macosko (1978), and Camargo et al. (1983), studied the RIM urethane by infrared spectroscopy and the adiabatic temperature rise method.



1,4 diphenylmethane
diisocyanate
(MDI)

AA

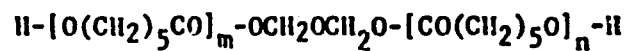
$M_n = 250$ 



1,4 butane diol
(BDO)

BB

$M_n = 90$ 

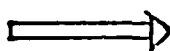


ϵ -caprolactone diol
(PCP-0240)

CC

$\bar{M}_n = 2000$

$m+n = 17$ 



segmented polyurethane

Figure 2.6 Domain formation of polyurethanes.

B. Properties and Applications

Major applications of polyurethanes include elastomers, flexible foams, and rigid foams (Saunders and Frisch, 1962; Sweeney, 1979; Schwartz and Goodman, 1982; Billmeyer, 1984).

Elastomer: Urethane elastomers are prepared by three processes (Schwartz and Goodman, 1982):

- a. Casting Method. The monomers are mixed in liquid state, poured into a casting mold, and allowed to cure to a solid, rubbery state in the mold. After demolding, additional postcure may be needed.
- b. Thermoplastic Method. Usually a prepolymer is prepared with some excessive -OH groups. The prepolymer is then chain extended by short-chain diol or diamine to a high molecular weight of highly soluble polymer.
- c. Millable Gum Method. The preparation is similar to thermoplastic method. The prepolymer (or gum) is mixed with isocyanate and then cured by milling and heating.

The elastomers generally can provide properties of elasticity, resilience, good abrasion resistance, high tear strength, shock-absorbing, and sometimes hardness. Other properties include

outstanding resistance to ozone, oxygen, and hydrocarbon. Major applications of urethane elastomers cover a wide range. For example, shoe heels and ski boots are among the many injection-molded goods which are made by thermoplastic urethanes. Others include injection-molded gears and O-rings, cast urethane encapsulants, extruded wire and cable insulations, gaskets, shock-absorbing pads, and cable jacketing.

Flexible Foams. Flexible foams can be defined as those urethane foams which possess high elongation, fast recovery rate, high elastic limits, and high tensile/compressive strength ratios (15/1 to 70/1). Polyols having molecular weight of 500 - 2,000 are usually used for flexible foams. The presence of blowing agent (i.e., water, or methylene chloride) cause the reaction of isocyanate and polyol (functionality of 2 or 3) to polymerize and expand into a cellular structure with the evolution of carbon dioxide. Catalysts are also added to force crosslinking and chain extension, and to control the evolution rate of carbon dioxide. Silicones or surfactants are used to control the size and the green strength of flexible foams, and its moldability. By far the biggest market for flexible foams is the comfort cushioning in furniture, which can provide ease of fabrication, light weight, and great strength economically. Mattress is another big market due to their superior durability, non-allergic, resistance to fungus, and freedom from odor.

Rigid Foams. Contrary to flexible foams, the rigid urethane foams can be defined as those urethanes having low tensile/compressive strength ratios (1/0.5), low elongation (<10%), low recovery rates from distortion, and low elastic limits. Glass transition temperature of rigid foams usually is above room temperature. High functionality (≥ 3) of polyols are generally used for rigid foams with high crosslinking density. Other properties include:

- a. Excellent adhesion to metals.
- b. Light weight and high strength.
- c. Excellent thermal insulation.
- d. Good heat resistance.
- e. Good energy-absorbing properties
(sound-dampening effect).

Typical applications of rigid urethane foams include refrigerator insulation, insulated pipes and tanks, structural uses, roof tops and wall panels, packaging for engine parts, and electronic tubes.

C. New Development.

In automotive industries, polyurethanes are manufactured mainly by RIM for the production of soft front and rear end fascias. The versatility of urethane provides various opportunities in automotive industries. Furthermore, the success of RIM process has

increased the demand of polyurethane applications such as the use for large auto body part and other structural applications. To do so, several modifications of polyurethanes have been proposed which are reviewed in the next section.

2.2.2 Modifications of Polyurethanes

To utilize the diversity and versatility of RIM and to expand applications of reactive polymer processing, three modifications have been proposed (Lee, 1980; Nguyen, 1984) :

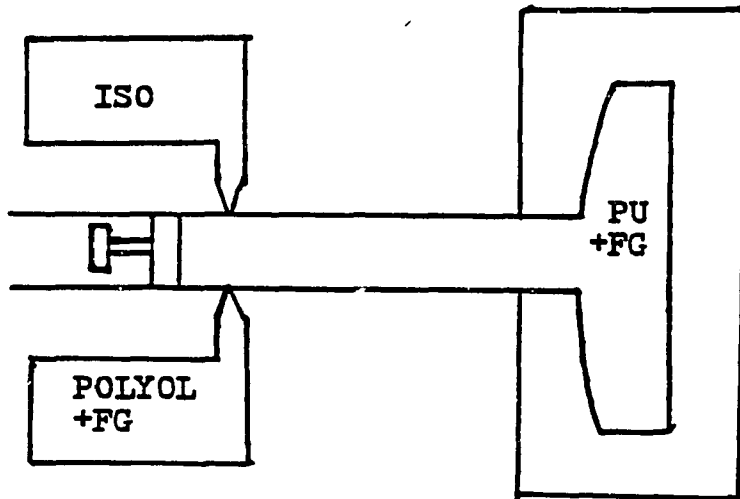
1. Addition of fillers such as fiber glass as a reinforcing agent.
2. Addition of other polymers to existing polyurethane.
3. Addition of fiber glass mats in the mold (Gonzalez and Macosko, 1983) -- mat reinforced RIM, structural RIM, or resin transfer molding.

All these modifications have been termed "composite materials." They can be further classified into two types:

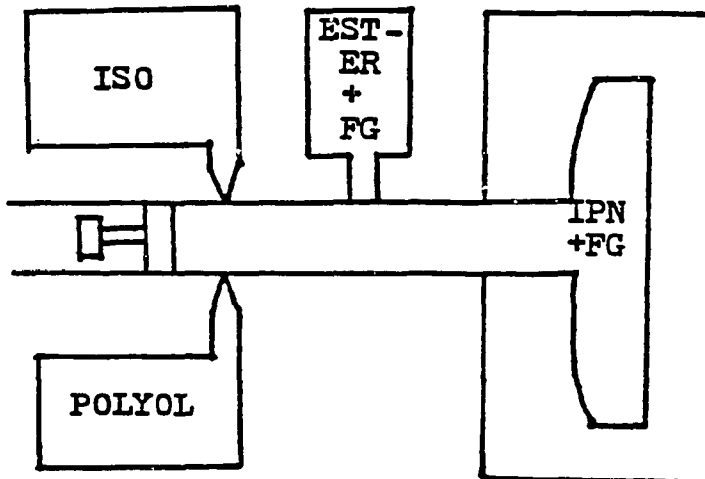
- A. External reinforcement.
- B. Internal reinforcement.

A. External Reinforcement

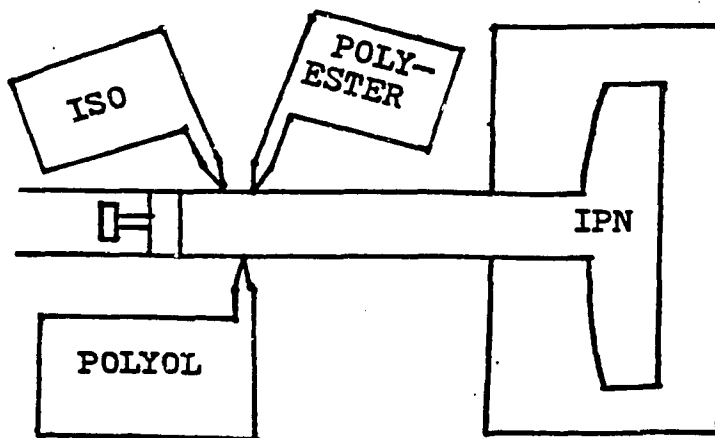
External reinforcement means the addition of fillers (i.e., milled or chopped fiber glass) to the reaction system or the addition of fiber glass mat in the mold to improve the mechanical properties and thermal stability of urethanes. This process is termed reinforced reaction injection molding (RRIM). Shown in Figure 2.7 are schematics of various modifications of RIM process. The materials of RIM and RRIM are quite similar. In an attempt to reinforce RIM urethane, some reinforcing agents such as glass fibers, carbon fibers, and others are added to the existing resin (Lawrence, 1974). Several research works in this area have been published over the last few years (Mikhail and Girgis, 1983; Sneller, 1986). Milled glass fibers have been the most preferred RIM reinforcement material due to their compatibility with the RIM machine and their low reduction of impact properties relative to other inorganic fillers. Milled glass fibers are glass filaments processed through a hammer miller with discharge screens of a specific opening size. The screen opening size determines the type and length (aspect ratio) of the milled glass. 1/16" milled glass at 25% weight load is currently the "state of the art" reinforcement for RIM urethanes. Several benefits can be expected from the fiber-loaded RIM urethanes (Schwarz, et al., 1979). These include:



A. Conventional RIM



B. External reinforcement of RIM



C. Internal reinforcement of RIM

Figure 2.7 Schematic diagram showing two possible routes for reinforced reaction injection molding (RRIM).

- a. Increase in stiffness.
- b. Reduction in thermal expansion coefficient.
- c. Reduction in heat sag.
- d. Reduction in modulus/temperature ratio.

One obvious drawback is that the impact strength and the elongation of reinforced RIM urethanes drop with increasing glass fiber content (Lee, 1980; Mighail and Girgis, 1983). No delay in curing time is expected for those urethanes with glass fibers added if process conditions were appropriately adjusted. In fact, the undesirable high exotherm during molding could be reduced through the heat sink effect of the filler. However, higher loading of glass fiber in RIM urethanes will cause handling problems because of the inability of RIM machine to process the highly viscous slurry.

In order to obtain better reinforcement, it is necessary to use fibers with longer lengths. Mighail and Girgis (1983) reported reinforcement in RIM urethanes using 1/8" milled glass fibers up to 20% by weight and 3 mm long chopped integral strands up to 13.4%. The results showed that with chopped integral strands, better impact strength, less heat sag, and less anisotropy were obtained. However, surface quality which is being considered by the automotive industries as its primary requirement for exterior body parts, was poor, with the chopped strands being the worst. It was also observed that due to the abrasion of glass fibers, leakage of material lines

and fiber breakage during impingement mixing were serious. The results indicated that processing of chopped glass fibers through the small nozzles of RIM machine was not very effective.

One possible route to accomplish the reinforcement is to process the prewetted glass fiber, either milled or chopped, through another stream into the mixing chamber. Since there is a highly turbulent flow generated in the mixhead, the turbulence may be able to provide thorough mixing of the third stream. Ideally, the polymerization of this third stream should begin immediately after mixing with urethane resin in the mixhead. Figure 2.7B schematically explains the process. The ideal candidate of this third stream is a free radical type resin with a temperature-initiated initiator which can utilize the high exotherm of urethane reaction to trigger its own polymerization. Unsaturated polyester with a moderate-temperature initiator, for example, is a good choice.

In RIM, another method of reinforcement is the mat reinforced RIM (Gonzalez and Macosko, 1983). A cold resin mixture is injected from RIM machine to a hot fiber mat which is present in the mold. Because of the well-structured long fiber reinforcement, the mat reinforced RIM may offer the reinforced RIM urethane an extremely high mechanical strength.

B. Internal Reinforcement

The internal reinforcement involves the introduction of another reactive liquid functional monomer into the reaction system (Figure 2.7C). The idea is based on the assumption that this polymer is able to compensate for the deficiencies of elastomeric urethane, especially the thermal and mechanical properties. This type of composite material have been termed "interpenetrating polymer networks." Nguyen and Suh (1986) studied the processibility of IPNs in RIM. In addition to the elastomeric RIM urethane, which accounts for two streams, they introduced a third stream of glassy unsaturated polyester resin into the reaction system. The impingement of these three streams was simultaneous with a drive pressure of up to 100,000 psi and a Reynolds number of up to 10,000 (a typical commercial RIM machine uses a pressure of about 1,000 - 2,000 psi and Reynolds number of about 200). The resulting products showed some improvement of thermal properties such as a reduction in heat sag.

2.2.3 IPNs

A. General IPNs

An IPN is a polymer alloy of two polymers which are crosslinked or synthesized in the presence of each other. Since there are two components in an IPN, the synthesis method of IPNs can

be classified according to the polymerization sequence and the polymer structure of the components. The polymer structure can be either crosslinked or linear. There are two types of IPNs according to the polymerization sequence. The first one is a simultaneous interpenetrating network (SIN) which is formed when the polymerizations of the components are simultaneous. Likewise, sequential polymerization of components results in a sequential IPN. According to the polymer structure, two IPNs can be distinguished. A full IPN is obtained when both components are crosslinked (i.e., thermosetting polymers). If there is one linear (i.e., thermoplastic polymers) and one crosslinked component in an IPN, a semi-IPN is formed. When both polymerization sequence and polymer structure are taken into account, four different IPNs can be classified as shown in Figure 2.8.

The history of IPNs can be traced back to at least 1941, when the British government granted a patent to Staudinger and Hutchinson (Staudinger and Hutchinson, 1951). The first United States patent was also given to them for the use of an IPN topology to prepare an improved optically smooth plastic surface. Since then, several patents have been issued in the United States. A list of IPNs related patents can be found in the literature (Sperling, 1981). Several groups in the United States, including Sperling, Manson, and their coworkers (University of Lehigh), Frisch, Klempner, and their coworkers (University of Detroit) have conducted

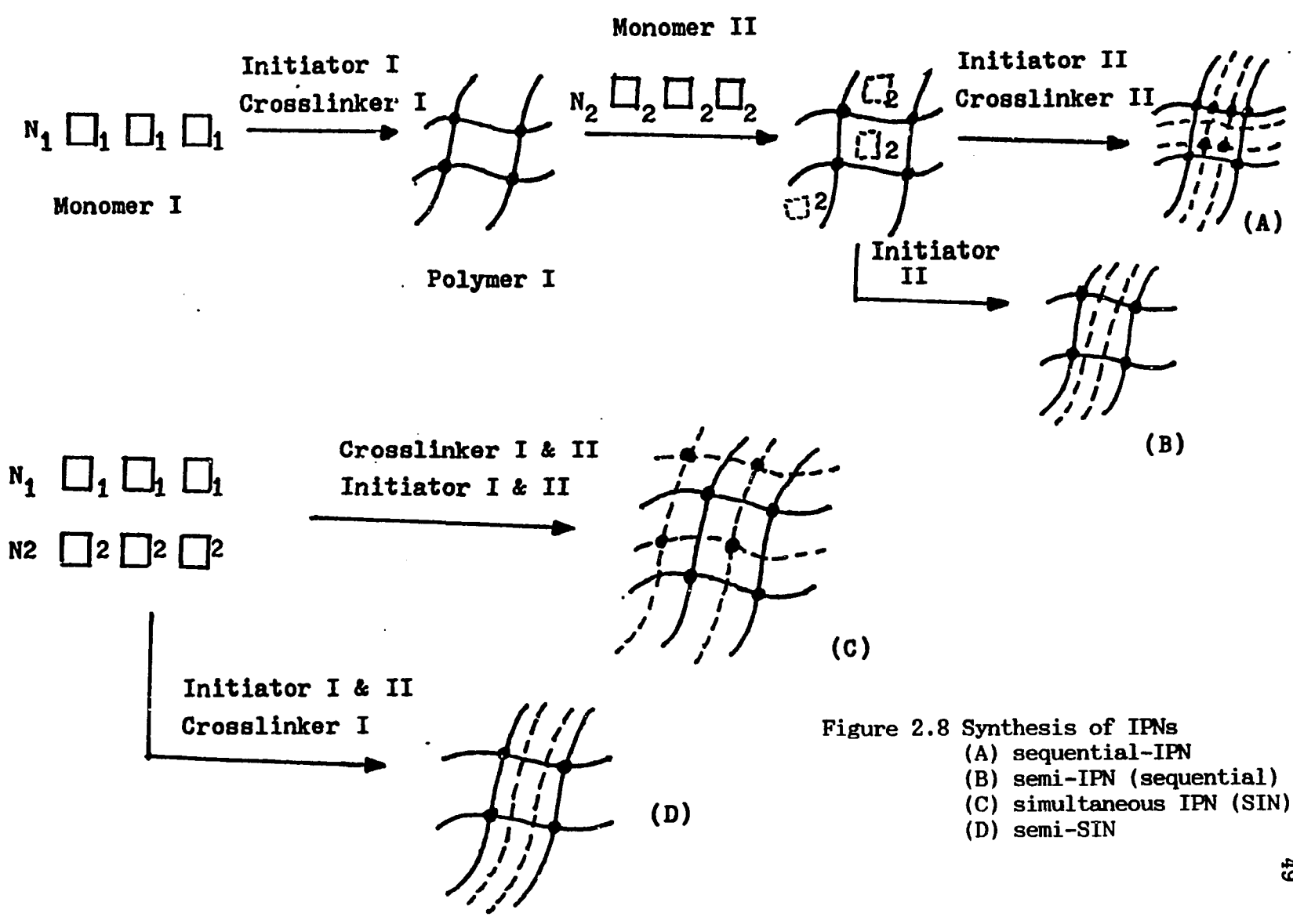


Figure 2.8 Synthesis of IPNs
 (A) sequential-IPN
 (B) semi-IPN (sequential)
 (C) simultaneous IPN (SIN)
 (D) semi-SIN

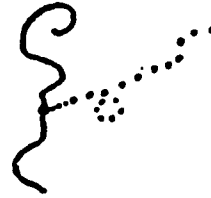
intensive research in this area. Several review papers have been published by these researchers (Manson and Sperling, 1976; Thomas and Sperling, 1976; Klempner, 1978; Sperling, 1980).

In comparison to polymer blends and other polymers, IPNs have several distinguished properties. Figure 2.9 shows schematically the topologies of some polymers of interest (Thomas and Sperling, 1976). A polymer blend can simply be defined as the combination of two polymers without any chemical bonding between them. It is well known that mechanical blending of two polymers results in a multiphase morphology due to thermodynamic incompatibility of its constituent polymers. Low interface strength is generally a serious problem in a polymer blend such as rubberized high-impact polystyrene (Lawrence, 1974). Also, because polymer blends are blended after the polymerization has been completed, only thermoplastic polymers fit into this category. On the other hand, if mixing starts at the beginning of the polymerization (i.e., when the constituents are monomer solution), such as in the case of IPNs, phase separation can be minimized. This is achieved by numerous permanent entangled locking. Furthermore, synthesis of IPNs is the only way to combine two crosslinked thermosetting polymers together.

Most IPNs studied in the literature have been prepared in slow processes where only synthesis method, morphology, mechanical testing, thermal behavior have been studied. Seldom have the method of processing, nor the reaction kinetics of IPNs, been explored.



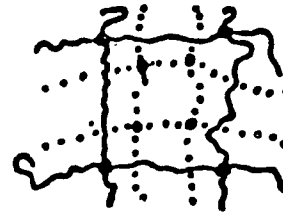
POLYMER BLEND



GRAFT COPOLYMER



BLOCK COPOLYMER



IPN

Figure 2.9 A comparison of various polymeric composites.

For the polymerization conditions, solution polymerization is the most popular method for IPNs synthesis since it is the easiest way to control the reaction rate. The reaction rate is typically slow, usually requires 3 or 4 days (only few seconds required in RIM process). Latex polymerization has also been explored (Frisch, et al., 1969) and the product is termed "interpenetrating elastomeric network (IEN)." However, these are not the preferred methods from the perspective of reactive polymer processing operations. For reaction injection molding, the only practical way is by bulk polymerization without any solvents being added to the system.

The synthesis of IPNs requires two independent and non-interfering reactions that can be carried out in the same reactor under the same reaction conditions. Both simultaneous and sequential IPNs have been mentioned in the literature (Manson and Sperling, 1976; Sperling, 1985). A sequential IPN begins with the swelling of the second monomer with its crosslinking agent and initiator, in a crosslinked primary polymer and polymerized in situ. This process is not suitable for mass production because it takes too long for swelling. The process also strongly depends on the mutual solubility of the two component networks. For a simultaneous IPN (SIN), a mixture of monomers, initiators, and crosslinkers of both components is prepared and poured into the mold for curing. For this reason, SINS are suitable for reaction injection molding and may become an

attractive alternative to SMC, BMC, fiber-reinforced RIM, and even sheet metals for exterior automobile body parts and other structural applications.

B. PU-Based IPNs

The urethane-based IPN systems, usually composed of a rubbery network (elastomeric urethane) and a glassy network (polyester, polystyrene, polyacrylate, epoxy, etc.), provides a wide spectrum of composite materials. Kim et al. (1976) investigated an IPN composed of a PU (a step-growth reaction) and a polystyrene or poly(methyl methacrylate) (a chain growth reaction). Djomo et al. (1983) and Morin et al. (1983) prepared PU-PMMA SINs. Yoon et al. (1976) reported a series of semi-SINs composed of polyurethane and polyacrylates. Summarized in Table 2.4 is a review of polyurethane-based IPNs dating back to as early as 1969. The review indicates that most research work on polyurethane-based IPNs dealt with the combination of polyurethane with free radical type resins such as polystyrenes, polymethyl methacrylates, polyesters, and other acrylates. Epoxies, ureas, and other condensation type polymers have also been studied. Most IPNs were cast in solution and bulk polymerization. Few of these work apply fast processes (e.g., RIM), except the work done by Nguyen and Suh (1986). In applying polyurethane-based IPNs in reactive polymer processing, research in processibility, moldability, and the property-structure-processing

Table 2.4 A review of PU-based IPN's

<u>2nd Phase</u>	<u>Method</u>	<u>Type</u>	<u>Investigators</u>	<u>Year</u>
Polystyrene	bulk	semi-SIN	Lipatov et al.	1977
Polystyrene	bulk	semi-SIN	Kim et al.	1975
Polystyrene	bulk	semi-SIN	Kaplan & Tschöegl	1975
PMMA	bulk	SIN	Kircher & Menges	1984
PMMA	bulk	semi-SIN	Djome et al.	1983
PMMA	solution	SIN	Kim et al.	1976
PMMA	bulk	seq-IPN	Alien et al.	1973
PMMA	bulk	semi-IPN	Hutchinson	1971
Polyacrylate	bulk	semi-SIN	Yoon et al.	1976
Polyacrylate	solution	semi-SIN	Frisch et al.	1974
Polyacrylate	emulsion	semi-IPN	Klempner	1970
Epoxy	solution	seq-IPN	Frisch et al.	1979
Epoxy	solution	SIN	Frisch et al.	1972
Epoxy	bulk	semi-IPN	Hawkin	1971
Polyester	bulk	SIN	Nguyen & Suh	1986
Polyester	bulk	SIN	Meyer & Mehrenberger	1977
Polyester	solution	semi-SIN	Frisch et al.	1974
Polybutadiene -acrylonitrile	emulsion	semi-IPN	Klempner et al.	1969
Urea and silicone	emulsion	semi-IPN	Klempner	1970

relationship is needed in order to have a better understanding of these composite materials for actual commercial applications.

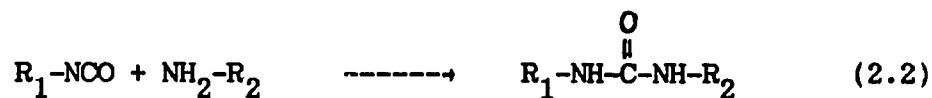
It is necessary to point out here that even in an SIN or a semi-SIN, the two rates of polymerizations and their approach to gelation or gel time may be the same or may be significantly different, depending on the nature of each component and reaction conditions such as temperature. In other words, SINs or semi-SINs also possess a sequential nature. For example, using a reduction/oxidation type initiator (e.g., a combination of methyl ethyl ketone peroxide and cobalt naphthanate) for PU-polyester SINs can promote the polymerization rate of polyester to almost the same as that of polyurethane; while using peroxide only as initiator for polyester delays its polymerization. The length of the delay depends strongly on the reaction temperature.

2.2.4 Polyureas

Despite the overwhelming success of polyurethane RIM in the production of bumpers, fascias, and others in the automotive industries, the generally soft elastomeric polyurethane can not meet various requirements if it is to be expanded to other structural applications. To meet the demands, current research efforts are focusing on the development of improved chemical systems of polyurethanes with faster reaction rate and better performance

properties. Faster reaction leads to reduced demolded time and cycle time. Better performance properties mean more applications of RIM in automotive and non-automotive industries.

The difference between polyurethane and polyurea is the replacement of functional polyol and diol in urethane by triamine and diamine in urea formation. The reaction kinetics of polyureas is a typical step-growth polymerization. This polymerization is generally regarded as an nth order reaction. The detailed chemistry of polyureas can be found elsewhere (Schwartz and Goodman, 1982; Ewen, 1985; Baumann et al., 1986; Nalepa and Eisenbraun, 1987). Basically, a commercial recipe of polyurea RIM includes three ingredients: a diisocyanate, a low molecular weight aromatic diamine, and a high molecular weight aliphatic triamine. The primary reaction that occurs during urea polymerization is



No catalyst is required since amine itself acts as a catalyst for urea reaction. Like the segmented linear polyurethane, polyurea also exhibits phase separation. Here, the hard domains are composed of diisocyanate and aromatic diamine (the chain extender), while the soft domains are composed of diisocyanate and the long chain triamine. In addition to phase separation, the functional triamine also makes polyurea system crosslinked, leading it to a

thermosetting polymer. This results in a very complicated chemical and physical system, rendering itself to a material of high thermal and mechanical properties. The reaction rate of polyurea can be affected by employing different amines, especially the aliphatic amine. It has been found that aliphatic amines can react with diisocyanate much faster than aromatic amines. Therefore, by selecting suitable combination of aliphatic and aromatic amines (Pannone, 1986; Vespoli et al., 1986), the reaction rate of polyurea can be controlled. Major characteristics of polyurea reaction include:

- a. Very fast reaction rate (gel time within 2 seconds).
- b. No catalyst needed.
- c. No postcure required.
- d. High mechanical strength (up to 100,000 psi flexural modulus).

Polyureas are mainly developed for RIM production of automotive fascia and body panels with flexural modulus ranging from 25,000 to 100,000 psi (Ewen, 1985). The success of Pontiac Fiero and the consumer's acceptance of a car with all plastic body have stimulated great demand of high modulus polyurea RIM systems. Compared to polyurethanes, polyureas possess better thermal and mechanical properties. At present, applications of polyureas in RIM

and other reactive polymer processing technologies are still in experimental and developing stage. Some of the material systems are actually not true polyureas, but rather modified polyurethanes which are chain-extended by short chain aromatic diamines. Table 2.5 lists current major suppliers. The achievement of 100,000 psi flexural modulus can be accomplished exclusively by varying the hard segment, which is mainly the aromatic short chain diamine. Also included in Table 2.5 are major suppliers of chain extenders.

Table 2.5 Current suppliers of polyureasA. Polyureas

<u>Company</u>	<u>Isocyanate</u>	<u>Amine</u>	<u>Flow time</u>	<u>Comment</u>
Mobay	Bayflex 110-80 (A)	Bayflex 110-80 (B)	2.5 sec	PU/ Polyurea
Dow	Dow-1305	Dow-1337	1.2 sec	Polyurea
Dow	1616E	XV15081.001	1.5 sec	PU/ Polyurea

B. Chain Extenders of Polyureas

<u>Company</u>	<u>Chain Extender</u>	<u>Molecular Weight</u>
Mobay	DETDA	178
Air Product	TBTDA	178
Du Pont	Dytek A	210
Allied Signal	Unilink 4100	---
	Unilink 4200	---
Ethyl	Ethacure 300	214

DETDA: Diethyl toluene diamine.

TBTDA: Tert-butyl toluene diamine.

CHAPTER III

PROCESSING OF IPN

SYNOPSIS

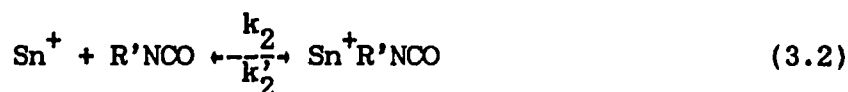
The kinetics and heat transfer during curing of a polyurethane-polyester interpenetrating polymer network (IPN) were investigated experimentally and theoretically. A model based on the additivity rule of constituent ingredients was used to predict the IPN's reaction kinetics and heat transfer. Compared with the experimental results measured by the differential scanning calorimetry, the adiabatic temperature rise during reaction injection molding, and the temperature profiles measured during a casting process, the prediction showed some deviations. This suggested that reaction interactions existed in the polymerization system.

3.1 PREVIOUS WORK ON IPN PROCESSING

3.1.1 KINETIC STUDIES OF POLYURETHANE REACTIONS

Polyurethane reaction is a typical step-growth polymerization. To date, kinetics of catalyzed polyurethane

reactions in the absence of solvent is still poorly understood. In particular, whether domain formation as well as gelation can affect the kinetics; and whether crosslink density has any effect on the kinetics are still questions remained unanswered (Ferber et al., 1984; Ferger and Macknight, 1985). The kinetics of polyurethane can further be complicated if reversible reaction (equilibrium) is considered (Stenile et al., 1980). Richter and Macosko (1978) proposed a Michaelis-Menten type kinetic mechanism for an organotin catalyzed urethane polymerization.



where SnOOCR is the organotin catalyst, k_1 , k_1' , k_2 , and k_2' are rate constants for catalyst, and k_3 is the rate constant for urethane formation. This mechanism can be summarized as a hyperbolic kinetic model as equation (3.4).

$$\frac{-dC}{dt} = \frac{k_1 C_{\text{NCO}} C_{\text{OH}} C_{\text{Sn}^+}}{1 + K C_{\text{OH}}} \quad (3.4)$$

where K is a lumpsummed parameter of k_i 's ($i = 1$ and 2). The model seems to be consistent with the experimental data. However, the overall order of reaction and the effect of catalyst concentration were found to change with varying temperatures.

In most theoretical studies of the curing step in the reactive polymer processing (Broyer and Macosko, 1976; Lee and Macosko, 1980; Castro et al., 1982; Castro and Macosko, 1982), the urethane reaction was modeled as a simple n th order reaction with an Arrhenius temperature dependence:

$$\frac{-dC}{dt} = A_0 \exp(-E/RT) C^n \quad (3.5)$$

where dC/dt is the reaction rate, A_0 is the frequency coefficient, E is the activation energy, n is the reaction order, and C is the concentration of functional group. The reaction order n varies from 1.5 to 3.0, depending on the catalyst level and may change at different conversion levels.

Making kinetic measurements during the reactive polymer processing is inherently difficult. Resin solidification due to chemical crosslinking, domain formation or crystallization adds complexity to the measurements. In addition, high polymerization temperature and pressure and fast reaction rate further complicate the task.

Since polymerization in reactive polymer processing is fast and highly exothermic, one of the simplest ways to follow overall conversion and reaction kinetics is to monitor the heat generation in the adiabatic condition. Several researchers have used the adiabatic temperature rise method, together with linear (Lipshitz and Macosko, 1977; Lee and Macosko, 1980; Richter and Macosko, 1980; Rojas et al., 1981; Camargo et al., 1983) or non-linear (Casey et al., 1982) regression method to predict the kinetic parameters for thermosetting polymers like polyurethane.

For slower reactions or systems which are not reactive at room temperature but are activated at elevated temperatures, differential scanning calorimetry (DSC) has been used extensively in the kinetic measurement (Kamal and Sourour, 1973; Barone and Caulk, 1979; Lee, 1981; Prime, 1982; Han and Lem, 1983, 1984; Osinski et al., 1983, 1985; Huang and Lee, 1985; Macosko and Lee, 1985; Fan and Lee, 1986; Fan et al., 1986; Stevenson, 1986; Huang et al., 1987). DSC and adiabatic temperature rise methods have the advantages of simplicity, less limitations, and the capacity to yield simultaneously information regarding kinetics, energetics, and thermal properties. However, both methods only measure overall heat release and cannot differentiate between multiple reactions or between reaction and physical changes such as crystallinity. They are also less sensitive at high conversions. The kinetic information

obtained tends to be less accurate due to their empiricism and lack of details in the kinetic sense.

Spectroscopic methods like infrared, ultraviolet or nuclear magnetic resonance can be much more specific to identify particular chemical bond formation. Recent development of computer-assisted instrument like FTIR has enabled accurate monitoring of fast and complex polymerizations (Mones and Morgan, 1981; Camargo et al., 1982; Ishida and Scott, 1986a and 1986b; Yang and Lee, 1987). Ishida and Scott (1986a and 1986b) have successfully interfaced a small RIM machine with an FTIR to follow the nylon-6 reaction and a polyurethane-acrylate reaction. The disadvantages of spectroscopic methods are that the instrument is more expensive and the data analysis are more time consuming compared to the thermal methods.

3.1.2 HEAT TRANSFER STUDIES OF POLYURETHANE FORMATION IN REACTIVE PROCESSING

Heat transfer of polyurethane formation in reactive processing was intensively studied by several researchers. The first study on the curing and heat transfer in polyurethane reaction molding was made by Broyer and Macosko (1976, 1978). An nth order reaction kinetics was assumed. Their model predicted the temperature profiles near the mold center reasonably well. Model predictions of temperature near the wall were too low due to failure of the

isothermal wall assumption. Domine and Gogos also developed a computer model to simulate the filling and curing steps of RIM process (Domine and Gogos, 1980). However, there was no experimental evidence to support this model. Lee and Macosko (1980) proposed a more realistic heat transfer model of RIM curing. Their model included the heat generation of a single-phase polymerization, heat build-up in the mold, and heat transfer to the temperature-control fluid. They studied both metal (steel and aluminum) and plastic molds with a wide range of mold wall temperatures. Measurements of temperature profiles in the polymer slab and mold wall compared well to the model prediction. Their results indicated that both mold wall temperature and mold material were important for the curing step. The curing and heat transfer in the RIM process was also analyzed by Castro and coworkers (Castro et al., 1980; Castro, 1985) and Osinski et al. (1985). In addition to the experimental measurement and numerical analysis, they mentioned several dimensionless parameters appearing explicitly in the balance equations, which tended to govern the curing behavior. These numbers include the Damkoehler number, Da , the dimensionless initial and wall temperatures, T_o^* and T_w^* , and the dimensionless activation energy, $E^* = E/RT_{ad}$. Following the analysis method developed by Castro and Macosko (1982), Estevez and Castro (1984) applied the dimensionless numbers mentioned above to analyze some phenomena in RIM process such as premature gelling, maximum temperature rise, and the control of demold time. The

results are presented as a set of graphs correlated using the relevant dimensionless groups of the process.

Most work on curing and heat transfer in RIM process is based on polyurethane systems. There are also a few studies associated with non-urethane systems. These include kinetic studies of the activated anionic polymerization of ϵ -caprolactam (Lin et al., 1985), material and process design of nylon-6 RIM polymerization (Sibal et al., 1984), modelling of the heat transfer process and reaction kinetics of urethane-modified isocyanate RIM system (Vespoli and Alberino, 1985), and moldability studies of epoxy in reactive polymer processing (Manziona and Osinski, 1984).

3.1.3 KINETIC STUDIES OF UNSATURATED POLYESTER REACTIONS

The reaction of unsaturated polyester resin is a free radical chain growth copolymerization between the styrene monomer and the unsaturated polyester molecule. The free radical chain copolymerization have been studied by many researchers (Bamford et al., 1958; Braudrup and Immergut, 1967; Odian, 1970). Several kinetic mechanisms have been proposed to predict the cure of SMC. Horie et al. (1968, 1969, 1970) indicated that most of the reaction was diffusion-controlled and the final conversion was never complete. The former was confirmed by other researchers (Galina, 1980); the latter was supported by infrared study. For reaction

kinetics, a simple kinetic model was used by Kamal et al. (1973), Pusatcioglu et al. (1979), and Han and Lem (1983, 1984) to empirically fit the reaction rate profiles obtained from DSC data. The empirical equation they used is:

$$\frac{d\alpha}{dt} = (K_1 + K_2\alpha)^m(1-\alpha)^n \quad (3.6)$$

where $d\alpha/dt$ is the reaction rate, α is the conversion, K_1 , K_2 , m , and n are four unknown parameters. This model fitted the experimental data well but lacked physical meaning for free radical polymerization.

Kuo et al. (1984) proposed methods for the determination of apparent rate constants of radical chain copolymerization. In his approach, the kinetics of radical-chain copolymerization was reduced to a pseudo-homopolymerization kinetics by introducing a single average rate constant. However, as Kuo claimed, the model was only good for chemical-controlled processes.

Stevenson (1980, 1982) and Lee (1981) developed a series of kinetic models for free radical copolymerizations based on the usually accepted reaction mechanism. Their models fitted the reaction rate profile fairly well. Unlike the empirical models (Kamal et al., 1973; Pusatcioglu et al., 1979; Han and Lem, 1983, 1984), these mechanistic models not only provided necessary kinetic information for the heat transfer modelling, but also elucidated the

functions of initiators, inhibitor, and monomers in the reaction up to the medium conversion region. However, as pointed out by Lee (1981), several important phenomena such as the incomplete conversion for isothermal cure and apparent diffusion control in the later stage of the curing reaction have not been considered.

To address the gel effect in chain growth polymerization, Bissenberger and Capinpin (1974, 1976) proposed kinetic models to analyze the effects of reaction parameters through computer studies. An empirical term was added to their model to account for the gel effect which caused a second exothermic peak from DSC measurement in styrene polymerization. The role of various dimensionless parameters in predicting thermal behavior was discussed. Chiu et al. (1983) took diffusion effect into account by adopting the free volume concept. Huang and Lee (1985) proposed a kinetic model which accounted not only the kinetic effect of the free radical copolymerization, but also the diffusion effect and the glass transition effect of the sheet molding compound (SMC). The model can be expressed by a single equation as:

$$\frac{d\theta}{dt} = (1-\beta) / \left\{ \frac{1}{[\pi_1 + (\pi_2 \pi_3)^2]^{1/2}} \right\} + \pi_4 \quad (3.7)$$

where π_i 's ($i = 1 \sim 4$) are parameters accounting for the kinetic and diffusion effect on propagation and termination respectively, and β

is the fractional conversion of unsaturated polyester reaction. Each parameter can be experimentally determined by DSC. Although the model is physically meaningful, it may not be easily applied to practical uses due to its complexity.

3.1.4. HEAT TRANSFER STUDIES OF STYRENE-UNSATURATED POLYESTER REACTION IN REACTIVE PROCESSING

Heat transfer analysis of free radical copolymerization, especially SMC, has been carried out by several researchers experimentally or theoretically. Barone and Caulk (1979) and Pusatcioglu et al. (1980) adopted the kinetic model developed by Kamal et al. (1973) to study the heat transfer in SMC molding. Although the results were satisfactory, the kinetic model used seemed to be inconsistent with the well known free radical reaction mechanism as discussed before. The heat flow during SMC molding was investigated by Herman (1978) and a method for designing an appropriate mold heating system was also proposed. Mallick and Raghupathi (1979) studied the effect of cure cycle on mechanical properties and suggested that preheating would offer advantages of reducing both mold cycle time and the thermal gradient. The variation of thermal conductivity and specific heat of a general-purpose unsaturated polyester resin during curing was investigated experimentally by Pusatcioglu et al. (1979). Their results indicated

that both thermal conductivity and specific heat of the cured unsaturated polyester increased nearly linearly with increasing temperature. The effect of the degree of cure on thermal properties during the early stage of cure was also investigated in their study.

Stevenson (1982) and Lee (1981) applied their kinetic models to investigate the heat transfer in the compression molded SMC. Without the consideration of diffusion effect during polymerization, the model predicted temperature profiles inside SMC parts during molding fairly well. However, model prediction of high conversion data was not satisfactory, possibly due to the fact that the propagation step is strongly influenced by the diffusion after the maximum exotherm, an important factor which was not considered in their kinetic model. The cure time of different part thickness, mold temperature, and initiator concentration were also predicted based on their kinetic models.

Stevenson and Lee's kinetic models were extended by Fan and Lee (1986) to a multiple initiator SMC system. The predictions compared well with experimental results except the limiting conversion. A set of predictive parameters were proposed from the model as guidelines for the optimal molding of SMC. In their studies, several moldability diagrams were also constructed which could easily be used to design the optimal SMC recipe for a given set of processing conditions.

Stevenson (1986) also proposed methods for generalizing the commonly accepted kinetic mechanism for free radical copolymerization. The approach simplified the kinetic models by various assumptions and restrictions to give several practical and realistic models for the simulation of industrial molding.

3.1.5 INTERPENETRATING POLYMER NETWORKS (IPNs)

Most research efforts on IPNs have been on synthesis method, morphology, and mechanical testings (Allen, et al., 1973; Frisch, et al., 1974, 1975; Kim, et al., 1976; Rosovizky, et al., 1979; Kircher, et al., 1984). Seldom have the processing aspects, nor the kinetic mechanism and heat transfer considerations been explored. Nguyen and Suh (1986) designed a high pressure RIM to study the processibility of polyurethane-polyester and other IPNs in RIM. In the processing aspect, they emphasized the mechanical design of a RIM machine, including a high pressure set-up, a multi-stage cascade impingement mixing, and the effect of impingement mixing on heat transfer. In the material aspect, they studied the effect of catalyst level and Reynolds number on the change of glass transition temperature of IPNs using dynamic mechanical analysis and by measuring other properties such as heat sag.

In this study, experimental and theoretical investigations of kinetics and heat transfer of polyurethane-polyester IPNs are

attempted. Experimentally, a slow casting process and a fast RIM process are studied and compared. Theoretically, a model based on the linear combination of the constituent components of IPN is proposed to simulate the kinetics and heat transfer of IPN reaction. Comparisons between experimental data and theoretical modelling are made and the differences are discussed.

3.2 EXPERIMENTAL

3.2.1 MATERIALS

A. Materials Used for DSC Measurement, Adiabatic Temperature Rise Measurement, and Casting Process.

The ingredients of the polyurethane-polyester IPN used in this study are listed in Table 3.1. The recipe can be divided into two parts, namely, a polyurethane and a polyester. The polyurethane chosen for this study consists of a soft segment based on a poly(ϵ -caprolactone diol) (TONE-0240, Union Carbide) and a hard segment based on a liquid form of 4,4'-diphenyl methane diisocyanate (MDI)(143-L, Dow Chemical Company) chain extended with 1,4-butanediol (BDO, Aldrich Chemical Company). MDI was degassed and demoiistured at room temperature for 20 minutes to remove water and

Table 3.1 Materials used in IPNs' study

<u>Ingredients</u>	<u>Percentage</u>
<u>Polyurethane (50%) in IPN</u>	<u>Part in Polyurethane</u>
MDI (Dow 143L)	41
Polyol (Union Carbide TONE-0240)	48
Butanediol (Aldrich BDO)	11
Catalyst (M&T Chemical, T-12)	0.033
<u>Polyester (50%) in IPN</u>	<u>Part in Polyester</u>
65% unsaturated polyester in styrene (OCF P-325)	67
Styrene	33
Initiator (Lucidol PDO)	1.38

air. The treated MDI solution was then filtered under vacuum. TONE-0240 is a long chain diol with a number average molecular weight of 2,000 and is a solid at room temperature. A heating plate was used to melt this material. BDO is a low molecular weight diol with a viscosity slightly higher than that of water. The combination of the molten TONE-0240 and BDO was degassed for 40 minutes at 60 °C using a heating plate and vacuum to remove water and air. The molar ratio of TONE-0240/MDI/BDO was set at 1/6/5 which is a typical recipe for RIM elastomers. The catalyst, dibutyltin dilaurate (T-12, M&T Chemical) was used as received. The amount of T-12 was 0.033% by volume of resin for a reasonable reaction time so that the kinetic study by DSC and the sample preparation for casting process was possible.

For the polyester part, styrene was used as a crosslinking agent for the unsaturated polyester resin (P-325, OCF) which is a 1:1 propylene-maleate polyester combined with 35% by weight of styrene. Styrene was not freed of inhibitor in all cases. Initiator PDO (Lucidol) was used as received. PDO, t-butyl peroxy-2-ethyl hexanoate, is a diluted high temperature initiator. The amount of PDO used was 1.38% by volume of polyester resin. The molar ratio of styrene to the double bonds of unsaturated polyester was adjusted to 2:1.

The ratio of polyurethane to polyester was fixed at 50/50 by weight for most IPNs prepared. In order to study the effect of compound composition on kinetics and heat transfer of IPN by DSC

measurement and in casting process, the ratio of polyurethane/polyester was also varied as 100/0, 75/25, 50/50, 25/75, and 0/100.

B. Materials Used for Moldability Test

To test the moldability of polyurethane-polyester IPNs, several commercial resins were tested. These resins include an unsaturated polyester from Ashland Chemical (Q6585), a triol (Union Carbide TONE-0300), and an isocyanate (BASF, M5030). Ashland Q6585 and BASF M5030 were used as received. The ratio of polyurethane/polyester was set at 50/50. Pretreatment of TONE-0300 was the same as TONE-0240. The amounts of T-12 and PDO were set at 0.5% by volume of polyurethane resin and 2.2% by volume of polyester resin respectively. A low temperature reduction/oxidation type initiator was also used for polyester reaction in the moldability test. This initiator was a combination of methyl ethyl ketone peroxide (MEKP) and cobalt naphthanate (Co-8).

C. Materials Used for RIM

In the reaction injection molding process, the amount of catalyst T-12 used for polyurethane was 0.1% by volume of polyurethane resin and the amount of PDO for polyester resin remained at 1.38% by volume of polyester resin. The molar ratio of TONE 0240/ MDI/BDO was set at 1/6/5. The polyester used was Q6585

from Ashland Chemical Company. The ratios of polyurethane/polyester chosen were 75/25 and 50/50.

3.2.2 INSTRUMENTATION AND EXPERIMENTAL PROCEDURE

A. Moldability Test of IPNs

Prior to the kinetics and heat transfer studies of IPNs, a series of tests were conducted in an effort to identify the processibility of IPNs. In the moldability test, the ingredients of IPN were mixed in a suction flask with a mechanical stirrer at 50 rpm. The temperature rise vs. time curve of the reacting system was recorded. For the thermal activated polyester reaction, the ingredients of polyester resin was preheated to 55 °C for MEKP/Co-8 initiated polyester and 95 °C for PDO-initiated polyester. These temperatures were chosen to provide enough heat for thermally induced polyester reaction.

B. Kinetic Measurement by DSC

A Perkin-Elmer differential scanning calorimeter (DSC-2C) was employed to follow the reaction course. Due to the volatile nature of styrene, all samples were prepared in volatile sample pans which are capable of withstanding at least 30 psia internal pressure after sealing. Ingredients of each sample were weighed in a balance (Mettler, Model-80) with a total weight in the range of 20-25 gram.

These ingredients were then thoroughly mixed to obtain a homogeneous solution. About 15 mg of the sample was then transferred to the sample pan. A dry nitrogen supply was employed to purge the oxygen and moisture that might exist inside the sample holder. An empty pan with the weight equivalent to that of the sample pan was put in the reference pan holder. The exothermic rate versus time was carried out in the isothermal mode. To check if residual activity existed after an isothermal run, a scanning run was performed from room temperature to 237 °C, which is far above the glass transition temperature of both polyurethane and polyester. This scanning run ensured the completion of the polymerization. A second scanning run was conducted immediately after the first scanning to determine the base line. The procedure of DSC experiment is schematically illustrated in Figure 3.1 for a typical polyester reaction.

The thermal data measured during the reaction were converted to the fractional conversion results as a function of time. Detailed information about DSC data treatment can be found in a previous work (Hsu and Lee, 1985). Several assumptions are made for the calculations. First, there is only one reaction taking place at a time and, second, the thermal properties of the system are assumed unchanged during the reaction. The kinetic parameters and the reaction exotherm of polyester reaction were determined by DSC too. Detailed procedure is explained in the section of Parameter Estimation.

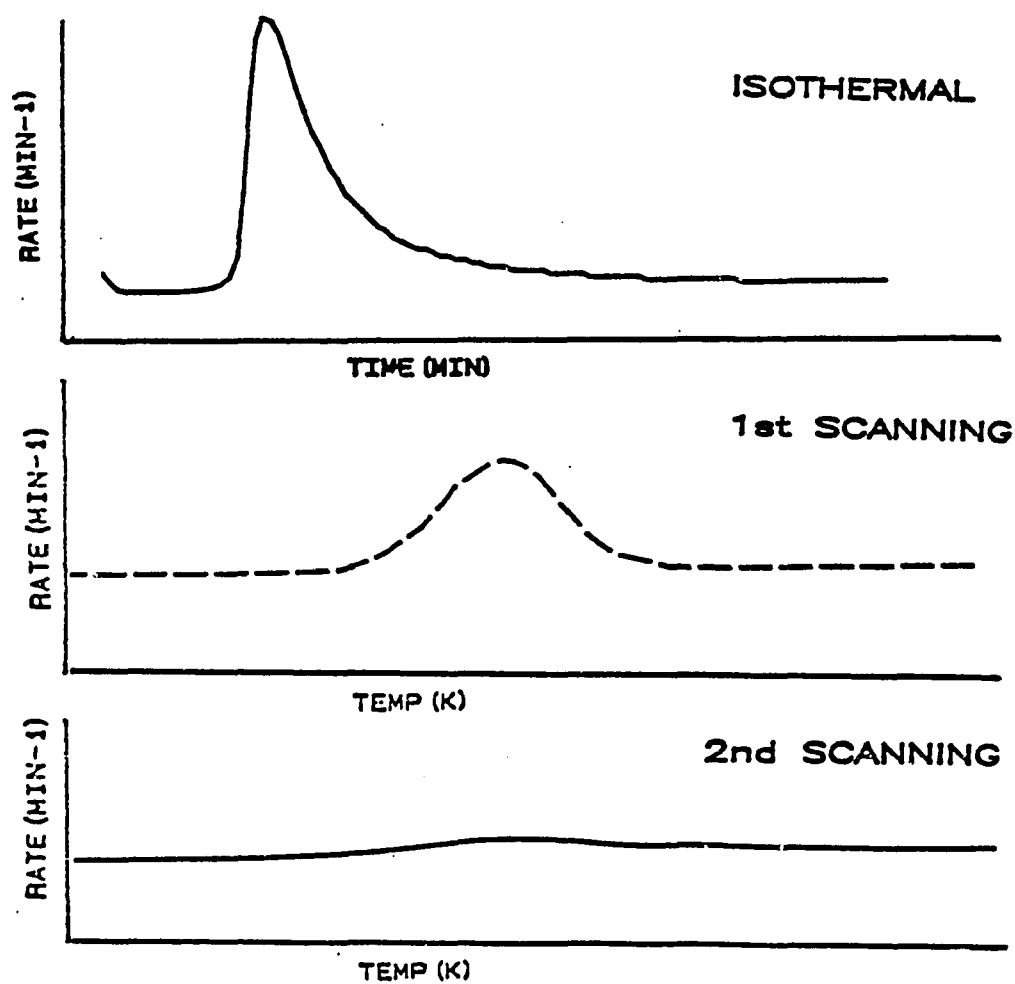


Figure 3.1 Procedure for DSC experiment, (A) isothermal run to determine the reaction rate, (B) 1st scanning to determine the residual activity, and (C) 2nd scanning run to determine the base line.

C. Kinetic Measurement by Adiabatic Temperature Rise Method.

For catalyzed urethane reaction, the conventional analytical tools are not able to measure the reaction rate because the reaction is too fast to follow. A very useful method to follow the reaction course is the measurement of adiabatic temperature rise (Lipshitz and Macosko, 1977; Lee and Macosko, 1980; Richter and Macosko, 1980). The kinetic parameters and the heat of reaction of polyurethane reaction were determined using the adiabatic temperature rise method. A paper cup was used as the reactor with a thermocouple inserted in the center and about 1 cm from the bottom of the paper cup to measure the temperature rise. To ensure the reaction was adiabatic, 0.1% by volume of catalyst T-12 was added to the reactive system. It took only a few seconds for polyurethane to polymerize. The reaction was so fast that the error due to adiabatic assumption was negligible. The measured temperature rise, along with the density and heat capacity, were used to calculate the heat of polyurethane reaction, assuming constant density and heat capacity. A mechanical stirrer was used to provide thorough mixing of the material. After the center temperature reached maximum, it cooled down at a rate less than 0.2 °C/min.

D. Reaction Injection Molding

A laboratory scale RIM machine was constructed to carry out the experimental work (Nelson, 1987). Figure 3.2 shows the machine

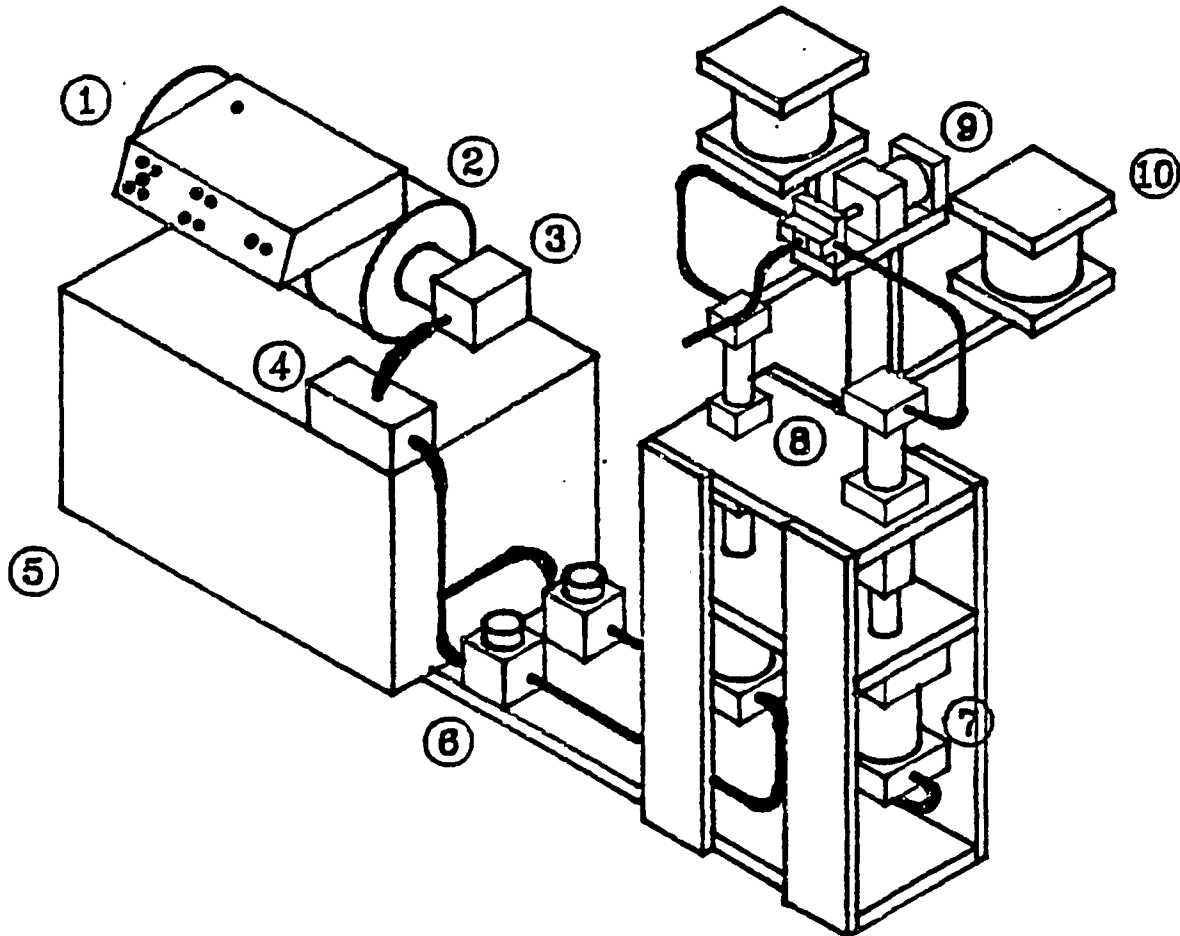


Figure 3.2 Schematic diagram showing the laboratory scale RIM machine. (1) control panel, (2) 7-1/2 Hp motor, (3) hydraulic pump, (4) directional solenoid, (5) hydraulic reservoir, (6) flow control valves, (7) drive cylinders, (8) material cylinders (9) mixhead, (10) material storage tanks.

design. Both the hydraulic drive system (item 1 to 7) and the material mixing system (items 8 to 10) are attached to a common support frame. The hydraulic drive unit consists of a 7-1/2 horsepower variable flow hydraulic pump and a 10 gallon hydraulic oil reservoir. A three position directional solenoid valve is used to control the flow direction. Flow rates into the individual drive cylinders are controlled by uni-directional flow control valves with load pressure compensation. The drive cylinders for this RIM machine are 8.255 cms (3-1/4 inch) diameter hydraulic cylinders with 7.62 cms (3 inch) stroke length. These cylinders are connected directly to the material cylinders which have a smaller diameter but with the same stroke length. This machine is capable of delivering up to 250 ml of liquid at rates up to 125 ml/sec and a maximum pressure of 2,000 psi in the material cylinder. Using a 0.635 cm (1/4 inch) diameter mixing chamber with 0.0794 cm (1/32 inch) diameter nozzles, these flow rates are able to produce nozzle Reynolds numbers (Re) in the order of 300 to 500 for the reaction systems explored in this work. The machine's reasonably small size allows it to be portable and can be interfaced with other analytical devices. More detailed description of this machine can be found elsewhere (Nelson, 1987).

To test the mixing and curing characteristics of the reaction systems, reactants were mixed by impingement mixing in the RIM machine and injected into an adiabatic reactor (i.e., an insulated paper cup). Adiabatic temperature vs. time was recorded

for mixtures produced. For IPN reactions, the initial material temperature was set at 55 °C. The high exotherm released from polyurethane can be used to trigger the polymerization of polyester.

E. Casting

To simulate slow processes in reactive polymer processing such as resin transfer molding (RTM) and pultrusion processes, a casting set-up was designed to study the heat transfer of polyurethane-polyester IPNs. A glass tube with inner diameter 2.25 cm and outer diameter 2.45 cm was used for the casting experiment (see Figure 3.3). The monomer mixture was thoroughly mixed before pouring into the reactor. IPN components were first mixed in a suction flask by a magnetic stirrer until no bubble was observed. This bubble-free mixture was then transported to the casting tube. A rubber stopper with two thermocouples passing through it was provided to seal tightly the casting tube in order to prevent any volatile loss of styrene monomer at high temperatures. Once the IPN mixture was in the tube, polymerization was allowed to proceed and the temperature profiles were recorded. One thermocouple was positioned near the center and the other near the wall to measure the temperature profile across the tube. The reactor was set in a constant temperature bath using aqueous ethylene glycol solution as heating/cooling medium. A mechanical stirrer was inserted in the bath to maintain homogeneous heating/cooling effect. Deviation of

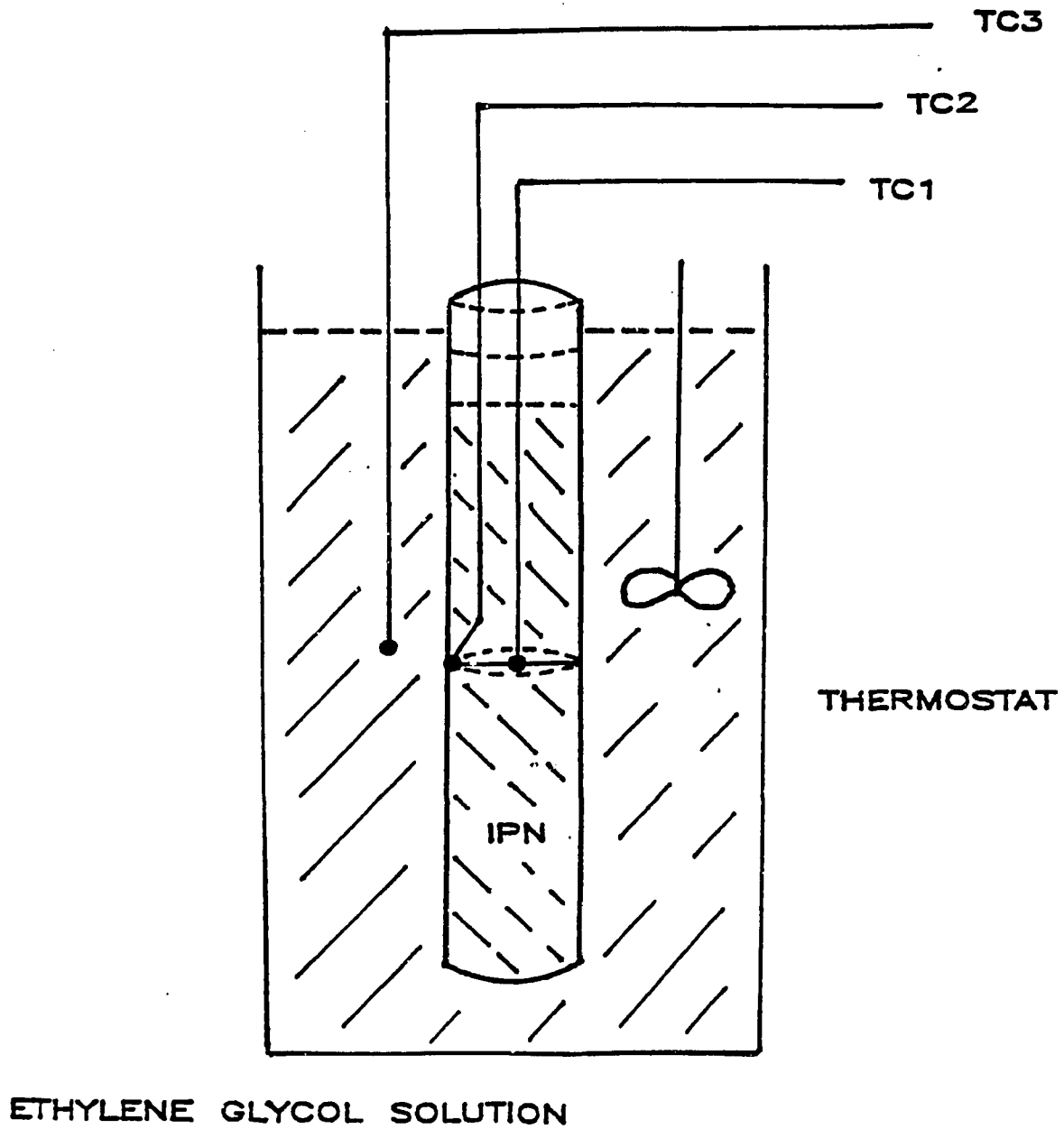


Figure 3.3 Schematic diagram of casting set-up.

bath temperature from set point was within 1%. Two casting temperatures of 80 °C and 120 °C were used.

F. FTIR

To check if there was residual activity in the cast IPN samples, a Fourier transform infrared spectroscopy (FTIR) (Nicolet, Model 20-DX) with a resolution of 4 cm^{-1} was employed. The cast sample from casting experiment was ground into powder (Cheever, 1978) using a grinder. The ground powder was then mixed and diluted with potassium bromide (KBr) powder, which is infrared inactive and transparent. About 10 mg IPN sample was diluted with 400 mg KBr. The mixture was then put into a Perkin-Elmer pellet-making device under a press with pressures up to 1,000 psi. A transparent thin KBr pellet (ca. 0.05 cm) of 1.3 cm diameter was obtained and was analyzed by FTIR at room temperature. An averaged spectrum was obtained with 10 scans.

3.3. RESULTS AND DISCUSSIONS

The detailed reaction mechanism of polyurethane-polyester IPN is schematically described in Figure 3.4. The long chains represent unsaturated polyester molecules which are prepolymers with molecular weight ranging from 500 to 3,000 and C=C bonds ranging

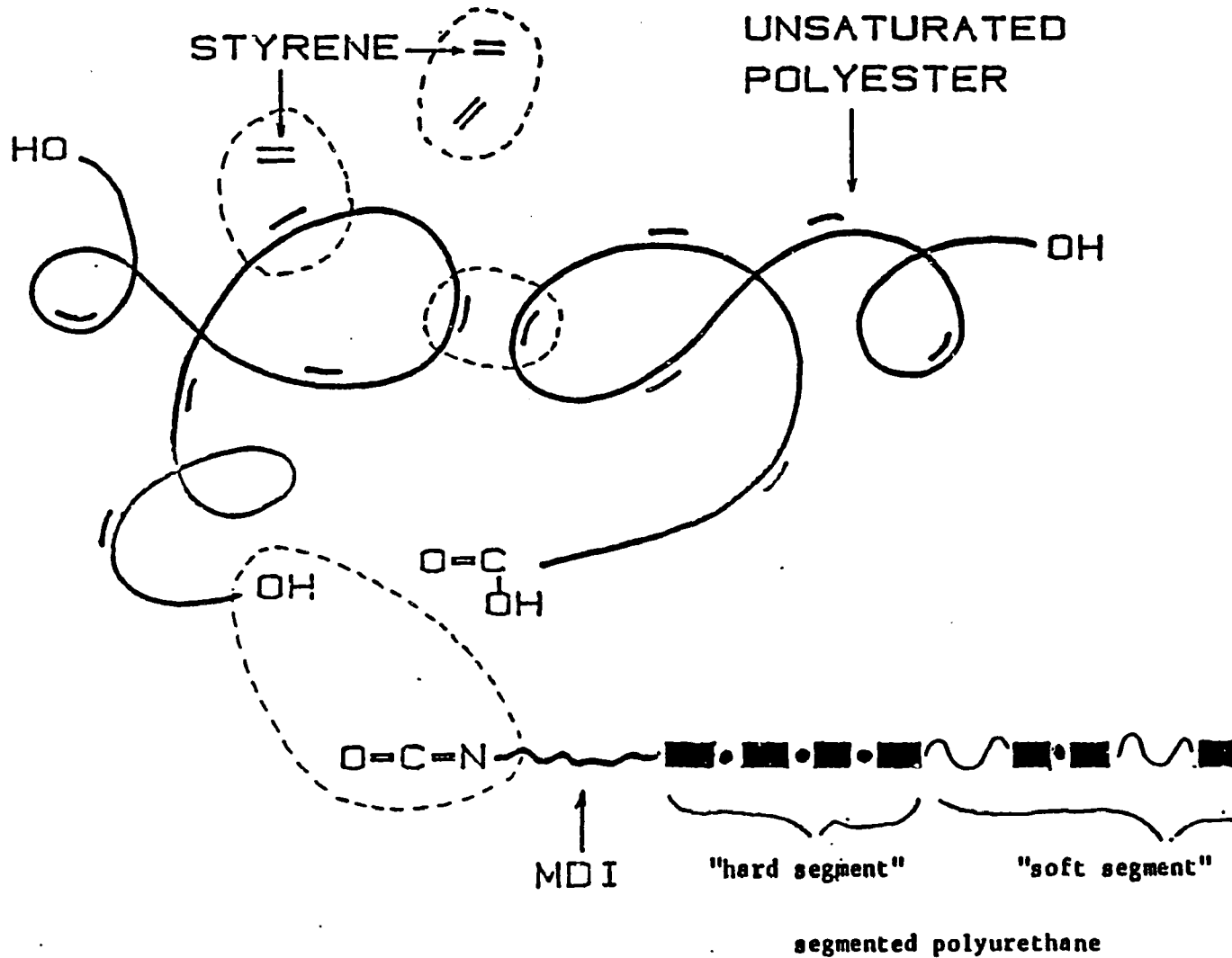


Figure 3.4 Schematic diagram showing the reaction mechanism of PU/PES IPN.

from 6 to 10 per molecule. Styrene monomer serves as a crosslinking agent to link C=C bonds on the adjacent polyester molecules.

Isocyanate reacts with polyols and diols to form a urethane network. Grafting between the two networks may occur through the reaction of isocyanate groups and hydroxyl or carboxyl groups at the end of polyester molecules. Such a multiphase system may be considered as a grafted IPN.

3.3.1 MOLDABILITY TEST

The dual reactions in an IPN system offer some advantages in processing. For example, the addition of usually less viscous chain growth type resins to the urethane material can reduce the resin viscosity and, consequently, to facilitate the mold filling. Furthermore, a mixing-activated step-growth polymerization can be utilized as an internal heat generator to initiate the polymerization of a thermally-activated chain growth polymerization. Here, one has to be sure that the heat released from the first reaction is large enough to trigger the second reaction. This imposes a constraint on the material selection of reaction pair in an IPN system. Figure 3.5 shows the adiabatic temperature rise vs. time curves of two polyurethanes and one polyester resin mentioned in Section 3.2.1. For the polyester resin, the high-temperature initiator PDO requires a temperature of about 100 °C to start the

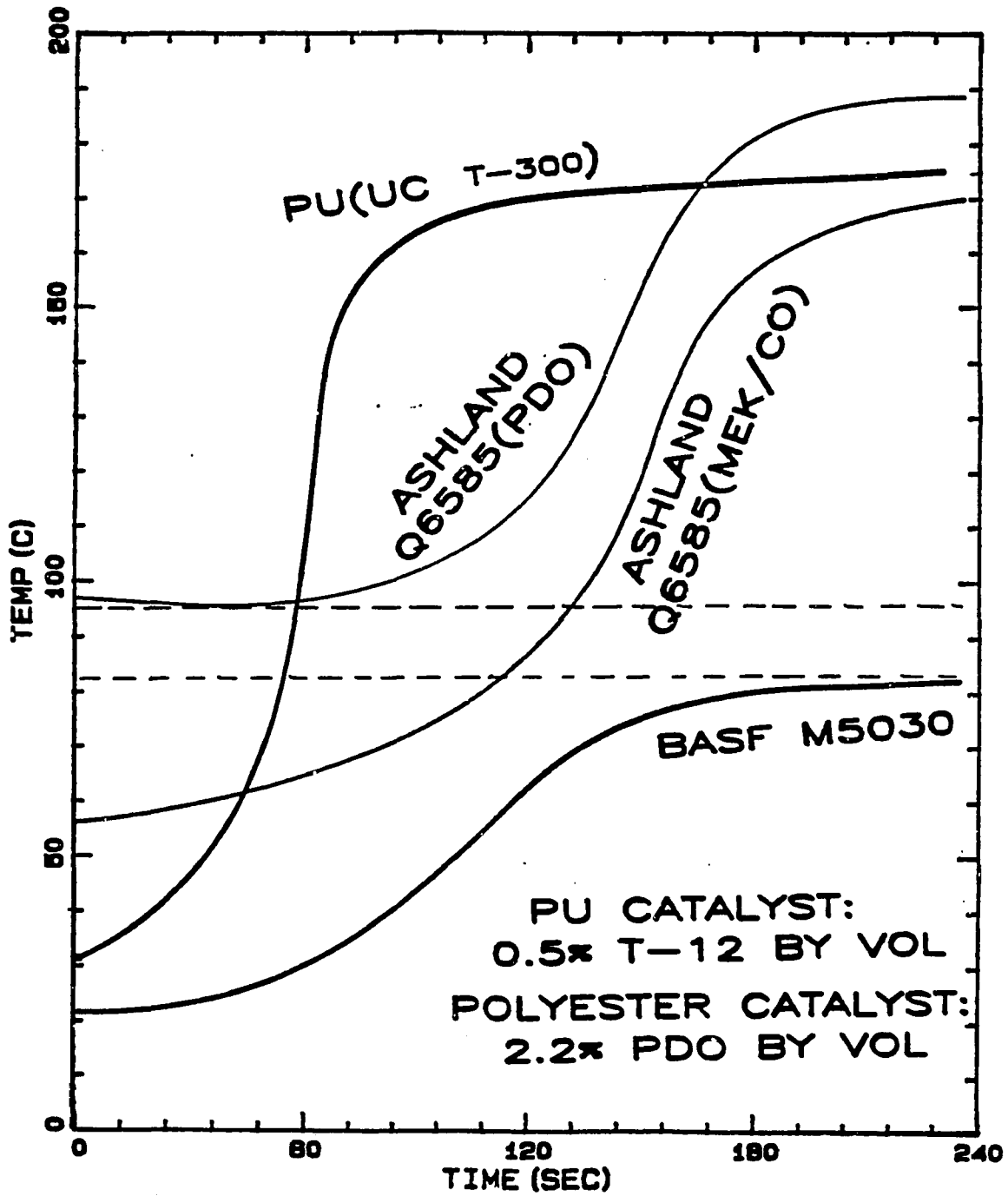


Figure 3.5 Adiabatic temperature rise vs. time of two polyurethanes and one polyester resin.

reaction, while the MEKP/Co-8 initiator may start the reaction at a much lower temperature. As shown in Figure 3.5, the crosslinked polyurethane (Union Carbide TONE-0300) is much more exothermic than the BASF urethane. For a low exothermic polyurethane, one needs to select a low-temperature initiator for the polyester reaction in order to reduce the curing temperature of polyester. Figure 3.6 demonstrates how the material selection can affect the IPN reaction. The results showed that the reaction exotherm of polyurethane (BASF M5030) was able to activate polyester reaction when MEKP and cobalt naphthanate were used as initiator. In the adiabatic temperature rise curve of IPN, the first temperature rise is due to the urethane reaction exotherm, while the second temperature rise is due to the polyester reaction exotherm. When PDO was used as initiator, the adiabatic temperature rise of urethane reaction was apparently not high enough to initiate the polyester reaction. One remedy is to increase the molding temperature for such systems if PDO is to be used.

3.3.2 KINETIC MEASUREMENT OF IPNS BY DSC

Figure 3.7 shows rate profiles of typical polyurethane and polyesters reactions in DSC isothermal mode. In general, the reaction of polyurethane (a step growth type) starts immediately after mixing. The maximum reaction rate happens at the very

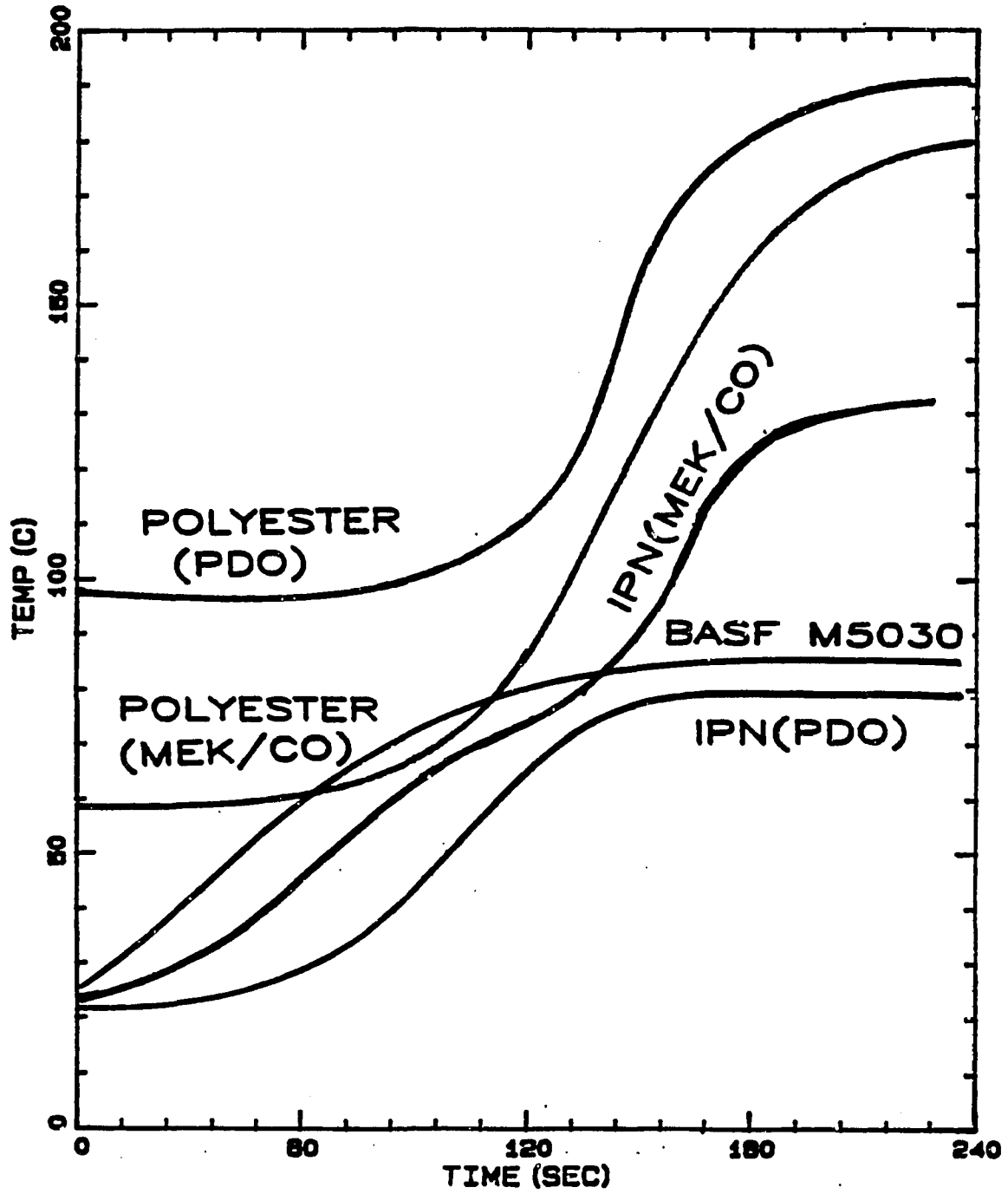


Figure 3.6 Adiabatic temperature rises of PU/PES IPNs using different initiators for polyester resin.

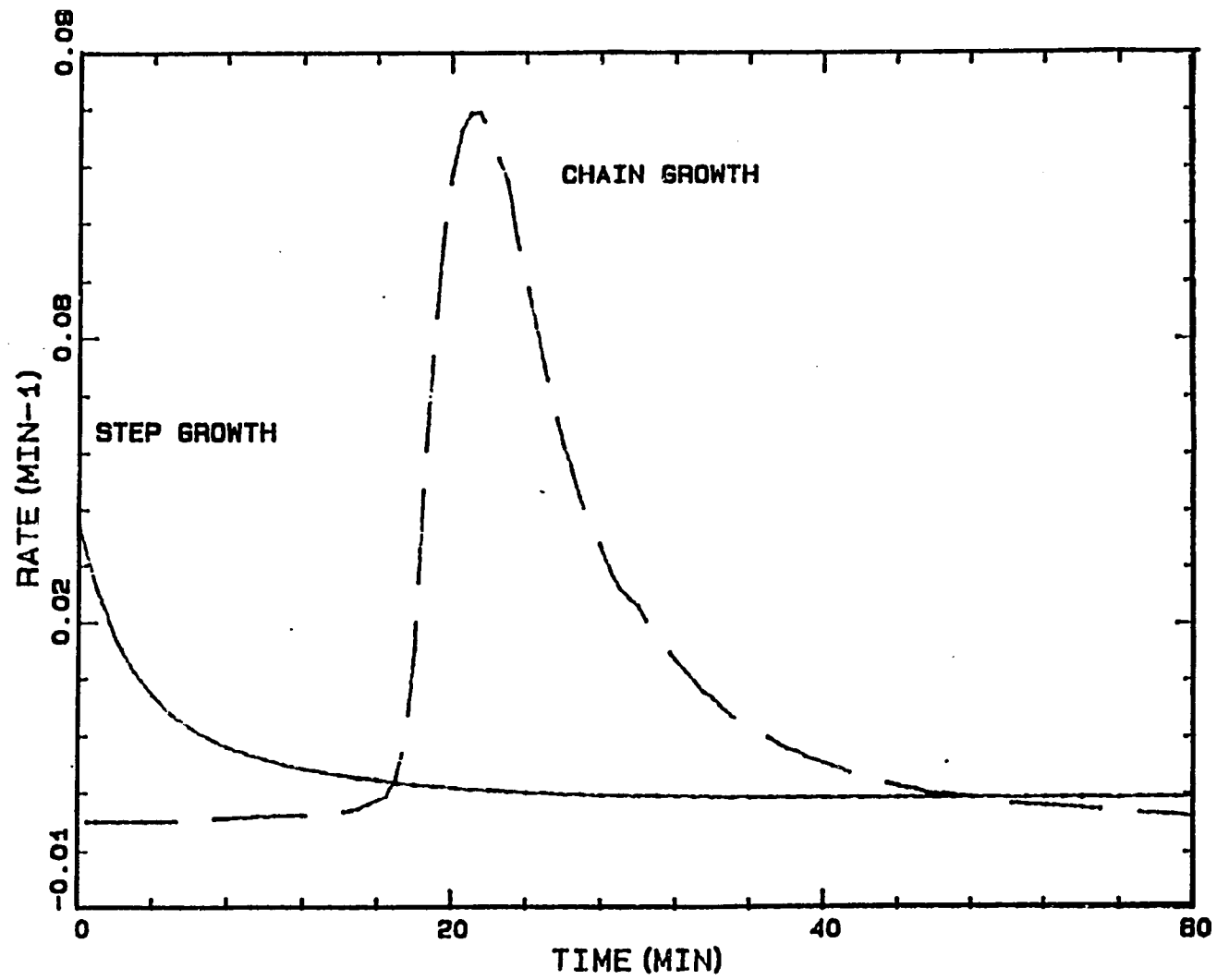


Figure 3.7 Chain growth and step growth polymerization measured by DSC isothermal mode.

beginning of polymerization. On the other hand, the reaction of styrene-unsaturated polyester (a free radical type) starts after an induction period. The initial reaction is relatively slow and then reaches a maximum exothermic rate. The induction time, t_z , and the time to reach the maximum exotherm, t_m , are temperature-dependent.

Figure 3.8 illustrates the compositional effect on the polyurethane-polyester IPN reaction measured by DSC. Due to different reaction mechanism (i.e., polyurethane is mixing-activated, while styrene-unsaturated polyester is often thermally activated), urethane polymerization always occurs in a condition where polyester phase is either unreacted or only partially reacted, which resembles a polyurethane solution polymerization with polyester resin serving as a solvent. On the other hand, styrene-unsaturated polyester polymerization often occurs in a condition where polyurethane phase is either totally or partially reacted, which means most polyester reaction occurs in the solid state.

Qualitatively speaking, while polyurethane reaction remained almost the same, increasing polyurethane content had a great effect on styrene-unsaturated polyester reaction. When the polyurethane content was increased, not only did polyester reaction peak move to the right, which indicates a longer induction time, but the peak also became broader, indicating a longer reaction time. This implies that the diffusion of polyester reactants in a high-polyurethane content IPN became more difficult.

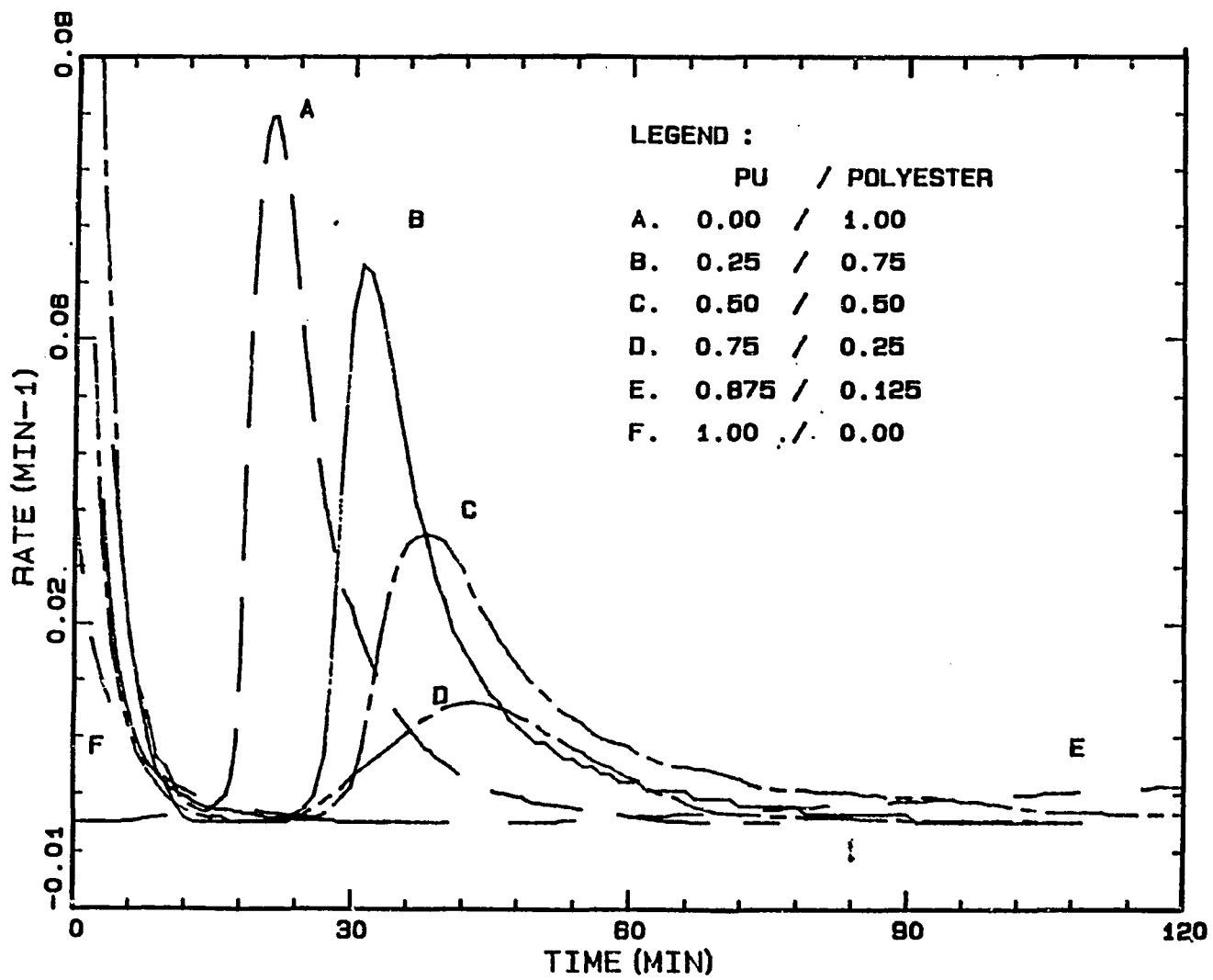


Figure 3.8 Compositional effect of PU/PES IPNs reacted at 353 °C.

Increasing polyester content in IPN promoted urethane reaction to completion. This was mainly due to the "solvent effect" of polyester and styrene monomers. For polyurethane reaction, adding polyester and styrene into polyurethane system had an effect of changing polyurethane reaction from bulk to solution polymerization. Therefore, diffusion barrier of urethane monomers was removed. As a result, there was almost no residual activity for polyurethane in IPNs with high-polyester content.

In general, the calculated total heat of reaction for polyester was reasonably consistent (about 100 cal/g) in each composition. These observations indicated that a gap existed at a composition around 50 to 60% by weight of polyurethane. When polyurethane content fell below this composition, the residual activity of polyester was small in isothermal runs and could be brought to complete polymerization by scanning of the isothermally cured samples. However, if the amount of polyurethane was greater than this margin, there was a great deal of residual activity of polyester in the isothermally cured sample and the polymerization could not be completed even if the sample was reheated by a scanning run. In other words, permanent residual activity of polyester existed for samples with 60% or higher polyurethane content.

In a polyurethane-polyester IPN, the reaction of polyurethane started first. With lower polyurethane content (up to about 50%), the reacted part of polyurethane had little effect on the kinetics

of polyester polymerization. However, if polyurethane content was increased above 50%, the reacted polyurethane content would have a "cage effect" on the polyester formation. The "cage effect" of the reacted polyurethane prevented styrene monomers from diffusion. In some cases, the mobility of styrene monomers was so prohibited that even with a following scanning run where the temperature went as high as 510 °K, the polyester reaction was still incomplete.

3.3.3 ADIABATIC TEMPERATURE RISE

Shown in Figure 3.9 is the adiabatic temperature rise of linear polyurethane with a gel time of less than 10 seconds and a maximum adiabatic temperature rise of 117.5 °C. The kinetic parameters of polyurethane reaction was determined from this temperature rise curve. Detailed analysis is presented in the section of Parameter Estimation.

3.3.4 REACTION INJECTION MOLDING

For IPNs (Figure 3.10), the addition of polyester phase promotes the maximum adiabatic temperature rise up to 127.5 °C for 75/25 (PU/PES) IPN and 167 °C for 50/50 IPN. The initial temperature rise of the 50/50 IPN is slower than that of 75/25 IPN, mainly due to the lower polyurethane content. However, the temperature rise of

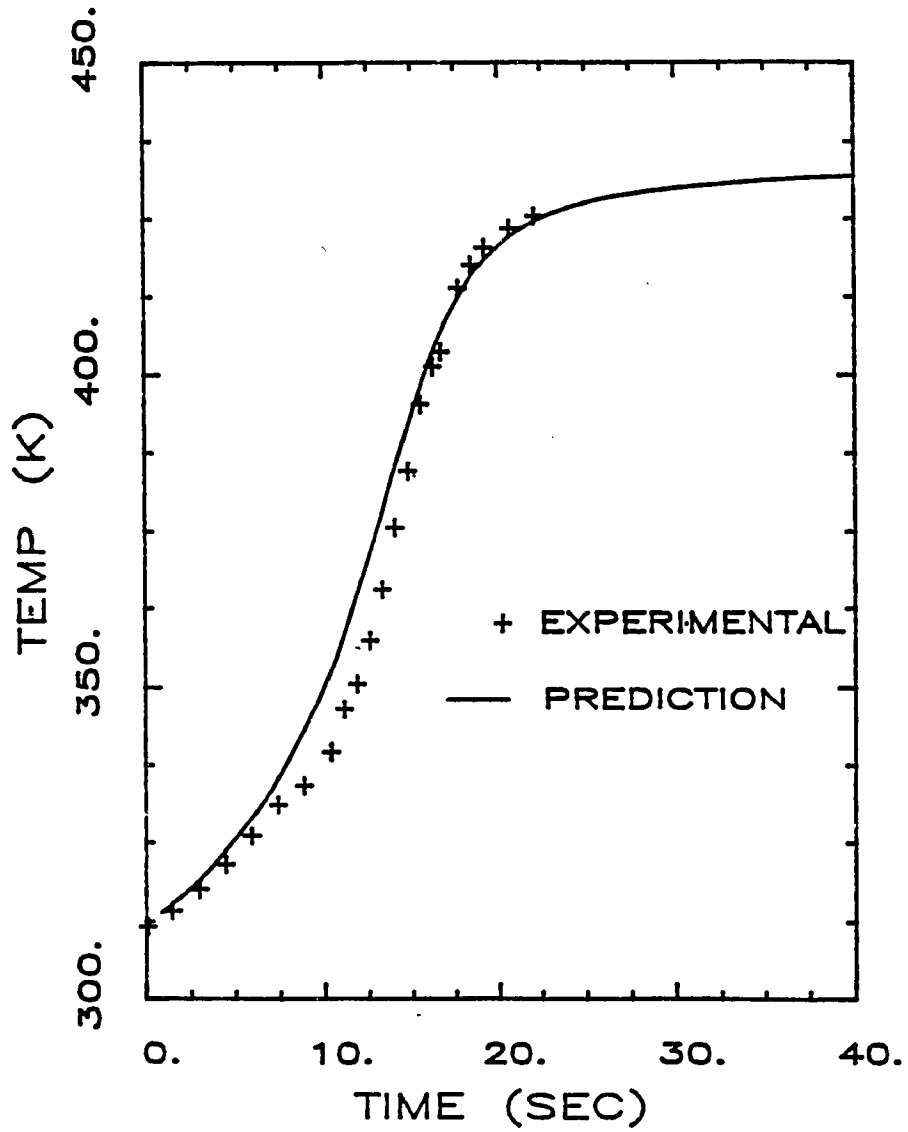


Figure 3.9 Adiabatic temperature rise of linear polyurethane. The solid line is curve fitted by multiple linear regression.

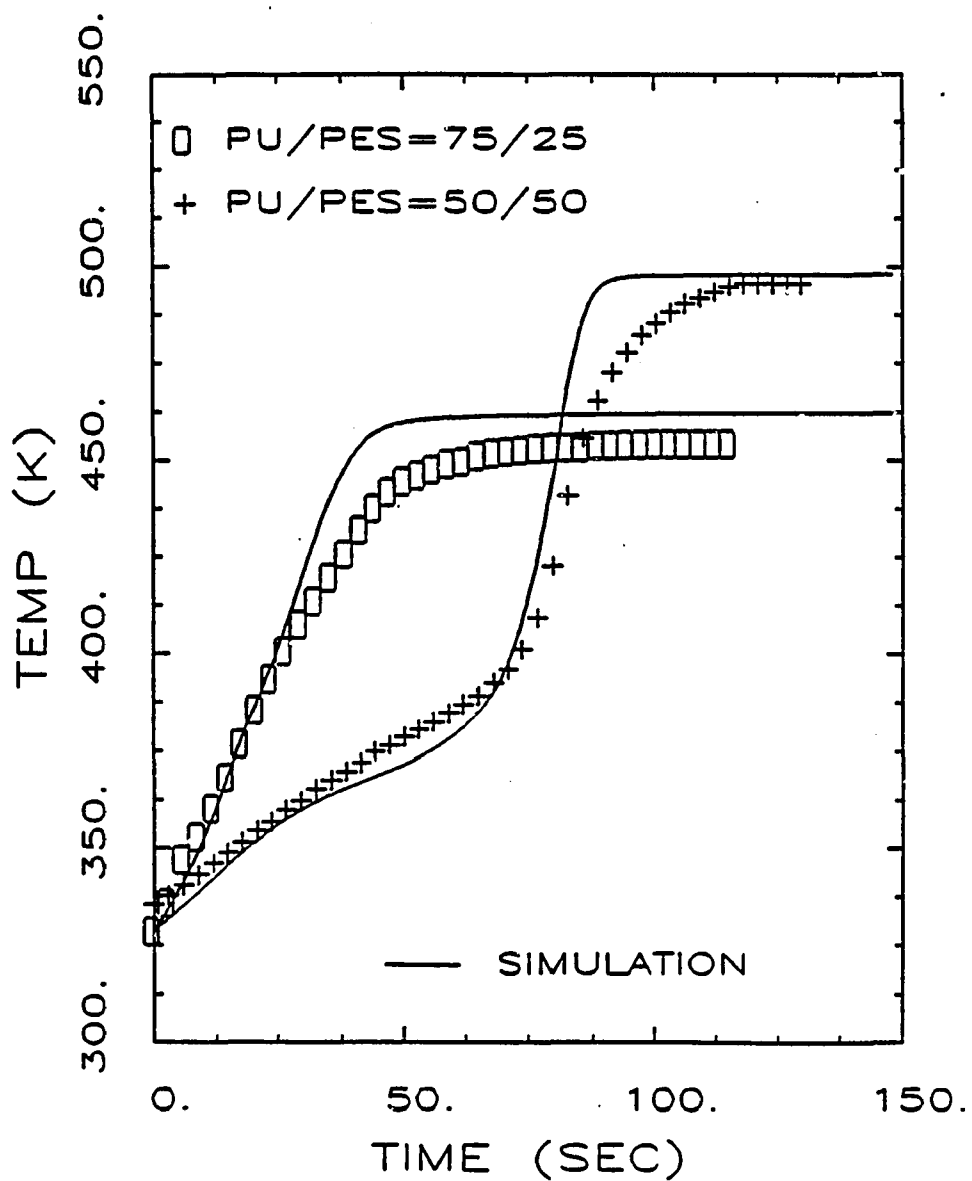


Figure 3.10 Adiabatic temperature rises of IPNs at two compositions. Model predictions are presented by solid lines.

PES is higher in the case of 50/50 IPN. In other words, the adiabatic temperature rise of IPNs is composition-dependent. This in turn indicates that the kinetics of IPNs is composition-dependent too. Since the PDO-initiated polyester is a thermally-activated reaction, the polymerization can only happen when sufficient heat is released from the polyurethane reaction. Therefore, the reaction of IPN in adiabatic condition is in a sequential order. The S-shaped temperature rise of the 50/50 IPN reaction shown in Figure 3.10 provides an evidence for this argument. In 75/25 IPN, the trend is not that obvious since the polyester phase consists only 1/4 of IPN.

3.3.5 CASTING

Casting results of polyurethane and polyester reactions at temperature of 353.5 °K are given in Figures 3.11 and 3.12 respectively. The difference of temperature profile at the center and the wall is obvious in both cases. With 353 °K wall temperature, the reaction started in the region near the wall. As heat was conducted through the resin phase, the temperature rise was greater at the center than at the wall. This phenomenon was common in all the casting experiment studied. Note also that for mixing-activated polyurethane reaction the reaction started upon heating. For the heat-initiated polyester phase, the reaction started after an induction period. In Figure 3.12, Zone I is the period during which

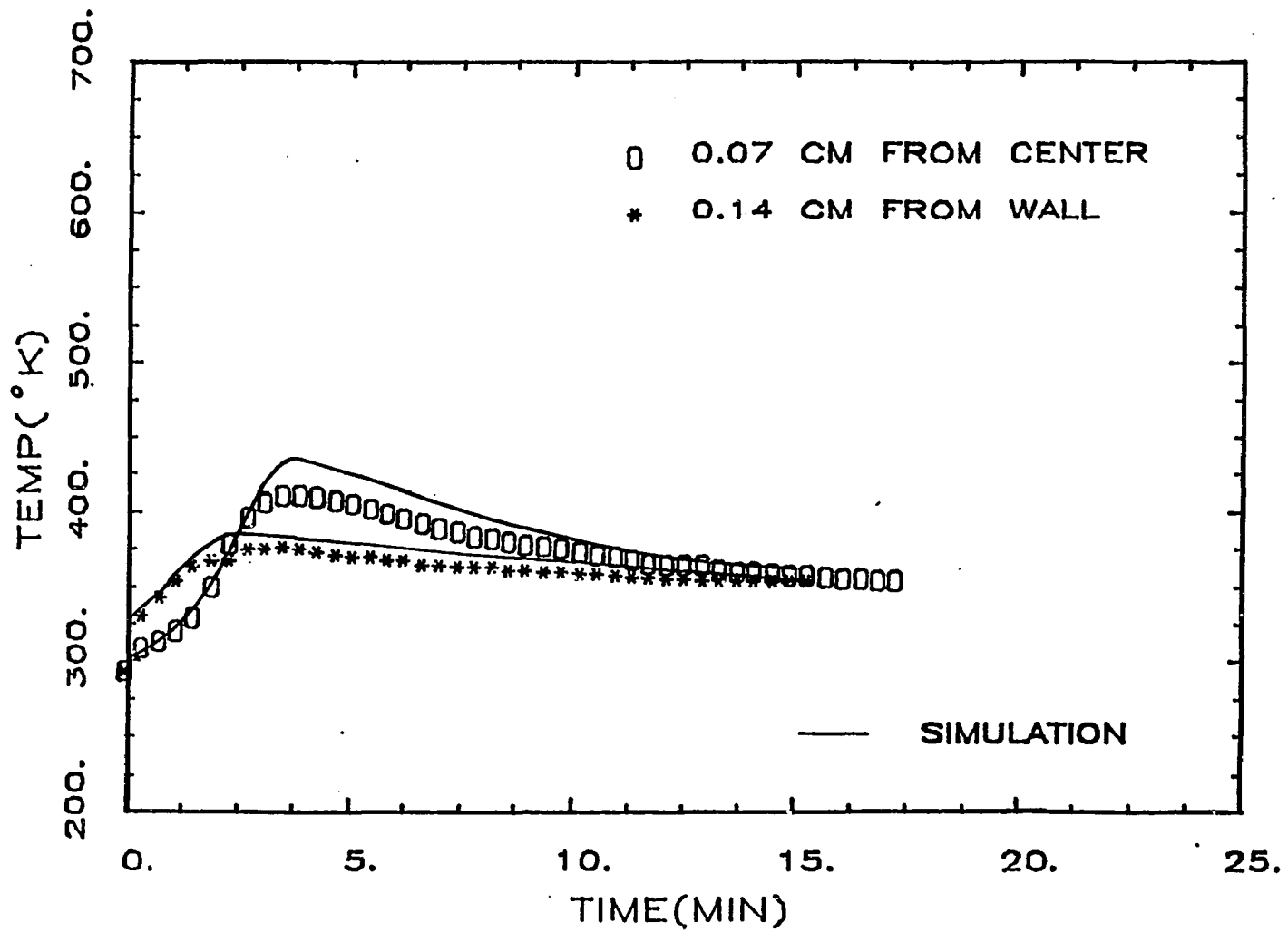


Figure 3.11 Casting of polyurethane at 353.5 K.

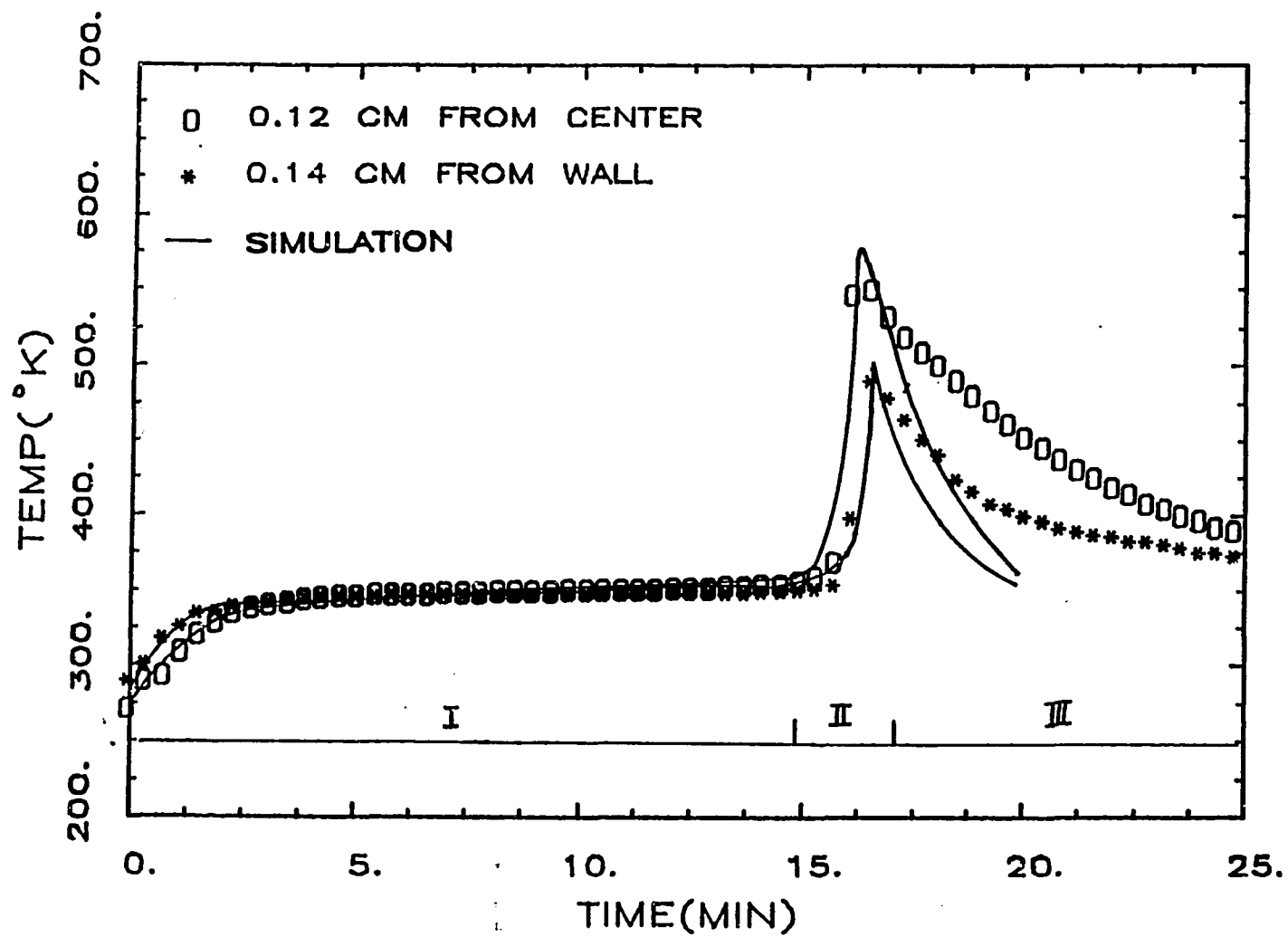


Figure 3.12 Casting of unsaturated polyester resin at 353.5 °K.

the temperature rise is mainly due to the heat input from the temperature bath. Zone II is the period during which the temperature increase is caused by heat generated during fast free radical polymerization. Finally, Zone III is a period during which heat transfers from the hot part to the cooler surroundings. For the material cured near the tube wall, the temperature change is moderated by heat exchange with the tube surface.

To explore the effect of compound composition on the curing of IPN, the composition ratio was varied. Casting results of IPN at 353 °K are given in Figures 3.13 to 3.15. The temperature profile, especially the maximum exotherm peak, is composition-dependent. Comparisons between IPNs (Figures 3.13 to 3.15) show that increasing polyester content in IPNs causes a higher exotherm. The maximum temperature of 75/25 IPN (Figure 3.13) is about 100 °C less than that of pure polyester resin. Figure 3.16 shows temperature profiles of a 50/50 IPN cast at 393 °K. Compared to the same material at 353 °K, the reaction time is shorter and the maximum exotherm is higher.

3.3.6 FTIR ANALYSIS OF CAST IPNs

FTIR analysis is based upon the peak change of functional groups or characteristic linkages during reaction period. Therefore, there is more than one peak which may change when reactions take place. For example, Figure 3.17 shows FTIR spectra for a 50/50 IPN

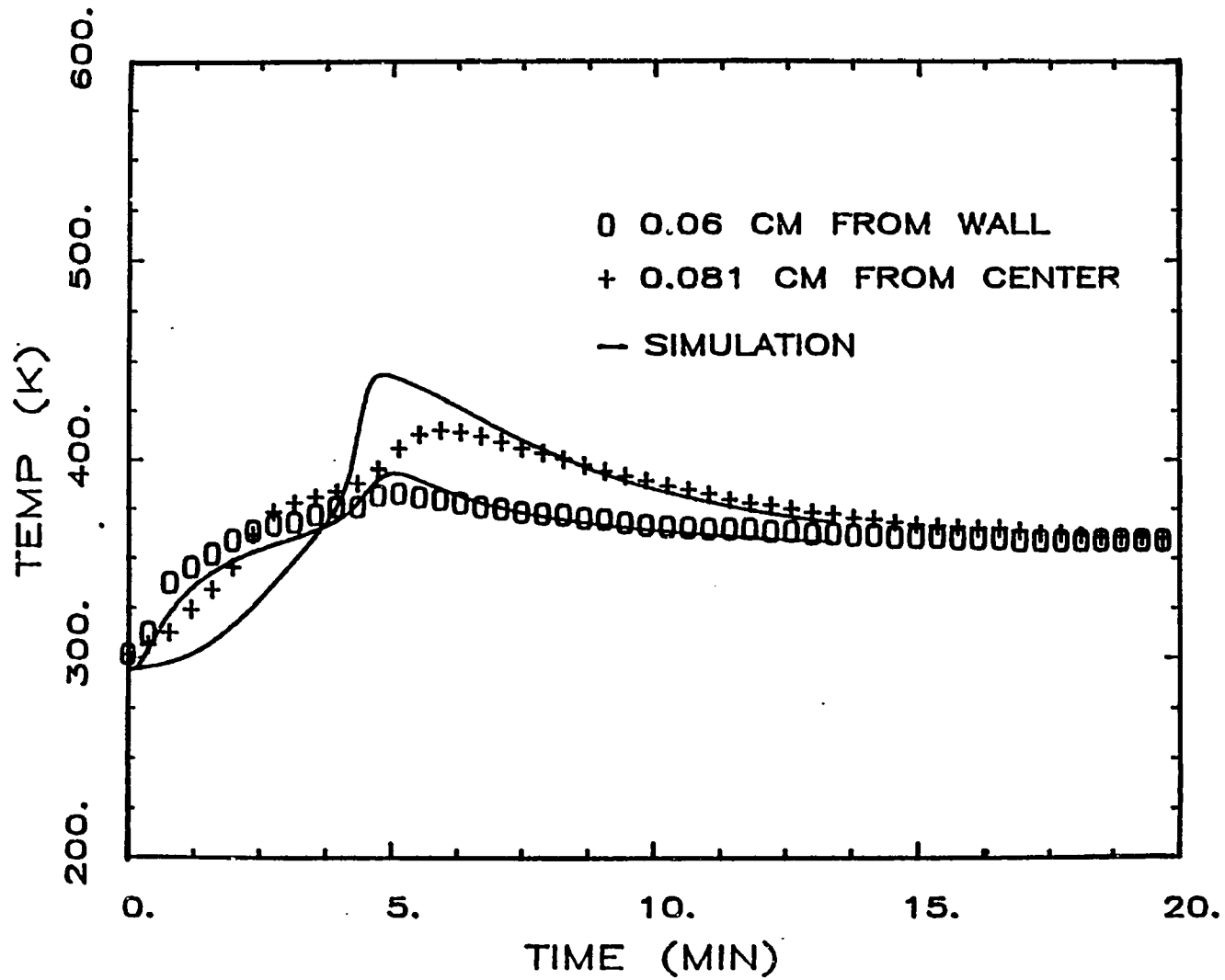


Figure 3.13 Casting of 75/25 IPN at 353.5 K.

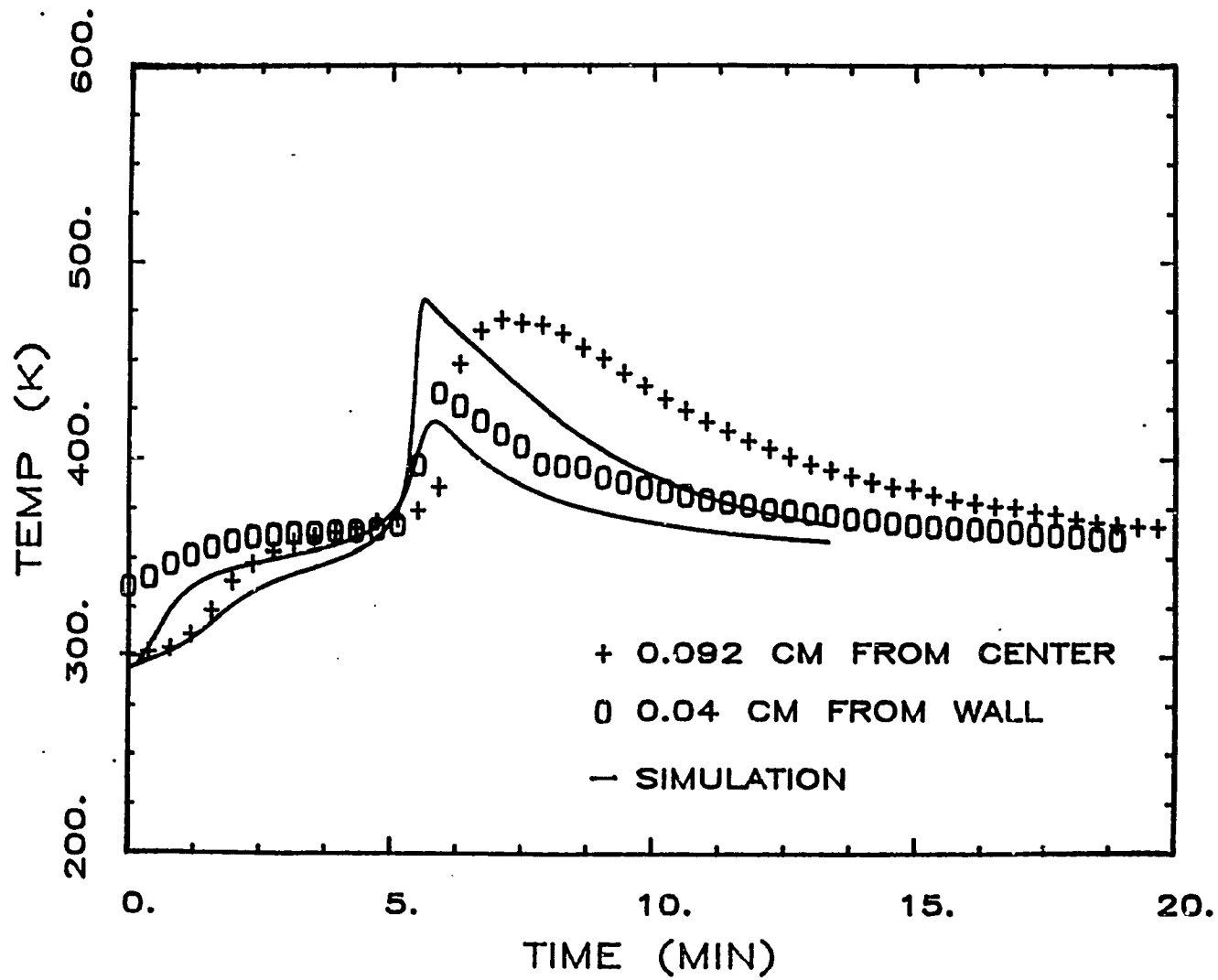


Figure 3.14 Casting of 50/50 IPN at 353.5 K.

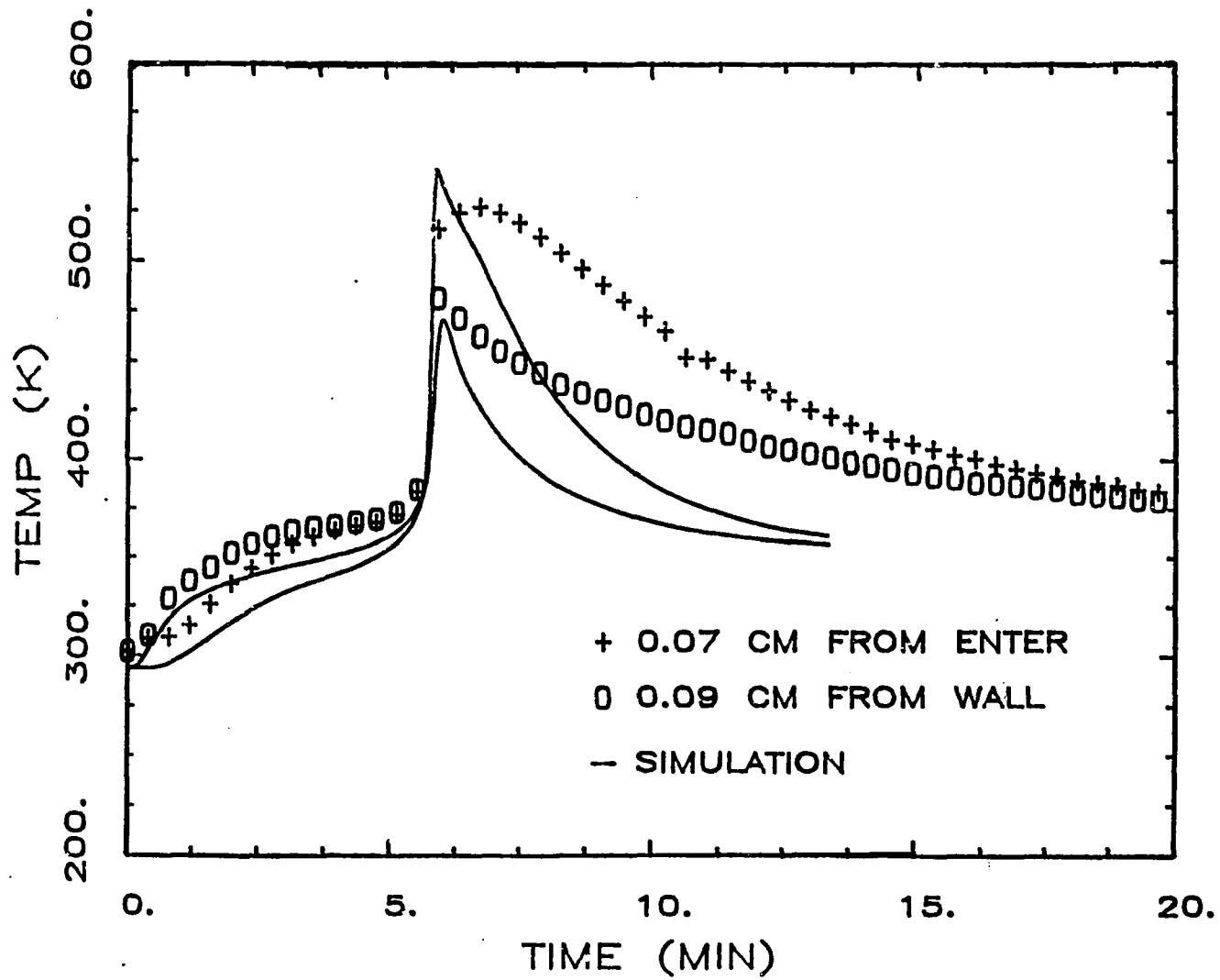


Figure 3.15 Casting of 25/75 IPN at 353.5 K.

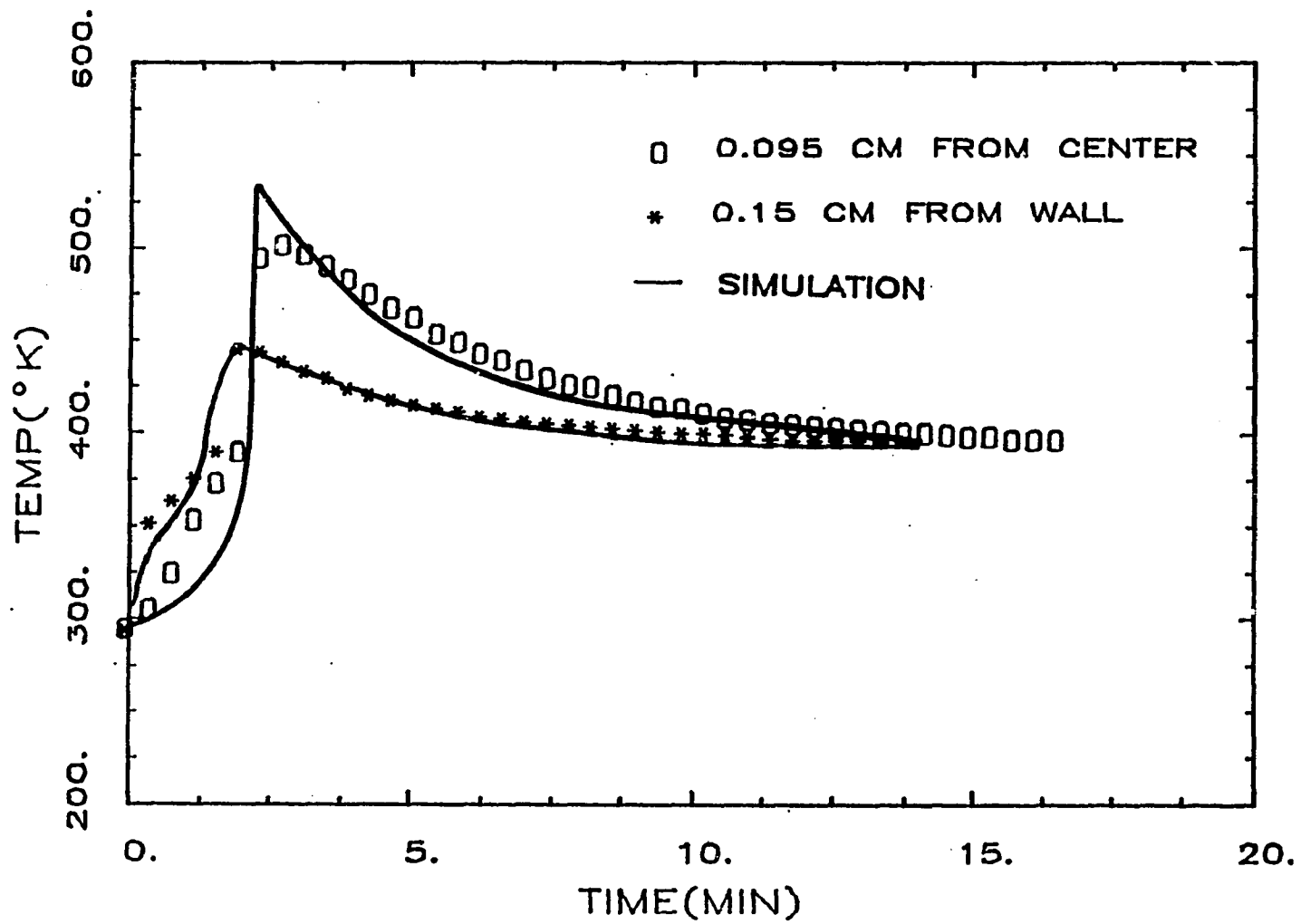


Figure 3.16 Casting of 50/50 IPN at 393.5 K.

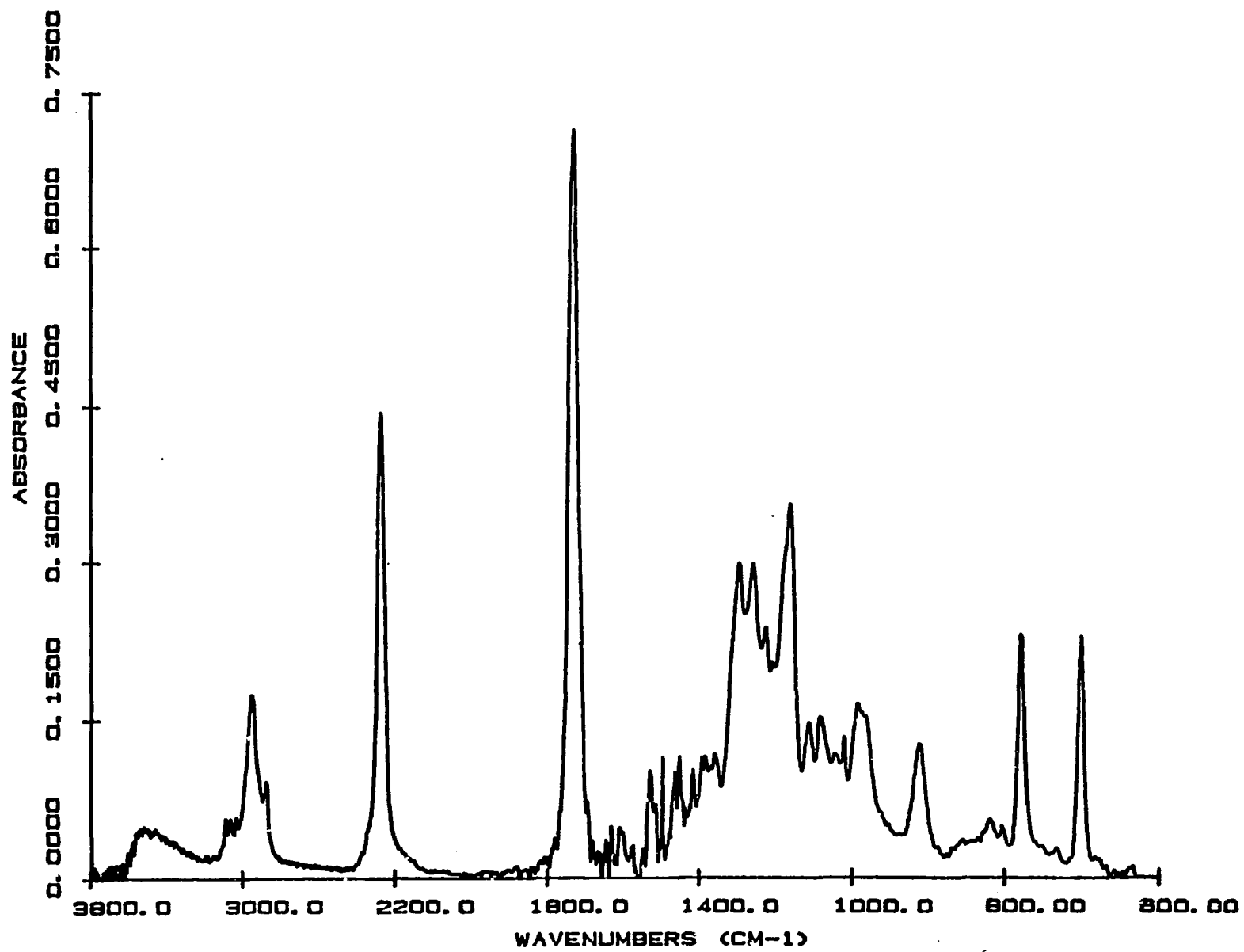


Figure 3.17 FTIR spectrum of 50/50 IPN before reaction (Yang and Lee, 1987).

system before reaction. In principle, isocyanate peak (2278 cm^{-1}), hydroxyl peak (3428 cm^{-1}) amine peak (3338 cm^{-1}) and urethane peak (trans at 1528 cm^{-1} , cis at 1414 cm^{-1}), can all be followed during urethane polymerization. However, the hydroxyl and amine peaks were found to be strongly affected by hydrogen bonding and tend to interfere with each other. The isocyanate peak at 2278 cm^{-1} was followed in order to calculate the fractional conversion of urethane reaction. Table 3.2 summarizes the IR peaks for different functional groups.

Polyester reaction can also be followed despite of urethane reaction (Yang and Lee, 1987). The peak at 1598 cm^{-1} indicates polystyrene formation, which is also located in a region where too many peaks are overlapped with one another. Therefore, the reaction conversion of polyester is better determined from the consumption of styrene C=C bonds at peaks 992 cm^{-1} and 912 cm^{-1} ($\text{CH}_2=\text{CH}$ deformation), and polyester C=C bonds at peak 982 cm^{-1} (trans CH=CH deformation). As shown in Figure 3.4, polyester reaction is a copolymerization of unsaturated polyester and styrene. There are three possible reactions: styrene-ester reaction, styrene-styrene reaction, and ester-ester reaction. Experimentally, these reactions can be quantitatively determined from infrared spectra. The consumption of styrene can be followed by the change of peaks at 912 and 992 cm^{-1} , while consumption of C=C bonds in unsaturated esters

Table 3.2 IR peaks for different functional groups of PU/PES IPN

<u>cm⁻¹</u>	<u>Functional Group</u>
<u>Polyurethane</u>	
2298	-NCO
3428	-OH (stretching)
3338	secondary -NH (stretching of amide)
1528	NH-COO- (urethane)
1414	cis NH-COO- (urethane)
2942	-CH (stretching) (internal standrad)
1737	amide I & II
1707	
1533	
<u>Polyester</u>	
1598	polystyrene
992	CH ₂ =CH ₂ (deformation)
912	
982	CH ₂ =CH ₂ (deformation)

may be followed by the change of peak at 982 cm^{-1} . These peak assignments are also summarized in Table 3.2.

Although it is not possible to monitor conversion profiles of polyurethane and polyester during casting, the final conversion of the cast samples can be analyzed using FTIR since an IR spectrum releases information about all the possible IR-active functional groups of polymers (Aldrich Chemical, Co., 1986). This not only gives final conversion data but also provides some ideas about the reaction mechanism during IPN polymerization. Table 2.3 details the possible reactions and the changes of functional groups during urethane reaction. For polyester reaction, the reactive groups (i.e., C=C bonds in polyester and styrene monomers) are transformed into C-C bonds by free radical polymerization.

Figure 3.18 shows FTIR spectra of samples taken from the center and wall of a cast 50/50 IPN. The wall temperature during casting was 393.5 K . Both spectra are normalized according to the internal reference peak at $2,942\text{ cm}^{-1}$ (-CH stretching), which did not alter during polymerization. For polyester phase, peaks at 912 cm^{-1} , 992 cm^{-1} (C=C for polystyrene) and 982 cm^{-1} (C=C for polyester) suggest that the reaction is nearly complete, with small amount of residual activity. For polyurethane, the complete disappearance of -NCO peak at $2,278\text{ cm}^{-1}$ suggests that polyurethane reaction is complete in both samples (wall and center). However, peaks at $3,428\text{ cm}^{-1}$ (-OH stretching), $3,338\text{ cm}^{-1}$ (-NH stretching of amide), and $1,737\text{ cm}^{-1}$,

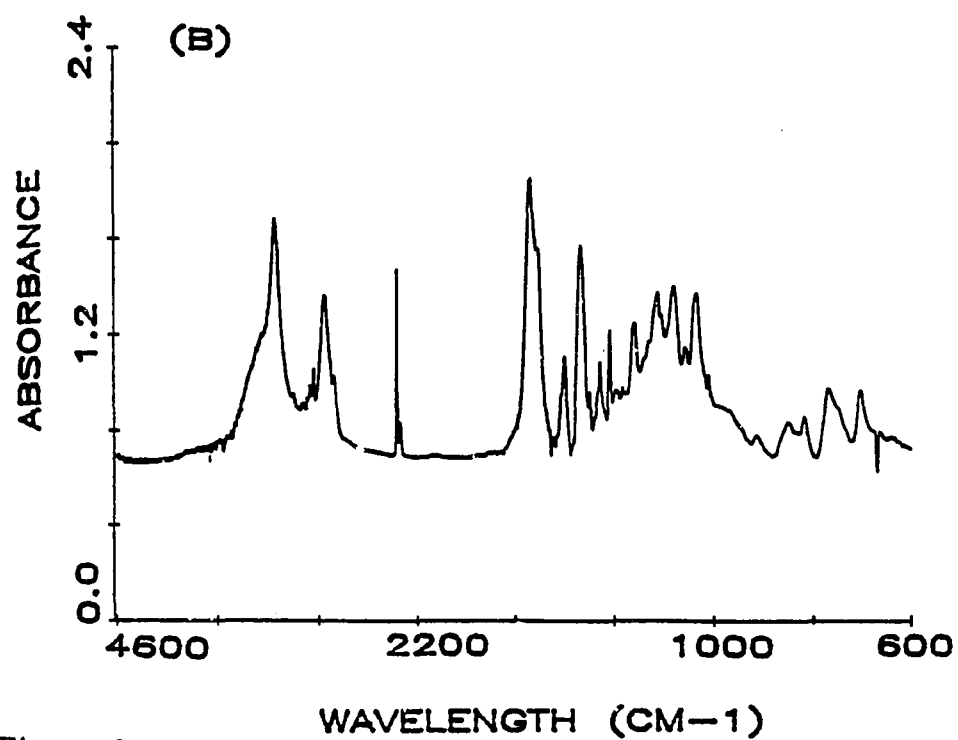
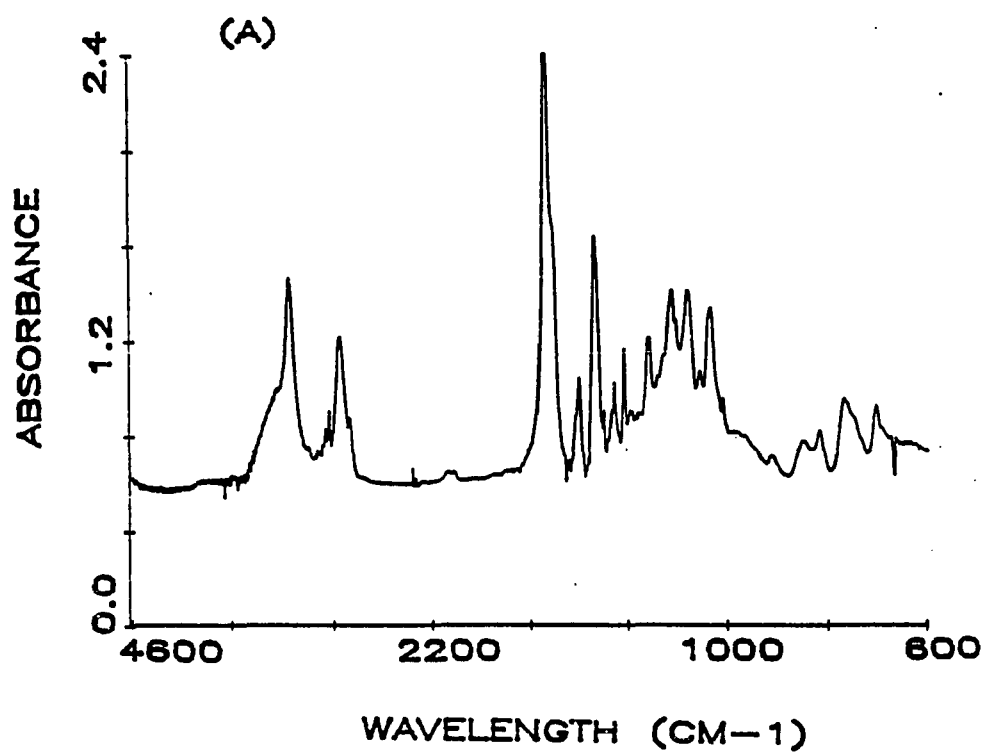


Figure 3.18

FTIR spectra of 393.5 °K-cast 50/50 IPN sampled (A) at wall and (B) at center of glass tube.

1,707 cm^{-1} , 1,533 cm^{-1} (amide I and II) all show different changes in peak height (i.e., compare Figure 3.19A and B). In Figure 3.19, the peak at 1737 cm^{-1} (amide I peak) of the IPN sample taken near the wall is higher than that of IPN sample taken near the center; while the peak at 3428 cm^{-1} (-OH stretching) of the IPN sample taken near the wall is lower than that taken near the center. Since the formation of urethane is the result of a reaction between isocyanate and hydroxyl groups, the consumption rate (change of peak height) of -OH peak should be equal to the consumption rate of -NCO peak and the appearance of amide I peaks if there are no side reactions. The results suggest that due to different thermal history along the radial mold direction, samples at different locations experienced different polymerization mechanism. Some possible side reactions might take place for the cast sample. These side reactions may include allophanate, biuret, urea, dimer, and trimer formations. Figure 3.19 implies that the sample at wall has more urethane formation than the sample at center. The formation of trimer (isocyanurate) at center is highly possible when reaction temperature exceeds 480 °K (Vespoli and Alberino, 1985). However, IR can not distinguish the formation of urethane from isocyanurate.

3.4 KINETIC AND HEAT TRANSFER MODELLING OF IPN REACTION

3.4.1 THEORETICAL MODEL

A. Kinetics

For kinetics of externally catalyzed step-growth polymerizations such as polyurethane, a simple nth order reaction model with Arrhenius temperature dependence is assumed.

$$r_u = C_{uo} \frac{d\alpha}{dt} = A_u \exp\left(-\frac{E_u}{RT_u}\right) C_{uo}^n (1-\alpha)^n \quad (3.8)$$

where r_u is the reaction rate of polyurethane, C_{uo} is the initial concentration of isocyanate functional groups, α is the extent of polyurethane reaction, E_u is the activation energy, R is the gas constant, T_u is the reaction temperature, and n is the reaction order. u stands for polyurethane phase. Kinetic parameters in eq. (3.8) were determined by adiabatic temperature rise measurement (Broyer and Macosko, 1978; Lee and Macosko, 1980). The assumptions made are as follows:

1. Homogeneous and well mixed system at $t=0$.
2. Negligible concentration change due to diffusion.
3. Reaction order n being the same throughout the entire reaction.

The energy equation for adiabatic condition is:

$$\rho_u C_{pu} \frac{dT_u}{dt} = -\Delta H_u r_u \quad (3.9)$$

where ρ_u is density, C_{pu} is heat capacity, ΔH_u is the heat of reaction of polyurethane. The extent of reaction is directly proportional to the amount of heat generated if constant density and heat capacity are assumed. Thus,

$$\frac{C_u}{C_{uo}} = (1-\alpha) = \frac{(T_{ad} - T_u)}{(T_{ad} - T_{uo})} \quad (3.10)$$

where C_u is the isocyanate concentration, T_{ad} is the measured maximum adiabatic temperature, and T_{uo} is the initial material temperature.

For free radical polymerizations such as styrene-unsaturated polyester, a kinetic model proposed by Stevenson (1980) and Lee (1981) is used. The following assumptions are made:

1. Diffusion of monomer is neglected in propagation step up to high conversion.
2. Negligible homopolymerization of unsaturated polyester.
3. Copolymerization of styrene monomer and C=C bonds on polyester chains can be described by a single average rate constant.

4. No monomer reacts until the number of initiator radicals created is equal to the effective number of inhibitor molecules initially present.
5. Free radical termination is significantly slower than that in the polymerization of low molecular weight species.

With these assumptions, the free radical reaction can be expressed as:

Initiation

$$\frac{dR^\bullet}{dt} = 2K_d I \quad (3.11)$$

Inhibition

$$\begin{aligned} qZ_o &= 2fI_o [1 - \exp(-\int_0^t 2K_d dt)] \\ &= 2f(I_o - \bar{I}_o) \end{aligned} \quad (3.12)$$

Propagation

$$\frac{dM}{dt} = -K_p MR^\bullet \quad (3.13)$$

or

$$r_e = C_{eo} \frac{d\beta}{dt} = 2f\bar{I}_o K_p \{ (1-\beta) [1 - \exp(-\int_{t_0}^{t-t_z} K_d(t-t_z))] \} \quad (3.14)$$

where R is the free radical concentration, I_o and Z_o are the initial concentrations of initiator and inhibitor. \bar{I}_o is the concentration of initiator after all the inhibitors having been consumed, f is the initiator efficiency, q is the inhibitor efficiency, t_z is the induction time before propagation, K_d and K_p are the rate constants of initiator decomposition and monomer propagation, M is the monomer concentration, and β is the fractional conversion. The value of K_d and K_p are assumed to be Arrhenius temperature dependent throughout the entire cure period, and

$$K_d = A_d \exp\left(-\frac{E_d}{RT_e}\right) \quad (3.15)$$

$$K_p = A_p \exp\left(-\frac{E_p}{RT_e}\right) \quad (3.16)$$

For model prediction of polyurethane-polyester IPN, the individual kinetic models are combined in a simple additive manner. No component interactions are considered here.

B. Heat Transfer Model (Casting and RIM Processes)

The following assumptions are made for the casting process:

1. One-dimensional heat conduction.
2. Negligible molecular diffusion.
3. Homogeneous and well mixing reaction system at $t=0$.
4. No flow.
5. Physical properties such as density ρ_I , heat capacity C_{pI} , heat of reactions ΔH_i 's, and thermal conductivities k_i 's are temperature independent.
6. No intercomponent chemical reaction.
7. Intimate contact of surface between reacting polymer and casting tube.

With these assumptions, the governing equations of the casting process can be described as follows:

(1) IPN phase

Heat transfer

$$\rho_I C_{pI} \frac{\partial T_I}{\partial t} = k \left[\left(\frac{\partial^2 T_I}{\partial r^2} \right) + \left(\frac{1}{r} \frac{\partial T_I}{\partial r} \right) \right] - \Delta H_u r_u - \Delta H_e r_e \quad (3.17)$$

where I stands for the IPN phase and

$$\frac{1}{k_I} = \frac{W_u}{k_u} + \frac{W_e}{k_e} \quad (3.18)$$

$$\frac{1}{\rho_I} = \frac{W_u}{\rho_u} + \frac{W_e}{\rho_e} \quad (3.19)$$

$$C_{pI} = W_u C_{pu} + W_e C_{pe} \quad (3.20)$$

where W_u and W_e are the weight fractions of polyurethane and polyester respectively. The initial conditions are:

$$T_I = T_{I0}, \quad \text{at } t = 0, \quad \text{for all } 0 \leq r \leq d_1 \quad (3.21)$$

$$\alpha = 0, \quad \text{at } t = 0, \quad \text{for all } 0 \leq r \leq d_1 \quad (3.22)$$

$$\beta = 0, \quad \text{at } t = 0, \quad \text{for all } 0 \leq r \leq d_1 \quad (3.23)$$

and boundary conditions are:

$$\frac{dT_I}{dr} = 0, \quad \text{at } r = 0, \quad \text{for } t > 0 \quad (3.24)$$

$$T_I = T_g, \quad \text{at } r = d_1, \quad \text{for } t > 0 \quad (3.25)$$

or

$$-k_I = \frac{dT_I}{dt} = -k_g \frac{dT_g}{dt}, \quad \text{at } r = d_1, \quad \text{for } t > 0 \quad (3.26)$$

(2) Glass phase:

$$\rho_g C_{pg} \frac{dT_g}{dt} = k_g \left[\frac{\partial^2 T_g}{\partial r^2} + \frac{1}{r} \frac{\partial T_g}{\partial r} \right] \quad (3.27)$$

with initial conditions:

$$T_g = T_o, \quad \text{at } t = 0, \quad \text{for } d_1 < r < d_2 \quad (3.28)$$

where T_o is the heating/cooling water temperature.

The boundary conditions are:

$$-k \frac{dT_g}{dr} = h_w (T_g - T_o), \quad \text{at } r = d_2, \quad \text{for } t \geq 0 \quad (3.29)$$

and equations (3.25) or (3.26), where h_w is the overall heat transfer coefficient between water and glass tube. The reaction equations have the following constraints:

$$\frac{dx}{dt} = r_u, \quad \text{for } t > 0 \quad (3.30)$$

$$\frac{d\beta}{dt} = 0, \quad \text{for } t < t_z \quad (3.31)$$

$$\frac{d\beta}{dt} = r_e, \quad \text{for } t \geq t_z \quad (3.32)$$

The coupled equations (3.17) - (3.32) are solved simultaneously using Advanced Continuous Simulation Language (ACSL) (Mitchell and Gauthier Assoc., Inc., 1981). The parameters used in computer simulation are listed in Table 3.3

The adiabatic reaction in the RIM process is a special case of the energy equation (3.17). The heat conduction term in the energy equation is removed and the boundary conditions are changed. Assuming no heat exchange with surrounding air, the energy equation becomes:

$$\rho_I C_{pI} \frac{dT_I}{dt} = - \Delta H_u r_u - \Delta H_e r_e \quad (3.33)$$

where r_u and r_e are represented by equations (3.8) and (3.14) respectively.

3.4.2 PARAMETER ESTIMATION

A. Polyurethane

The kinetic parameters of polyurethane reaction are estimated from the adiabatic temperature rise method. Combining equations (3.8), (3.9), and (3.10) gives

$$\ln \frac{dT_u}{dt} = \ln \left[\frac{\Delta H_u A_u}{\rho_u C_{pu}} \right] + \frac{E_u}{RT_u} + n \ln \left[\frac{T_{ad} - T_u}{T_{ad} - T_{uo}} \right] \quad (3.34)$$

Equation (3.34) can be rewritten in the following form:

$$\ln \frac{dT_u}{dt} = C_1 + C_2 \frac{1}{T_u} + C_3 \ln \left(\frac{T_{ad} - T_u}{T_{ad} - T_{uo}} \right) \quad (3.35)$$

where $C_1 = \ln[\Delta H_u K_u / \rho_u / C_{pu}]$, $C_2 = E_u / R$, and $C_3 = n$. The variables dT_u/dt , $1/T_u$, and $[(T_{ad} - T_u) / \Delta T_{ad}]$ can be evaluated from the temperature vs. time curve of the adiabatic polymerization. By using a multiple linear regression procedure, one can obtain the order of reaction n , the activation energy E_u , and the frequency coefficient of reaction rate K_u . The parameters obtained are listed in Table 3.3.

Table 3.3 Parameters used in modelling of IPN

<u>Parameters</u>	<u>PU</u>	<u>PES</u>	<u>IPN</u>	<u>Glass</u>
ρ (gm/cc)	1.14	1.10	1.12	2.375
C_p (cal/gm/K)	0.4	0.4	0.4	0.18
λ (cm ² /s)	7.9×10^{-4}	8.2×10^{-4}	8.0×10^{-4}	8.42×10^{-4}
ΔH_r (cal/gm)	139.2	95.95	-----	-----
A_d (pp unit)	-----	2.8×10^{16}	-----	-----
E_d (Kcal/gmole)	-----	31.0	-----	-----
A_p (app unit)	2.0×10^7	4.6×10^3	-----	-----
E_p (Kcal/gmole)	10.6	10.0	-----	-----
n (reaction order)	2.0	-----	-----	-----

B. Styrene-Unsaturated Polyester

The kinetic parameters of polyester reaction are estimated following Lee's method (1981). Equation (3.12) is rearranging in the following form:

$$\ln t_z = \ln\left\{-\frac{1}{A_d} \ln\left(1 - \frac{qZ_0}{2fI_0}\right)\right\} + \frac{E_d}{R} \frac{1}{T_e} \quad (3.36)$$

By plotting $\ln t_z$ vs. $1/T_e$ of isothermal DSC runs, a straight line is obtained. The slope gives the activation energy of initiator decomposition, $E_d = 31.0$ kcal/g-mole, and the intercept gives $A_d = 2.8 \times 10^{16}$. The exact amount of inhibitor in the resin is unknown. It is assumed that $qZ_0/2fI_0 = 0.01$. For isothermal DSC curves, the maximum rate of reaction occurs at a point where

$$\frac{dR}{dt} = \frac{d^2\beta}{dt} = 0 \quad (3.37)$$

Combining equations (3.37), and (3.14), we have

$$(2fI_0 A_p) \exp\left(-\frac{E_p}{RT}\right) = \frac{K_d \exp[-K_d(t_m - t_z)]}{1 - \exp[-K_d(t_m - t_z)]} = D \quad (3.38)$$

If we define $2f\bar{I}_0 A_p = \bar{A}_p$, the kinetic parameters \bar{A}_p and E_p can be calculated by the same way to calculated A_d and E_d . The result is $A_p = 4.6 \times 10^5$ and $E_p = 10.0$ kcal/g-mole. The activation energy of propagation is of the right order compared to typical value of $E_p = 6 \sim 12$ kcal/g-mole for styrene homopolymerization (Bamford, et al., 1958). Kinetic parameters of polyester reaction are listed in Table 3.3, along with other physical properties used in simulation.

3.4.3 MODEL PREDICTION

A. Isothermal Reaction

Comparison of model prediction and measured reaction rates of pure polyurethane and polyester by DSC in isothermal mode is shown in Figure 3.19. The prediction of each component is reasonably accurate. Figure 3.20 compares the model prediction and experimental data of IPNs measured by DSC in isothermal mode. The results show that for an IPN with lower polyurethane content (i.e., 25/75 IPN), the deviation of model prediction from experimental data is small. As the amount of polyurethane is increased to 50%, the prediction of polyurethane reaction remains satisfactory, a large deviation, however, exists in the prediction of polyester reaction. Compared to the predicted results, the experimental data show a delay of the onset of polyester exotherm and a lower and broader

DSC ISOTHERMAL AT 353.5K

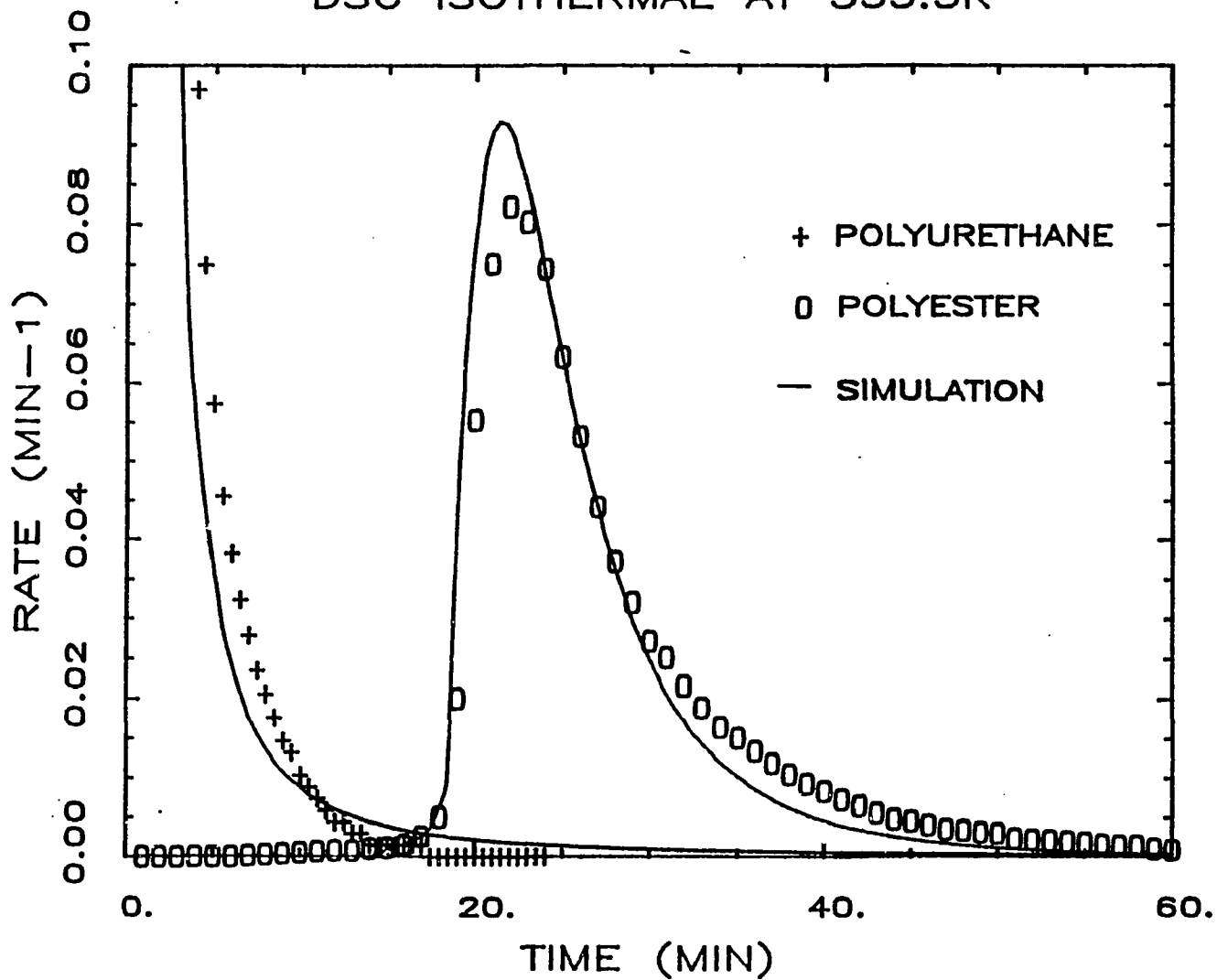


Figure 3.19 Predicted reaction rate vs. time of polyurethane and polyester at 353.5 °C.

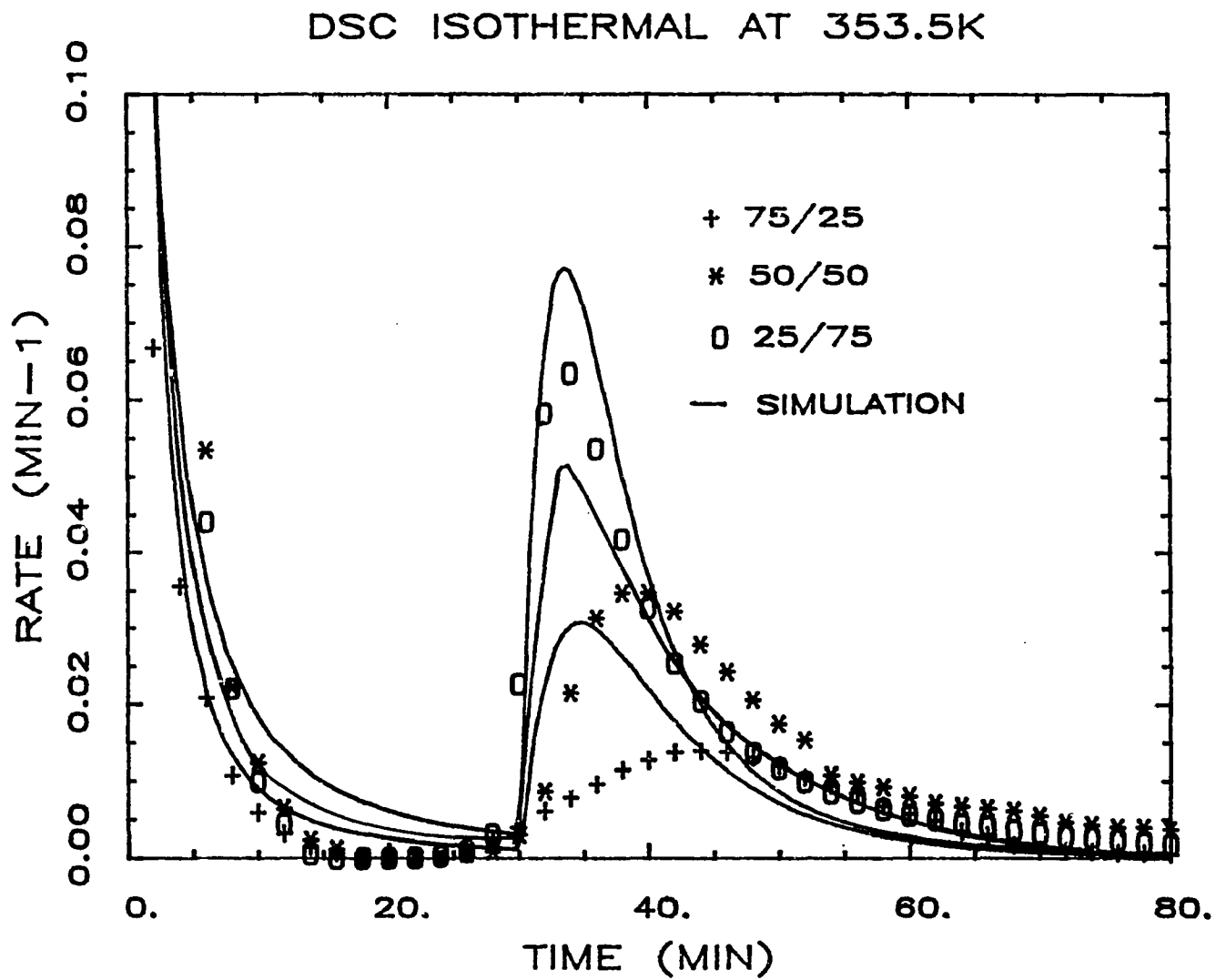


Figure 3.20 Predicted reaction rate vs. time of IPNs at three compositions (353.5 °K).

exothermic peak. In the prediction of IPNs with higher polyurethane content (i.e., 75/25 IPN), a much larger deviation is observed.

Since the IPN model used is a simple combination of two component models in an additive mode, the discrepancy between model prediction and DSC experimental results may be attributed to some possible component interactions. Since polymerizations of both components are diffusion-controlled, especially in the high-conversion region, a diffusion limitation may exist in the polyester phase because polyester polymerization took place after polyurethane polymerization.

B. Reaction Injection Molding

The predicted temperature rise vs. time curves of IPN reactions in RIM are shown in Figure 3.10. The predictions follow the experimental data closely, which are much better compared to the predictions of isothermal reactions where large deviations were observed. This may be because that the adiabatic reaction is so fast and exothermic that component interactions are totally or partially eliminated; whereas in the isothermal reactions measured by DSC, the heat released from polyurethane and polyester reactions is removed, the reaction rate profiles reflect the reaction kinetics at low temperatures, which may be more diffusion affected.

C. Casting

Model predictions of temperature profiles in the casting of pure polyurethane and polyester resins are given in Figures 3.11 and 3.12. Considering the highly simplified model for each component, the comparison between experimental data and predicted results is reasonably well. The predicted polyester curve rises more sharply at the beginning of the reaction and descends more sharply at the end of the reaction. This is probably a result of the model assumptions that the polymerization starts instantaneously at time t_z when the inhibitor is completely consumed and the lack of free radical termination as the reaction progresses (Lee, 1980).

These two individual models are then combined to predict IPN's reaction. The results of casting at 353 °K are shown in Figures 3.13 to 3.15 for three compositions of IPNs. The prediction of 75/25 IPN (Figure 3.13) is reasonably good. For the 50/50 IPN (Figure 3.14) and the 25/75 IPN (Figure 3.15), the prediction is good in terms of reaction exotherm, but it shows a much sharper temperature drop in the cooling region. For these IPNs with low-polyurethane content, the error in the cooling region is due to the lack of free radical termination in the modelling of polyester reaction. Figure 3.16 shows the comparison of predicted and measured temperature profiles of a 50/50 IPN cast at 393 °K. The prediction is much better than that at lower molding temperatures. Figure 3.21 shows the predicted conversion profiles of a 50/50 IPN sample cast at 353 °K.

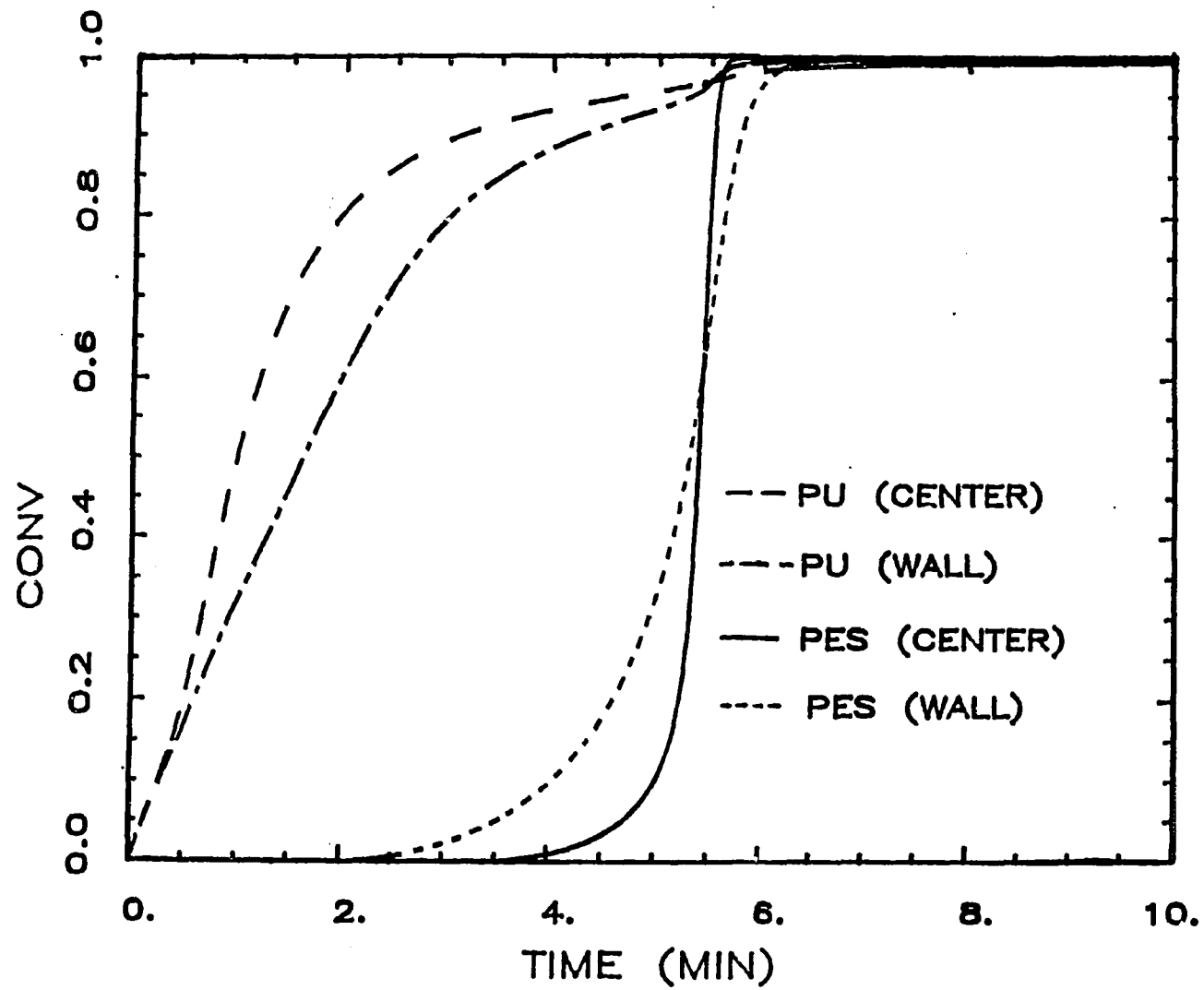


Figure 3.21 Predicted conversion profiles of 50/50 IPN cast at 353.5 K.

The reaction at center is faster than the reaction at wall in both polyurethane and polyester phases.

Generally speaking, the model gives a reasonably good prediction of temperature profiles for adiabatic reactions, but not for isothermal reactions. The prediction of casting is fairly well at high molding temperatures. The discrepancy may largely resulted from component interaction since the model proposed is based on the additivity rule of constituent components and without any consideration of interaction. These interactions can be categorized as either physical interactions or chemical interactions. The physical interactions mainly come from the "cage effect" of polyurethane on polyester and the "solvent effect" of polyester on polyurethane. Chemical interaction may happen between the isocyanate group of polyurethane and the hydroxyl and carboxylic groups of unsaturated polyester.

CHAPTER IV

PROPERTY-STRUCTURE-PROCESSING RELATIONSHIPS OF IPN

SYNOPSIS

Solid state characterization of polyurethane-polyester IPNs is presented in this chapter. The characterization ranges from the morphological study by transmission electron microscopy, the dynamic mechanical analysis using a Weissenberg Rheogoniometer, to the tensile test using an Instron tensile tester. The measured physical properties are related to processing variables such as molding temperature and degree of mixing, and material variables such as the type and concentration of initiator, and the chemical structure of constituent components.

4.1 PREVIOUS WORK ON MORPHOLOGY AND MECHANICAL PROPERTIES OF IPNS

4.1.1 Survey of Morphological Studies

Major studies of IPN morphology have been centered around the degree of interphase penetration, the shape and size of each

phase, the extent of intersystem chemical grafting, and the influence of morphology on the mechanical properties of IPNs.

Phase separation is an intrinsic phenomenon in IPN formation. Elastomeric polyurethanes are segmented polymers due to the incompatibility of the hard and soft segments. When another component is added to this already segmented system, phase separation becomes more complicated. However, due to the interpenetrating nature of molecule chains, phase separation can be reduced to a lesser extent in IPN than the mechanically mixed polymer blends.

The most important factor that determines the degree of phase separation is the thermodynamic compatibility of the constituent components in IPNs. For a highly compatible system such as PMMA and poly(ethyl acrylate), the dispersed phase with a domain size less than 100 Å was observed using the electron microscope (Huelck et al., 1972). For a less compatible system like poly(ethyl acrylate) and polystyrene, an additional cellular structure of about 1,000 Å domain size was found. Composition also plays an important role in determining the domain size. For a polyurethane-PMMA simultaneous interpenetrating network (SIN) with comparable polymerization rates, Kim et al. (1976) found that the phase inversion occurred at a composition of about 30% PMMA by weight. In studying the influence of morphology on the mechanical properties of SBR/PS IPNs, Donatelli et al. (1976) found that an optimum degree of

toughness was obtained at an intermediate level of crosslinking of SBS.

Polymerization rate is another important factor. If polymerization rates of constituent reactions are significantly different, then the one that polymerizes first will form the continuous phase and will subsequently "freeze" the phase formation of the other component. One way to identify the degree of interphase mixing is by measuring the glass transition temperature, T_g , of an IPN. Frisch et al. (1974) applied DSC to measure T_g 's of polyurethane-epoxy, polyurethane-polyacrylate, and polyurethane-polyester IPNs and found that all IPNs exhibited a single T_g which was as sharp as the T_g 's of each component network. This T_g was located approximately in the middle of the T_g 's of the two components. They claimed that phase separation might not occur because of the heavy chain entanglement (interpenetration). Nguyen and Suh (1983) used dynamic mechanical analysis to measure T_g 's of a series of polyurethane-polyester SINs and found that the T_g 's of the two components had a tendency to shift together to form a single T_g , indicating a substantial interphase mixing.

Donatelli et al. (1976) studied the morphology of several IPNs and semi-IPNs synthesized from a styrene-butadiene copolymers (SBR) as polymer I and a polystyrene as polymer II. By controlling the level of crosslinking, they found that the polymer synthesized first formed the more continuous phase and tended to control the

morphology. The second polymer formed a cellular structure whose size was determined primarily by the degree of crosslinking of polymer I, with an increase in crosslinking producing a finer structure. Their results were similar to the investigations on polyurethane-poly(methyl methacrylate) IPNs done by Kim et al. (1976) who concluded that the physical interlocking prevented the demixing of IPN, thereby producing a better mixing of component networks.

Several theoretical models have been developed to predict the phase domain size (Jordhamo et al., 1984; Sperling, 1984). Sperling proposed the following equation to predict the domain diameter of the second component in a full sequential IPN:

$$D_2 = \frac{4 \gamma}{RT(A*V_1 + B*V_2)} \quad (4.1)$$

$$A = 1/2(1/\phi_2)(3\phi_1^{1/3} - 3\phi_1^{4/3} - \phi_1 \ln\phi_1) \quad (4.2)$$

$$B = 1/2(\ln\phi_2 - 3\phi_2^{2/3} + 3) \quad (4.3)$$

where D_2 : "sphere" domain diameter of polymer II.
 γ : interfacial tension.
 V : crosslink density.
 ϕ : volume fraction of each phase.

T : temperature.

The predicted results were in good agreement with the experimental data. Another model was proposed by Jordhamo et al. (1984), which was used to describe the morphology of the castor oil-based polyester-polystyrene IPNs. The equation used to predict the phase inversion point is

$$\eta_1/\eta_2 * \phi_1/\phi_2 = 1 \quad (4.4)$$

where η is the viscosity and ϕ is the volume fraction. This prediction did not work very well. However, the experimental technique designed to measure the phase volume fraction by centrifugation is plausible. Djomo et al. (1983) investigated the effect of intersystem grafting and its influence on mechanical properties of polyurethane-acrylate IPNs and found that there were only 7×10^{-6} grafts per gram of polyacrylate. They concluded that the number of grafts was so low that its influence on mechanical properties was negligible. Neubauer et al. (1977, 1978) used a hydrolyzable crosslinker and a permanent crosslinker in a poly(ethyl acrylate)-polystyrene semi-IPN. They observed a significant modulus change upon annealing when the decrosslinker was increased from 0 to 100 %. The results suggested that morphological change occurred when the semi-IPN was changed from a crosslinked one to a linear one.

The morphology of polyurethane-polystyrene IPNs was studied by Kim et al. (1975). They found that at a composition of about 75% polyurethane, a phase inversion occurred, the continuous phase being polystyrene at polyurethane composition less than 75%. Their results from electron microscopy showed phase separation with some chain interpenetration. The optical microscopy of polyurethane-polysiloxane IPNs was studied by Ebdon et al. (1984). They found that from 90% to 50% polyurethane component, the urethane network was continuous and the polysiloxane was present as a dispersed phase. From 40% to 10% of urethane, the situation was reversed. Some degree of interchain mixing at phase boundaries was also detected using C^{13} nuclear magnetic resonance spectroscopy. The morphology of interstitial polymerization of vinyl monomers and polyurethane elastomers was investigated by Allen et al. (1973). The structure was found to consist of PMMA domains embedded in a PU matrix. Some molecular interaction between the polymeric species, mainly at the domain boundaries was also observed. The effect of polymerization temperature on the morphology of styrene-divinyl benzene copolymer/poly(vinyl chloride) IPNs was studied by Hayashi et al. (1987). The IPNs studied showed a two-phase structure in which styrene was the dispersed phase. The phase inversion of a polyacrylate/poly(urethane-urea) IPN was found at a composition of 30% polyacrylate by Matsuo et al. (1970). Morphological study of polyurethane/poly(methyl methacrylate) IPNs by Kim et al. (1976)

also suggested a two-phase structure and the phase inversion was observed to occur between 60 and 80% polyurethane concentration. More detailed morphological characterization of multiphase polymers by electron microscopy can be found in the literature (Thomas, 1977).

4.1.2 Survey of Mechanical and Thermal Studies

An ideal IPN should possess better mechanical and thermal properties than those of its components. In fact, the motivation of using IPNs is based on this hypothesis. In many cases, IPNs do show some enhancement in mechanical properties. However, the enhancement may occur only at a certain composition range. Beyond that range, a decrease of mechanical properties may occur. Figure 4.1 shows the measured tensile strength vs. composition for a series of polyurethane-epoxy SINs (Frisch et al., 1974). A maximum tensile strength occurred at 25% by weight of polyurethane, which was considerably higher than the tensile strength of its individual networks. A minimum, below the tensile strength of each individual network, occurred at 75% polyurethane. This finding implies the importance of the composition of IPN in controlling its mechanical properties. The enhancement of mechanical properties, together with the measured single glass transition temperature by DSC (Klempner and Frisch, 1970; Frisch et al., 1974) suggested that chain

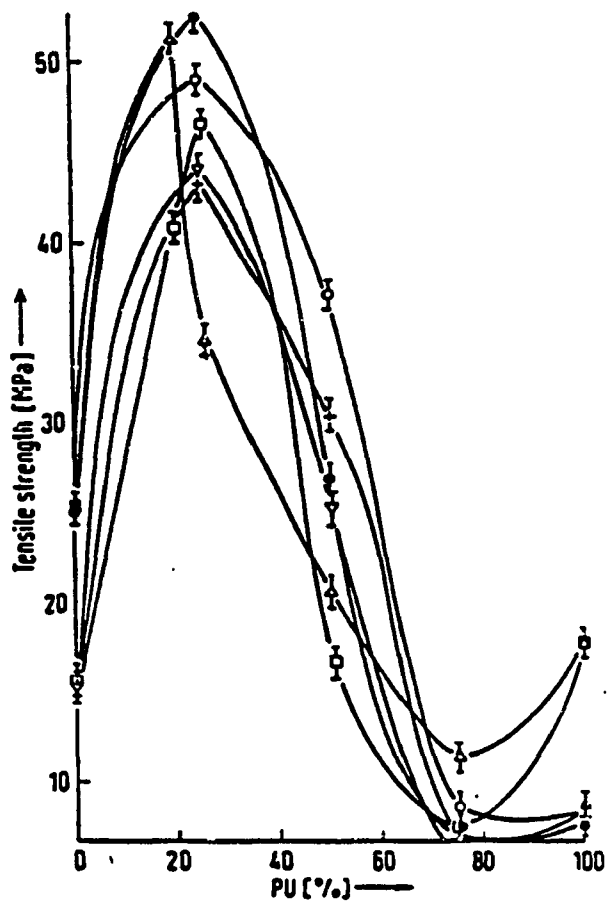


Figure 4.1 Tensile at break vs. polyurethane concentration for polyurethane/epoxy SINs (Frisch et al., 1974).

interpenetration, and consequently, an increase in crosslink density through physical chain entanglement must occur during the formation of polyurethane-epoxy IPNs. Measurements from thermogravimetric analysis (TGA) also showed an improved thermal resistance of polyurethane-epoxy IPNs (Frisch et al., 1974). For polyurethane-acrylic IPNs, the same maximum tensile strength was observed at PU/PAC = 80/20 by weight (Klempner, 1978). Morin et al. (1983) and Djomo et al. (1983) studied the polyurethane-PMMA IPNs. They found that, while most mechanical properties were fairly constant, the elongation at break decreased with increasing crosslink density of PMMA. The IPNs also became more brittle when crosslink density of PMMA was increased.

Several theoretical models were proposed to predict the mechanical properties of IPNs or other polymer blends. Allen et al. (1974) used a model proposed by Davies (1971) to predict the shear modulus of polyurethane/vinyl monomer interstitial polymers (a synonym of IPN used by Allen et al.). The equation used is

$$G^{1/3} = \phi_1 G_1^{1/3} + \phi_2 G_2^{1/3} \quad (4.5)$$

where G_i 's ($i = 1, 2$) are the shear modulus and ϕ_i 's are the volume fraction of individual networks. Equation (4.5) is derived on the basis of continuity of both phases. Applying Davies' theory (a non-interacting theory), they found the existence of particle-particle

interaction between polyurethane and polyvinyl molecules in the interdomain regions.

The Takayanagi's model (Takayanagi, 1964) has been applied to predict the mechanical behavior of polymer blends when the mechanical characteristics of the individual networks are known. The equation used in the model is

$$G^* = (1-\lambda)G_A^* + \lambda[(1-\phi)/G_A^* + \phi/G_B^*]^{-1} \quad (4.6)$$

where G_i^* are the moduli of the respective phases A and B, $\lambda\phi = V_B$, V_B is the volume fraction of the phase B, and λ and ϕ are parameters of the model. The equations for the real and imaginary components of the modulus of the composite, G' and G'' , are

$$G' = (1-\lambda)G_A' + \lambda X/(X^2 + Y^2) \quad (4.7)$$

$$G'' = (1-\lambda)G_A'' + \lambda Y/(X^2 + Y^2) \quad (4.8)$$

where $X = (1-\phi)G_A''/(G_A'^2 + G_A''^2) + [\phi G_B''/(G_B'^2 + G_B''^2)]$ (4.9)

and

$$Y = (1-\phi)G_A''/(G_A'^2 + G_A''^2) + [\phi G_B''/(G_B'^2 + G_B''^2)] \quad (4.10)$$

Rosovizky et al. (1979) applied this model to predict the dynamic Young's modulus of polyurethane-polyurethane acrylate IPNs and found

a pronounced two-phase behavior in the concentration range of polyurethane acrylate $\geq 50\%$, confirming the heterogeneous character of the IPN structure. Matsuo et al. (1970) used the same model to study the mechanical properties of polyacrylate-poly(urethane-urea) IPNs and found that the model fitted the G' reasonably well with appropriately adjusted parameters λ and ϕ .

Most researches on the morphological and mechanical properties of IPNs do not relate processing conditions to the properties of finished products. The fact that enhanced mechanical and thermal properties exist in most IPNs does not guarantee that a good property may be obtained for an IPN in any processing condition. The relative reaction rate, the chemical structure of constituent components, and the processing variables such as molding temperature and pressure, may all affect the morphology, and accordingly, the mechanical and thermal properties of an IPN. In this study, the morphology and the mechanical properties of polyurethane-polyester IPNs prepared by both transfer molding and RIM are investigated. These properties are then related to the processing variables such as molding temperature and mixing power. Other effects also studied are compound composition, reaction sequence, and crosslinking density.

4.2 EXPERIMENTAL

4.2.1 MATERIALS

The materials used in this study are listed in Table 4.1. The description and treatment of these materials are described in the preceding chapter. In the series of PDO-initiated IPNs (L/C, C/C, C/L, L/L), the first letter indicates the phase structure of polyurethane and the second letter indicates the phase structure of polyester. C is crosslinked structure; L is linear structure. The series RA, RB, and RC are MEKP/amine/Co-8 catalyzed IPN samples.

4.2.2 SAMPLE PREPARATION

A. Transfer Molding

Figure 4.2 shows the schematic of the transfer mold used to prepared IPN samples. The mold has a single cavity. The sprue plate is 0.635 cm thick, and has four conical sprues with an entrance diameters of 0.635 cm and an exit diameter of 0.127 cm. The spacer right below the sprue plate is 0.3175 cm thick and has a rectangular cavity of 10.16 x 15.24 cms. The plunger diameter is 3.81 cms. IPN components were first mixed in a suction flask by a magnetic stirrer until no bubble was observed. This bubble-free mixture was then transported to the mold cavity through the transfer pot. Once it was

Table 4.1 Recipe used in property-structure-processing relationships study of IPN

Ingredients	Sample DEsignation						
	L/C	C/C	C/L	L/L	RA	RB	RC
PU in IPN	Part by wt. in PU						
MDI (Dow 143L)	41	44	44	41	41	41	41
Polyol (UC T-2400)	48	--	--	48	48	48	48
Diol (Aldrich BDO)	11	--	--	11	11	11	11
Triol (UC T-310)	--	56	56	--	--	--	--
Catalyst (Lupersol T-12)	0.033	0.033	0.033	0.033	--	--	--
Structure	L	C	C	L	L	L	L
Polyester in IPN	Part by wt. in polyester						
Unsat. polyester (OCF P325)	67	67	--	--	67	67	67
Styrene	33	33	100	100	33	33	33
PDO	1.38	1.38	1.38	1.38	--	--	--
MEKP	--	--	--	--	0.23	0.7	1.15
Amine	--	--	--	--	0.11	0.33	0.55
Co-8	--	--	--	--	0.11	0.33	0.55
Structure	C	C	L	L	C	C	C

*C = Crosslinked structure

L = Linear structure

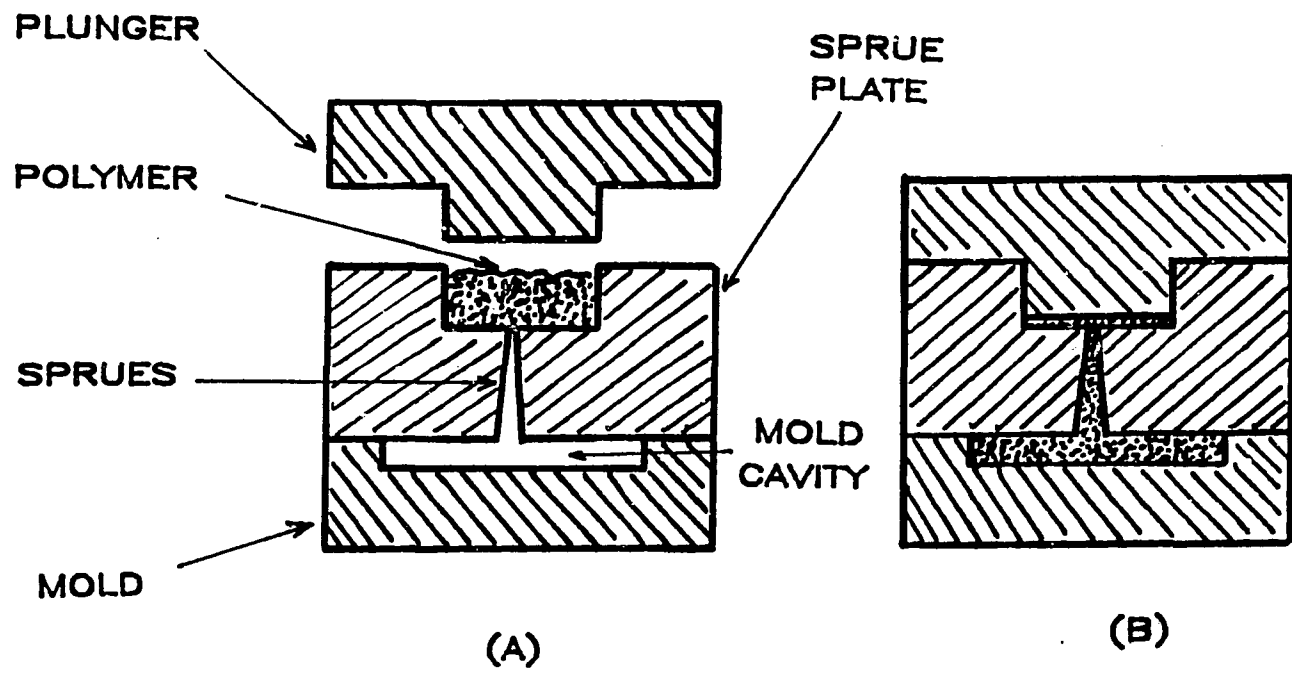


Figure 4.2 Schematic of the transfer mold. (A) before molding, (B) after molding.

in the mold, polymerization was allowed to proceed for two hours before demolding. Two molding temperatures were used: 80 °C and 120 °C. Half of the 80 °C-molded samples were further postcured at 120 °C for six hours. The concentrations of catalyst and initiator were chosen in such a way that the mixture would not reach gelation in at least two minutes which was required for material preparation (i.e., mixing and transfer molding). The transfer molding technology was found to be successful in the preparation of bubble-free samples.

B. Reaction Injection Molding

The procedure of reaction injection molding process is described in Chapter III. IPN samples from RIM were prepared using a rectangular mold of 15 x 3 x 0.3175 cm in size. The mold temperature was controlled at 120 °C. The samples were demolded after 2 hours in the mold.

4.2.3 METHODS OF MEASUREMENT

A. Transmission Electron Microscopy

The morphology of transfer molded IPN samples and samples from RIM was observed using a Philips EM-300 transmission electron microscope (TEM). The materials were prepared for the microscope by an LKB HT-2B ultramicrotome and stained with 1% osmium tetroxide

solution. A low temperature ultramicrotome unit (Ultracut E, Reichert-Jung) was used for soft samples like polyurethane and 75/25 IPNs. Samples were examined at a power of 60 KV at various magnifications.

B. Dynamic Mechanical Analysis

Dynamic mechanical analysis has been widely used in the study of polymer compatibility and rubber-glass transition. With this technique, the dynamic modulus can be measured as a function of temperature over a range of frequency (Nielsen, 1974; Ferry, 1980; Ward, 1983). The dynamic shear storage modulus (G') and the dynamic shear loss modulus (G'') can be obtained as a function of temperature at a fixed frequency.

$$G^* = G' + iG'' \quad (4.11)$$

where G^* is the complex shear modulus, G' is the real part of the modulus, G'' is the imaginary part of the modulus, and $i = (-1)^{1/2}$. The glass transition temperature T_g (or T_g 's) of the IPN is defined as a temperature corresponding to the maximum in G'' or $\tan\delta$ ($\tan\delta = G''/G'$), which marks the onset of main chain segmental mobility corresponding to the glass transition.

The glass transition behavior of IPNs and its individual networks are measured from dynamic mechanical analysis using a

Weissenberg Rheogoniometer (Model R18). Detailed experimental set-up and procedure can be found in the literature (Wang, 1985; Sangamo Controls Ltd.). The measurements were performed on solid IPN samples with 0.09 x 0.30 x 2.5 cm in size. Three torsion bars with specification of 27 (≥ 100 °C), 98 (10 ~ 100 °C), and 430 (-60 ~ 10 °C) dyne/cm²/micron were used between -60 and 130 °C at a frequency of 1 Hz. The temperature was controlled using an aqueous ethylene glycol solution and liquid nitrogen as heating/cooling media and was monitored by an Omega 871 digital thermometer. An IBM personal computer was linked to the Weissenberg Rheogoniometer for real time data acquisition (Dash-8, Metrabyte) with voltage ranging from -5 to 5 V. The temperature dependence of the storage modulus G' and the lose modulus G'' was measured and calculated.

C. Tensile Test

Tensile tests were carried out on an Instron tensile testing machine (Model 1137) at -2, 25 ,and 93 °C. Sample specimens were made with a heated die cutter to the dumbbell shape of 13.97 cms long and 2.54 cms wide with the narrow testing section 6.35 cms long and 1.27 cms wide. The thickness of the samples was 0.3175 cm. The specimen was stretched until failed. The crosshead speed of the tensile tester was set at 0.05 inch/min. Tensile properties were determined from the average of 3 to 5 specimens.

D. Thermal Analysis

The limiting conversions of molded parts were measured by a Perkin-Elmer differential scanning calorimeter (DSC-2C). The molded part was cut and weighed in a balance (Mettler, Model-80) with a weight in the range of 10 - 15 mg. This sample was then loaded into the sample pan of DSC. To check if residual activity existed, the reaction exotherm vs. temperature was carried out in the scanning mode with temperatures increasing from room temperature to 237 °C at 20 °C/min. Because 237 °C is far above the glass transition temperature of both polyurethane and polyester, the completion of polymerization was ensured. A second scanning run was conducted immediately after the first scanning run to determine the baseline. For IPNs, the limiting conversion is based on the polyester reaction only (Hsu and Lee, 1985). For TONE-0240 based IPNs, the crystallinity of polyurethane phase in the molded samples was also measured by DSC.

4.3 MORPHOLOGY AND DYNAMIC MECHANICAL PROPERTIES

To differentiate polyurethane from polyester in transmission electron microscopy, a staining technique using osmium tetroxide is applied. The osmium tetroxide technique was originally developed for rubberized polymers in which the C=C bonds of rubber phase are

stained. This technique gives excellent contrast of many multiphase polymers in electron microscopy (Keto, 1967). Generally speaking, it is possible to observe the microtexture of a two-phase polymer system under TEM if one component contains C=C, -OH, -NH₂, or -C-O-C- groups which can react with osmium tetroxide. Others such as C=N and styrene can only be slightly stained (Ninomi et al., 1975). In PU-PES IPNs, previous research work has shown that polyurethane can be stained by OsO₄ (Matsuo, 1970; Ninomi et al., 1975; Kim, 1976; Kircher 1979; Menges, 1984), although actual staining mechanism is still unknown. For a linear segmented polyurethane such as RIM elastomer, however, the hard segments which exhibit crystallinity, can not be stained by OsO₄ (Kim, 1976). This is probably due to the rigid crystalline structure of the hard segments which prohibit free diffusion of OsO₄ vapor into them.

For polyester, since most C=C bonds are transformed into C-C bonds, no segment in polyester phase should be greatly stained by OsO₄. The -OH and -COOH groups at the end of polyester molecule may also be stained by OsO₄ although the amount of these functional groups is relatively small compared to polyurethane (less than 4% by mole). Therefore, in analyzing the TEM picture of PU/PES IPNs, the dark areas (OsO₄ stained) indicate the polyurethane phase and the bright areas indicate the polyester phase in general.

4.3.1 A Comparison of Morphology of IPNs Prepared by Transfer Molding and RIM Processes

IPNs can be prepared with different degree of mechanical mixing. The effects of mixing on mechanical properties of various polymers have been studied previously (Silberberg and Han, 1978; Lee, 1981; Nguyen and Suh, 1986). Silberberg and Han (1978) studied the effect of intensity of agitation on the morphology of high impact polystyrene. Using phase-contrast microscopy as a way to measure rubber particle size, they related rubber particle size to impact and tensile properties. As expected, the rubber particle size decreased with increasing agitation. Lee (1981) pointed out that a minimum Reynolds number was required for a complete polymerization of polyurethane in RIM mixing. Nguyen and Suh (1986) found that increasing mixing of IPNs in RIM process (i.e., higher Reynolds number) shifted T_g 's of component networks to a single T_g , which was located between the T_g 's of component networks. This indicated that a phase interpenetration occurred for RIM molded polyurethane-polyester IPNs.

Shown in Figure 4.3 are micrographs of 50/50 IPNs processed by RIM and transfer molding. The transfer molding process represents a slow process; whereas the RIM process represents a fast process. In Figure 4.3, the RIM processed IPN has a more homogeneous matrix, indicating that phase interpenetration is better achieved in RIM

(A)



(B)

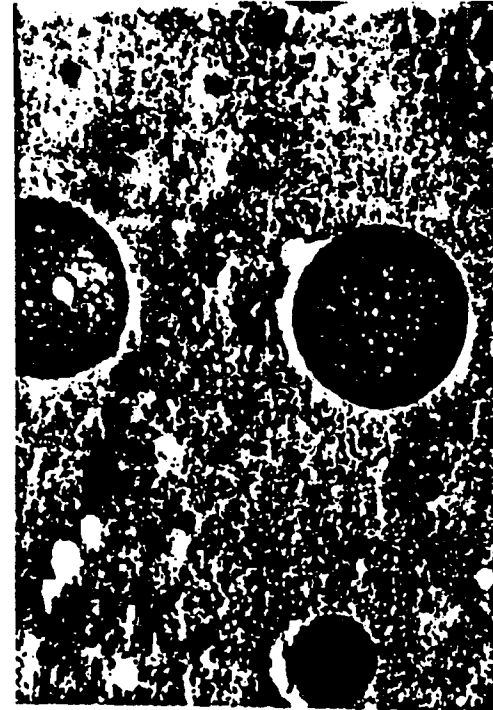


Figure 4.3 Transmission electron microscopies of 50/50 IPNs by (A) RIM, (B) transfer molding.

process. On the other hand, the transfer-molded IPN shows phase separation. The continuous phase is relatively brighter for the 120 °C-molded sample, indicating a high level of polyester. Both polyurethane and polyester are able to form dispersed droplets with diameters ranging from 0.5 to 4.0 μm for polyurethane and 0.1 to 0.6 μm for polyester. Within polyurethane droplets, one can clearly see some dispersed polyester spheres. Such a structure may be considered as a polyester-dominated matrix reinforced by both polyurethane and polyester spheres.

Shown in Figures 4.4 and 4.5 are results of dynamic mechanical analysis (DMA) of the 50/50 IPNs processed by transfer molding and RIM. Also included are the DMA spectra of neat polyurethane and polyester processed by transfer molding. Plots of storage modulus vs. temperature in Figure 4.4 suggest that the RIM-processed IPN has a better molecular mixing than the transfer-molded IPN. Unlike the transfer-molded IPN which shows a sharp drop of G' at about 60 °C (Figure 4.4), the RIM-mixed IPN has a gradual transition in the temperature range tested. The $\tan\delta$ vs. temperature plots shown in Figure 4.5 indicate that there are two T_g 's for the segmented polyurethane phase, one at 10 °C (the soft segment) and the other at 60 °C (the hard segment). The polyester phase has a single T_g at 95 °C. For IPN processed by transfer molding, there are three T_g 's located at 10 °C, 55 °C, and 93 °C respectively. These T_g 's correspond to those of its individual networks. In other words, the

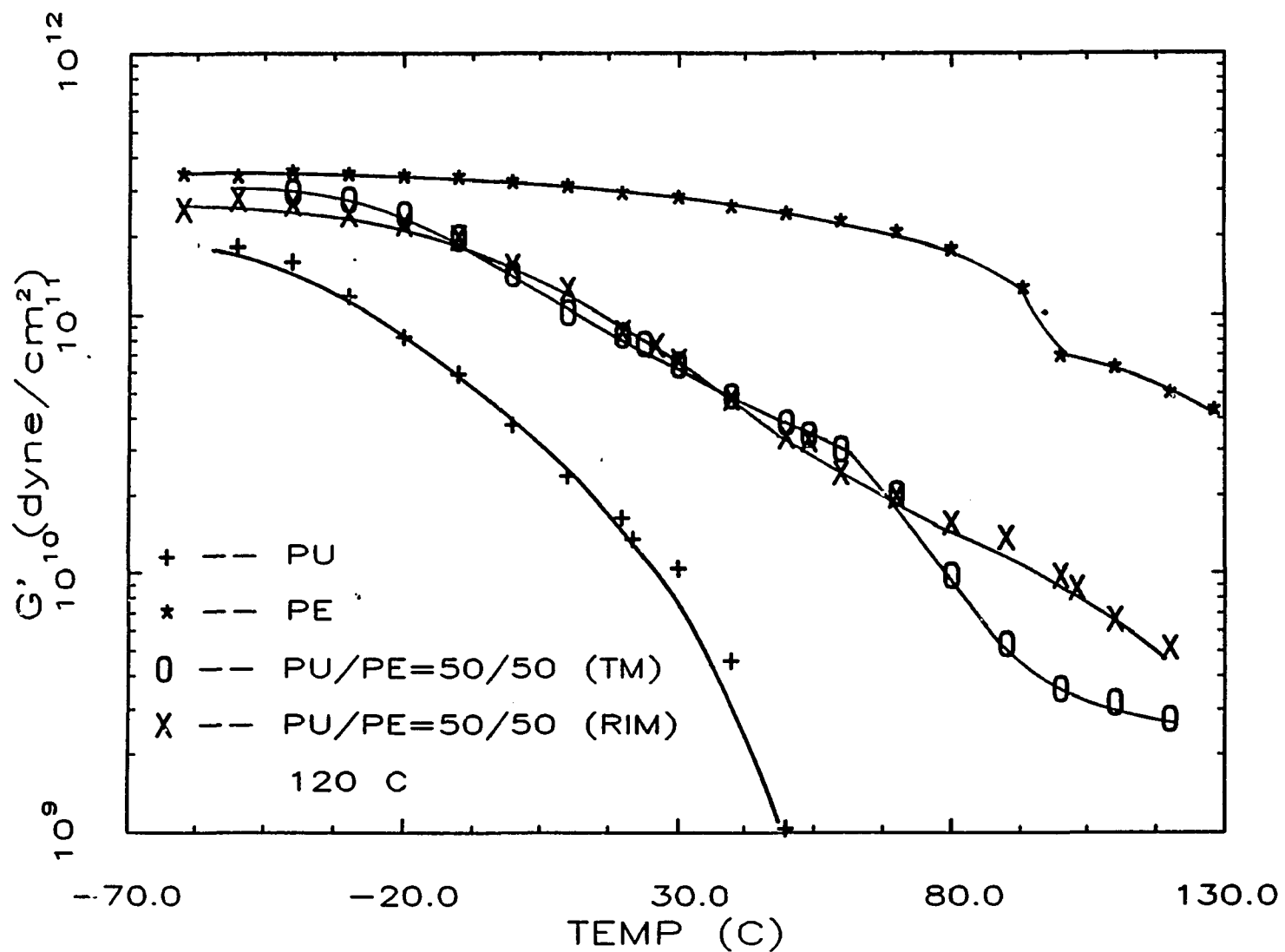


Figure 4.4 Dependence of storage modulus G' on temperature of 50/50 IPN by transfer molding and RIM. Individual networks molded by transfer molding.

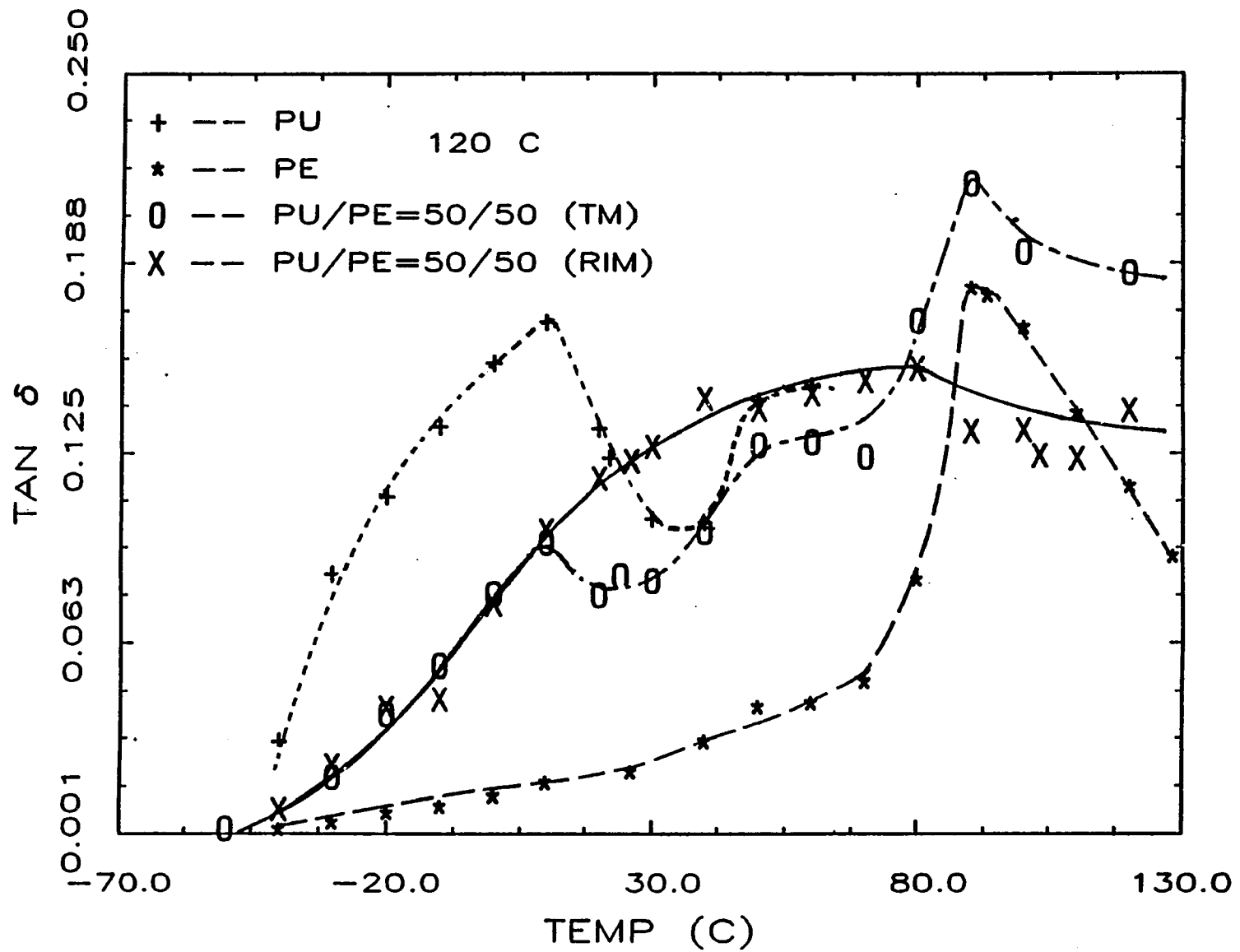


Figure 4.5 Dependence of $\tan \delta$ on temperature of 50/50 IPNs by transfer molding and RIM at 120 °C.

transfer-molded IPN possesses phase separation, much like the mechanically blended two-phase polymers. The RIM-molded IPN, however, does not show any distinguishable T_g 's. Instead, a broad $\tan\delta$ peak exists from 40 to 80 °C, which again implies a strong phase mixing between the two constituent polymers. These results suggest that the morphology and mechanical properties of finished IPN products may be greatly affected by the processing method even with the same polymer composition.

4.3.2 Effect of Molding Temperature

Figure 4.6 shows the transmission electron micrographs of 50/50 polyurethane/polyester IPNs transfer molded at 80 °C and 120 °C respectively. For the 80 °C-molded sample, the continuous phase mainly consists of polyurethane because it reacted first, while polyester tends to form large dispersed phase with diameter ranging from 1.0 to 2.0 μm . Within polyester droplets, there is a substantial amount of polyurethane forming small droplets. The overall structure may be considered as a polyester sphere reinforced polyurethane matrix. On the other hand, the 120 °C-molded sample resembles more a polyester dominated matrix reinforced by polyurethane droplets.

These observations suggest that processing temperature has a profound effect on IPN's morphology. Generally speaking, higher

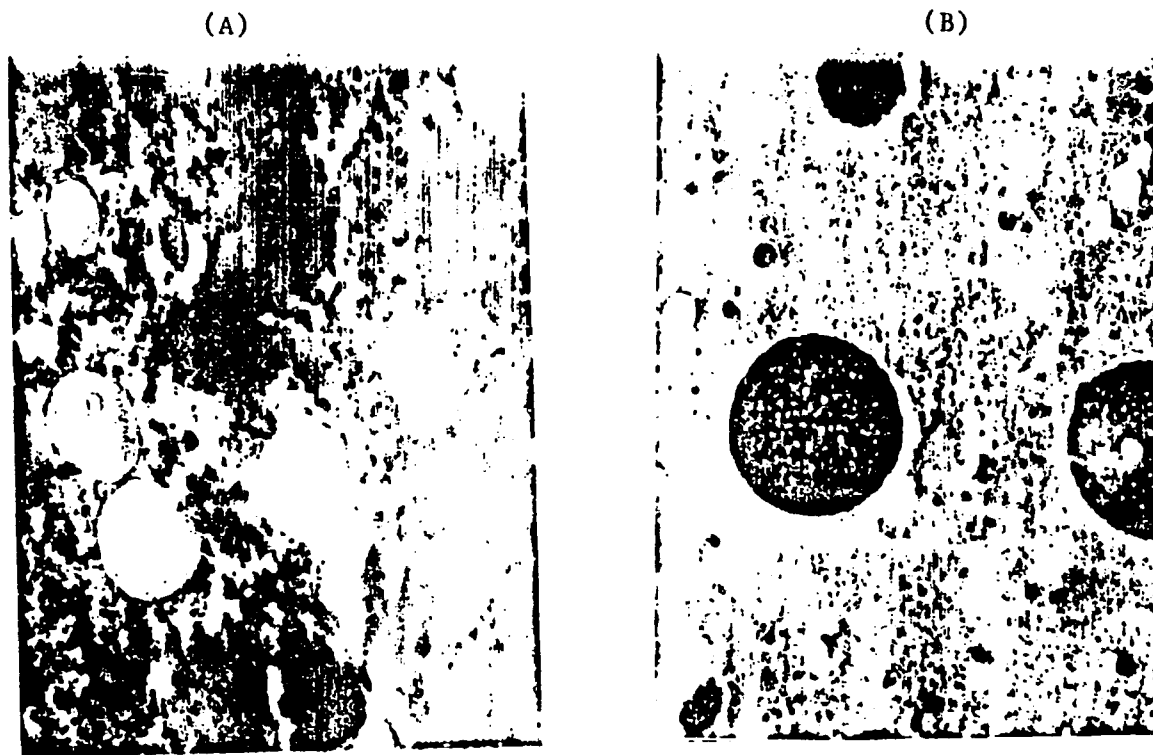


Figure 4.6 Transmission electron microscopies of 50/50 IPNs transfer molded at (A) 80 °C, and (B) 120 °C.

molding temperature allows the two polymerizations in an IPN to occur simultaneously, which results in a more polyester contained continuous phase and smaller domain size of polyester. Same observation has been found in the literature for epoxy/acrylic SINs (Touhsaent et al., 1974). Other IPNs in this study (i.e., 75/25 and 25/75 IPNs) also show the same observations when comparison is made between 80 °C and 120 °C -molded samples (i.e., Figure 4.8 to Figure 4.11).

4.3.3 Effect of Compound Composition

Two sets of IPNs are analyzed in this section: the 80 °C and the 120 °C-molded IPNs. Shown in Figure 4.7 are micrographs of 80 °C-molded IPN samples with various compositions. The micrograph of the 75/25 IPN shows a polyurethane-dominated matrix and a dispersed polyester phase with average domain size of 2.0 μm . Increasing the polyester content to 50%, the 50/50 IPN possesses a well dispersed polyester phase in the continuous polyurethane matrix. The domain size of polyester ranges from 1.0 to 2.0 μm . As polyester content is further increased to 75%, the polyurethane phase tends to become dispersed with particle sizes in the order of 0.1 μm . There are also several large polyester-swollen polyurethane droplets with size

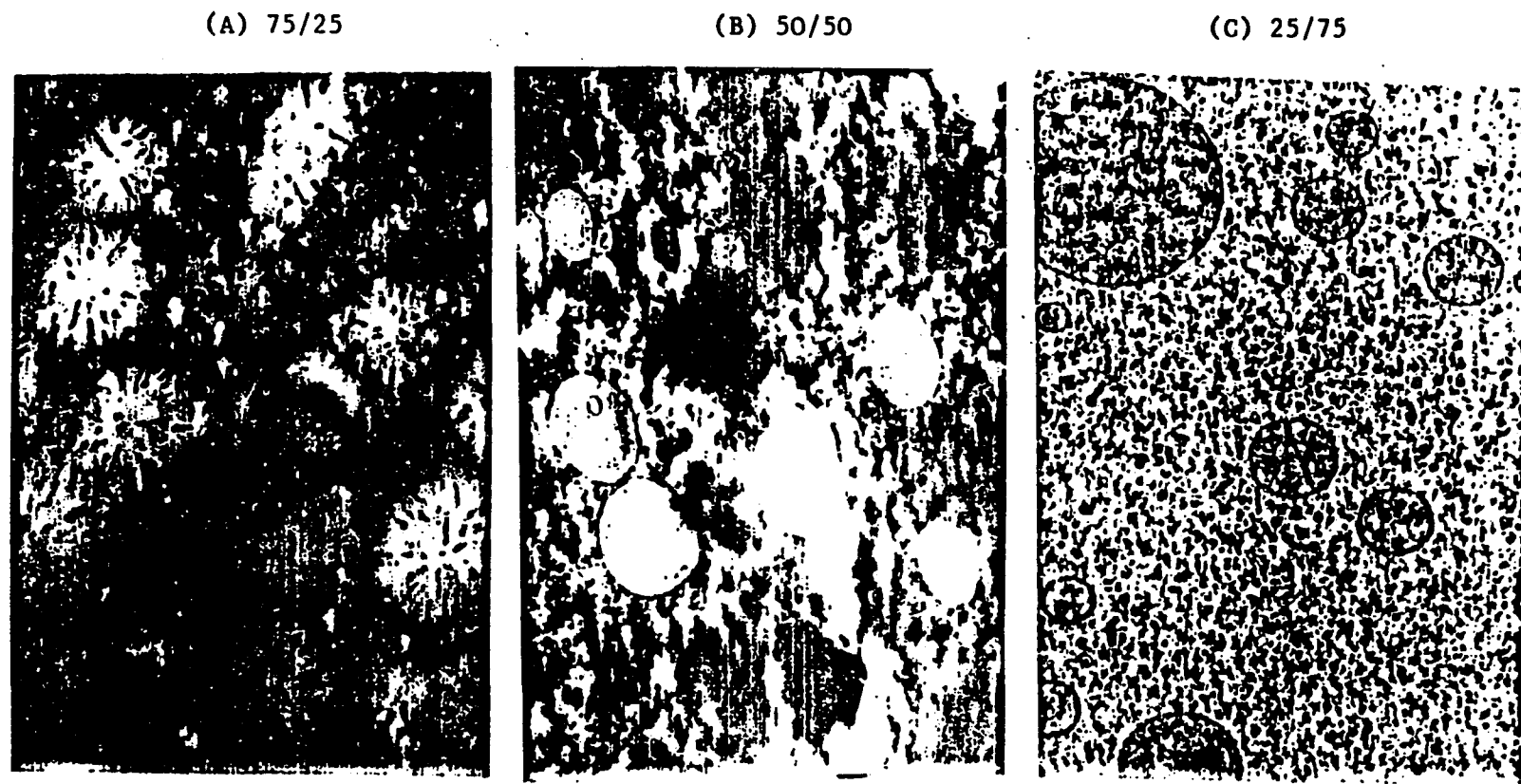


Figure 4.7 Transmission electron microscopies of 80 °C-transfer molded IPN samples with compositions of (A) 75/25, (B) 50/50, and (C) 25/75.

ranging from 1.0 to several μm . The matrix is primarily polyester-dominated. These observations suggest that phase inversion must occur between 50/50 and 25/75 composition.

The temperature dependence of the dynamic storage modulus (G') and the $\tan\delta$ of three 80 °C-transfer molded IPNs (PU/PES = 75/25, 50/50, and 25/75) are shown in Figures 4.8 and 4.9 respectively. Plots of storage modulus vs. temperature in Figure 4.8 show that the IPNs with more polyester content has a higher G' than those IPNs with more polyurethane. The $\tan\delta$ curve of 75/25 IPN shows a T_g at 10 °C and a T_g at about 53 °C, both are characteristic of the segmented polyurethane. The T_g of polyester phase in the 75/25 IPN could not be obtained since the sample was too soft to conduct DMA measurement when testing temperature exceeded 60 °C. The 50/50 IPN has T_g 's at about 5 °C, 30 °C (soft and hard domains of polyurethane), and 80 °C (polyester). The 25/75 IPN has two T_g 's at -6 °C and 25 °C (soft and hard domains), and a sharp T_g at 83 °C (polyester). In general, as polyurethane content in IPN increases, the T_g 's of both soft and hard domains in polyurethane increase and approach the T_g 's of pure polyurethane (i.e., see Figure 4.5); while the T_g of polyester decreases, deviated more from the T_g of pure polyester. The increase of T_g 's in polyurethane and the decrease of T_g in polyester as the polyurethane content in IPN is increased are indications of phase interpenetration in IPN. The $\tan\delta$ curve of the 25/75 IPN resembles that of pure polyester, while the $\tan\delta$ curve of

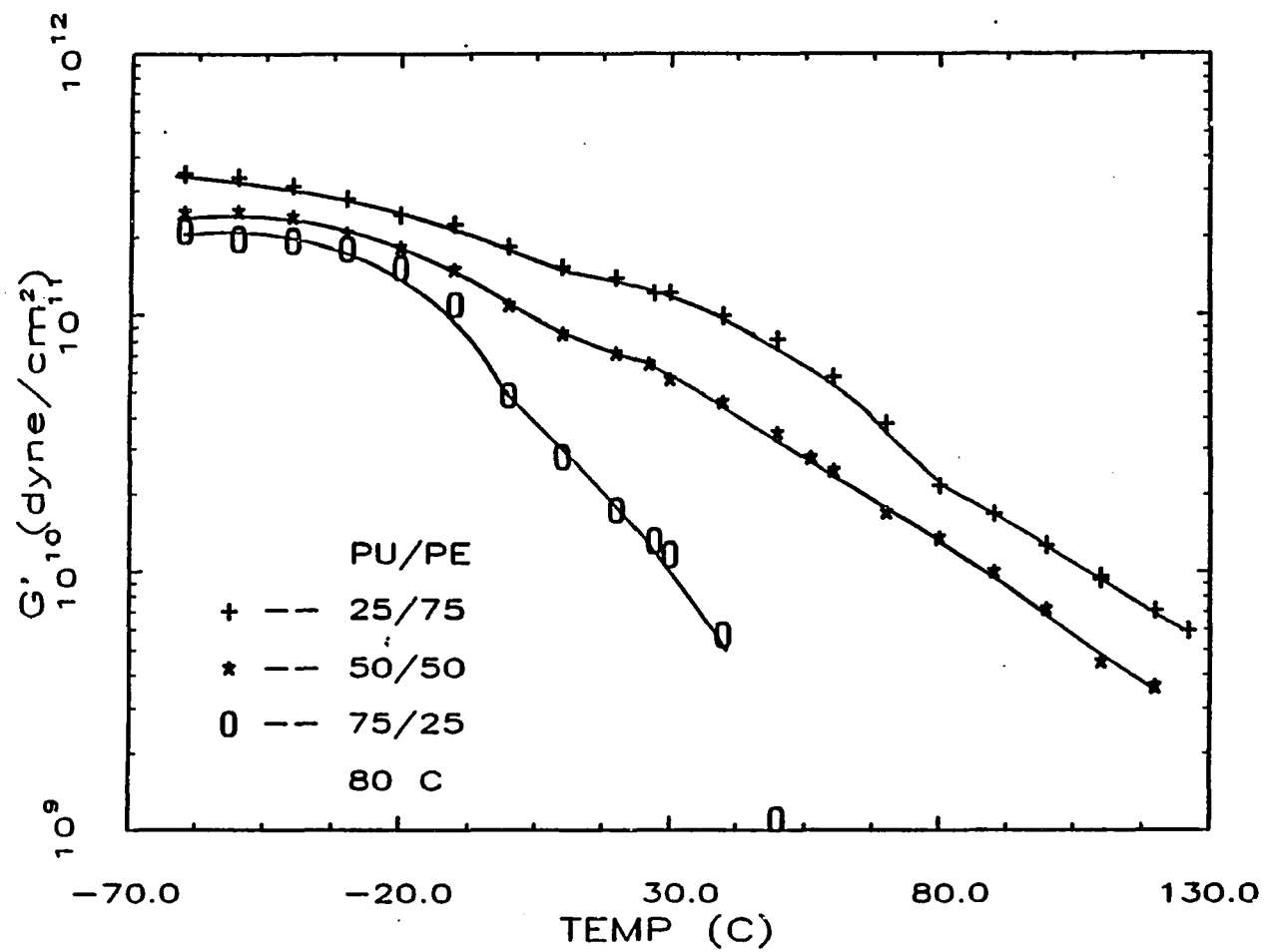


Figure 4.8 Dependence of storage modulus G' on temperature of 80 °C-transfer molded IPNs with three compositions.

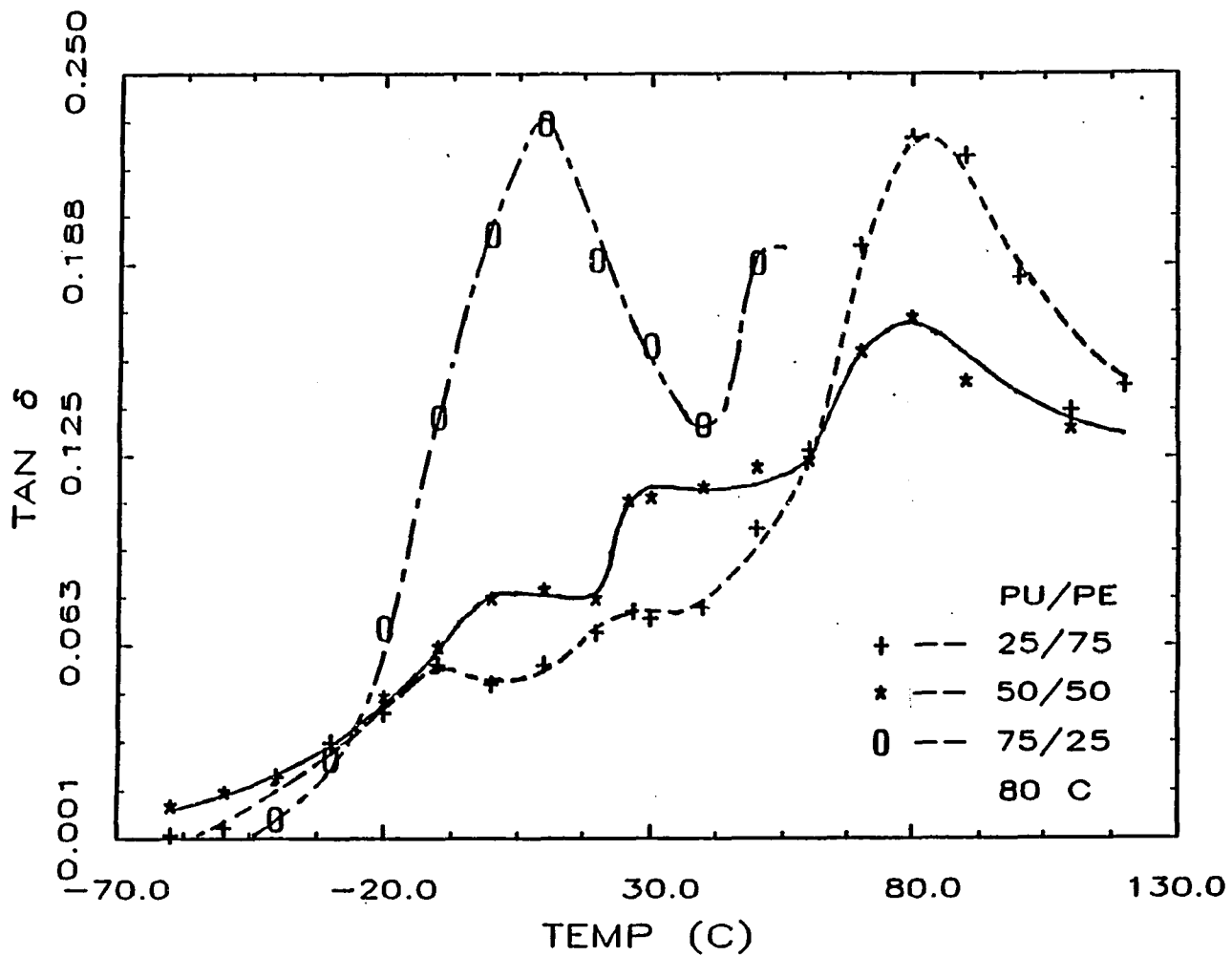


Figure 4.9 Dependence of $\tan\delta$ on temperature of 80°C-transfer molded IPNs with three compositions.

the 75/25 IPN resembles that of pure polyurethane. This further confirms the result from TEM (Figure 4.8), in which the continuous phase is the major component of an IPN.

Electron micrographs of 120 °C-molded IPN samples with three compositions are presented in Figure 4.10. The 75/25 IPN has a continuous polyurethane phase and polyester particles of about 0.5 μm . One can see that the dispersed phase consists of both polyurethane and polyester droplets. The continuous phase is not well defined. When the polyester content is increased to 50%, several large polyurethane droplets are formed. These particles have sizes ranging from 1.0 to 3.0 μm . One can also observe a large amount of small polyester particles (0.5 μm or less) distributed among the very large polyurethane particles. The matrix is primarily polyester-dominated. The 25/75 IPN has a continuous polyester phase. The dispersed phase consists of both polyurethane and polyester of about 0.5 μm in diameter. From this observation, one can conclude that phase inversion occurs at a composition between 75/25 and 50/50.

4.3.4 Effect of Reaction Sequence

Although the IPN samples produced by transfer molding were prepared with the same extent of mixing, their morphology can be different if the samples experienced different thermal history. This

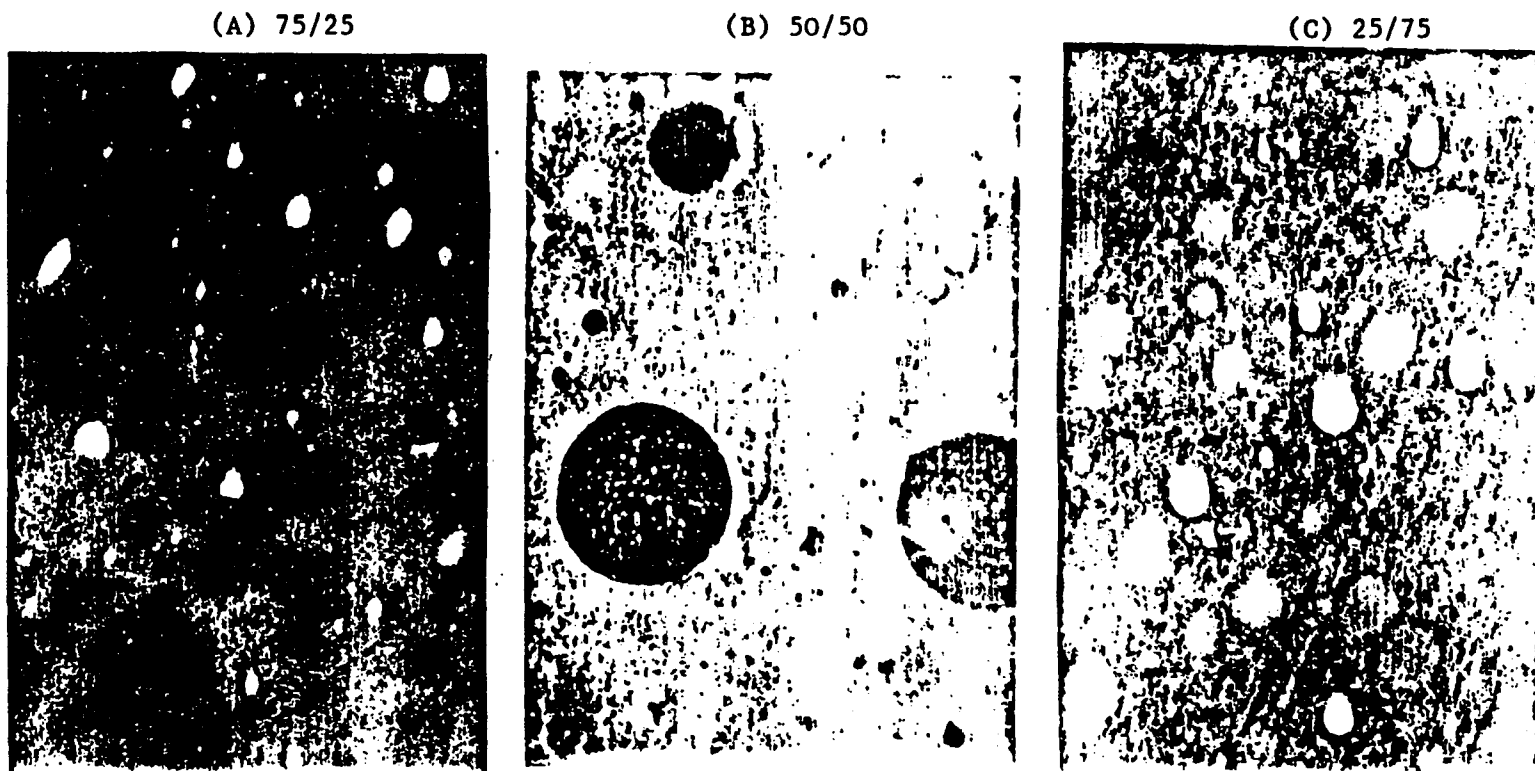


Figure 4.10 Transmission electron microscopy of 120 °C-transfer molded IPN samples with compositions of (A) 75/25, (B) 50/50, and (C) 25/75.

has been shown in the section of temperature effect since thermal history can have an effect on the reaction sequence in an IPN. Another way to change the reaction sequence is by employing different initiators for polyester reaction. In this study, PDO was replaced by a combination of MEKP, a tertiary amine, and cobalt naphthanate (Co-8), a reduction-oxidation type low temperature initiator. Figure 4.11 shows TEM pictures of two 50/50 IPNs transfer molded at 80 °C with different redox initiator concentrations. The domain size of polyester is greatly reduced as the MEKP/amine/Co-8 concentration is increased three times. At low MEKP/amine/Co-8 concentration, the domain of polyester in a continuous polyurethane phase is clearly defined. At high MEKP/amine/Co-8 concentration, not only does the polyester domain become smaller, but some polyurethanes are also excluded from its continuous matrix. With mixing effect being equal, the earlier polymerization of polyester in IPN prevents polyurethane phase from forming continuous matrix. The dark particles in Figure 4.11B are polyurethane particles which are excluded as a result of early polyester polymerization.

4.3.5 Crosslinking Effect

As the two reactions in an IPN become simultaneous at a molding temperature of 120 °C, the physical structure of polyurethane could be a major factor in controlling IPN's morphology. When the

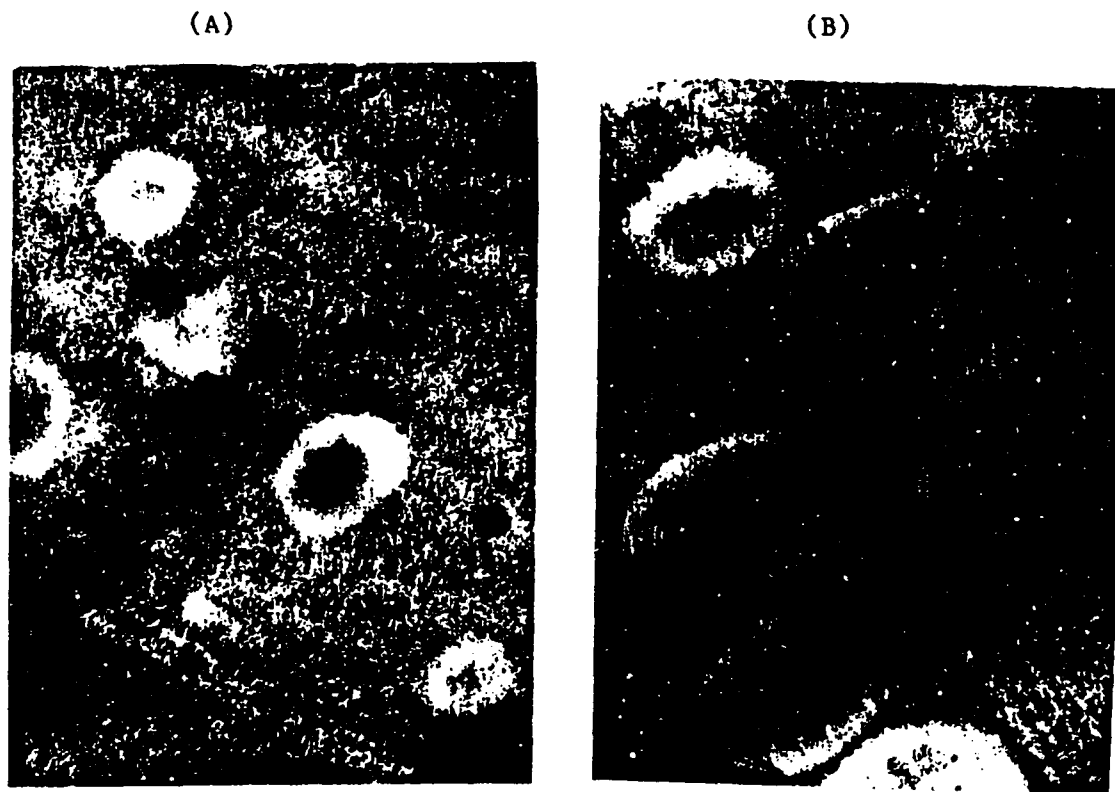


Figure 4.11 Transmission electron microscopies of 80 °C-transfer molded MEKP/amine/Co-8-initiated 50/50 IPNs at (A) 2.0% MEKP, 0.67% amine, and 0.67% Co-8, (B) 0.67% MEKP, 0.22% amine, and 0.22% Co-8.

linear thermoplastic polyurethane is replaced by a crosslinked thermosetting polyurethane, the particle size of polyurethane becomes smaller, tighter, and well dispersed (Figure 4.12, 50/50 IPNs, molded at 120 °C). The IPN resembles a polyurethane-reinforced polyester with polyurethane particles of 0.5 μm . Same experimental results were reported in the literature for PU/PMMA IPNs (Kim et al., 1976).

4.4 TENSILE PROPERTIES

Figure 4.13 shows typical stress-strain curves of a TONE-0240 based polyurethane, polyester, and their 50/50 IPN (L/C sample, PU/PES = 50/50) tested at 25 °C. As expected, the rigid polyester has a high tensile modulus and strength but very low elongation, whereas the elastomeric polyurethane shows a much lower tensile strength but a longer elongation. IPN has a stress-strain behavior between those of its constituent polymers.

4.4.1 Compositional and Temperature Effects

Figure 4.14 shows the compositional effect on the tensile strength of 80 °C-molded samples tested at 25 °C, along with their limiting conversions measured by DSC. The dashed line indicates a

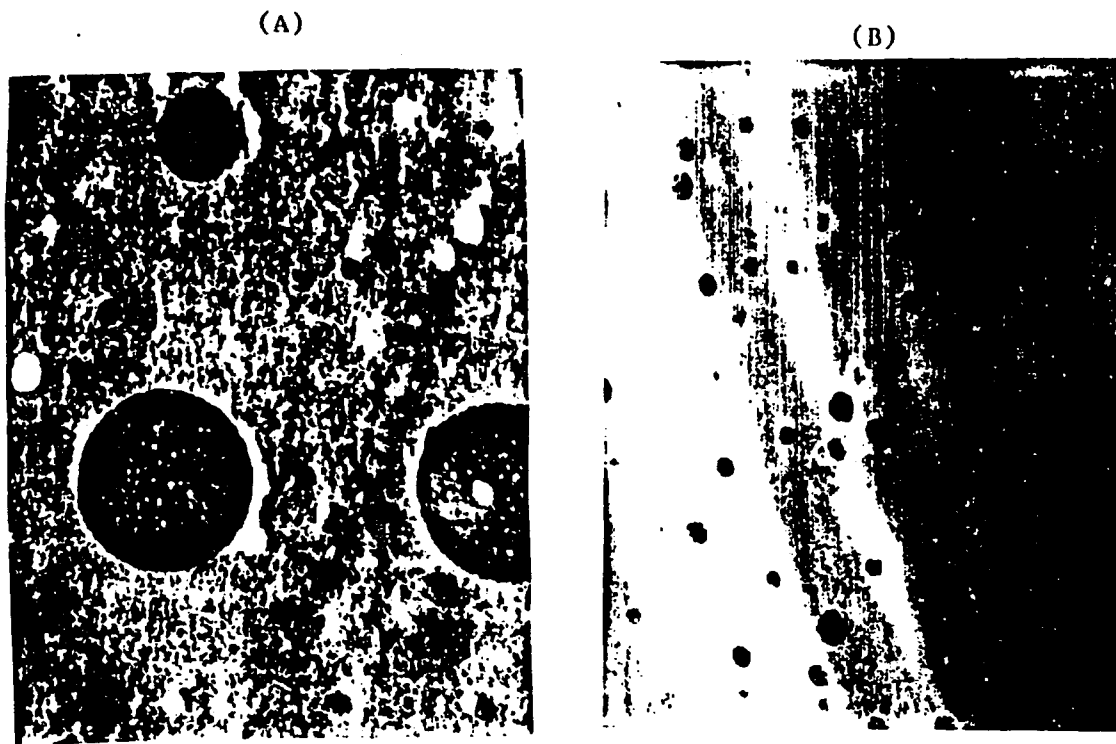


Figure 4.12 Transmission electron microscopies showing the crosslinking effect of 120 °C-molded 50/50 IPNs, (A) with linear polyurethane, (B) with crosslinked polyurethane.

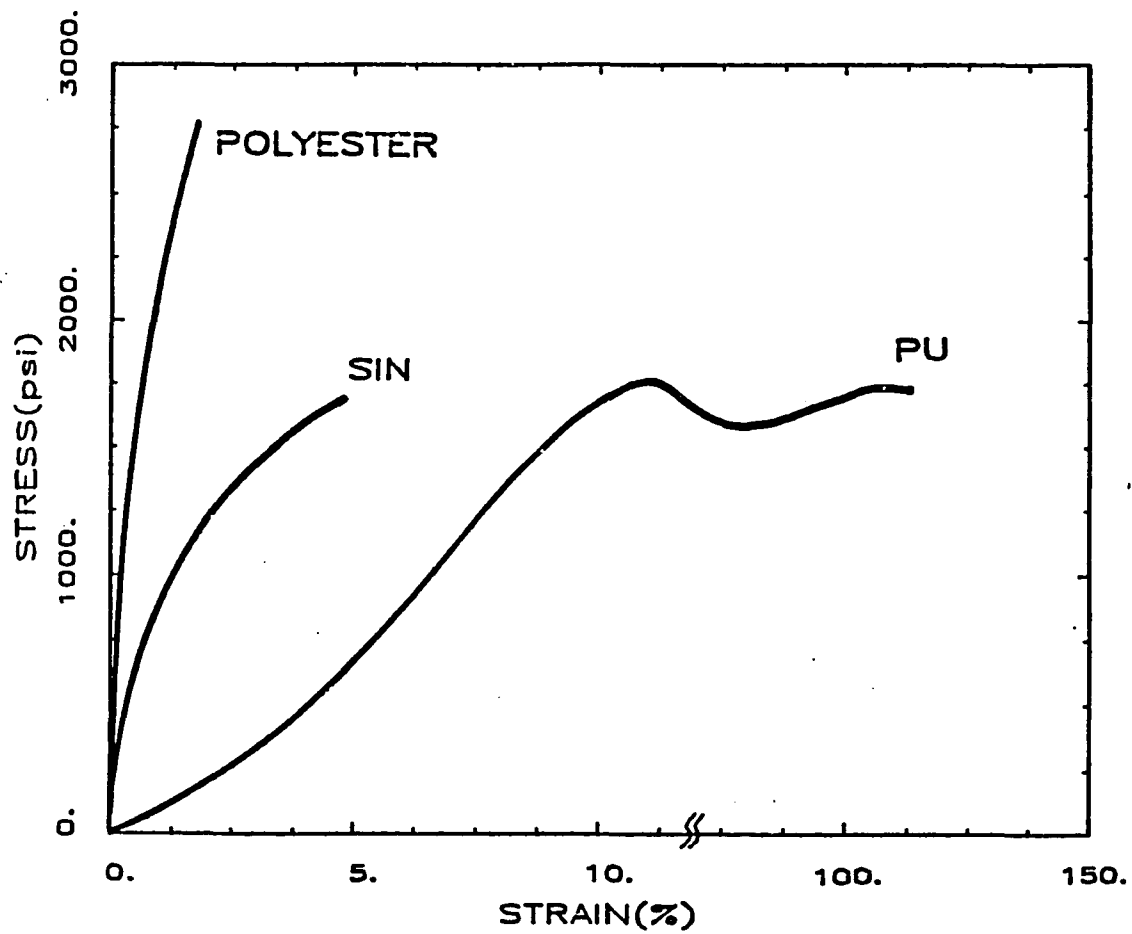


Figure 4.13 Typical stress-strain curves of linear polyurethane, polyester, and IPN (L/C sample, 50/50) tested at 25 °C. Samples were molded at 80 °C and postcured at 120 °C for 6 hours.

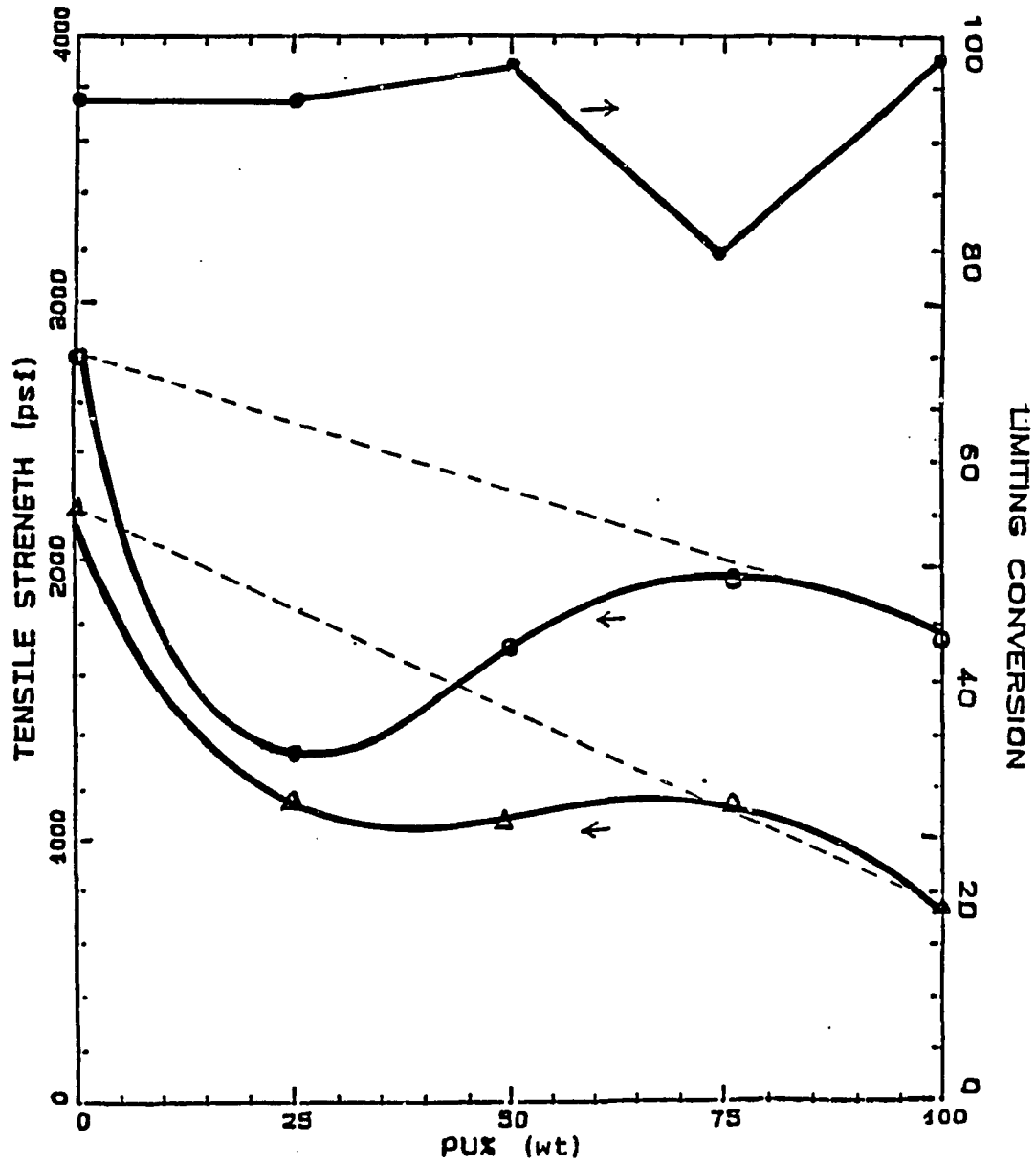


Figure 4.14 Tensile strength and limiting conversion of 80 °C-transfer molded L/C samples before (Δ) and after (\circ) postcure. Test temperature is 25 °C.

relationship based on the additivity rule. The 80 °C-molded L/C samples show a negative deviation of tensile strength from its linear average. DSC measurement of residual activity of these samples is very similar to that measured in the thermal kinetic study, which shows that polymerization is incomplete for all samples molded at 80 °C. The IPN with 75% polyurethane has the lowest limiting conversion among all samples. To improve the physical properties, the 80 °C-molded samples were postcured at 120 °C for 6 hours. In general, improved tensile strength is observed for all samples, as shown in Figure 4.14, but the negative deviation from linear average still exists. Numerical data from tensile tests are summarized in Table 4.2. The improvement is more significant for samples with a higher polyurethane content. DSC measurements of crystallinity of polyurethane phase in the molded and postcured L/C samples are shown in Figures 4.15 and 4.16. Apparently, the crystallinity structure of polyurethane phase is composition dependent. Adding polyester to the reaction system sharply reduces the amount of crystallinity. The melting peak of polyurethane crystal shifts to a higher temperature after postcure.

The results shown in Figures 4.14 through 4.16 indicate that the mechanical properties of IPN and their constituent polymers depend on the conversion and morphology of the molded parts. At a molding temperature of 80 °C, polymerization cannot reach completion and the final conversion is composition dependent (Fara, 1972;

Table 4.2 Tensile strength and ultimate elongation of 80 °C-transfer molded and 120 °C-postcured I/C samples tested at three different temperatures.

<u>Tensile Strength (psi)</u>	<u>PU Content</u>				
<u>Temperature (°C)</u>	<u>0%</u>	<u>25%</u>	<u>50%</u>	<u>75%</u>	<u>100%</u>
-2	3044	1808	2148	2675	2739
25	2790	1318	1623	1933	1733
93	2509	998	969	1043	640
$\frac{-2}{93}$	1.2	1.8	2.2	2.6	4.3

<u>Elongation (%)</u>					
<u>Temperature (°C)</u>					
-2	1.4	1.9	3.9	21.0	31.0
25	1.8	1.6	4.3	76.5	112.3
93	2.5	4.6	13.2	90.0	164.0
$\frac{-2}{93}$	0.6	0.4	0.3	0.23	0.2

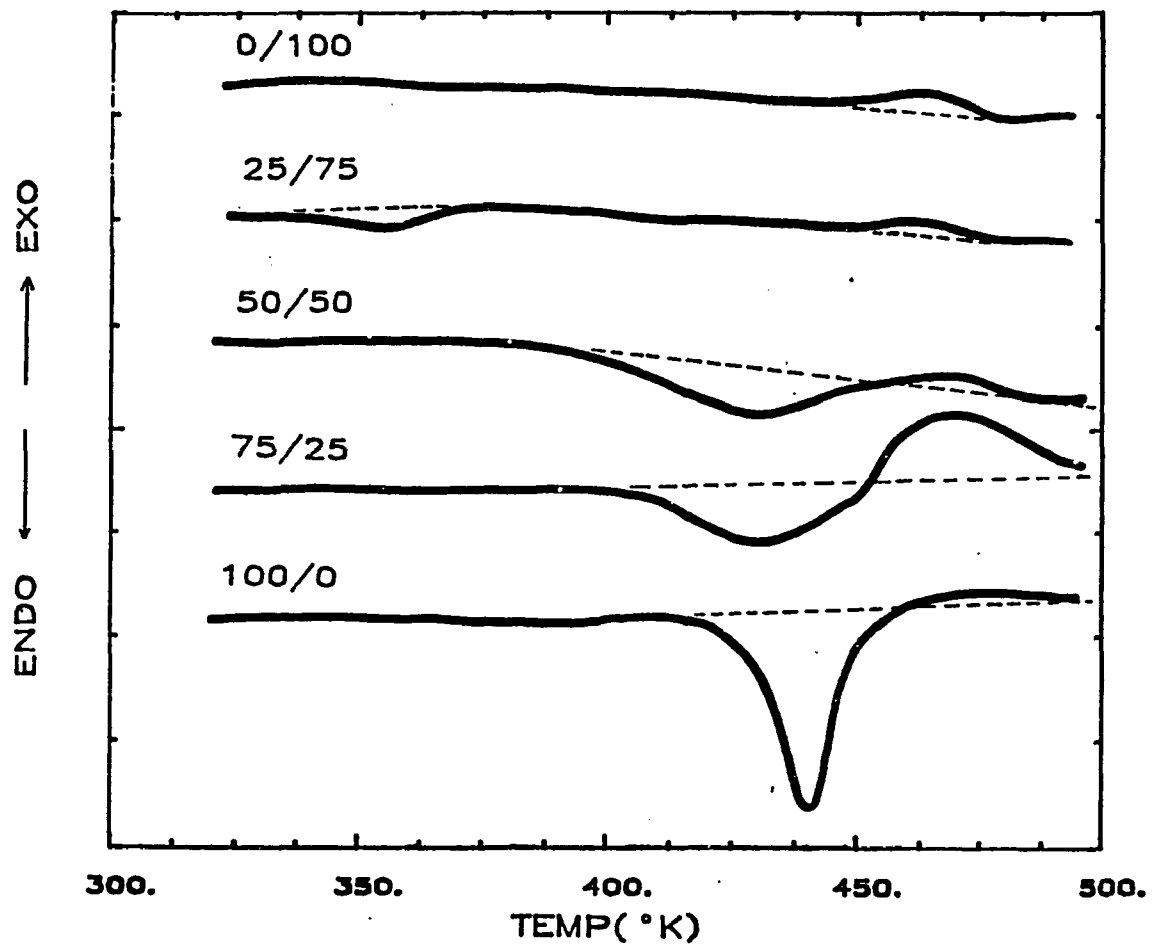


Figure 4.15 Scanning DSC results of 80 °C-transfer molded L/C samples.

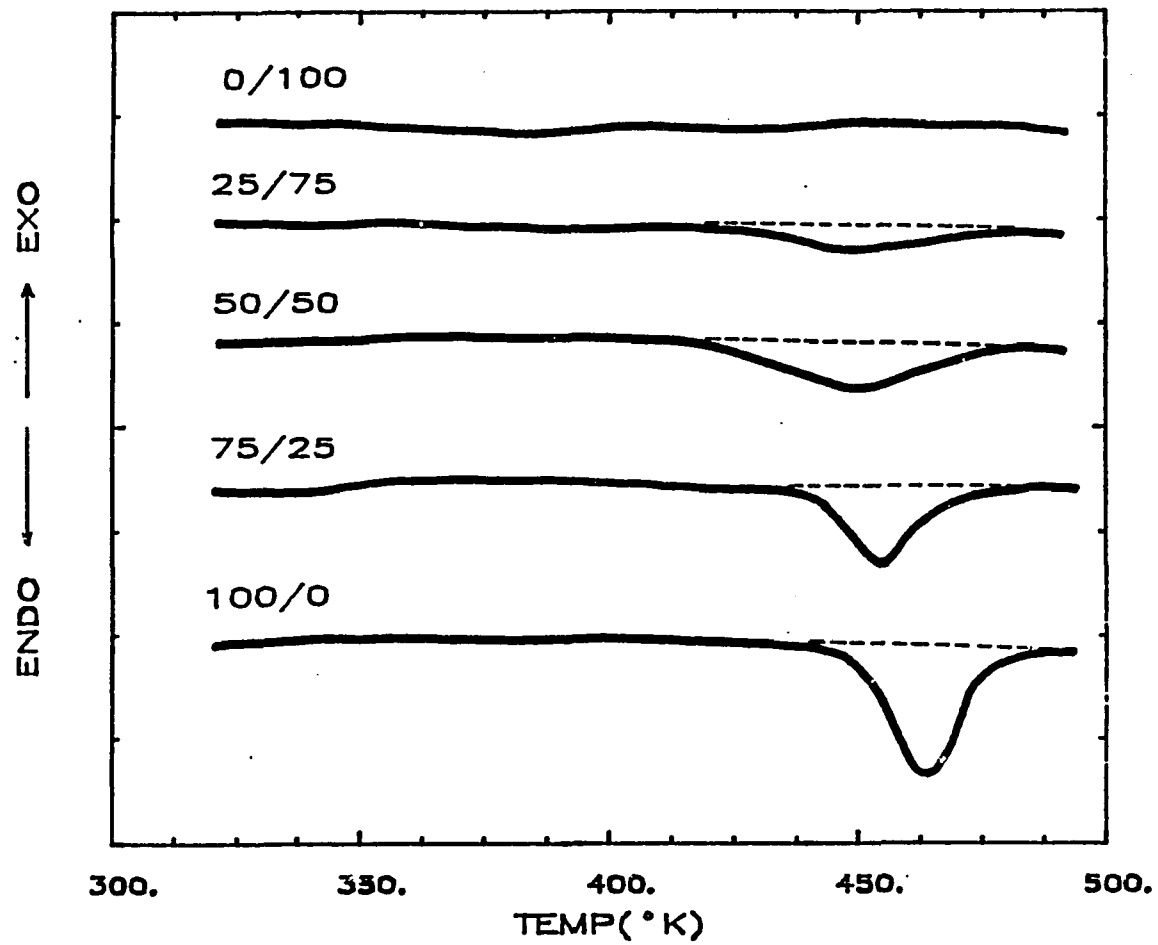


Figure 4.16 Scanning DSC results of 80 °C-transfer molded L/C samples after postcure treatment.

Gilliam, 1979; Huang and Lee, 1985). Postcure has an effect of promoting the reaction to a higher conversion, which improves the mechanical properties of the molded parts. It is evident that the tensile strength of postcured samples is higher than that of unpostcured samples for all composition. For IPN and pure polyurethane, the morphological change due to postcure treatment may also play an important role in the improvement of tensile strength. It is found that postcure has the effect of shifting the melting peak of polyurethane phase from a lower temperature to a higher temperature, which implies a more stable crystallinity structure (Fridman et al., 1980) in polyurethane phase. Accordingly, increase of tensile strength is also more significant for IPN samples with a higher polyurethane content.

When the mold temperature was raised to 120 °C, tensile strength was greatly improved. A comparison is made between 80 and 120 °C molded L/C samples tested at 25 °C, as shown in Figure 4.17. Unlike the 80 °C-molded samples, the 120 °C molded IPNs show a positive deviation of tensile strength from linear additivity. Higher molding temperature, however, does not greatly affect tensile strength of constituent polymers. From previous thermal kinetic study (Hsu and Lee, 1985), it is noted that molding temperature has a significant effect on polymerization rate of IPN. For PDO-initiated polyester, a temperature of 100 °C or higher is required to generate a high reaction rate, but polyurethane polymerization is

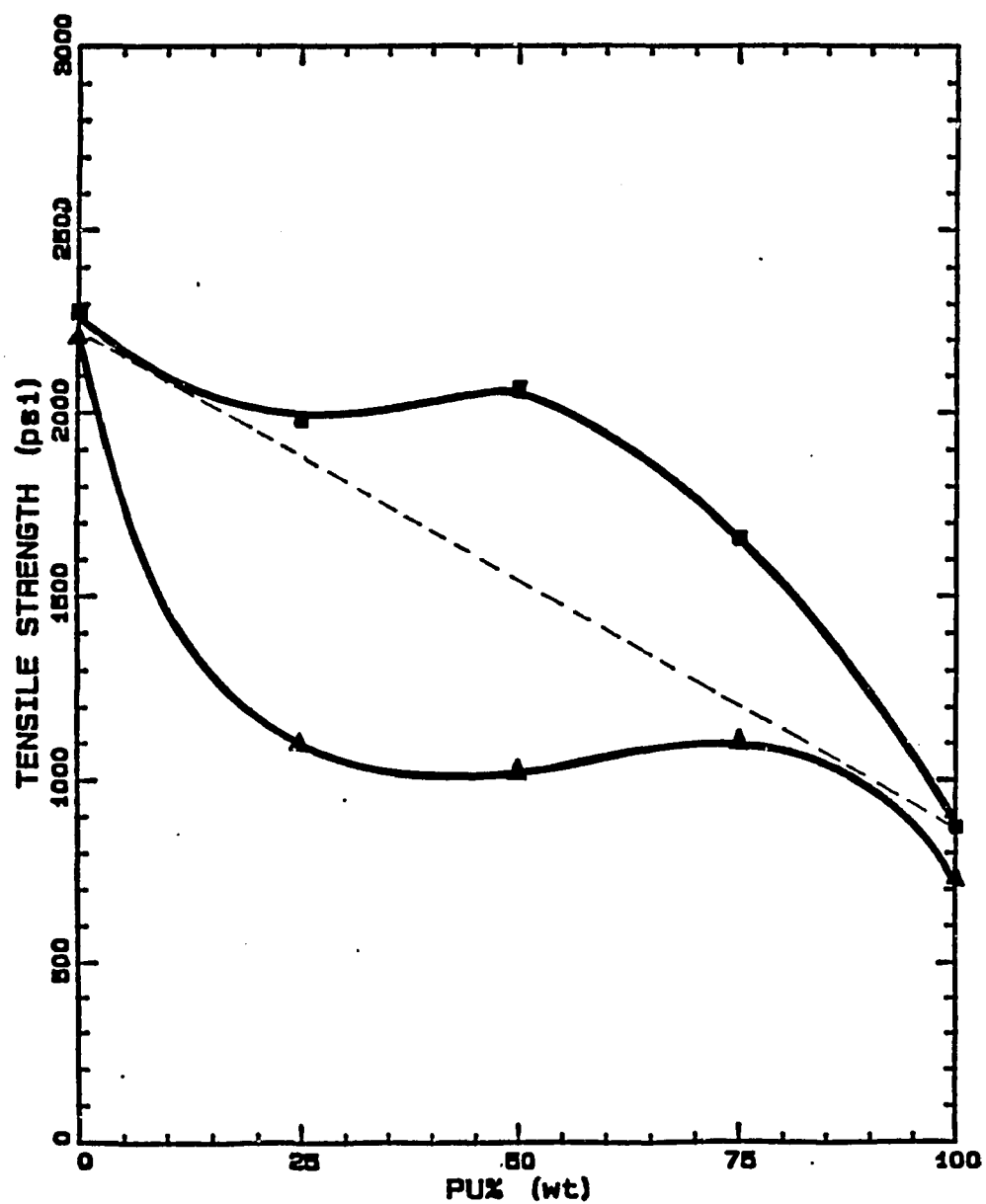


Figure 4.17 Comparison of tensile strength of 80 °C- (Δ) and 120 °C (■) transfer molded L/C samples. Test temperature at 25 °C.

relatively fast even at low temperature since the reaction is initiated by mixing. For a polyurethane-polyester IPN reaction at 80 °C, polymerization of urethane resin occurs much earlier than that of polyester. DSC results show that residual activities exist in the 80 °C molded samples (see Figure 4.15). At 120 °C, both urethane and ester reactions occur almost at the same time (Hsu and Lee, 1985). DSC results indicate all samples reach complete reaction. This seems to suggest that a higher final conversion and simultaneous reactions of urethane and ester are very helpful for increasing the mechanical properties of IPN.

The tensile strength of the 120 °C-molded 50/50 IPN is close to that of the pure polyester. The TEM picture of 50/50 IPN suggests that the 120 °C transfer molded IPN sample resembles a polyurethane reinforced polyester. On the other hand, the tensile strength of the 80 °C-molded 50/50 IPN is close to that of the pure polyurethane. Again, the TEM picture described in Figure 4.6 shows that this IPN resembles a polyester reinforced polyurethane.

DSC measurements of crystallinity of 120 °C molded L/C samples are shown in Figure 4.18. Compared to Figures 4.15 and 4.16, higher molding temperature tends to broaden the melting peak of polyurethane phase but does not shift the melting peak to a higher temperature as in the case of postcure treatment.

Thermal stability is a very important consideration for polymeric materials used in the automobile industry. To explore this

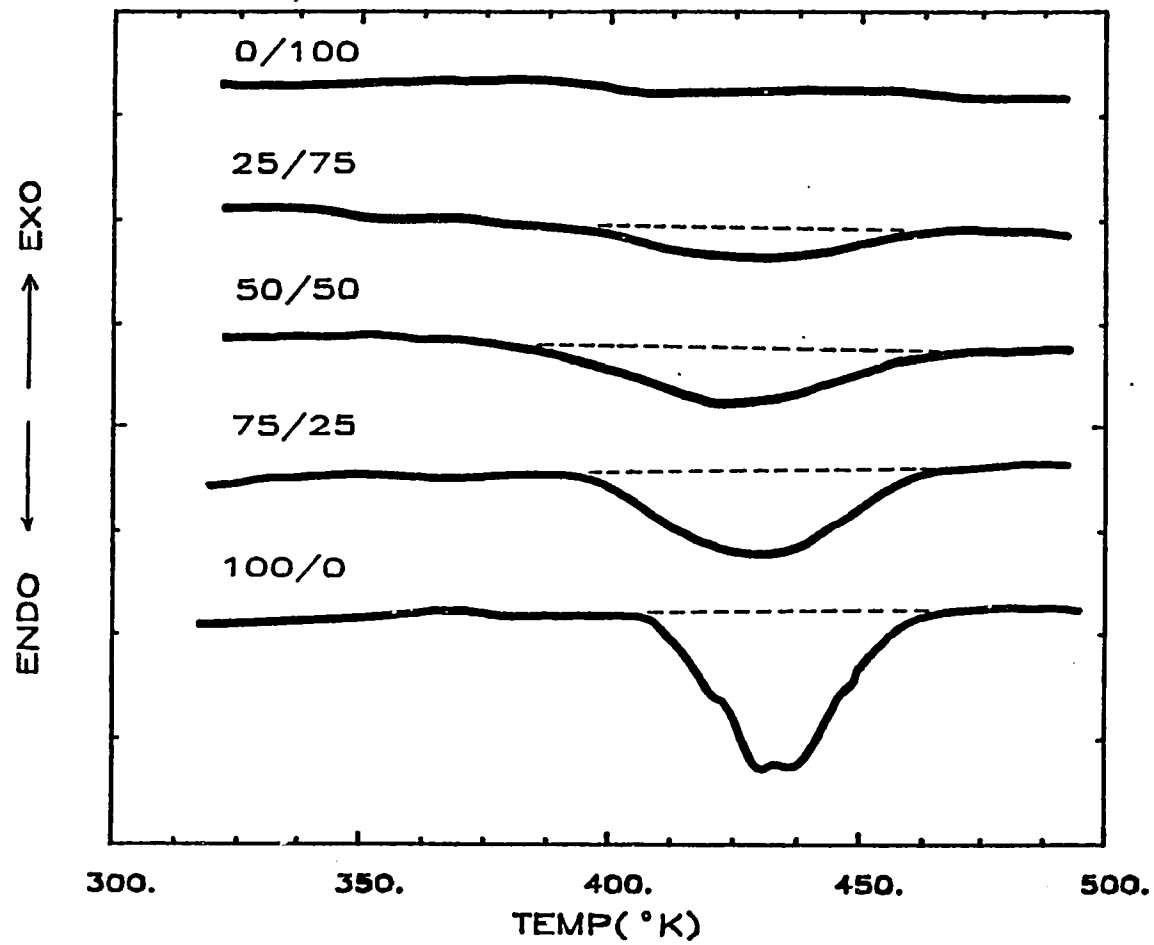


Figure 4.18 Scanning DSC results of 120 °C-transfer molded L/C samples.

property, tensile strength of 80 °C molded and 120 °C postcured L/C samples was measured under three different temperatures: -2, 25, 93 °C. Figure 4.19 and Table 4.2 summarize the results. Temperature of 93 °C was chosen because it is located in the middle of the glass transition temperature of polyurethane hard domain (50-70 °C) and the glass transition temperature of unsaturated polyester (near 100 °C). When the testing temperature was increased from -2 to 93 °C, tensile strength of polyurethane dropped from 2739 to 640 psi, whereas much less difference was observed with polyester sample. This is because linear polyurethane is soft and elastomeric in nature and the highly crosslinked polyester is extremely rigid. In general, increasing the temperature decreases tensile strength of all IPNs. IPNs with high polyurethane content show more reduction in tensile strength than those with low polyurethane content. Ultimate elongation of IPN also shows an intermediate value between those of the constituent polymers. The ratio of tensile strength at -2 °C to that at 93 °C can be used as a measure of temperature sensitivity. As shown in Table 4.2, the ratios range from 1.2 for pure polyester to 4.3 for pure polyurethane. IPNs have ratios between these two extremes.

4.4.2 Sequential Effect

The two polymerizations in IPN do not necessarily occur at the same time. The actual polymerization sequence depends on the

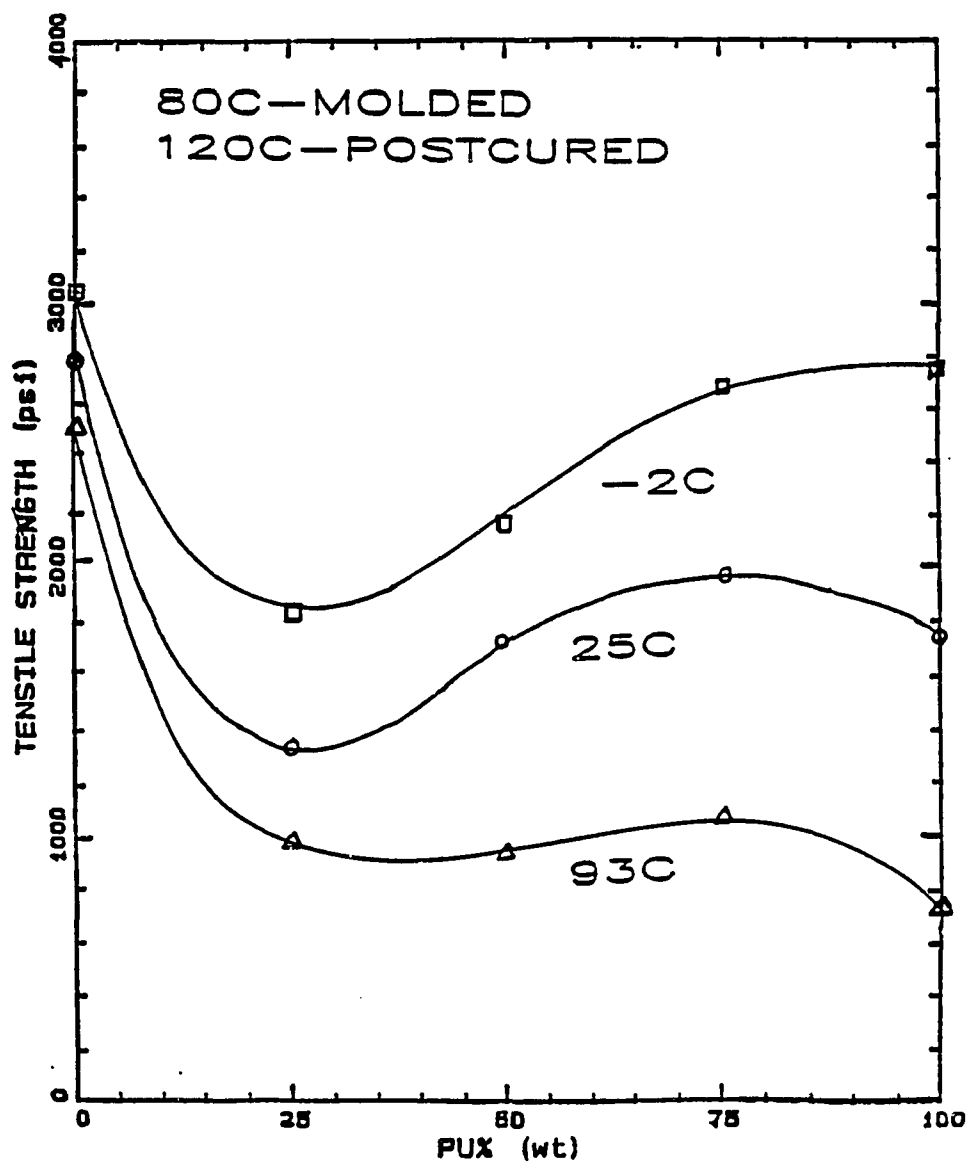


Figure 4.19 Tensile strength of 80 °C-transfer molded, 120 °C-postcured L/C samples tested at -2 °C (□), 25 °C (○), and 93 °C (Δ).

molding temperature and catalyst in each constituent polymer. All 80 °C molded IPN samples discussed so far have been in the sequence that polyurethane reacted first and polyester reacted later by employing a high-temperature peroxide initiator, PDO, which required a long period of induction time at 80 °C.

To study the effect of reaction sequence, a redox type initiator, MEKP/amine/Co-8, was used to substitute for PDO in polyester reaction. The combined initiator is a reduction-oxidation (redox) initiator that may start free radical polymerization at low temperatures. The ingredients of polyurethane phase remained the same, but without the catalyst T-12, because tertiary amine is also known to be a weak catalyst for polyurethane. By changing the amount of this combined initiator, the reaction rates of polyester and polyurethane can be adjusted. Previous thermal kinetic study (Hsu and Lee, 1985) showed that substantial overlapping occurred between polyurethane reaction and polyester reaction when MEKP/amine/Co-8 was employed as the initiator. Increasing the concentration of MEKP/amine/Co-8 increased the extent of overlapping. Tensile strength of IPN samples molded at 80 °C with different redox type initiator concentrations is presented in Table 4.3. The ratio of Polyurethane/polyester was set at 50/50. For comparison, tensile properties of a similar IPN initiated by PDO and T-12 are also listed in Table 4.3.

Table 4.3 Tensile strength, ultimate elongation, and limiting conversion of 80 °C-transfer molded I/C samples with different initiator concentrations (PU/PES = 50/50, testing temperature was 25 °C).

Sample Designation	<u>L/C</u>	<u>RA</u>	<u>RB</u>	<u>RC</u>
Tensile (psi) strength	1050	2344.5	1489.1	1440
Ultimate (%) elongation	4.26	7.59	5.58	4.18
Limiting (%) conversion	96.7	97.2	95.3	78.2

It is found that the PDO-initiated IPN has a lower tensile strength and ultimate elongation than the MEKP/amine/Co-8 initiated IPN. Since no T-12 was added to polyurethane phase, reaction rate of urethane slowed down; while polyester reaction became faster due to low temperature redox initiation. This resulted in enhanced mechanical properties of IPNs. The results are also very similar to molding the PDO-initiated IPNs at high temperatures (i.e., 120 °C). Among those redox samples, the one with the lowest concentration (i.e., sample RA) shows the highest tensile strength and ultimate elongation. This is probably due to the influence of limited conversion, as shown in Table 4.3. The effect of reaction sequence on crystallinity of polyurethane phase is presented in Figure 4.20. It seems that the overlapping of polyurethane and polyester reactions reduces the degree of crystallinity in polyurethane phase.

Tensile properties among different IPN samples may be affected by both polymerization kinetics and sample morphology. Factors such as phase separation, chain interpenetration, crystallinity structure of polyurethane phase and network structure of polyester phase may all play important roles.

4.4.3 Crosslinking Effect

Since there are two constituent polymers in a polyurethane-polyester IPN and each polymer can either be linear or crosslinked,

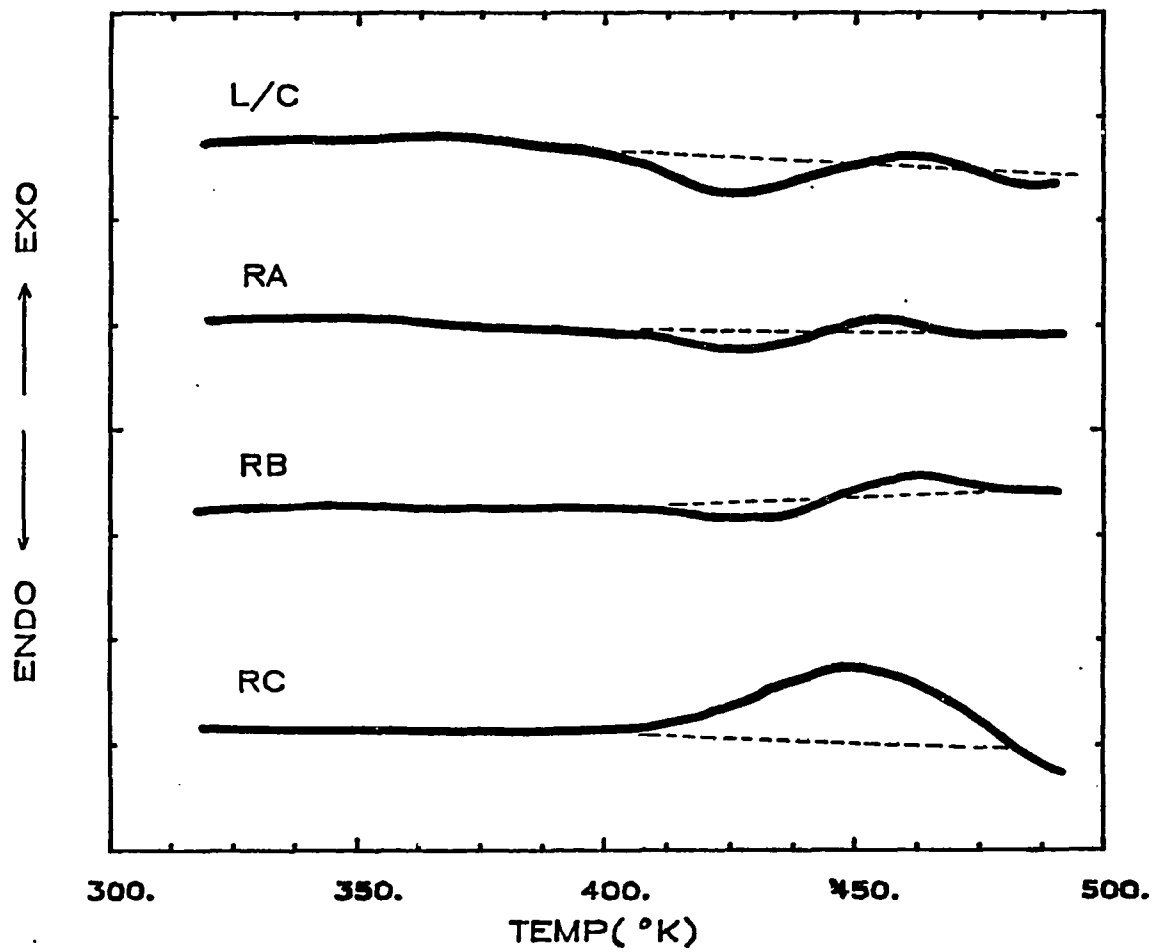


Figure 4.20 Scanning DSC results of 80 °C-transfer molded L/C samples with different initiator combination (PU/PES = 50/50).

the mechanical properties of IPNs may depend on the crosslinking nature of the two constituent polymers (Donatelli et al., 1977; Neubauer et al., 1977, 1978). Table 4.4 summarizes the crosslinking effect of both polyurethane and polyester on the tensile properties of IPNs. In this Table, U_c is TONE-0300-based thermosetting polyurethane and U_l is TONE-0240-based linear polyurethane. All samples have a polyurethane-polyester ratio of 50/50, molded at 80 °C and tested at 25 °C. Limiting conversions of molded and postcured samples are also listed in Table 4.4. Results show that postcure improves tensile strength of all samples, but to a different extent. For crosslinked polyurethane, the increase of tensile strength from 956 to 1828 psi owing to postcure treatment can be attributed to the increase of polyurethane conversion from 92 to almost 100%, which not only reduces residual monomers, but also increases crosslinking density. For linear polyurethane, postcure treatment only slightly increases its limiting conversion; therefore, the significant increase in tensile strength must attribute to a change in morphology, such as crystallinity structure and phase separation.

For the two polyester-based IPNs, the molded C/C sample shows a higher tensile strength than that of L/C sample. This is apparently due to the dual network structures of C/C sample. Postcure increases the limiting conversion of C/C sample substantially. Consequently, its tensile strength also greatly increases. For L/C sample, limiting conversion does not change much

Table 4.4 Effect of crosslinking on tensile strength and limiting conversion of 80 °C-transfer molded samples before and after postcure treatment (PU/PES = 50/50, testing temperature was 25 °C).

Sample Designation		<u>80°C-molded</u>	<u>Postcured</u>
C/C	σ (psi) [*]	1496	1961
	α (%) ⁺	86	~100
L/C	σ (psi)	1050	1623
	α (%)	96.7	~100
C/L	σ (psi)	954	1528
	α (%)	93	~100
L/L	σ (psi)	1280	2080
	α (%)	98.7	~100
U _c	σ (psi)	956	1828
	α (%)	92	~100
U _l	σ (psi)	730	1733
	α (%)	97.5	~100

* Tensile strength

+ Limiting conversion

by postcure treatment; the morphological change must be the reason for the increased tensile strength. Postcure treatment shows a more significant influence on tensile strength for the polystyrene-based IPNs than for the polyester-based IPNs. One may again attribute the influence of tensile strength on C/L samples to an increased limiting conversion. For L/L sample, the substantial increase in tensile strength due to postcure treatment cannot be attributed to the increase in limiting conversion. Thermal analysis of molded and postcured samples by DSC shown in Figure 4.21 again suggest that morphological changes, such as rearrangement of crystallinity structure in polyurethane phase, must be a main reason for this improvement. The linear polystyrene phase is less rigid than the crosslinked polyester phase at the postcure temperature. Thus, postcure treatment is more beneficial for the polystyrene-based IPNs than for the polyester-based IPNs.

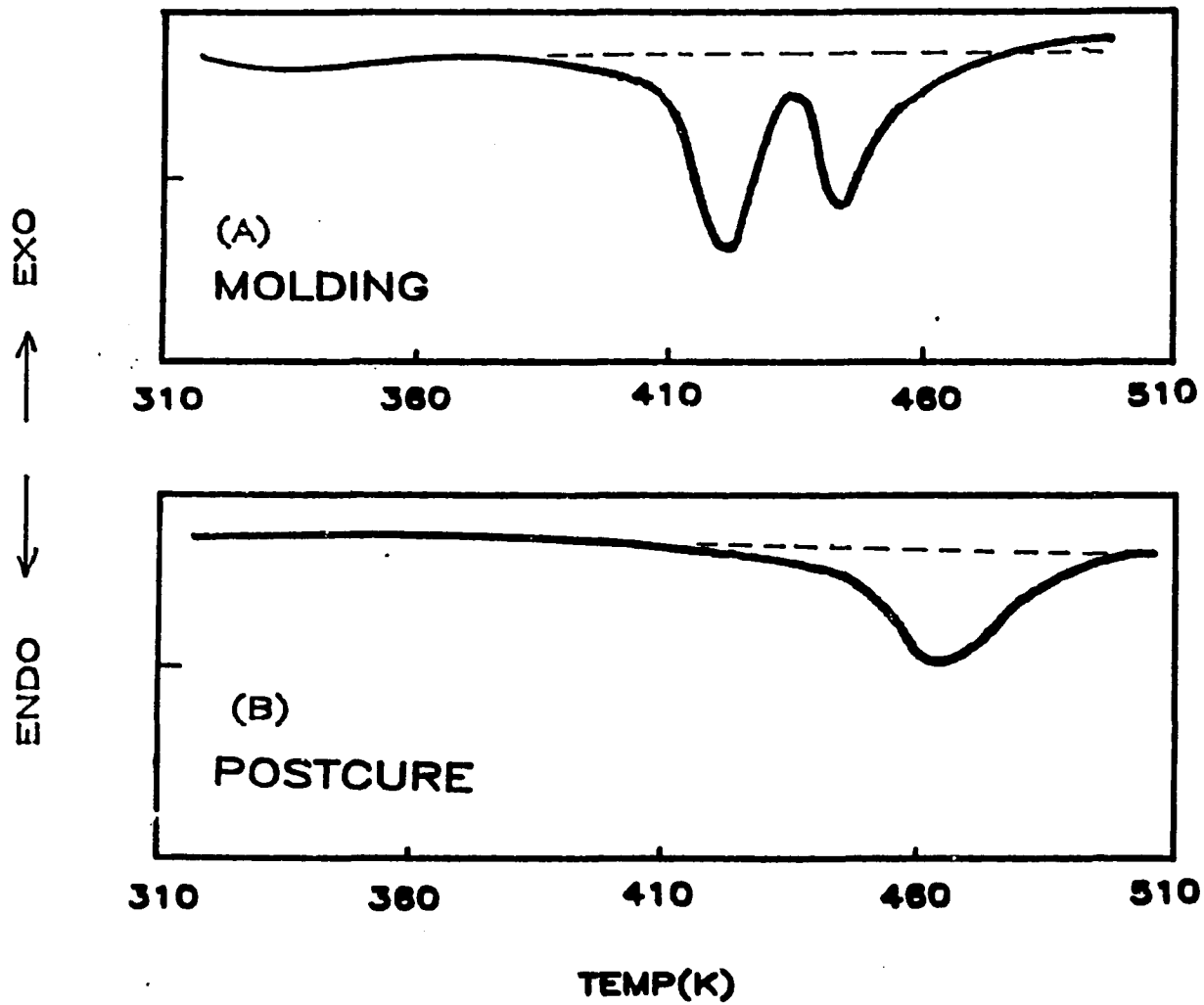


Figure 4.21 Scanning DSC results of 80 °C-transfer molded L/L samples. (A) molding, and (b) after postcure.

CHAPTER V

PROCESSING OF POLYUREA

SYNOPSIS

Summarized in this chapter are the experimental results and mathematical modelling of processing of polyureas. The experimental part includes the applications of solution polymerization to study the rheology and kinetics of polyureas. The theoretical part includes a kinetic and heat transfer model which can apply solution polymerization data to predict the bulk polymerization of polyurea in RIM process.

5.1 PREVIOUS WORK ON POLYUREA RIM

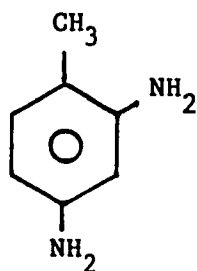
5.1.1 MATERIALS

In order to increase the reaction rate of RIM materials and to provide RIM products with better properties, many RIM products, especially in the automotive applications, have shifted from

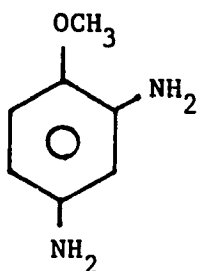
polyurethane to polyurethane/polyureas and total polyureas. The main difference is that the latter two systems use a low molecular weight diamine as a chain extender instead of butanediol and ethylene glycol (Nissen and Markovs, 1983). Diamines are much more reactive than diols. Aliphatic diamines react almost instantaneously with isocyanates, while aromatic diamines, in particular, hindered diamines such as bis(orthochloroaniline) (MOCA) and 3,3'-dichlorobenzidine (DCB) react considerably slower. Because of the proven health hazards, uses of MOCA and DCB have been discontinued in some countries and restricted in The United States (Frisch, 1980). Today, diethyl toluene diamine (DETDA) is the major chain extender used in the polyurethane/polyurea and total polyurea RIM systems. Its reactivity is much higher than that of MOCA and DCB (i.e., pot life in seconds rather than in minutes). Other diamines commercially available include Ethacure 300 (Ethyl Chemicals Corp.), Unilink 4,100, 4,200 (UOP Inc.), tert-butyl toluene diamine (TBTDA, Air Product Chemicals Co.), Dytek (Du Pont), 4'4'-methylene-bis(3-chloro-2,5-diethylaniline) (MCDEA, Lonza Ltd.), ditert-butyl ethylene diamine (Virginia Chemical), and XPA series (UOP Inc.). The use of secondary aromatic diamines (Unilink 4200) as chain extenders and reactive carriers for polyurethane and polyurethane/urea was studied by Baumann et al. (1986). They found that the addition of secondary aromatic diamines provided formulators the versatility of controlling the degree of crosslinking and the capability of

adjusting the polymer structure so that the desired properties of finished product can be obtained.

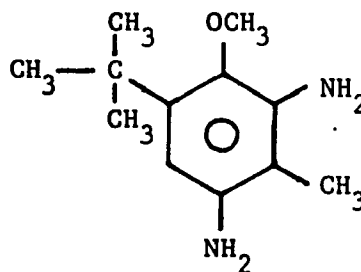
Since urea-linkage is thermally more stable than urethane-linkage, many researchers have been working on total polyurea resins for the RIM applications, i.e., amine-terminated polyether resins with amine chain extenders (Dominguez, 1984; Wood, 1984; Casey, 1985; Grigsby and Dominguez, 1985; Ewen, 1985; Vespoli et al., 1985; Sneller, 1986). These systems, however, react too fast to fill large, complex molds (Vespoli et al., 1985). Currently, a major effort in the development of polyurea RIM is to slow down the reactivity of diamine chain extender by modifying its chemical structure. The relative reactivity and the structure-activity relationships of several aromatic diamines were studied by Casey et al. using Hammet correlation (1985). For example, for the three diamines shown below, structure B has about half of the reactivity as structure A, while structure C reacts six times slower than structure A due to the steric hindrance effect.



(A)

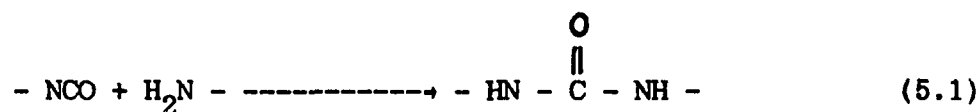


(B)



(C)

The reaction of polyureas is a typical step-growth polymerization. This polymerization is generally regarded as an nth order reaction. Basically, a commercial recipe of polyurea RIM includes three ingredients: a diisocyanate, a low molecular weight aromatic diamine, and a high molecular weight aliphatic triamine. The basic reaction which forms the urea linkage is,



Even without any catalyst, the urea formation is much faster than the catalyzed urethane formation (i.e., activation energy 1 ~ 8 kcal/mole vs. 10 ~ 15 kcal/mole) (Lee and Macosko, 1980; Macosko, 1983; Vespoli, 1985).

5.1.2 POLYUREA RIM

Diamine extended RIM systems build viscosity rapidly after mixing, leading to less turbulence during mold filling and often to faster and cleaner demolding. Processing conditions of polyurea RIM are similar to those of polyurethane RIM except that mold temperature must be higher (i.e., ~ 100 °C) in order to achieve desirable physical properties (Dominguez, 1984; Grigsby and Dominguez, 1985; Ferber, 1986). Since polyurea RIM is a relatively

new area, little research work have been done so far. Three related work, namely, the studies of reaction kinetics of a polyurea RIM system by Pannone (1986), the mold filling studies of polyurea RIM systems by Vespoli et al. (1986), and the studies of mechanical properties of RIM polyurea by Ewen (1985) are reviewed.

Since polyurea reaction is a step growth type polymerization, the reaction kinetics is generally modelled as an nth order reaction with an Arrhenius temperature dependence. Pannone (1986) found that the aliphatic amines reacted with isocyanates much faster than the aromatic amines. Therefore, the reaction of aliphatic amine was considered instantaneous and only the reaction kinetics of aromatic amine was studied using an unreactive polyether as the solvent to replace the aliphatic amine. The reaction rate of aromatic amines and isocyanate was described by a third order model (1st order in isocyanate, 2nd order in amine) to fit the adiabatic temperature rise for a two component polyurea system. The kinetic parameters were determined from solvent-diluted polyurea systems. Adiabatic temperature rises for all the RIM experiments studied were in good agreement with the values predicted by heat of reaction measured in solution polymerization.

In the mold filling studies by Vespoli et al. (1986), the flow times were determined by the pressure build-up in the mold. They also found that the aliphatic amine reacted much faster with isocyanate than the aromatic amine. When injecting the two component

polyurea (isocyanate and aliphatic triamine) into the mold, the RIM machine shut down due to excessive back-pressure from the gelled material trying to fill the mold. Therefore, the aliphatic triamine was diluted with a slowly reacting triol. A kinetic model of 2nd reaction order was developed for the polyureas studied by assuming that the aliphatic amine reacted instantaneously and could be ignored in the model. Comparison of model prediction and experimental data was fairly good. The mechanical properties of RIM polyureas for automotive fascia and body panels were studied by Ewen (1985). The flexural modulus ranges from 25k to 100k psi. They found that the polyureas tested (RIMSOURCE series, Dow Chemical U.S.A.) possess better thermal and impact properties than polyurethanes and polyurethane/ureas. They indicated that no postcure and no catalyst were needed, and that the RIM molded polyurea could be painted on line with metal body components at high temperatures.

Due to its superior thermal and mechanical properties mentioned above, polyurea is a desirable RIM material. However, the system reacts so fast that most of the reaction actually takes place during mixing and subsequently during mold filling. In many cases, this exhibits processing difficulties and may result in poor properties such as insufficient mixing and low conversion. To solve this problem, a thorough understanding of the reaction kinetics and heat transfer is required. In this study, an experimental investigation of polyurea RIM is first conducted and several processing

difficulties are pointed out. A solution polymerization technique is proposed to slow down the reaction rate such that rheological and kinetic information can be obtained. Finally, the solution polymerization data are applied to the bulk polymerization of polyurea in RIM. A model is proposed based on the solution polymerization data to predict the kinetic and heat transfer of polyurea in RIM.

5.2 EXPERIMENTAL

5.2.1 MATERIALS

Before conducting the quantitative analysis, three commercial RIM materials from different suppliers were tested. The description of these three materials is listed in Table 2.4. The Bayflex 110-80 series (Mobay Chemical), currently used in the production of Fiero body panels, is not a total polyurea but rather a hybrid of polyurethane and polyurea. Reported flow time is approximately 2.5 seconds in the typical RIM process. The Dow's XV15081.001 resin reacts with 1616E isocyanate with a reported 1.5 second flow time. The XV15081.001 resin is a blend of polyol and polyamine; therefore, it is also a hybrid of polyurethane and polyurea. The Dow's 1337

resin reacts with 1305 (isocyanate) with a reported 1.2 seconds flow time. This material is a total polyurea system.

The ingredients of the polyureas used in this study and the sample designations are summarized in Table 5.1. The recipe consists of a soft segment based on a triamine (Jeffamine T5000, Texaco Chemicals Corp.) and a hard segment based on a liquid form of 4,4'-diphenyl methane-diisocyanate (MDI) (1305, Dow Chemical Company) chain extended with a diamine (TBTDA, from Air Product Co.). T5000 is a polyamine with functionality of 3 and a molecular weight of about 5,000. The aromatic diamine chain extender tert-butyl toluene diamine (TBTDA) used has a functionality of 2 and an equivalent molecular weight of 89. The Dow's 1305 is a blend of isocyanate monomer (50% by weight) and a high molecular weight polymer (50% by weight) with an equivalent molecular weight of 210. Polyureas I and II in Table 5.1 were formulated to obtain the kinetic parameters for reactions of diisocyanate with aliphatic and aromatic amines respectively. To determine the kinetic parameters by FTIR measurement, polyurea I was diluted in 92.5% nitrobenzene solution and polyurea II was diluted in 90% nitrobenzene solution. After the individual kinetic parameters were obtained, polyurea III was studied at dilution levels of 90%, 85%, and 80% nitrobenzene for kinetic measurements. Polyurea III has a molar ratio of $T5000/1305/TBTDA = 11.1/100.0/88.9$ (70/77/30 by weight) which is typical in RIM process. In order to study the relative reactivity of

Table 5.1 Recipe of polyurea systems used

		<u>I</u>	<u>II</u>	<u>III</u> *
<u>Ingredients</u>	<u>Name</u>	<u>% by Weight</u>		
Diisocyanate	1305 (Dow)	10.90	69.50	43.50
Diamine	TBTDA (Air Product)	-----	30.50	16.95
Triamine	T5000 (Texaco)	89.10	-----	39.55

* Triamine/Diisocyanate/Diamine = 11.1/100/88.9 (molar ratio).

1. TBTDA : tert-butyl toluene diamine with molecular weight = 178.
2. T5000 : Jeffamine T5000 from Texaco with molecular weight about 5,000.
3. 1305 : a mixture of isocyanate monomer (50% by weight) and a high molecular weight polymer (50% by weight), equivalent weight is 210.
4. Most polyurea systems were diluted in nitrobenzene with 80%, 85%, 90%, and 95% for various applications in solution polymerization.
5. In RIM process, system III was used with 15% nitrobenzne dilution or no dilution.

aliphatic and aromatic amines, the composition was also varied from total aliphatic to total aromatic amine with equivalent molar amount of isocyanate. For rheological measurements, polyurea III solutions at dilution levels of 90%, 85%, and 80% nitrobenzene were used. In RIM process, polyurea III was used both in bulk and in 15% nitrobenzene solution. All ingredients were degassed and demoiistured under vacuum at room temperature for 12-16 hours to remove water and air. To prepare polyurea samples for kinetic and rheological measurements in solution polymerization, a homogeneous solution of isocyanate and nitrobenzene was first prepared in a vial of 50 cm³. The aliphatic and aromatic amines were then added to the mixture. The whole vial was shaken vigorously for complete mixing. In RIM process, The isocyanate solution and the amine solution were loaded directly into the RIM machine, where a nitrogen blanket was maintained.

5.2.2 INSTRUMENTATION AND EXPERIMENTAL PROCEDURE

A. Viscosity Measurement

A Haake viscometer (Model MVII) and a Brookfield viscometer were used to measure the system viscosity before gelation. Model MVII has a cup with an inside diameter of 42 mm and a rotor with an outside diameter of 36.8 mm and a length of 60 mm. Water was

circulating in a heating jacket outside the measuring cup to control the system temperature at a fixed value which was checked occasionally by inserting a thermocouple into the gap between the cup and the rotor during reaction. Shown in Figure 5.1 is the schematic diagram of the experimental set-up.

During polymerization, different shear rates, ranging from 3.3 to 176.3 (1/sec), were applied to the system by changing the gear to different slots. Thus, one could study the shear rate dependence of the system viscosity during reaction. The system viscosity was measured every few seconds before the sharp rise of viscosity, and was continuously measured thereafter.

A Brookfield viscometer (Model RVTD) was also employed to measure the viscosity of diluted polyurea solution. By selecting a suitable combination of the size of spindle and the rotation speed, the Brookfield viscometer can measure viscosities up to 80,000 cp. In this study, a disposable glass tube with the same dimension of the spindle (#7) was used. The system viscosity was measured continuously by using a chart recorder.

B. FTIR

A FTIR spectrometer (Nicolet 20DX) with a resolution of 4 cm^{-1} in the transmission mode was used for kinetic measurements. After the reactants were mixed, about 0.05 cc. of mixture was pasted between two sodium chloride (NaCl) plates which were then mounted on

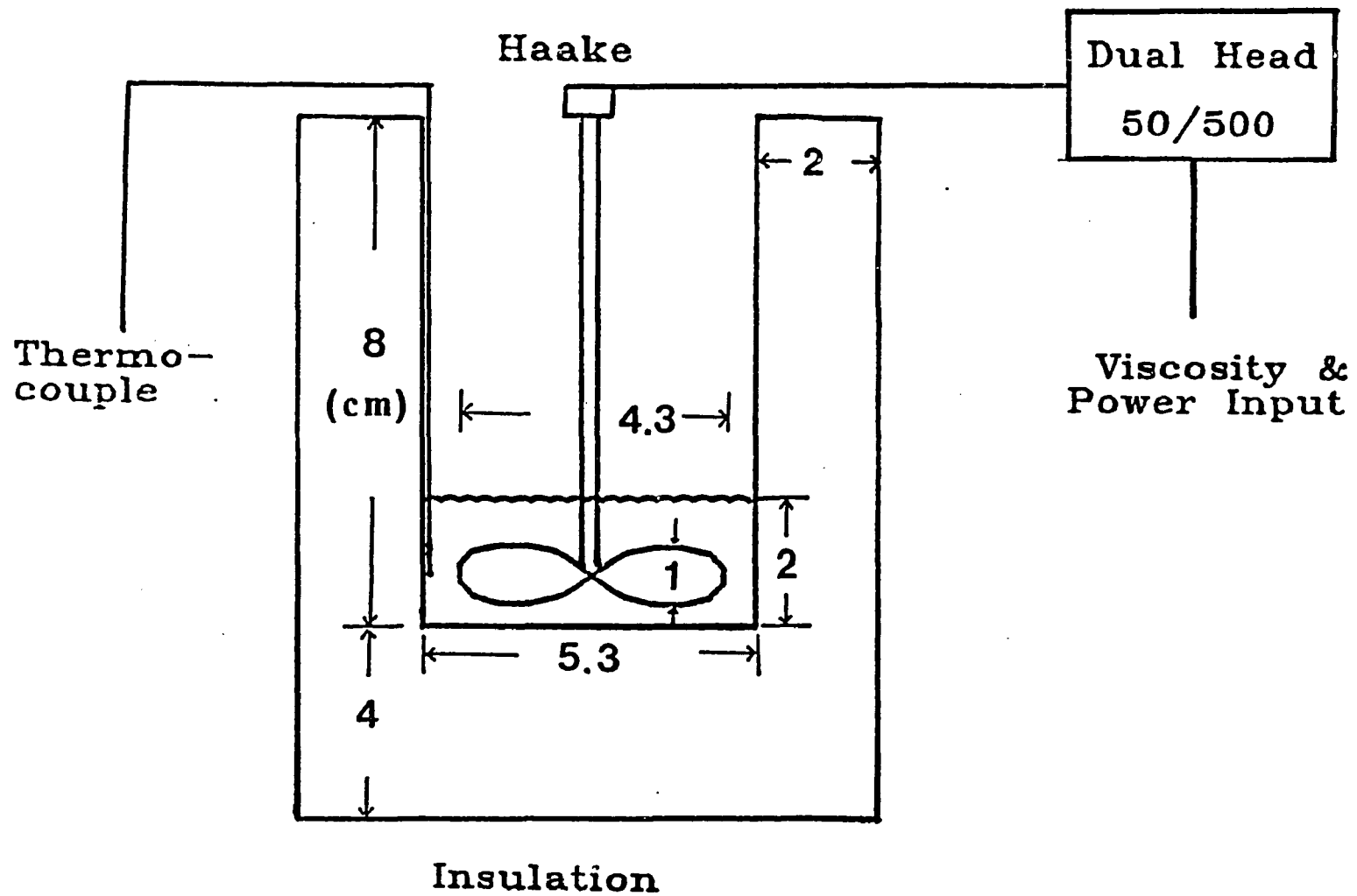


Figure 5.1 Experimental set-up for rheological measurements (Lee, 1986).

a sample holder. No spacer was used between the two NaCl plates. A temperature chamber was designed to maintain the reaction temperature isothermally. Three consecutive one-second scans were taken, averaged, and stored in a floppy disk at each sampling time. The sampling interval was one minute during most of the reaction, but was longer at high conversions because the reaction was very slow at these regions. Measurement was ended at a preset time. All IR spectra in this study were expressed in absorbance. FTIR measurement is in contrast to the principle used in the DSC measurement since DSC detects the amount of monomer reacted. FTIR is found very useful for the kinetic measurement of multicomponent reaction systems and is also sensitive at high conversions.

Infrared absorption is based on the fact that each chemical group in a sample absorbs infrared radiation at some characteristic frequencies. The amount of light intensity transmitted relative to the amount of light intensity incident on the sample can be related directly to the concentration of the absorbing species by Beer's law (Kendall, 1966),

$$A_i = \beta_i l C_i \quad (5.2)$$

where A_i is the absorbance of species which can be determined from the peak height or peak area, β_i is the absorptivity which is characteristic of the absorbing species, l is the sample length, and

C_i is the concentration of the absorbing species i . To compensate for the thickness changes in the sample during polymerization, a ratio is taken between the absorbance of the functional group of interest and that of an internal standard, i.e., a group whose concentration does not change during polymerization. Either the peak height or the peak area is used to calculate the absorbance. Reaction conversion can then be determined from the change of the normalized absorbance.

In this study, the C-H peak at 2942 cm^{-1} was chosen as the internal standard and the peak height method was used to calculate the amount of unreacted monomers or functional groups left in the reaction system.

$$\alpha = 1 - \bar{A}_t / \bar{A}_0 \quad (5.3)$$

where \bar{A}_t and \bar{A}_0 are normalized absorbances of the monomer functional group before the reaction and after a reaction time t .

Before applying Beer's law for any quantitative analysis, the absorptivities of reacting species need to be determined. Calibration curves of isocyanate peak based on the change of both the peak height and the peak area have been established in our laboratory (Yang and Lee, 1987). The calibration curves were established by preparing mixtures of isocyanate monomer and dichloro-methane of known concentration. For the isocyanate peak,

the calibration curves based on both peak height and the peak area formed straight lines. In this study, the change of the peak height of isocyanate peak was followed to determine the reaction kinetics of polyurea.

C. Reaction Injection Molding

The lab-RIM machine described in Chapter III was used to carry out the experiment. An IBM PC/XT was linked to the lab-RIM for real time data acquisition (Nelson, 1987). Detailed description about this RIM machine can be found in Section 3.2.2, Chapter III. To measure the adiabatic temperature rise of polyurea, a paper cup was used as the adiabatic reactor with a thermocouple inserted in the center and about 1 cm from the bottom of the paper cup. It took only a few seconds for polyurea to polymerize. The reaction was so fast that the error due to the adiabatic assumption was negligible. The measured temperature rise, along with the density and heat capacity, were used to calculate the heat of polyurea reaction, assuming constant density and heat capacity. After the center temperature reached maximum, it cooled down at a rate less than 0.2 °C/min. Initial material temperature T_0 was set at 35 °C and 55 °C for bulk polyurea. For 15% nitrobenzene diluted polyurea, $T_0 = 25$ °C. T5000 and TBTDA mixture formed one stream, while diisocyanate formed the other stream. The volume ratio was $V_{\text{amine}}/V_{\text{iso}} = 1.55$. No catalyst was added in the system.

5.3 RESULTS AND DISCUSSION

5.3.1 REACTION INJECTION MOLDING OF POLYUREA

Experimental results of polyurea bulk polymerization in RIM shown in Figure 5.2 indicate that about 90% of the adiabatic temperature rise took place within five seconds at initial material temperatures of 35 °C and 55 °C respectively. For $T_o=55$ °C, the maximum temperature rise, ΔT_{ad} , is 92 °C ($Re = 409$, based on the amine stream), whereas for $T_o=35$ °C, $\Delta T_{ad}=65$ °C only ($Re = 144$ based on the amine stream). The viscosity of isocyanate prepolymer is 736 cp at 35 °C and 250 cp at 55 °C. In amine solution, the viscosity is 740 cp at 35 °C and 260 cp at 55 °C. The results suggest that the initial material temperature not only affect the reaction kinetics but also the viscosity, and subsequently, the efficiency of mixing. Figure 5.3 compares the bulk polymerization and 15%-nitrobenzene diluted polyurea polymerization in RIM. The temperature rise of 15%-nitrobenzene diluted polyurea reaction also took place within five seconds with a $\Delta T_{ad} = 75$ °C, a value which is equal to 81.5% of ΔT_{ad} in bulk polymerization at 55 °C. The effect of isocyanate/amine ratio on temperature rise is shown in Figure 5.4. The T_{ad} 's for three runs (isocyanate/amine ratio = +4.6%, +1.75%, and -2.90%) reached about 145 °C, with ± 5 °C difference. The initial temperature rises during the first 2 seconds did not show any difference.

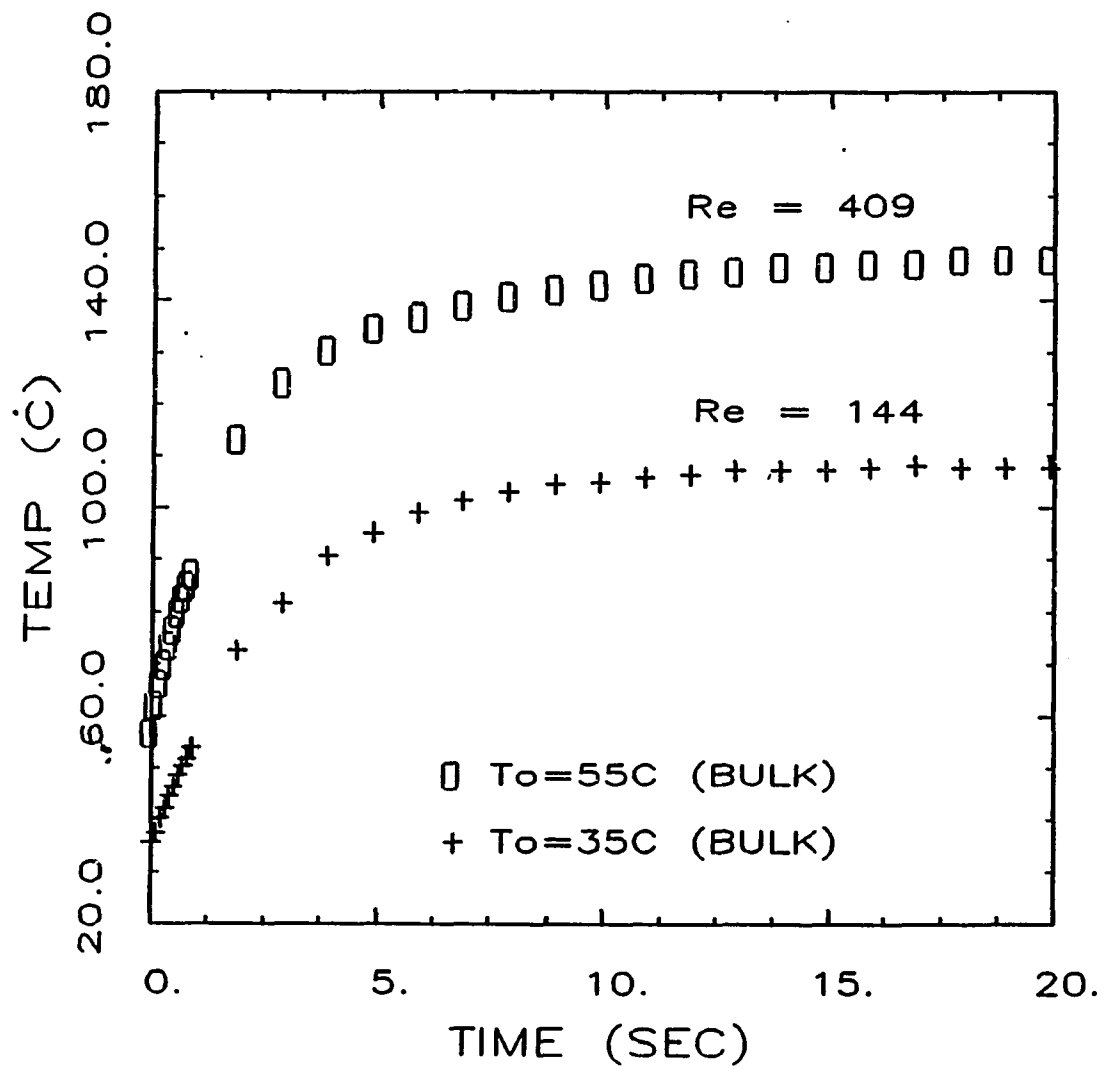


Figure 5.2 Reaction injection molding of polyurea III at 35 °C and 55 °C.

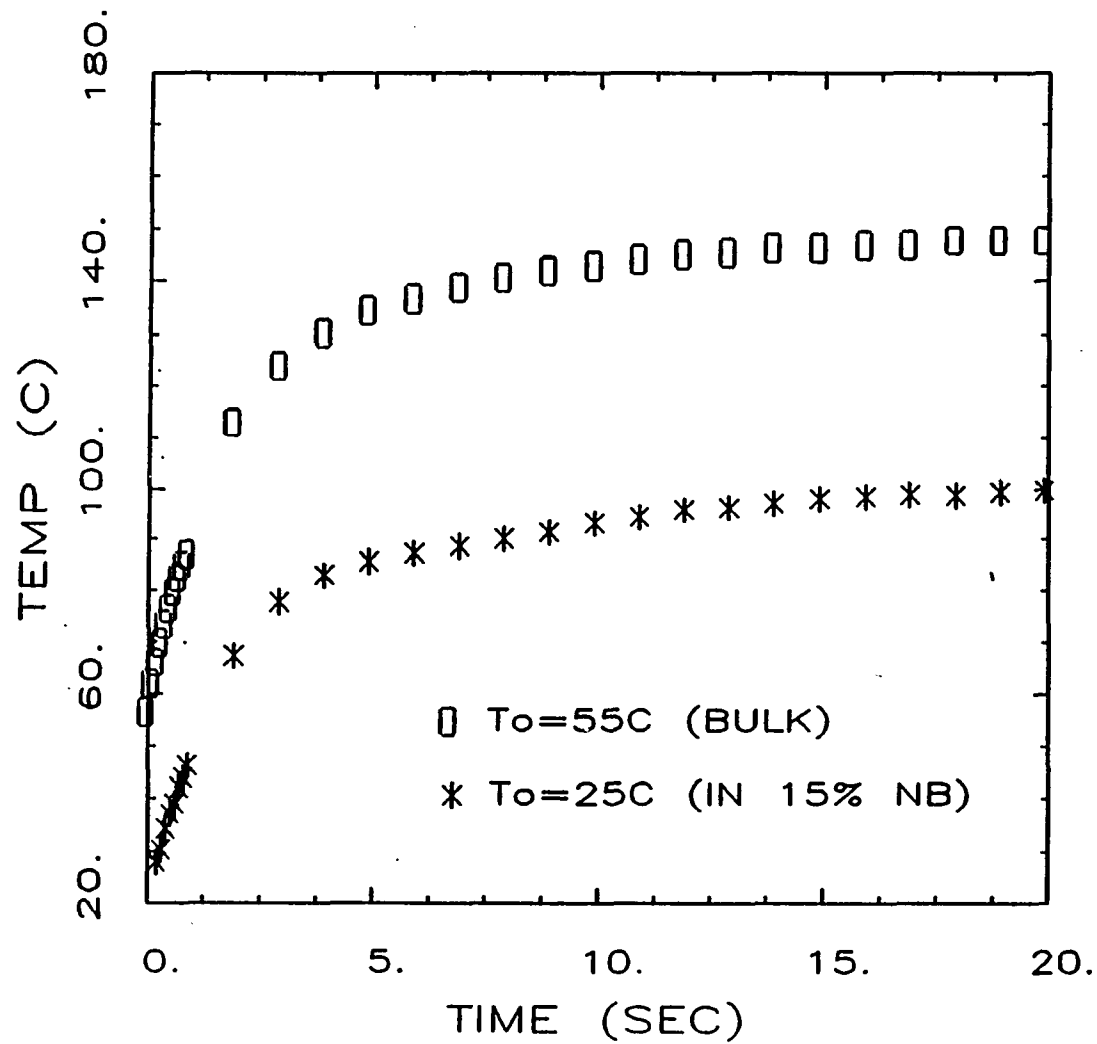


Figure 5.3 Reaction injection molding of polyurea III in bulk and in 15% nitrobenzene.

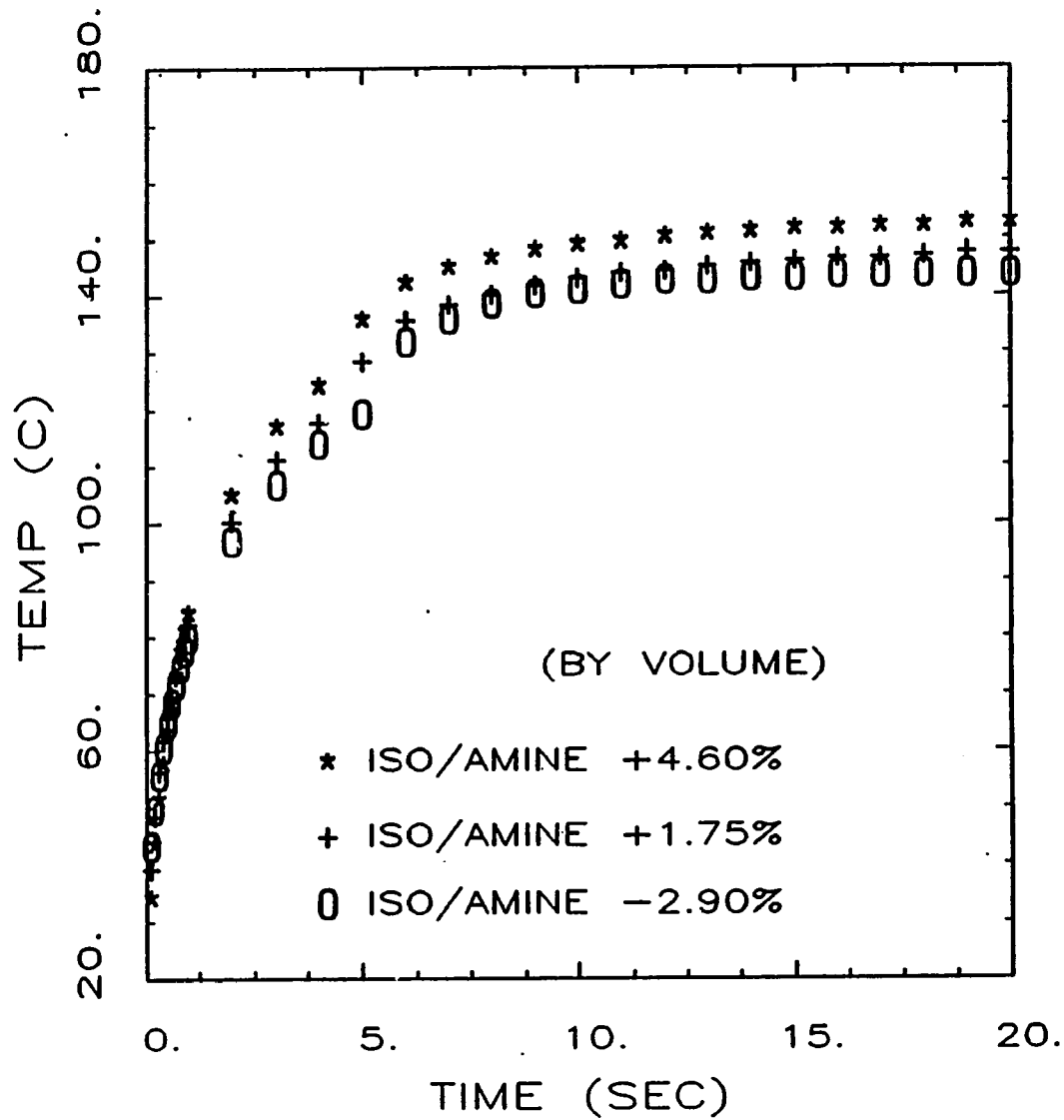


Figure 5.4 Maximum adiabatic temperature rises of three different isocyanate/amine ratios of polyurea III.

Results from Figures 5.2 to 5.4 indicate that polyurea reaction in RIM is so fast that no existing analytical instrument (e.g., differential scanning calorimetry, Fourier transform infrared spectroscopy, etc.) can follow the entire reaction course. This necessitates the study of solution polymerization of polyurea in which the reaction rate is substantially reduced.

5.3.2 SOLUTION POLYMERIZATION

A. Rheological Measurements

In order to understand the detailed reaction kinetics, heat transfer, and rheology of polyurea RIM, and to evaluate various commercial polyurea resins, solution polymerization was carried out.

Since the gel time (or flow time) is almost impossible to measure in RIM process, the polyurea systems were diluted with nitrobenzene (a solvent which does not react with polyurea) and the rheological changes during polyurea reaction were studied using a Brookfield and a Haake viscometers. Figure 5.5 shows the rheological changes of three commercial materials currently being developed for RIM. They were diluted in 80% nitrobenzene. Compared to the Dow 1616E and Bayflex 110-80 systems which are hybrids of polyurethane and polyurea, the Dow 1305, a pure polyurea system, shows a faster viscosity rise measured by the Brookfield viscometer. This indicates

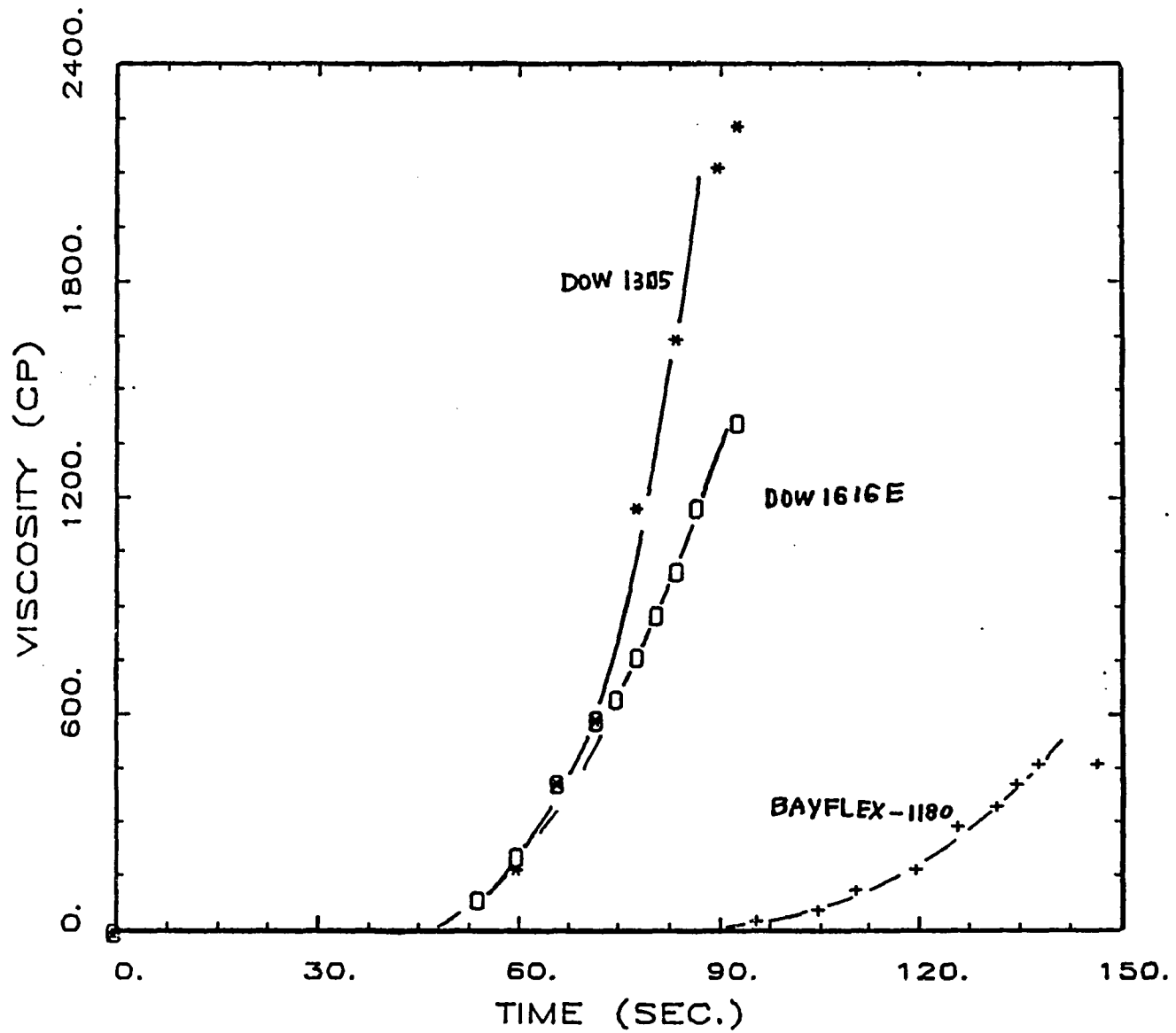


Figure 5.5 Comparison of three material systems currently developed for RIM process.

that as the system shifts from polyurethane to polyurea, it imposes more processing difficulties in RIM (Ewen, 1985). Current suppliers of polyurea resins provide many types of chain extenders (the aromatic short chain diamines). Their effects on the viscosity rise are displayed in Figure 5.6. Their chemical structures are shown in Figure 5.7. The Dytex (Du Pont) is an aliphatic diamine. Its reaction with isocyanate was so fast that even at 80% dilution with nitrobenzene, the viscosity rise still could not be measured. The viscosity rise curve of Dytex shown in Figure 5.6 is based on an estimation. Among the primary aromatic diamine chain extenders (TBTDA and DETDA), DETDA has an earlier onset of viscosity rise than TBTDA. This may be due to the hindrance effect of the bulky tert-butyl side group which reduces the activity of the adjacent amine groups. The Unilink 4200 has the slowest viscosity rise because it is a secondary aromatic diamine. The reaction of secondary diamine is generally slower than that of primary diamine (Baumann, et al., 1986).

The viscosity rises of 70/30 polyureas (70% triamine and 30% diamine by weight with equivalent moles of isocyanate) diluted with 90%, 85%, and 80% nitrobenzene are presented in Figure 5.8. As expected, at a higher concentration of polyurea, the system gave an earlier onset of viscosity rise.

Shown in Figure 5.9 is the effect of soft segment/hard segment ratio (by weight) on the rheological changes of polyurea formation

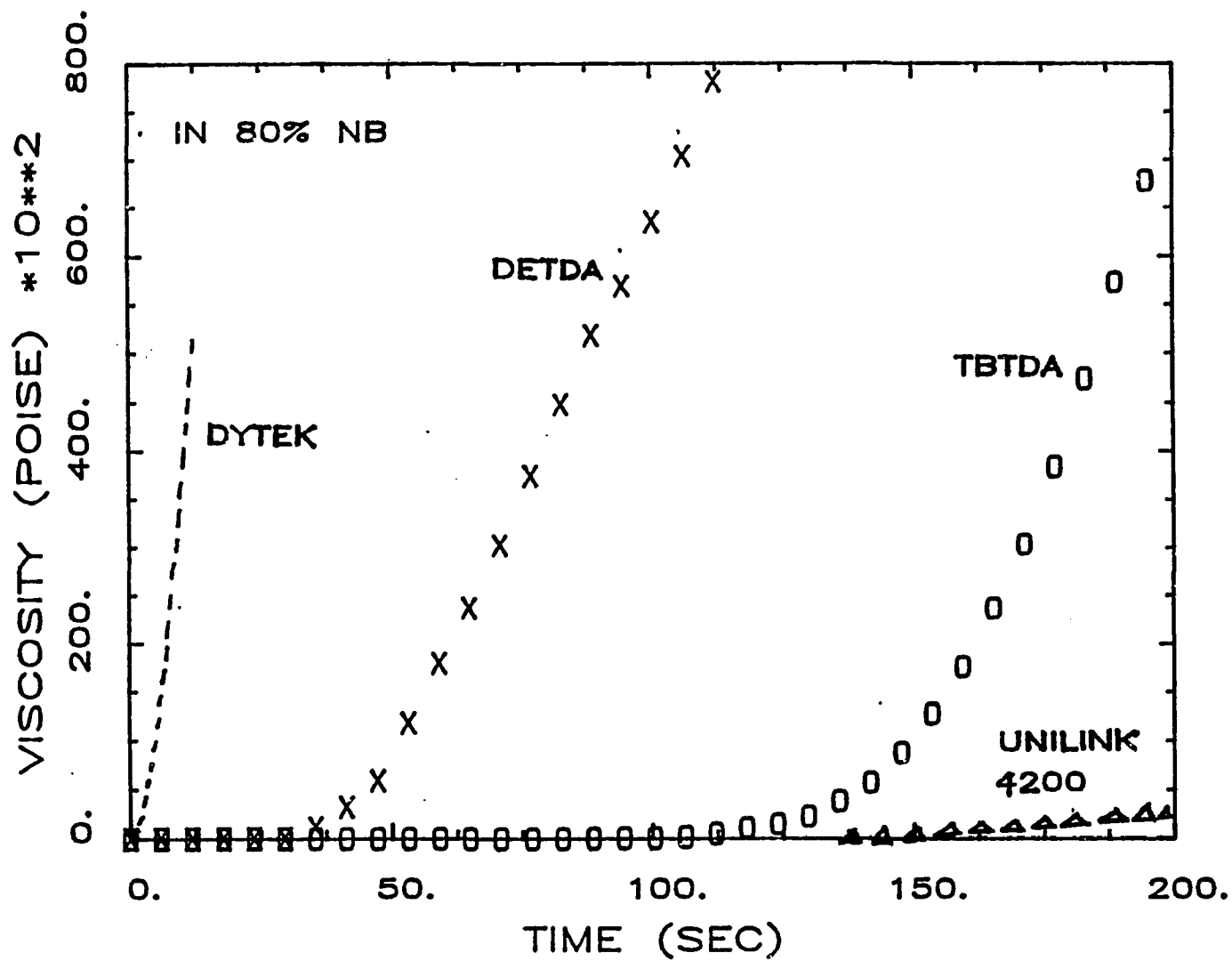
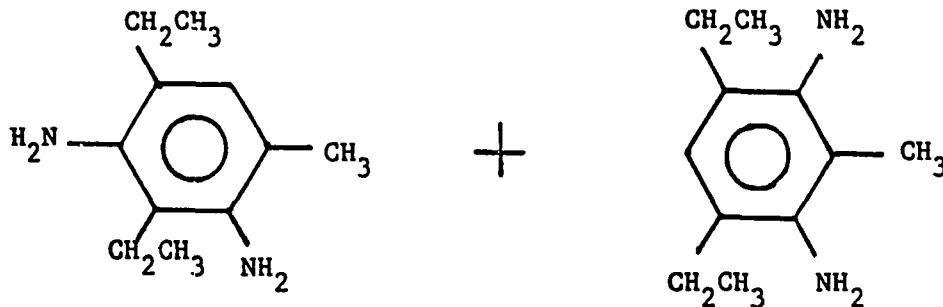


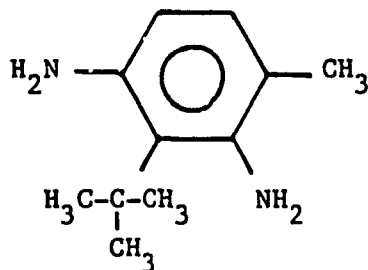
Figure 5.6 Chain extender effect of T5000/1305/X using Brookfield viscometer, where X stands for different diamine chain extenders studied at 80% nitrobenzene solution at 25 °C.

Figure 5.7 Chemical structures of various amine chain extenders.

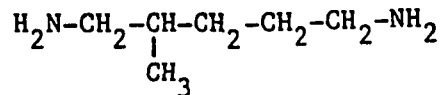
DETDA



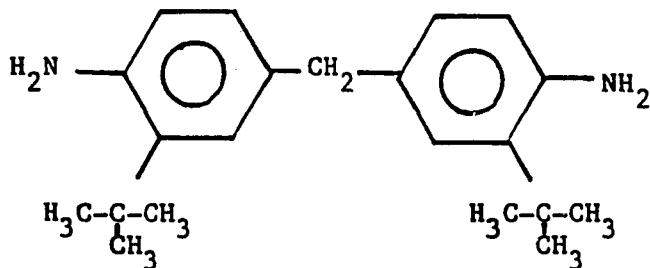
TBTDA



DYTEK



UNILINK 4200



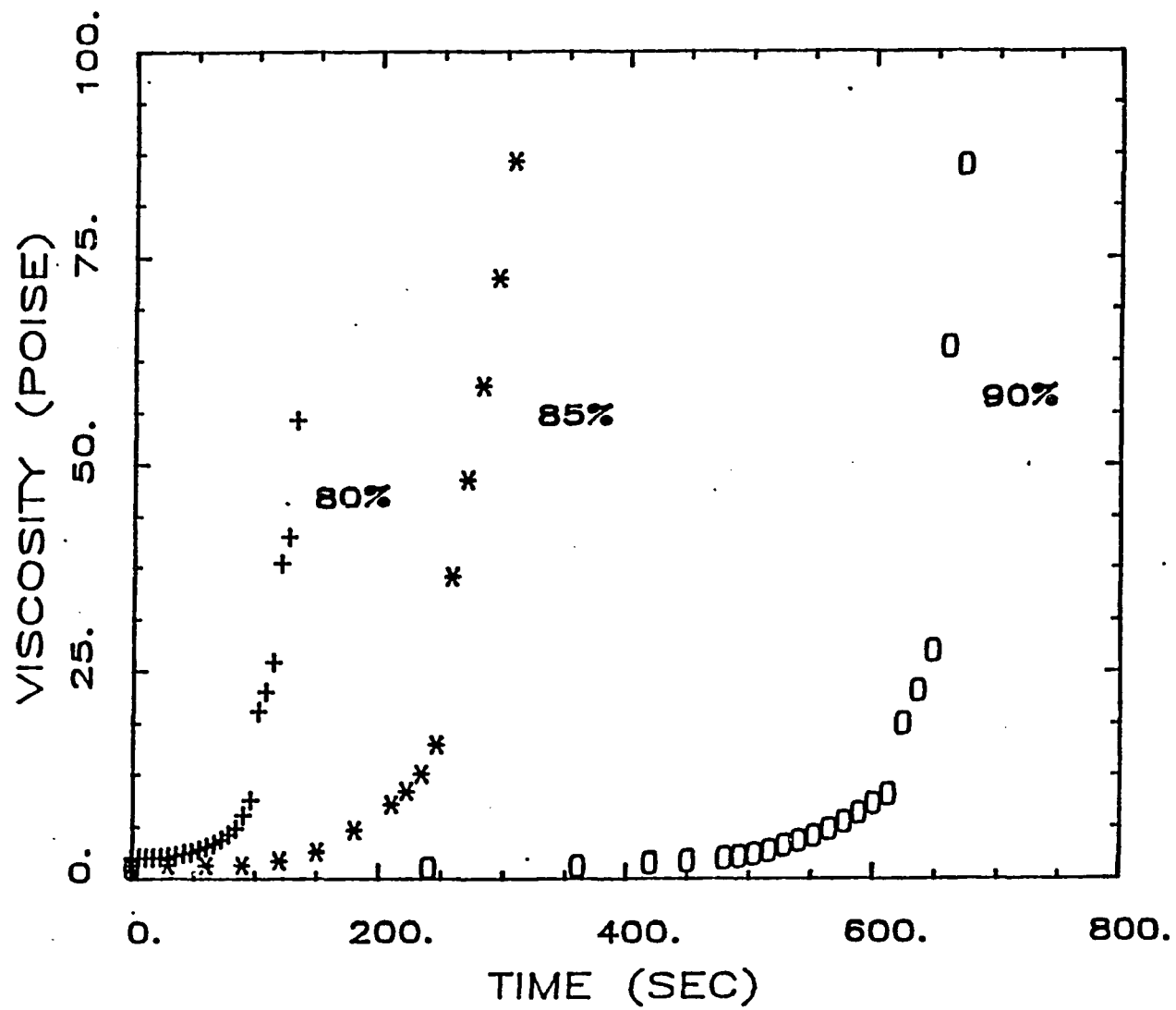


Figure 5.8 Viscosity vs. time plot of polyurea III at three concentrations by Haake viscometer at 25 °C.

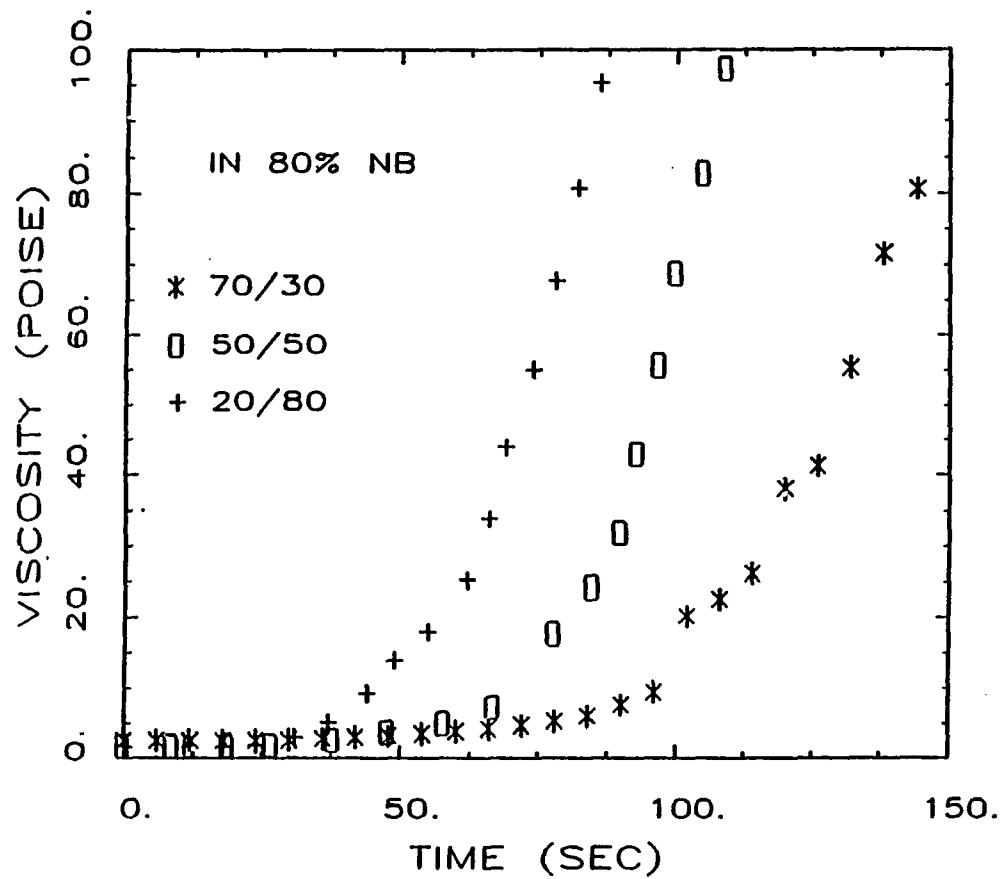


Figure 5.9 Effect of soft segment/hard segment ratios on viscosity rise in 80% nitrobenzene solution of T5000/MDI/TBTDA using Haake viscometer at 25 °C.

with 85% nitrobenzene dilution by Haake viscometer. The stoichiometric ratio between amines and isocyanates is equivalent to one in each composition. The gel times of polyureas with composition of 70/30 (70% triamine and 30% diamine by weight with equivalent moles of isocyanate), 50/50, and 20/80 are 310, 200, and 145 seconds respectively. This indicates that with more aromatic amine in polyurea, the viscosity rise tends to take place earlier. However, when the aliphatic triamine and the aromatic diamine were separated and allowed to react with the diisocyanate independently (Figure 5.10), the viscosity rise of polyurea I (i.e., aliphatic amine and isocyanate only, sample designation 100/0) took place much earlier than that of polyurea II (i.e., aromatic amine and isocyanate only, sample designation 0/100). In Figure 5.10, the gel time is 22 seconds for polyurea I and is 112 seconds for polyurea II, which indicates that aliphatic amine reacts much faster with isocyanate than aromatic amine. This seems to be contrary to the results shown in Figure 5.9. The same experimental results were also found for polyurea reaction in 80% dilution as shown in Figures 5.11 and 5.12 (compared to Figures 5.9 and 5.10). Because of less dilution, the gel time of each 80% diluted polyurea reaction was shorter than the corresponding reaction at 85% dilution, but the trend was still the same.

The viscosity rises of 85%-diluted polyurea reactions with the compositions ranging from 80/20 to 95/5 were also measured. As the

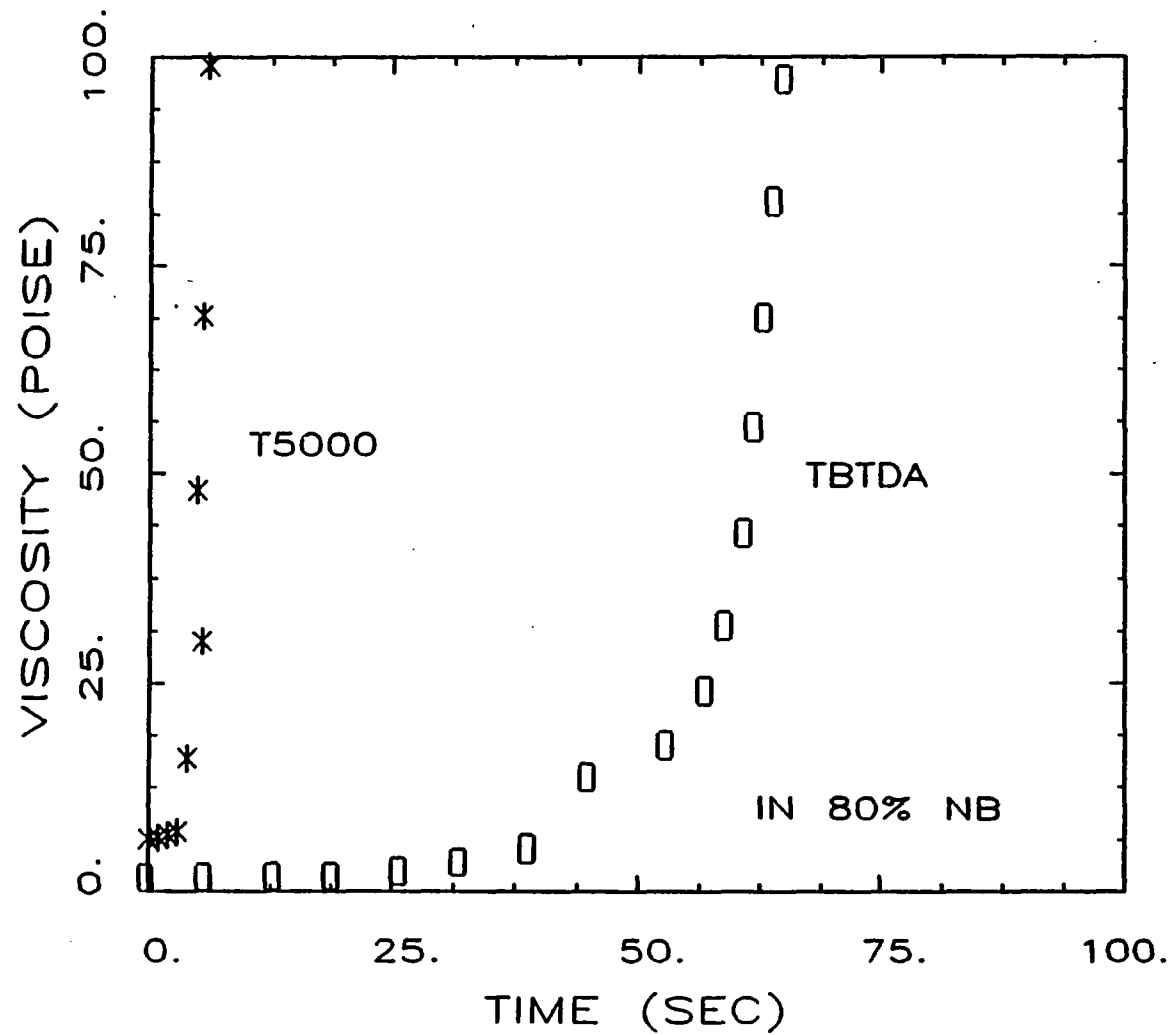


Figure 5.10 Viscosity rise vs.time plot of polyurea I and II in 80% nitrobenzene.

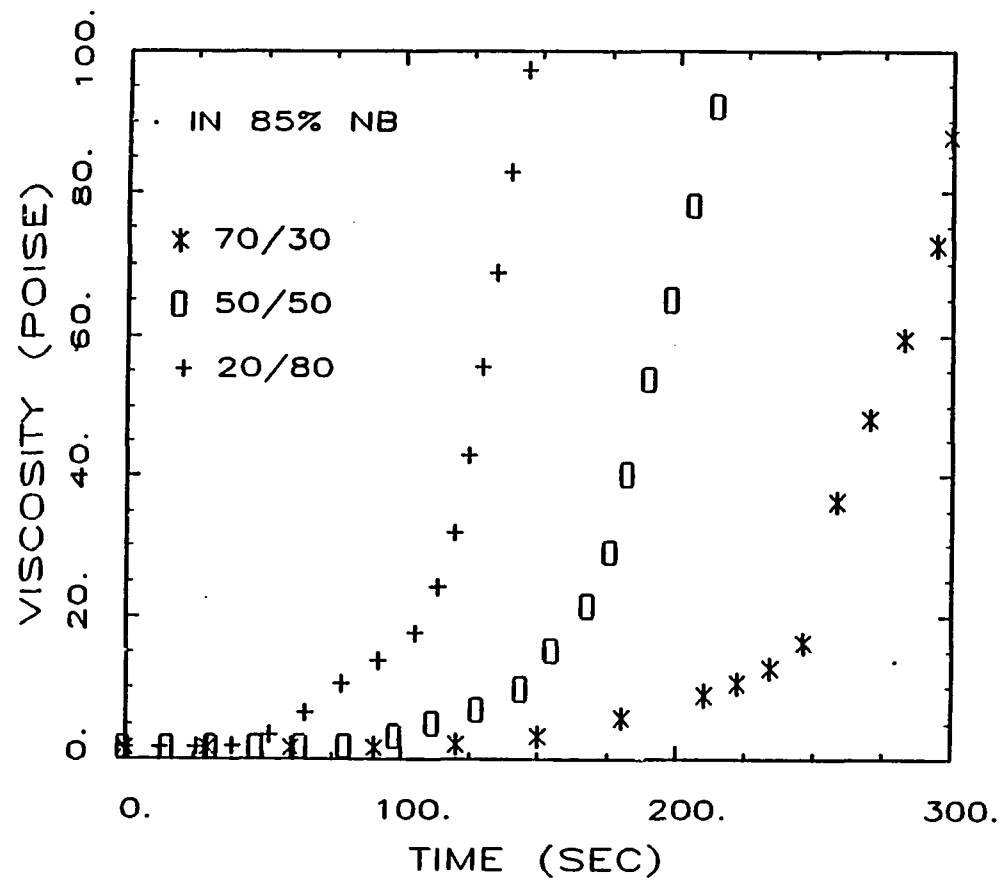


Figure 5.11 Effect of soft segment/hard segment ratios on viscosity rise in 85% nitrobenzene solution of T5000/MDI/TBTDA using Haake viscometer at 25 °C.

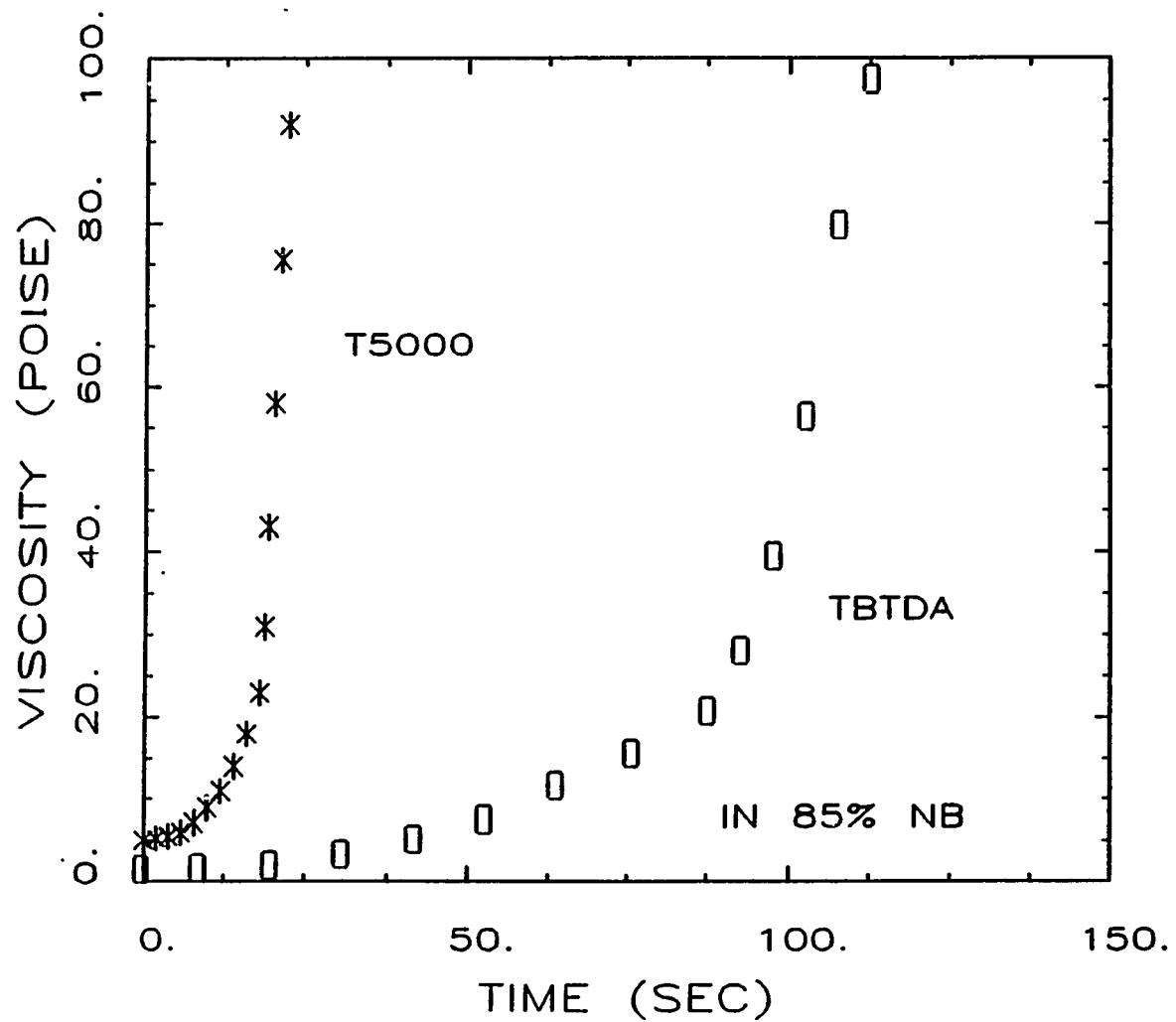


Figure 5.12 Viscosity rise vs. time plot of polyurea I and II in 85% nitrobenzene.

weight ratio of aliphatic triamine was further increased from 70/30 to 95/5, a critical (transition) point occurred around the ratio of 85/15. Above this point, increasing the amount of aliphatic amine decreased the gelation time; while below this point, gelation time increased at higher content of aliphatic amine. The gel times at various compositions of polyureas with 85% dilution are listed in Table 5.2 and shown in Figure 5.13. In Figure 5.13, the gel time is plotted vs. weight percent soft segment in the reaction system. The soft segment content is defined as aliphatic amine plus an equivalent molar amount of isocyanate. For 85% diluted systems, the maximum soft segment content is 15%. The calculated soft segment contents for various compositions of polyureas are listed in Table 5.2. Figure 5.13 and Table 5.2 indicate that a critical concentration exists at 8.2% soft segment content. The viscosity rise of polyurea reaction is primarily aliphatic amine-dominated above 8.2% soft segment content. Below 8.2%, although the reaction of aliphatic amine with isocyanate is still faster than the reaction of aromatic amine and isocyanate, the amount of soft segment formed is not high enough to cause viscosity build-up. The measured viscosity rise is mainly due to the reaction between aromatic amine and isocyanate. This is why that in the 80% and 85% nitrobenzene diluted polyurea reactions shown in Figures 5.6 and 5.12, increasing the amount of aromatic amine in polyurea increased the viscosity rise since all the reaction systems have soft segment contents lower

Table 5.2 Variations of soft segment/hard segment ratios

C	soft segment + hard segment					soft segment only	
	t_{gel} (sec)	P_{NB} (%)	SP (%)	P_F (%)	P_a (%)	S_{NB} (%)	t_{gel} (sec)
100/0	22	85.0	15.0	70.0	---	15.0	0.0
95/5	50	85.0	13.0	81.6	---	13.0	1.2
90/10	84	85.0	11.0	86.9	---	11.0	3.0
85/15	116	85.0	9.8	90.1	---	9.8	6.1
80/20	340	85.0	8.2	92.2	---	8.2	---
75/25	325	85.0	7.4	93.7	---	7.4	---
70/30	310	85.0	6.6	94.9	59.0	---	---
50/50	200	85.0	2.01	97.5	53.0	---	---
20/80	145	85.0	1.2	99.4	44.0	---	---
0/100	112	85.0	0.0	100.	---	---	---
70/30 (RIM)	---	44.4	---	---	---	---	---

no
gel

- C : weight composition of polyurea (soft segment/hard segment)
 P_{NB} : % nitrobenzene in solution
 SP : % by weight soft segment of polyurea in solution
 P_F : gel conversion calculated according to equation (5.5)
 P_a : actual gel conversion measured
 S_{NB} : % by weight (T5000 + 1305) in solution.

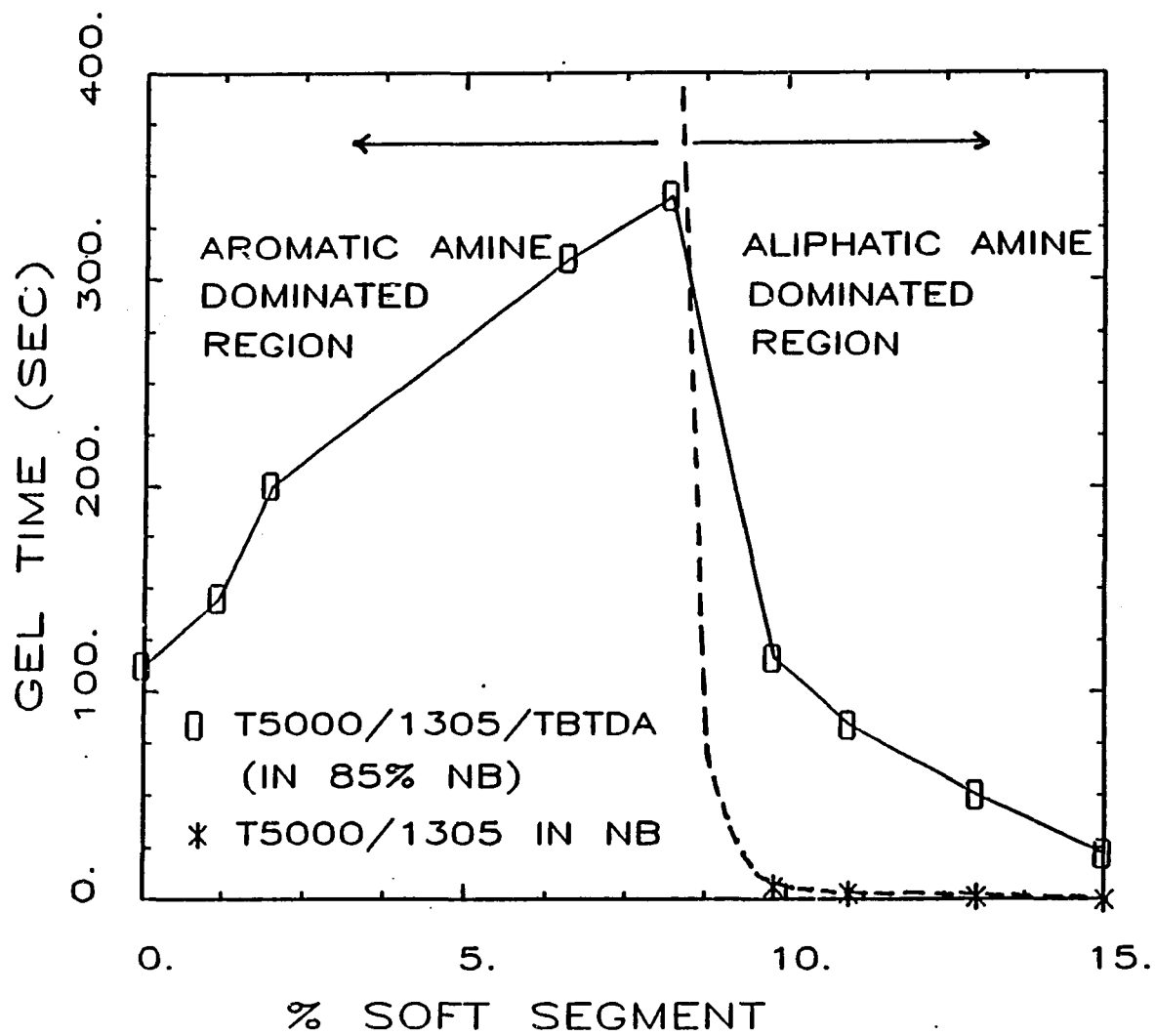


Figure 5.13 Gel time vs. the amount of soft segment.

than the critical point, except polyurea I solutions. Figure 6, therefore, reflects mainly the relative reactivities of various aromatic diamine chain extenders. To further check this argument, the gel times of polyurea reactions with aliphatic triamines only were measured in 85% nitrobenzene and the results are plotted in Figure 5.13. It was found that a critical concentration also existed at about 8.2% polymer in nitrobenzene, which agrees well with other experiments. Above this concentration, the solution could form a gel; while below this concentration, the solution stayed in a liquid state even after several days of reaction time.

The detailed reaction mechanism of polyurea formation is schematically described in Figure 5.14. The long chains represent aliphatic triamine molecules with molecular weight about 5,000 and a functionality of 3. Aromatic diamine serves as a chain extender with molecular weight of 178. diisocyanate reacts with both amines to form urea linkage. Compared to the size of aliphatic amine, the size of aromatic amine is so small that its contribution to the increase of molecular weight during polyurea formation is relatively small. In addition, the reactivity of aliphatic amine is greater than that of aromatic amine (Pannone, 1986; Vespoli et al., 1986), which further reduces the influence of aromatic amine on the molecular weight growth of polyureas. Therefore, the viscosity rise of polyurea reaction mainly reflects the polymer formation between aliphatic amine and isocyanate. However, when the polyurea system is

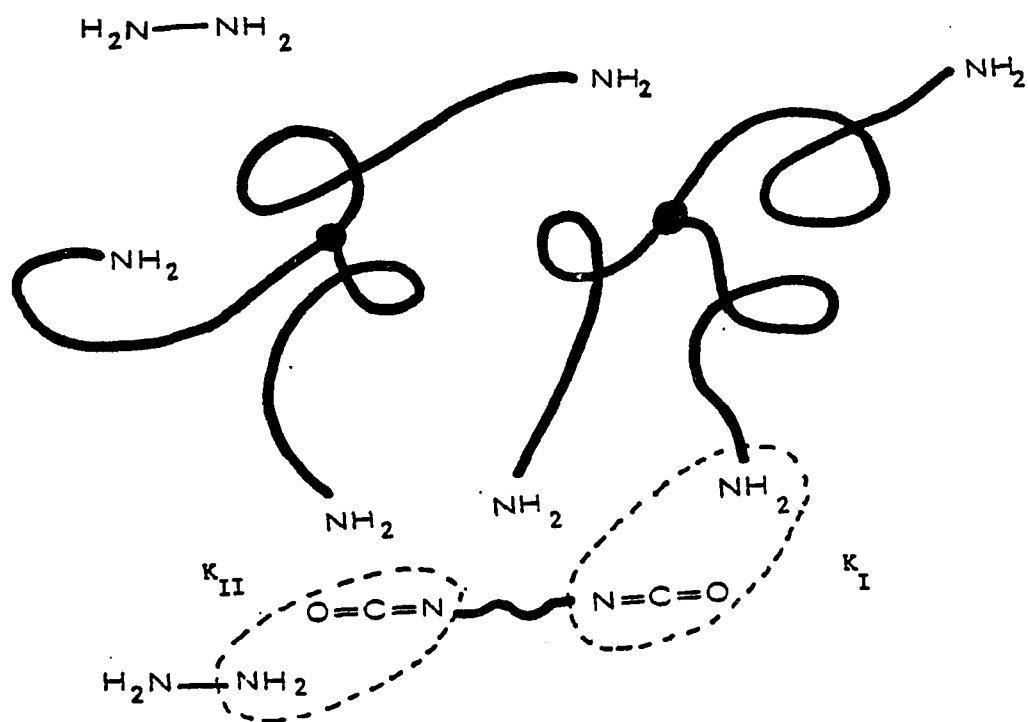


Figure 5.14 Schematic diagram showing the formation of polyurea.

highly diluted in nitrobenzene, there is a critical concentration of aliphatic amine. Below this concentration, the aliphatic amine, even though totally reacted with isocyanate to form polyurea, is not able to build up a network structure. The observed viscosity rise is caused by the physical crosslinking through the reaction of aromatic amine and isocyanate, which will be explained in next section. This critical concentration was found to be 8.2% soft segment in 85%-diluted polyurea system.

In RIM process, the polymerization occurs in bulk, the soft segment content of 70/30 polyurea is 44.4% by weight, a value far above the critical concentration (8.2%). Therefore, the rheological data, measured at 85% dilution, are applicable in extrapolation to bulk polyurea polymerization only when the soft segment exceeds 8.2%.

B. Kinetic Measurements

The reaction kinetics of polyureas was measured using Fourier transform infrared spectroscopy (FTIR). The FTIR analysis is based upon the peak change of functional groups or characteristic linkages during reaction period. Therefore, there are more than one peaks which may change when polyurea reaction takes place. In principle, the isocyanate peak (2273.4 cm^{-1}), amine peak (3338 cm^{-1}), and the amide peak (NH stretching, around 3312.5 cm^{-1}) can be followed

during urea formation in which both isocyanate and amine monomers are consumed and amide is formed. However, the amine peak and the amide peak are found to be strongly affected by hydrogen bonding and also tend to interfere with each other. The isocyanate peak can be more precisely monitored since it is located in an isolated area and its absorbance are much higher than the amine and amide peaks.

Figure 5.15 shows a portion of the infrared spectra (i.e., wavelengths 2,000-3,600) for a 70/30 polyurea reaction diluted with 80% nitrobenzene. Figure 5.16 shows the measured conversion profiles of polyureas in 95% nitrobenzene solution with two different chain extenders TBTDA and DETDA. For comparison, the isocyanate conversion of Dow's XV15081.001 experimental polyurea is also shown (solid line). The conversion data based on the peak of the 2nd NH- stretching of amide (3312.5 cm^{-1}) scatter more than those based on the -NCO peak because the amide peak is strongly affected by hydrogen bondings. Nevertheless, following the changes of both peaks gave the same results. The conversion profiles reported in this chapter were based on the change of -NCO peak.

Figure 5.17 shows conversion vs. time plots of 90%-diluted polyureas at three reaction temperatures: 25 °C, 47 °C, and 67 °C. Figure 5.18 shows conversion profiles of isothermal polyurea reactions at 25 °C and three levels of dilution: 80%, 85%, and 90% nitrobenzene. As expected, a higher temperature and a higher polyurea concentration exhibit a faster reaction rate.

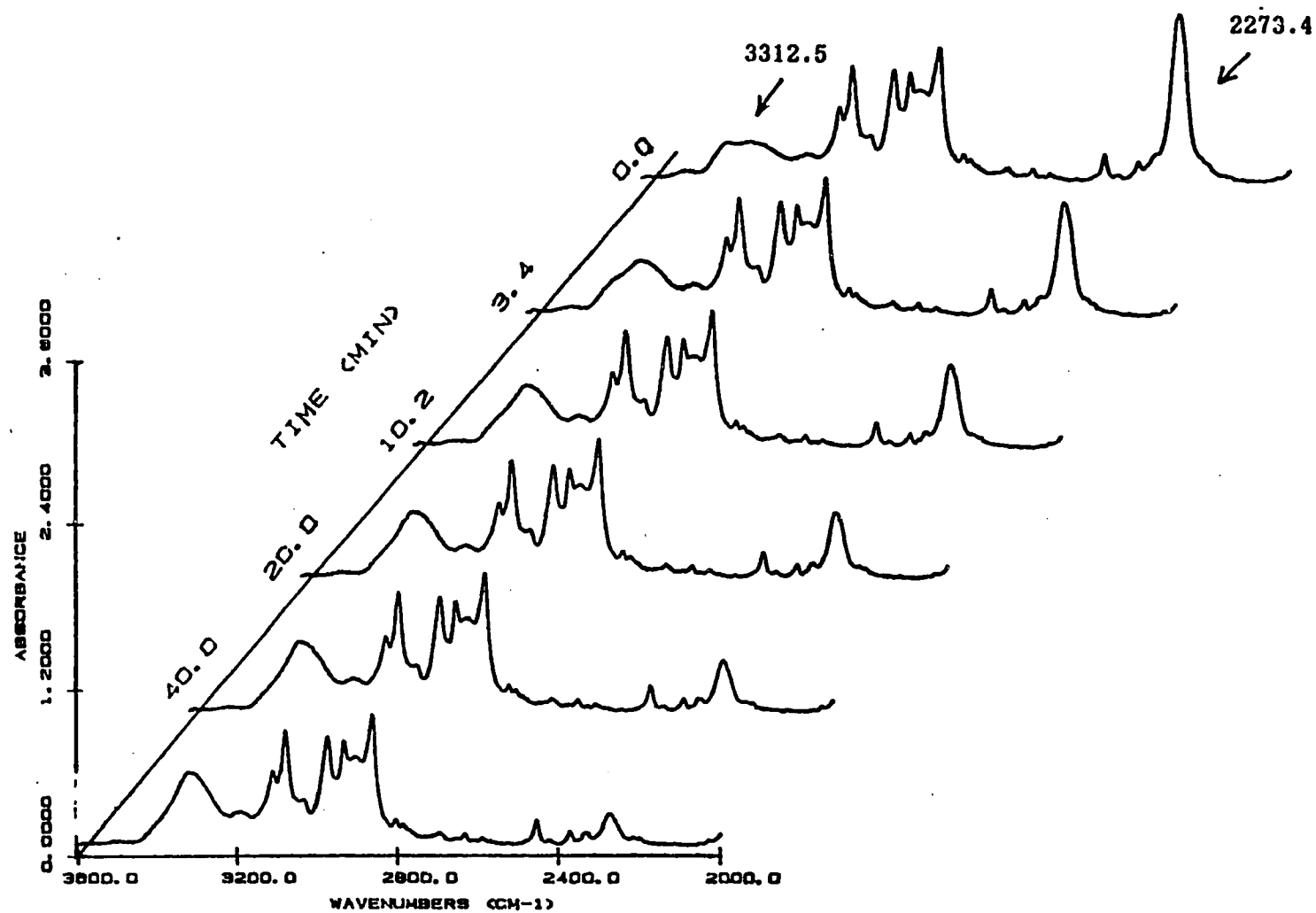


Figure 5.15 FTIR spectra of polyurea III in 80% nitrobenzene solution recorded at several reaction times. Reaction temperature = 25 °C.

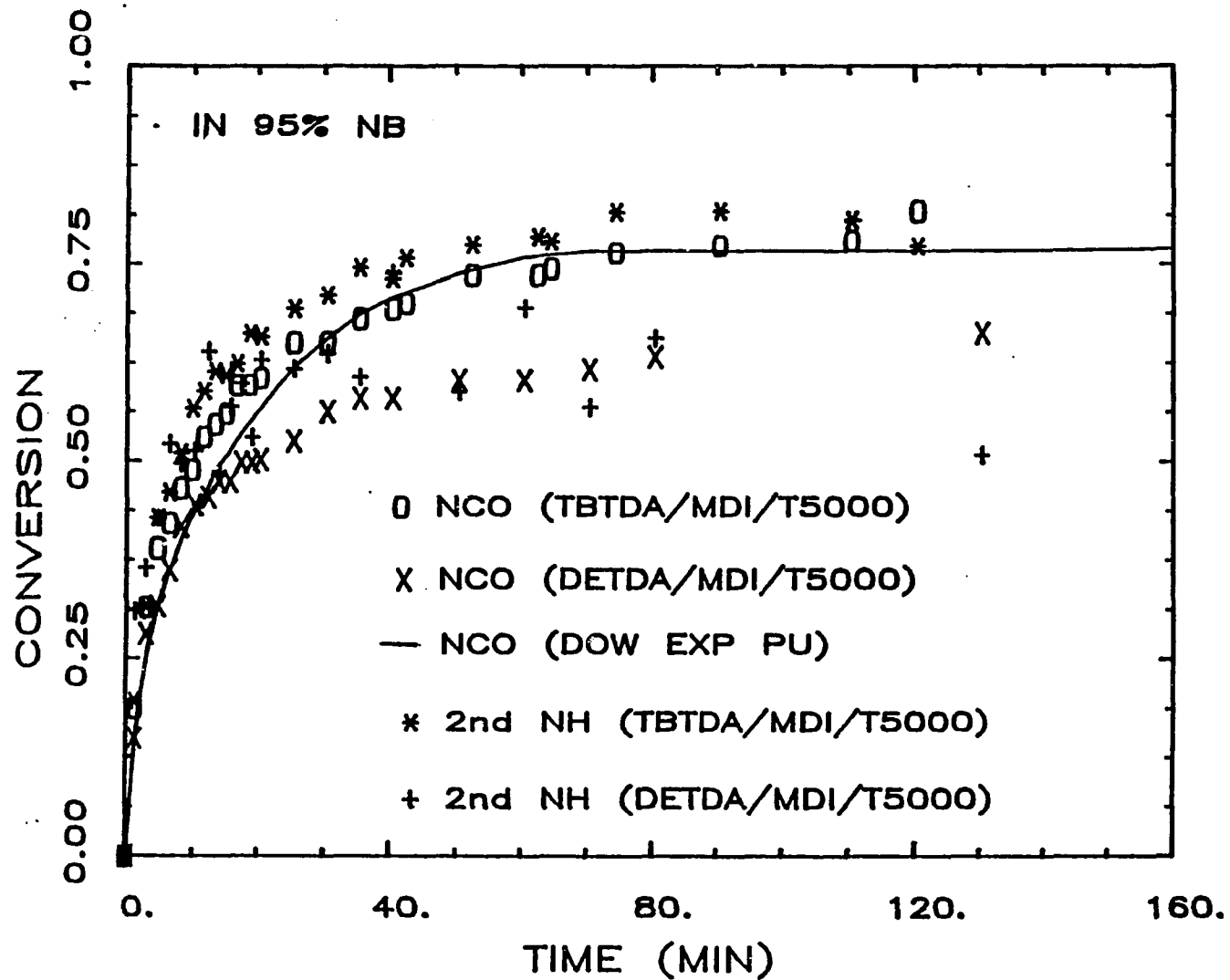


Figure 5.16 Conversion vs. time plot of polyurea III in 95% nitrobenzene with two different chain extenders.

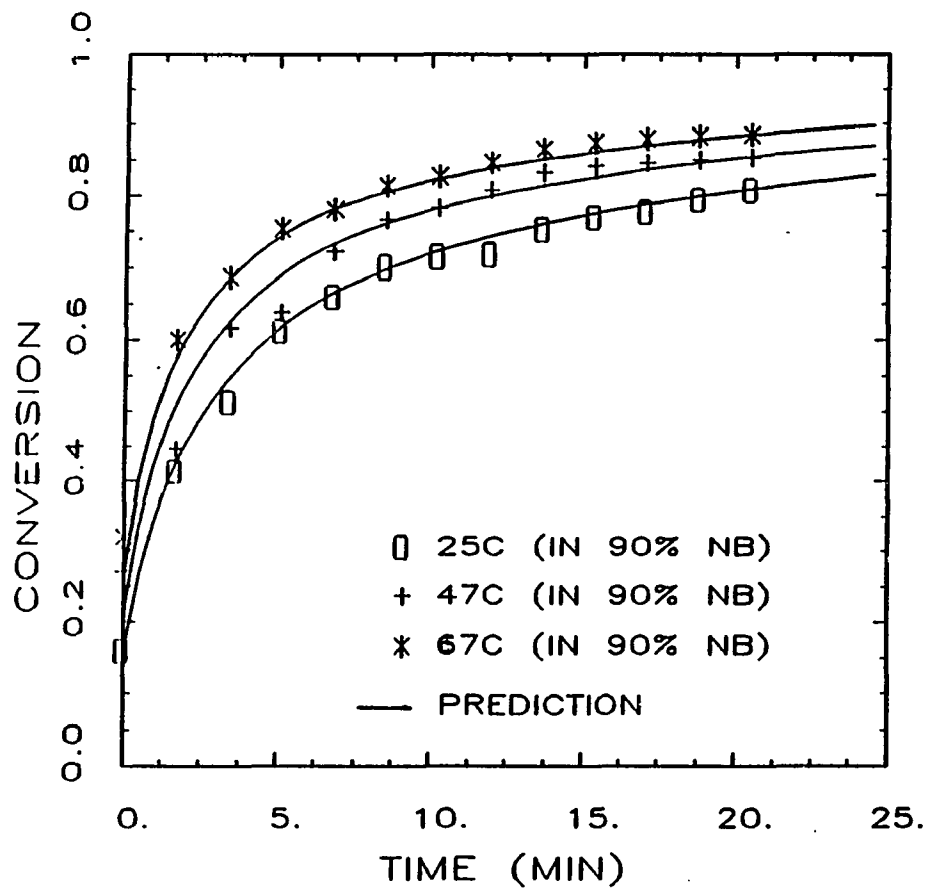


Figure 5.17 Conversion vs. time plot of polyurea III in 90% nitrobenzene at three temperatures. Data were obtained according to the NCO peak at 2273.4 cm^{-1} and the NH stretching peak at 3312.5 cm^{-1} from FTIR spectra.

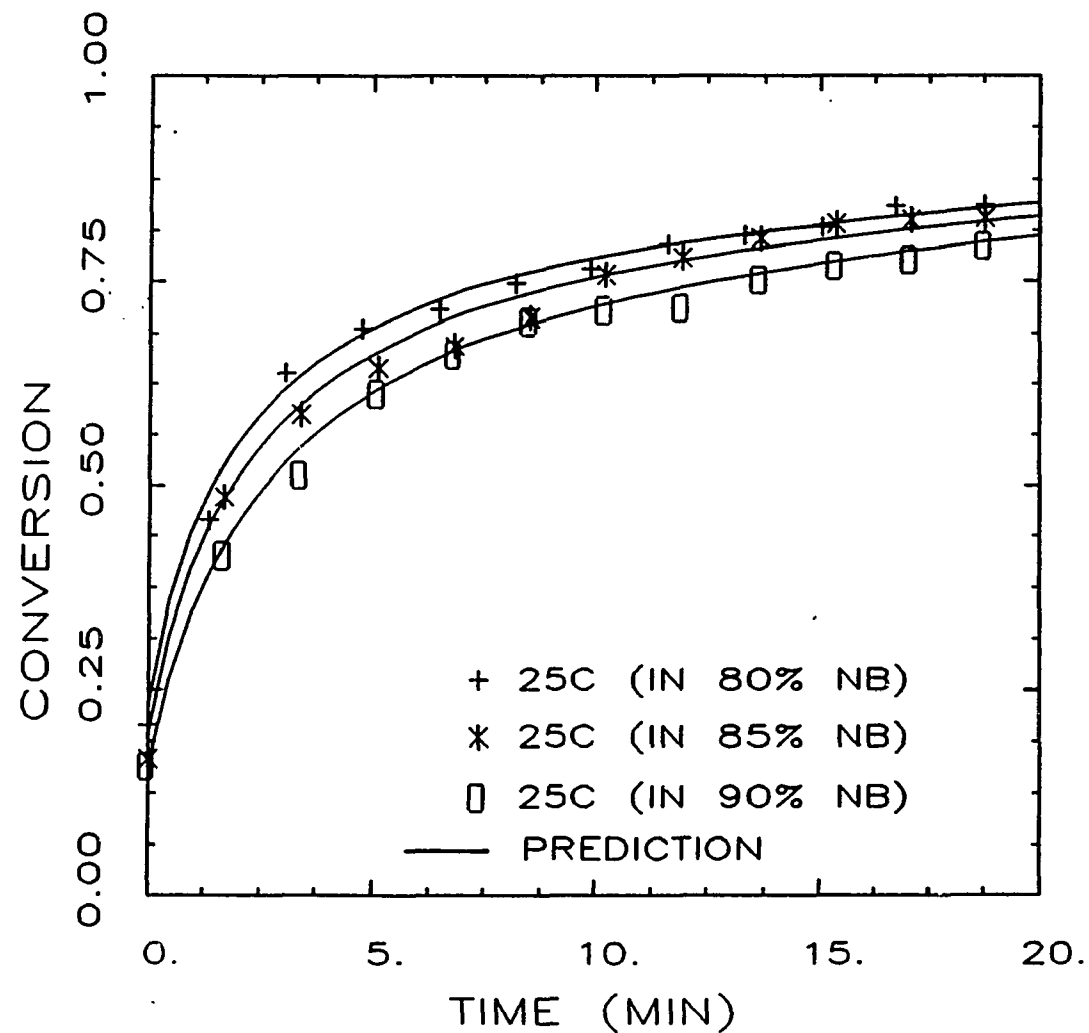


Figure 5.18 Conversion vs. time plot of polyurea III at three concentrations from FTIR measurements. Reaction temperature = 25 °C.

Combining viscosity data from Haake viscometer and conversion data from FTIR, a viscosity vs. conversion plot is obtained as shown in Figure 5.19 for the same data in Figure 5.18. The gel conversions are between 50% and 60%. The more the polyurea is diluted, the higher the gel conversion is. Similar results were also experimentally observed by Stepto and Waywell (1972) and Stanford and Stepto (1977) in the studies of intra-molecular reaction for linear and branched polyurethane reactions. It was found that the extent of intra-molecular reaction increased when the reaction system was diluted by solvent, as indicated by a delay of gelation. Figure 5.20 shows the viscosity vs. conversion curves for 85%-diluted polyurea reactions at three compositions: 70/30, 50/50, and 20/80. The gel conversions are between 40% and 60%, and are lower for systems with higher content of hard segment.

According to Flory's theory of gelation (Flory, 1953), for a branched system $A_3 + A_2 + B_2$, the gel conversion can be calculated from the following equation:

$$\begin{aligned} 1/(f-1) &= \gamma p_A^2 \varepsilon / [1 - \gamma p_A^2 (1-\varepsilon)] \\ &= p_B^2 \varepsilon / [\gamma - p_B^2 (1-\varepsilon)] \end{aligned} \quad (5.4)$$

where f is the functionality of the branch units A_3 in this case, ε is the ratio of A groups (amine) on branch units to all A groups in

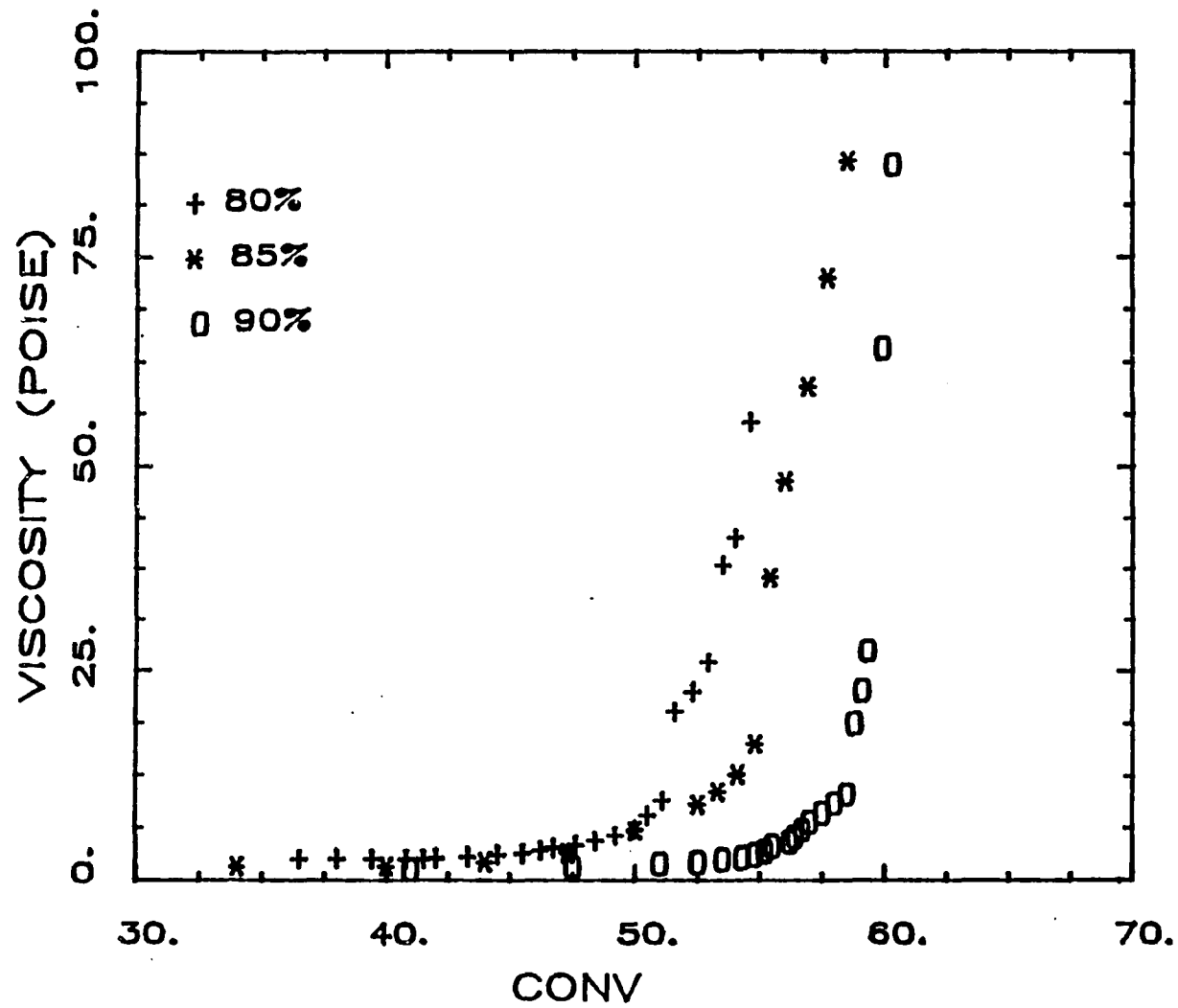


Figure 5.19 Viscosity vs. conversion plot of polyurea III at three concentrations measured at 25 °C.

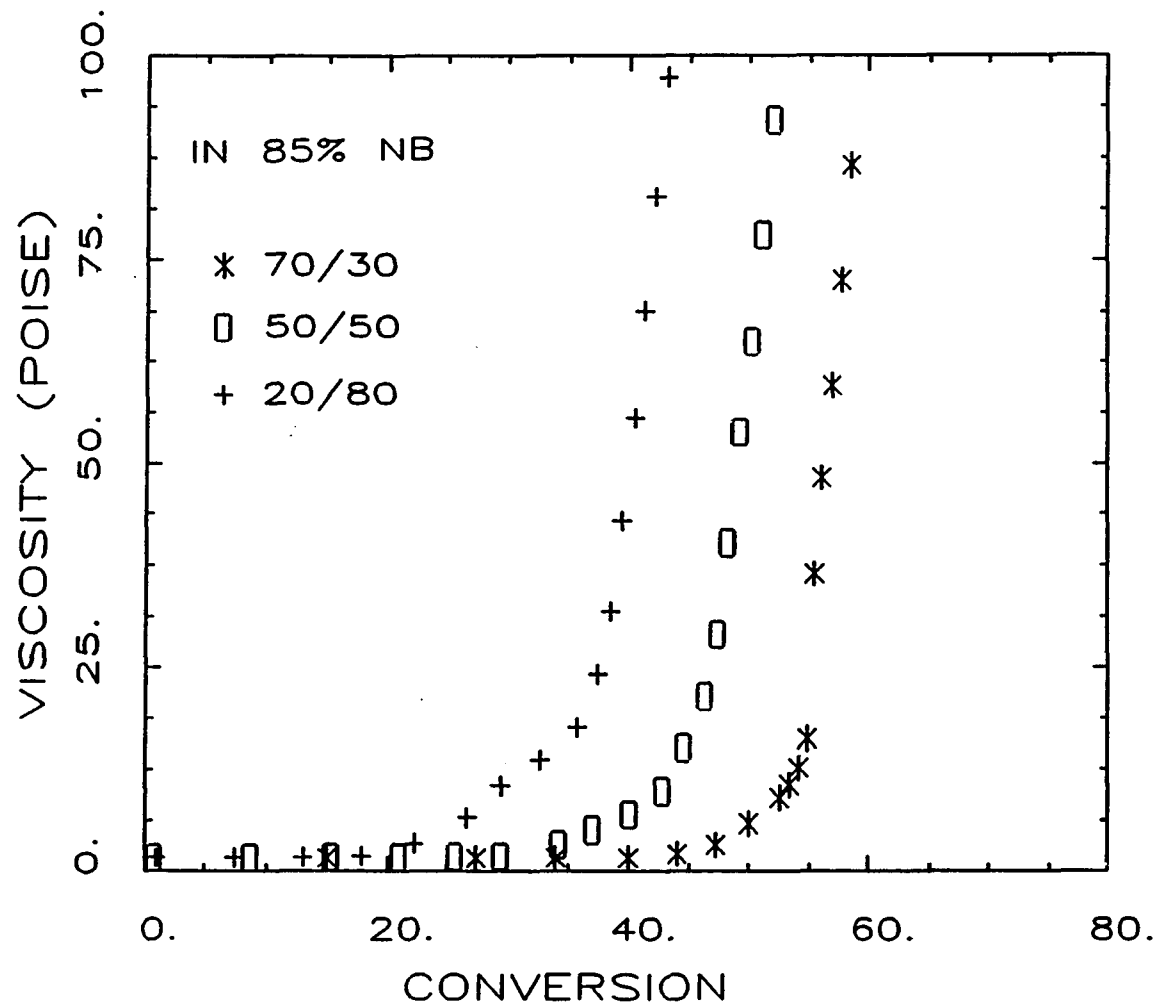


Figure 5.20 Viscosity vs. conversion plot of polyurea III at three compositions in 85% nitrobenzene measured at 25 °C.

the mixture, $\gamma = N_A/N_B$ (hence $p_B = \gamma p_A$), and p_A and p_B are the extents of reaction for A and B groups at gel point. N_A and N_B are moles of functional monomers A and B. In this study, A is defined as the amine functional groups (including bothiphatic and aromatic amines) and B is defined as the isocyanate functional groups. It is assumed in equation (5.4) that the reactivities of aliphatic and aromatic amines are equal. If equal numbers of A and B groups are present, $\gamma = 1$ and $p_A = p_B = p$, then equation (5.4) becomes

$$1/(f-1) = p^2 \epsilon / [1 - p^2 (1 - \epsilon)] \quad (5.5)$$

When there are no diamine units such as in the case of diisocyanate and triamine reaction (i.e., polyurea I), $\epsilon = 1$, and equation (5.5) is further simplified to

$$1/(f-1) = p_A^2 \gamma = p_B^2 / \gamma \quad (5.6)$$

With $f=3$ and $\gamma=1$, equation (5.6) predicts a gel conversion of 70% for polyurea I and 94.9% for the 70/30 polyurea (i.e., polyurea III). The measured gel conversions in Figures 5.19 and 5.20, however, are far below the predicted values by Flory's theory. This can be attributed to the following reasons: First, the aliphatic amine has a higher reactivity than the aromatic amine, which violates the equal reactivity assumption in Flory's theory.

Secondly, the reaction between aromatic amine chain extender and isocyanate, although does not greatly increase the molecular weight of polymer chains, may form hard domains in solution. These hard domains may cause a physical crosslinking in the reaction system and result in a sharp increase of system viscosity. Such phenomenon has been reported for a segmented polyurethane system (Castro, et al., 1981). The measured viscosity rises in highly diluted systems shown in Figures 5.19 and 5.20 are probably mainly caused by the reaction of aromatic amines and isocyanates. Physical crosslinking may be the major reason of viscosity rise.

5.4 KINETIC AND HEAT TRANSFER MODELS FOR POLYUREA REACTIONS

5.4.1 MODELS

A. Kinetic Model

For kinetics of step-growth polymerizations such as polyurea reaction, a simple nth order reaction with Arrhenius temperature dependence is assumed. In this study, the kinetics of polyurea I and II are treated separately as follows:

$$\begin{aligned}
 r_I &= \frac{dC_I}{dt} = K_I C_I^{m_I} C_i^{m_I} = A_I \exp\left(-\frac{E_I}{RT}\right) C_I^{m_I} C_i^{m_I} \\
 &= A_I \exp\left(-\frac{E_I}{RT}\right) C_I^{n_I}
 \end{aligned} \tag{5.7}$$

$$\begin{aligned}
 r_{II} &= \frac{dC_{II}}{dt} = K_{II} C_{II}^{l_{II}} C_i^{m_{II}} = A_{II} \exp\left(-\frac{E_{II}}{RT}\right) C_{II}^{l_{II}} C_i^{m_{II}} & (5.8) \\
 &= A_{II} \exp\left(-\frac{E_{II}}{RT}\right) C_{II}^{n_{II}}
 \end{aligned}$$

where r_I and r_{II} are reaction rates of isocyanates with aliphatic and aromatic amines respectively, C_I and C_{II} are concentrations of aliphatic and aromatic amine functional groups, K_I and K_{II} are rate constants, A_I , A_{II} , A_I , and A_{II} are frequency coefficients, E_I and E_{II} are activation energies, R is the universal gas constant, l_I and l_{II} are reaction orders of aliphatic and aromatic amines, m_I and m_{II} are reaction orders of isocyanate monomers, and n_I and n_{II} are the overall reaction orders of soft and hard segments respectively.

Assumptions used in the kinetic model include:

1. Homogeneous and well mixed system at $t=0$.
2. Negligible concentration change due to diffusion.
3. Reaction order n being the same throughout the entire reaction.

B. Heat Transfer Model

The following assumptions are made for heat transfer model:

1. One-dimensional heat conduction.
2. Negligible molecular diffusion.

3. Homogeneous and well mixing reaction system at $t=0$.
4. Physical properties such as density ρ , heat capacity C_p , heat of reaction ΔH , and thermal conductivity k are temperature independent.
5. No intercomponent reaction.
6. Heat of reaction ΔH is assumed to be the same for the reactions of aliphatic and aromatic amines with isocyanates.

With these assumptions, the governing equations for heat transfer in the cylindrical coordinate can be described as follows:

$$\rho C_p \frac{\partial T}{\partial t} = k \left[\left(\frac{\partial^2 T}{\partial r^2} \right) + \left(\frac{1}{r} \frac{\partial T}{\partial r} \right) \right] - \Delta H_I r_I - \Delta H_{II} r_{II} \quad (5.9)$$

$$= k \left[\left(\frac{\partial^2 T}{\partial r^2} \right) + \left(\frac{1}{r} \frac{\partial T}{\partial r} \right) \right] - \Delta H D_I r_I - \Delta H D_{II} r_{II}$$

where T is temperature, D_I and D_{II} are molar fraction of aliphatic and aromatic amines respectively. The initial conditions are:

$$T = T_0, \quad \text{at } t = 0, \quad \text{for all } 0 \leq r \leq d \quad (5.10)$$

$$C_I = C_{I0}, \quad \text{at } t = 0, \quad \text{for all } 0 \leq r \leq d \quad (5.11)$$

$$C_{II} = C_{II0}, \quad \text{at } t = 0, \quad \text{for all } 0 \leq r \leq d \quad (5.12)$$

where C_{I_0} and C_{II_0} are initial aliphatic and aromatic amine concentrations respectively. The boundary conditions are:

$$\frac{dT}{dr} = 0, \quad \text{at } r = 0, \quad \text{for } t > 0 \quad (5.13)$$

$$T = T_0, \quad \text{at } r = d, \quad \text{for } t > 0 \quad (5.14)$$

The adiabatic reaction in the RIM process is a special case of the energy equation (5.9). The heat conduction is removed in the equation and the boundary conditions are changed. Assuming no heat exchange with surrounding air, the energy equation becomes:

$$\rho C \frac{dT}{pdt} = -\Delta H_I r_I - \Delta H_{II} r_{II} \quad (5.15)$$

Due to the rapid reaction and low thermal conductivity of the polymer, heat loss was assumed to be negligible. The heat of reaction of polyurea can be calculated from the maximum adiabatic temperature rise, ΔT_{ad} , assuming constant density and heat capacity, i.e.,

$$-\Delta H = \rho C_p \Delta T_{ad} / C_0 \quad (5.16)$$

where T_0 is the initial material temperature and C_0 is the initial isocyanate concentration. The measured ΔH is 22.6 kcal/g-mole, which

is in the same range mentioned by other researchers (i.e., 15 ~ 30 kcal/g-mole) (Vespoli, et al., 1986; Pannone, 1986).

5.4.2 PARAMETER ESTIMATION

The kinetic parameters in equations (5.7) and (5.8) were estimated from FTIR measurements. Equations (5.7) and (5.8) can be expressed in the following forms,

$$\begin{aligned} \log(dx_I/dt) &= \log[A_I C_{Io}^{n_I-1} \exp(-E_I/RT)] + n_I(1-\alpha_I) \quad (5.17) \\ &= G_I + n_I(1-\alpha_I) \end{aligned}$$

$$\begin{aligned} \log(dx_{II}/dt) &= \log[A_{II} C_{IIo}^{n_{II}-1} \exp(-E_{II}/RT)] + n_{II}(1-\alpha_{II}) \quad (5.18) \\ &= G_{II} + n_{II}(1-\alpha_{II}) \end{aligned}$$

where α_I and α_{II} are fractional conversions of reactions of isocyanates with aliphatic and aromatic amines respectively. The conversion vs. time plots were first generated from FTIR measurements at three temperatures, 25, 47, and 67 °C. Figure 5.21 shows the FTIR results of these measurements for polyurea II. To obtain the reaction rate dx_{II}/dt at each reaction time, the conversion vs. time data shown in Figure 5.21 are treated by a polynomial curve fitting. Plotting of $\log(dx_{II}/dt)$ vs. $(1-\alpha_{II})$ for

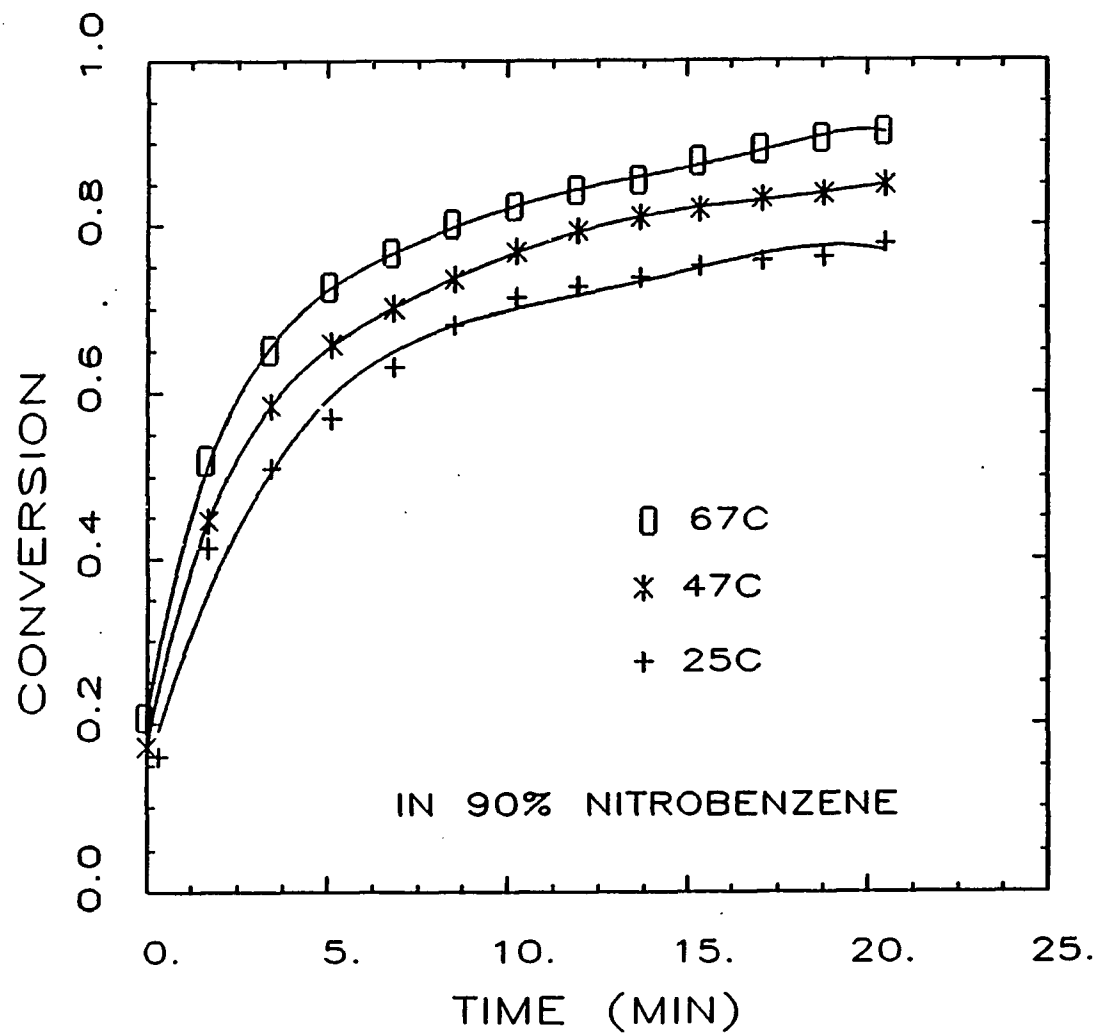


Figure 5.21 Curve fitting of conversion vs. time of polyurea II in 90% nitrobenzene at three temperatures.

three temperatures yields three parallel straight lines as shown in Figure 5.22. As shown in Figure 5.16, FTIR data at high conversions tend to scatter. This is because the peak change of isocyanate is relatively small at high conversions. Therefore, those high conversion data are not included in the determination of kinetic parameters. The interception in Figure 5.22 gives G_{II} and the slope gives the reaction order n_{II} . The G_{II} 's at three temperatures vs. $1/T$ are then plotted as shown in Figure 5.23. The frequency coefficient A_{II} and the activation energy E_{II} are obtained from the interception and the slope in Figure 5.23. The results are $A_{II} = 2.0 \times 10^5$, $E_{II} = 4.21$ kcal/gmole, and $n_{II} = 2.15$. Figures 5.24 to 5.26 are the results of polyurea I using the same procedure described above. The results are $A_I = 3.14 \times 10^6$, $E_I = 1.60$ kcal/gmole, and $n_I = 2.10$. The kinetic parameters and other physical properties used in the model are listed in Table 5.3. The calculated activation energy is similar to those mentioned by others (i.e., 1 ~ 8 kcal/g-mole) (Vespoli et al., 1986; Pannone, 1986). For aliphatic amines, the initial reaction rate was difficult to measure, only the kinetic data in the middle range of conversion were used for the parameter estimation. Deviations of linear regression from experimental data are higher for aliphatic amine-isocyanate reactions than for aromatic amine-isocyanate reactions (i.e., see Figures 5.25 and 5.26). However, the prediction of the conversion profiles of polyurea II is reasonably well as shown in Figure 5.27.

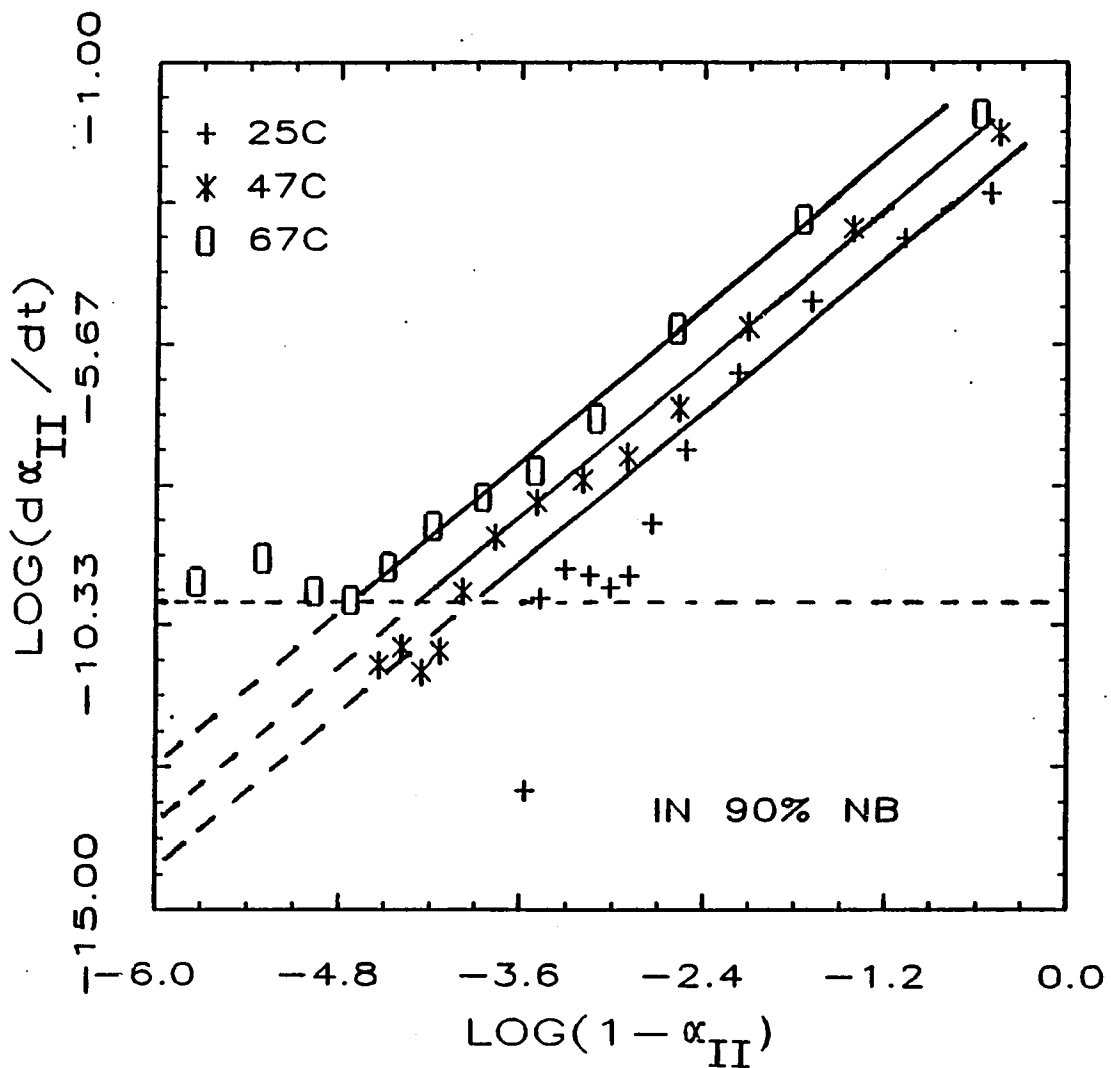


Figure 5.22 Plot of $\log(d\alpha_{II}/dt)$ vs. $\log(1-\alpha_{II})$ of polyurea II.

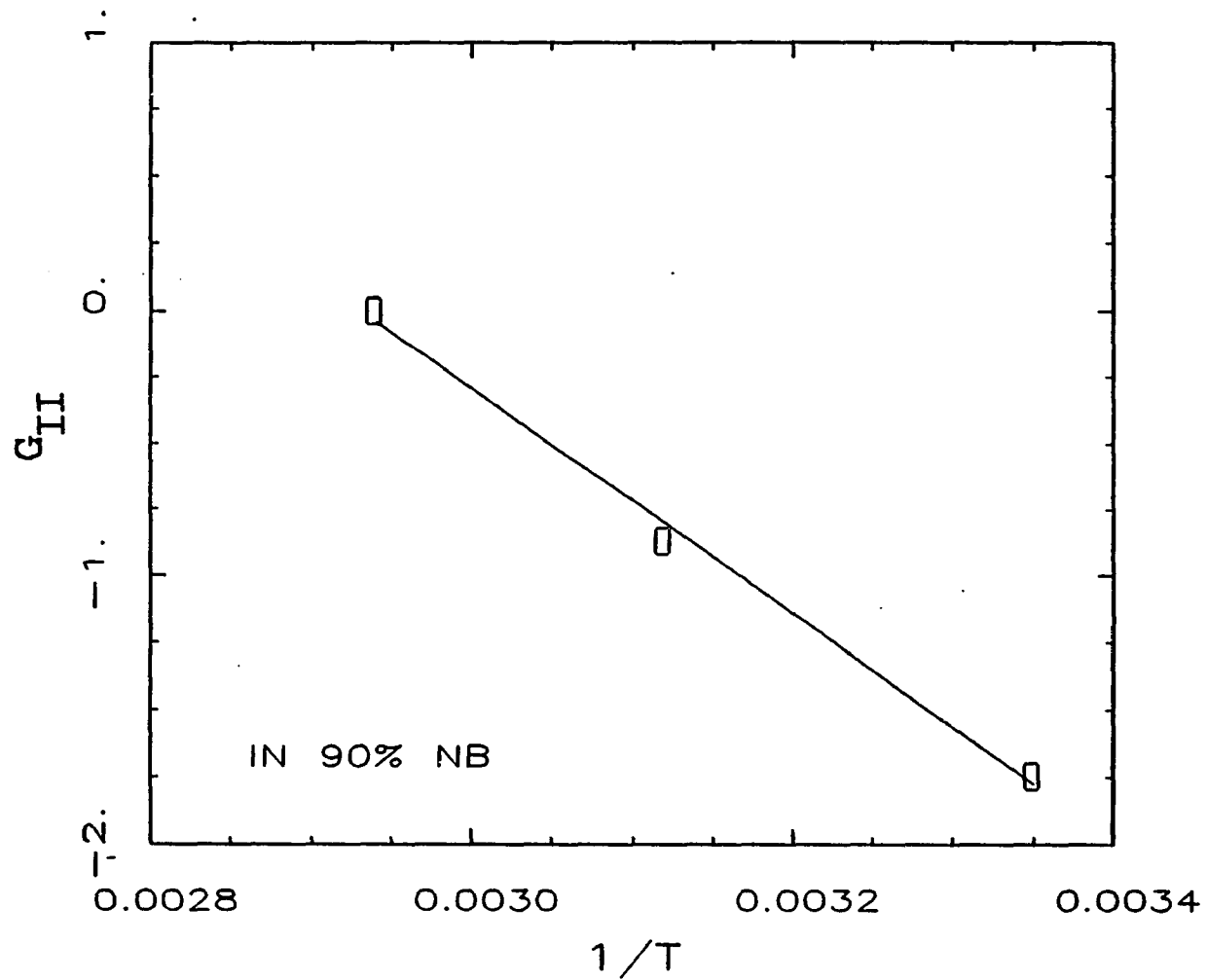


Figure 5.23 Plot of G_{II} vs. $1/T$ of polyurea II.

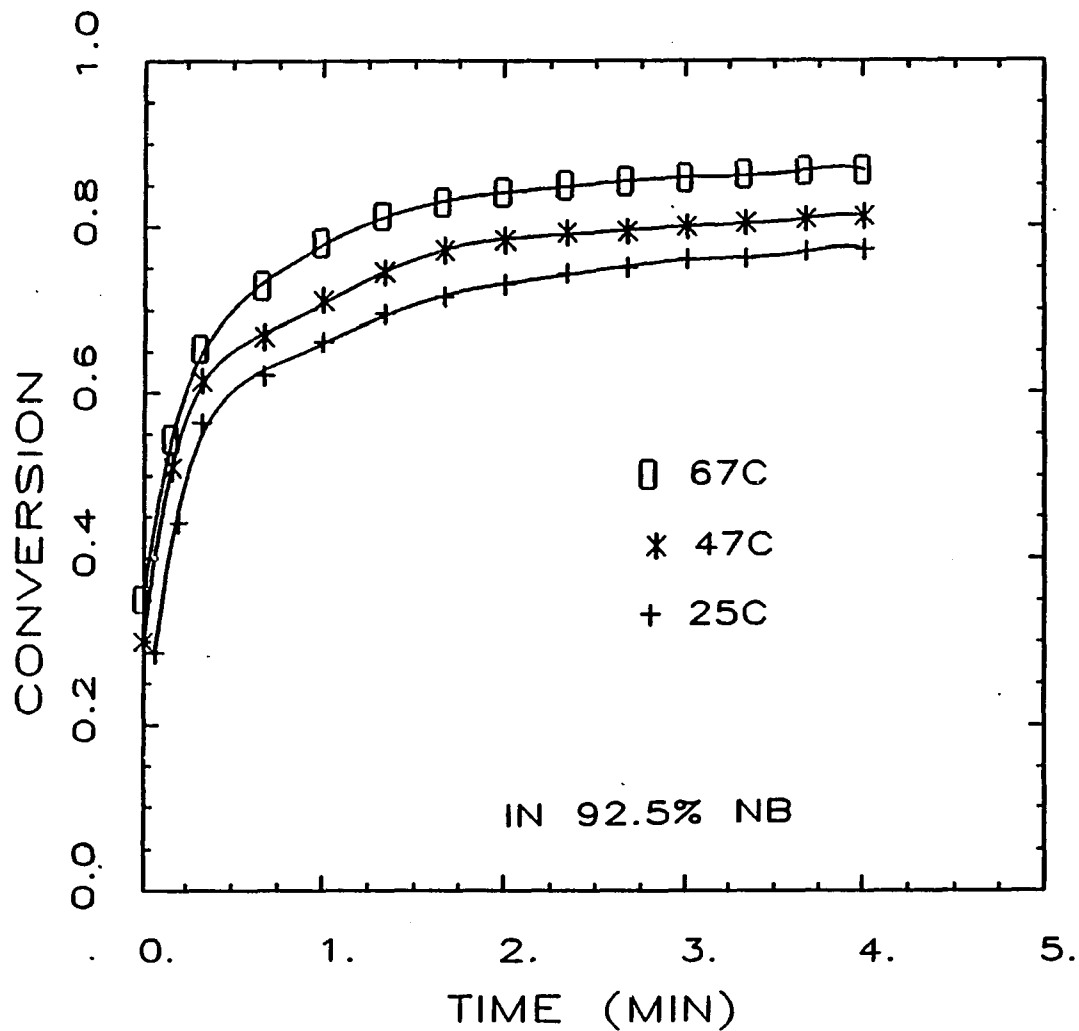


Figure 5.24 Curve fitting of conversion vs. time of polyurea I in 92.5% nitrobenzene at three temperatures.

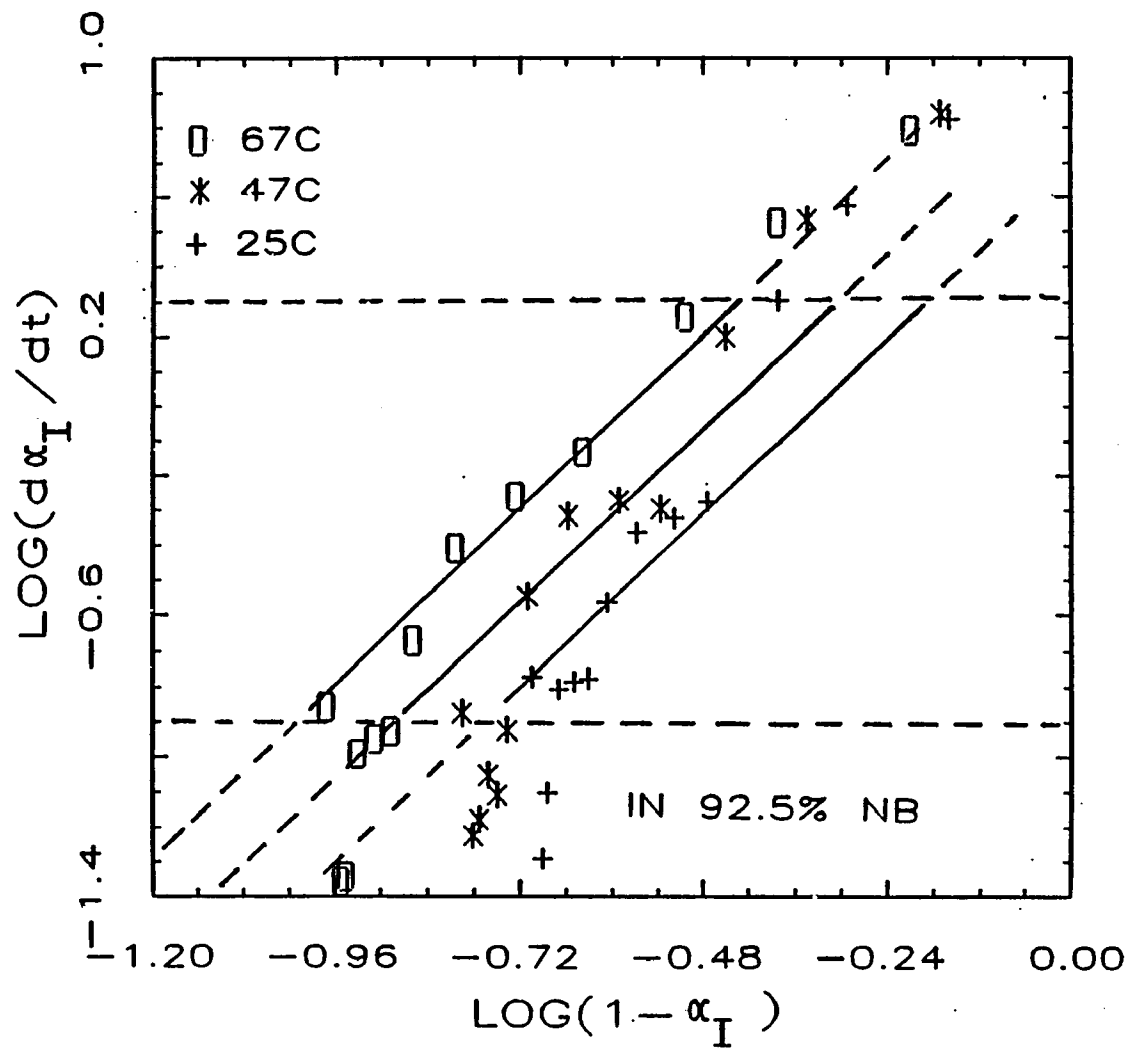


Figure 5.25 Plot of $\log(dx_I/dt)$ vs. $\log(1-\alpha_I)$ of polyurea I.

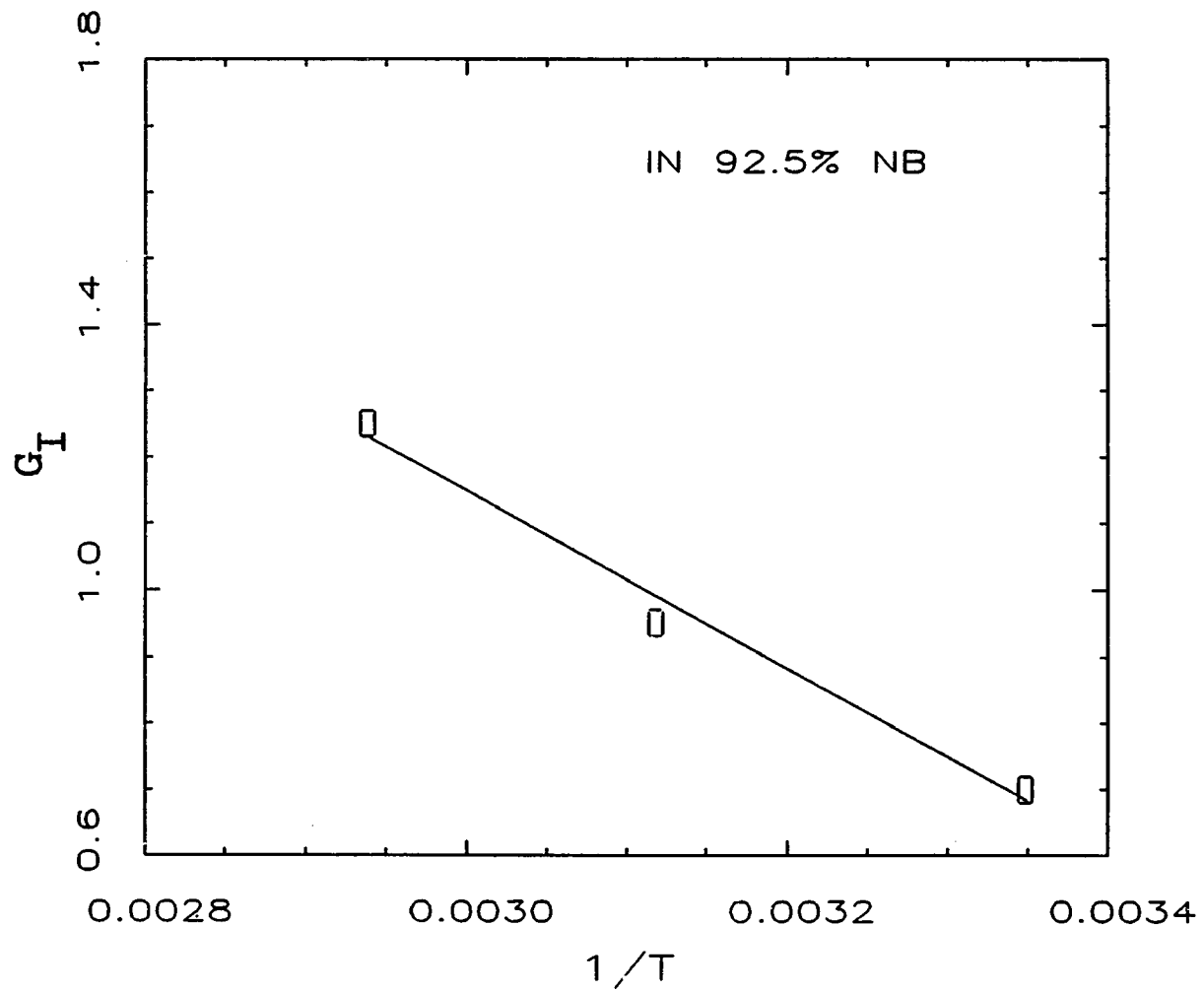


Figure 5.26 Plot of G_I vs. $1/T$ of polyurea I.

Table 5.3 Parameters used for modelling of polyurea

	<u>Aliphatic</u> I	<u>Aromatic</u> II	<u>Polyurea</u> III
E (kcal/gmole)	2.01	4.21	-----
A (app. unit)	5.25×10^6	2.0×10^5	-----
n	3.0	2.15	-----
D	0.111	0.889	-----
H (kcal/gmole)	-----	-----	22.6
C_p (cal/g/ °C)	-----	-----	0.4
ρ (g/c.c)	-----	-----	1.081

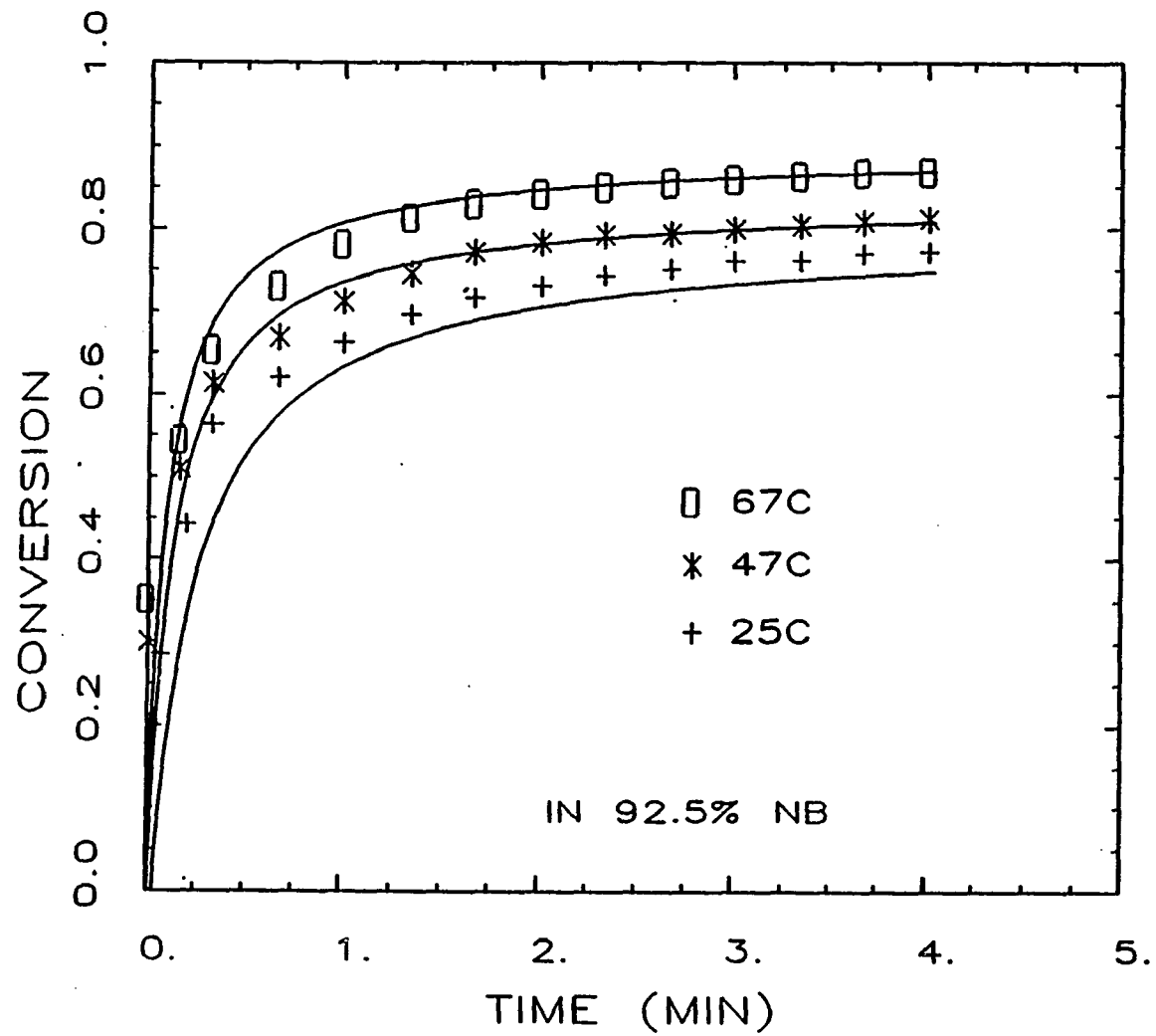


Figure 5.27 Comparisons of predicted and observed conversion profiles of polyurea I in 92.5% nitrobenzene solution.

5.4.3 Model Prediction

Using the parameters determined from the preceding section, the conversion vs. time curves for the 70/30 polyurea reactions with 90% dilution at three reaction temperatures are simulated by the model and the results are given in Figure 5.16. Figure 5.18 compares the model prediction and experimental results for polyurea reactions at three dilution levels at 25 °C. The predictions are very good. The predictions of the adiabatic temperature rises in polyurea RIM are presented in Figures 5.28 and 5.29. Results in Figure 5.28 indicate that the predictions are also very good. The slight deviation is probably due to the model assumption that reactions of aliphatic and aromatic amines with isocyanates are independent of each other. In polyurea formation, the reaction of aliphatic and aromatic amines with isocyanates are actually parallel and competitive. The deviation may also result from the physical interactions from domain formation. Since the kinetic parameters were obtained from solution polymerization data, the extrapolation from solution to bulk polymerization may also result in some errors in prediction. Figure 5.29 displays model predictions of polyurea RIM at initial material temperatures of 35 °C and 55 °C. For the case of 35 °C, the model predicts a higher maximum temperature rise. This is because the low Reynolds number ($Re = 144$) prohibits good mixing. Therefore, experimental data shows a lower adiabatic temperature rise.

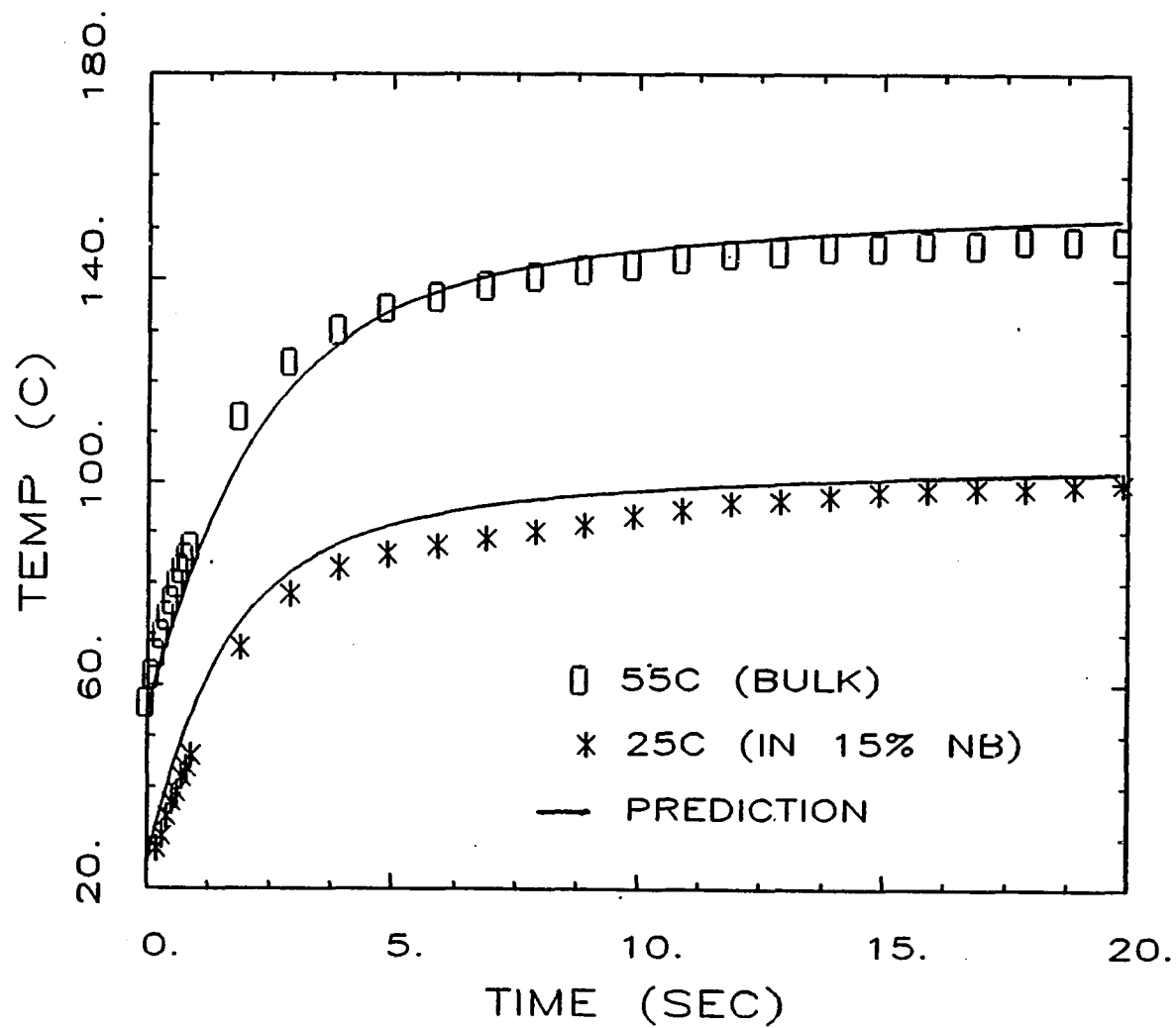


Figure 5.28 Model predictions of temperature profile for polyurea III by RIM in bulk and 15% nitrobenzene.

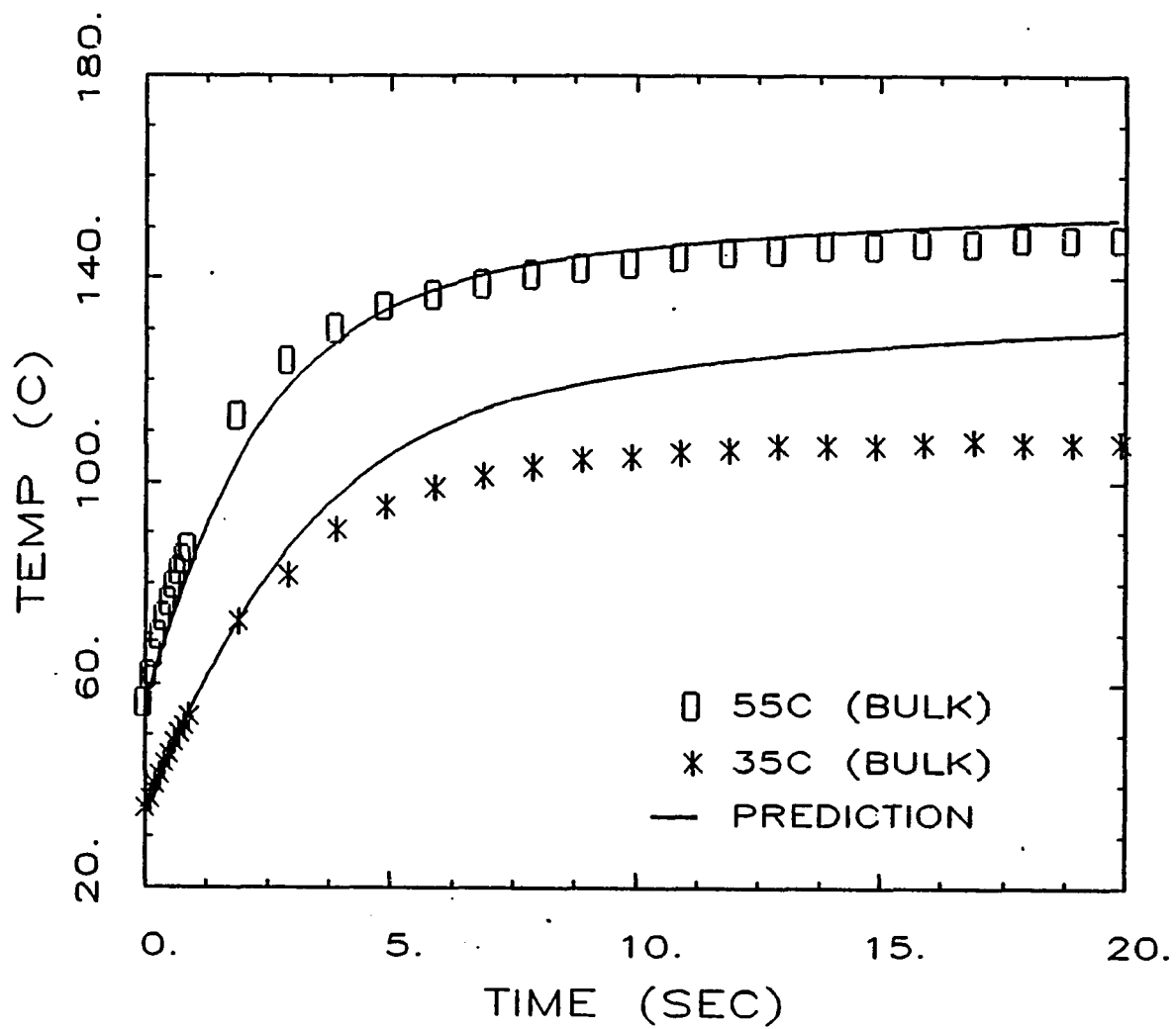


Figure 5.29 Model predictions of temperature profile for polyurea III by RIM at 35 and 55 °C.

Figure 5.30 shows the predicted conversion profiles of polyurea III and its soft and hard segments in adiabatic condition ($T_0 = 55^\circ\text{C}$). The reaction of soft segment is much faster than that of hard segment at the beginning of the reaction. For polyurea III, the overall conversion profile is similar to that of hard segment except at the initial stage. This is because of the high molar concentration of aromatic amine in the reaction system (88.9%).

Figures 5.31 and 5.32 show model predictions of adiabatic temperature profiles of polyurea reactions with various soft segment/hard segment ratios. In Figure 5.31, the temperature rise of the 95/5 polyurea reaction is lower than the 100/0 polyurea (polyurea I). As the hard segment is increased above 15% (i.e., 85/15 polyurea), the temperature rise curve begins to show a crossover (i.e., 1.5 seconds after impingement for 85/15 polyurea). As shown in both figures, increasing the hard segment content increases the maximum adiabatic temperature rise, even though the reaction of hard segment is much slower than that of soft segment. Figures 5.33 and 5.34 show the predicted conversion profiles of polyurea III with various compositions. Figure 5.33 shows that increasing the hard segment content results in a crossover of conversion profile and an increase of the overall conversion rate of polyurea reaction. The results suggest that a major function of aromatic amine chain extender is to increase the reaction

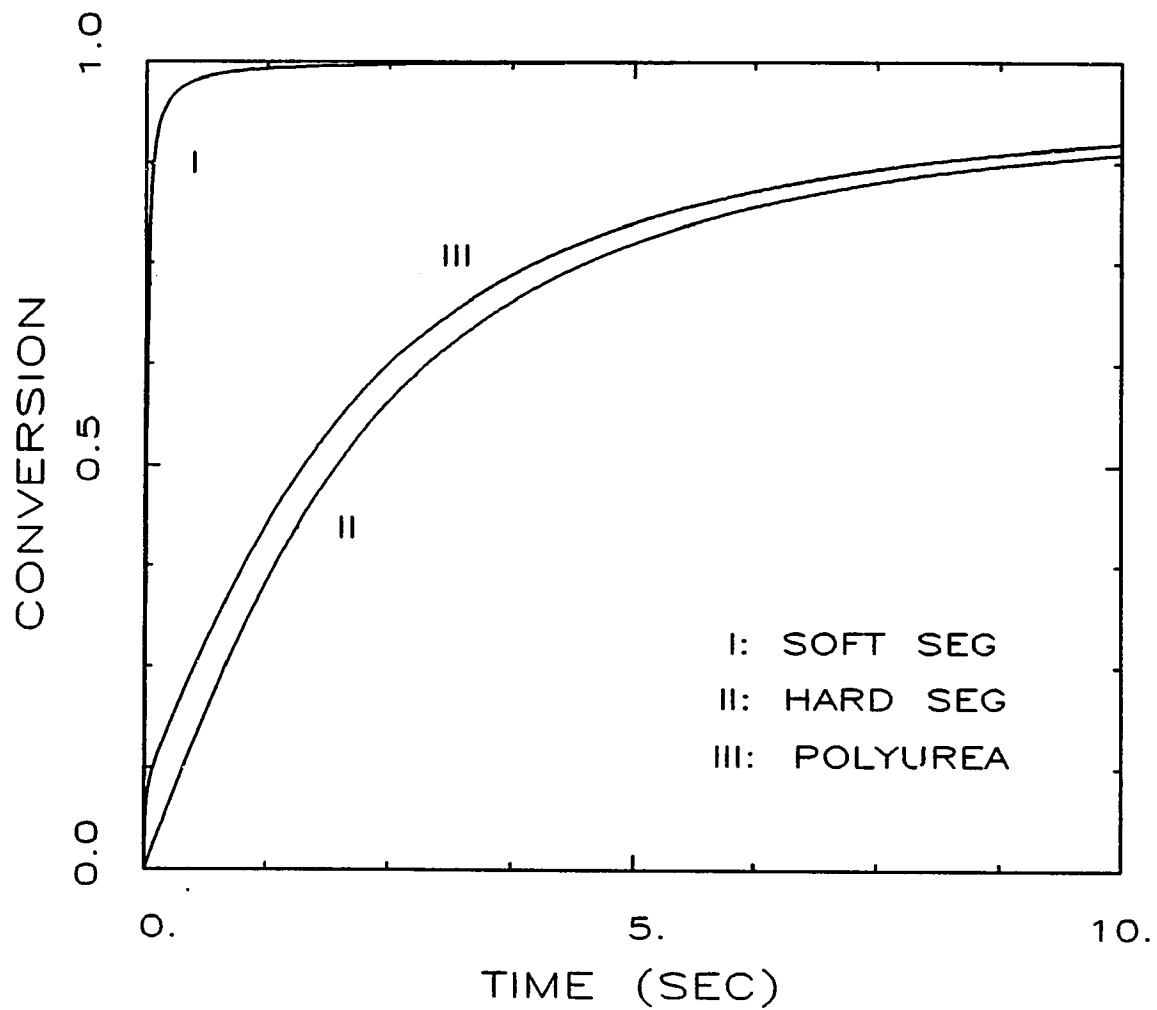


Figure 5.30 Predicted conversion profiles of 70/30 polyurea III in bulk in adiabatic condition.

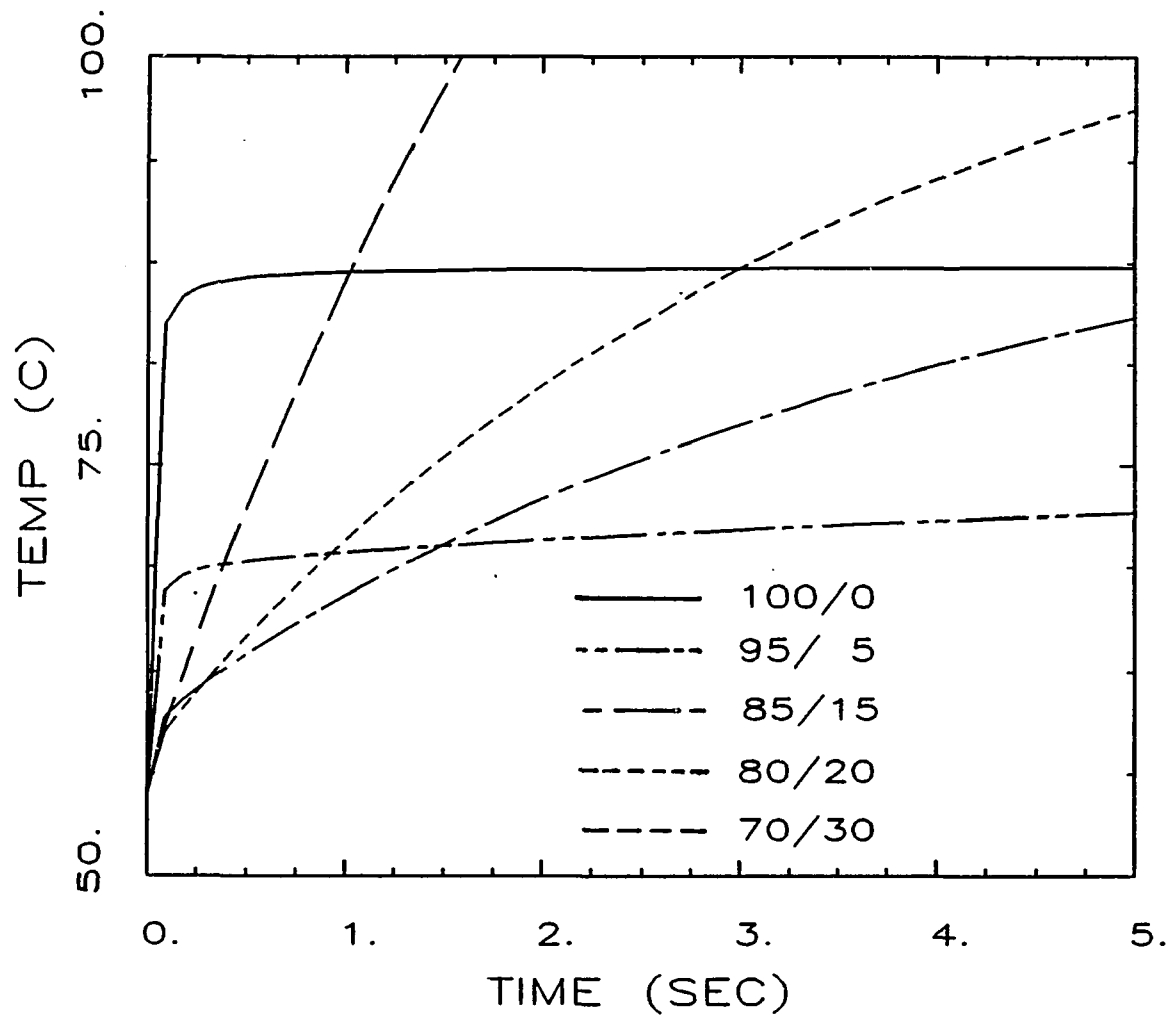


Figure 5.31 Predicted adiabatic temperature profiles of polyurea III in bulk with various compositions (100/0 ~ 70/30).

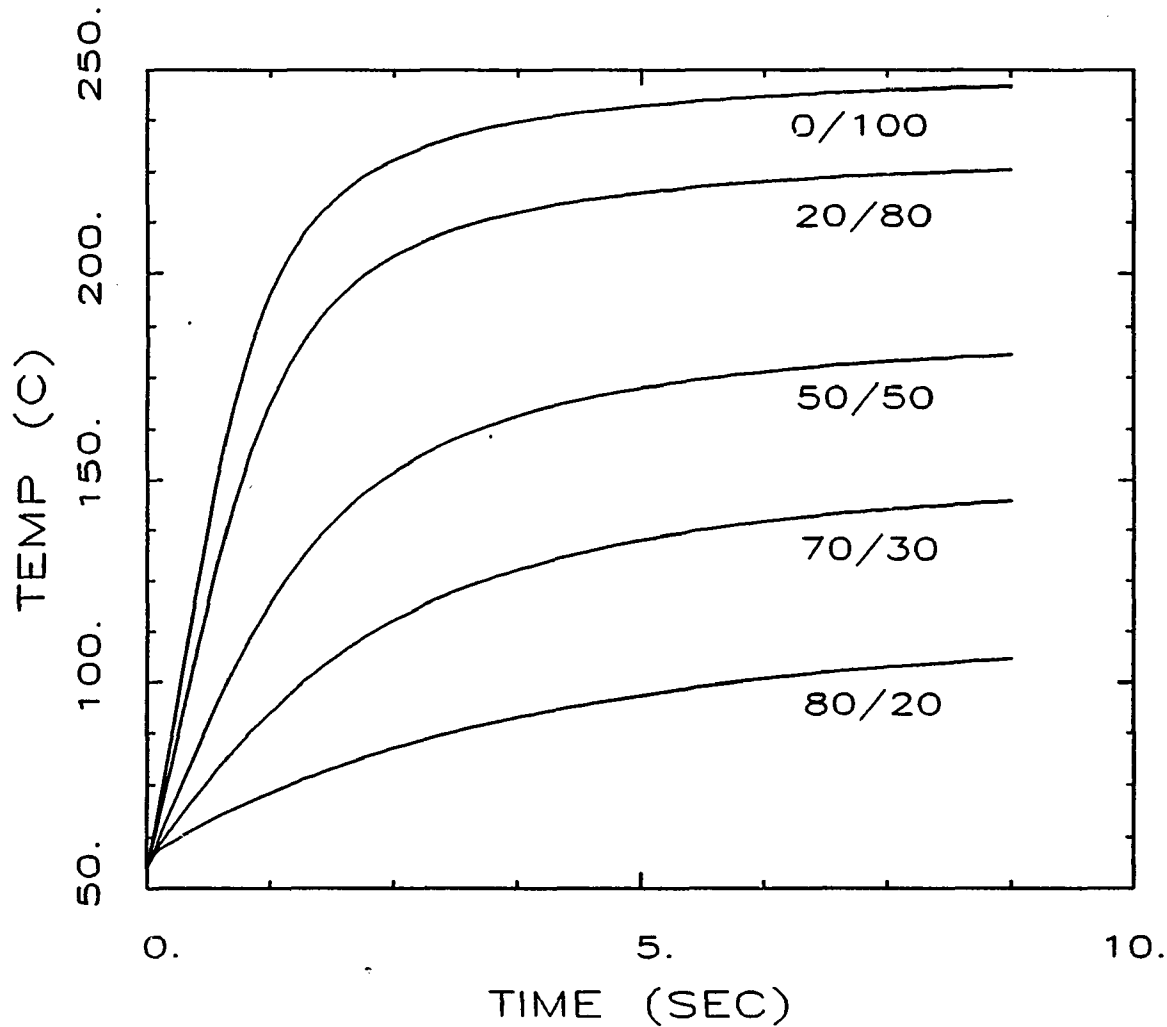


Figure 5.32 Predicted adiabatic temperature profiles of polyurea III in bulk with various compositions (80/20 ~ 0/100).

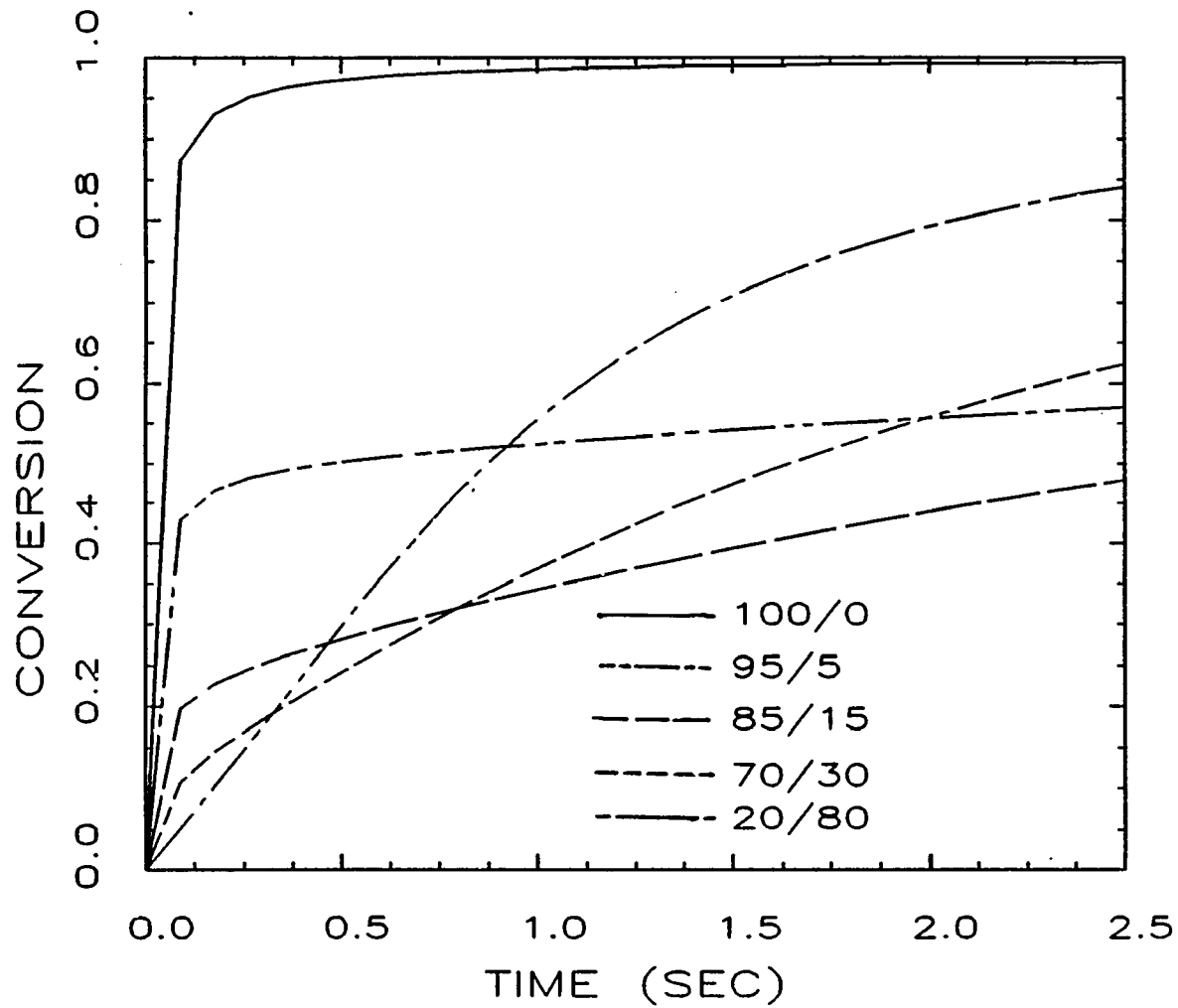


Figure 5.33 Predicted adiabatic conversion profiles of polyurea III in bulk with various compositions (100/0 ~ 20/80).

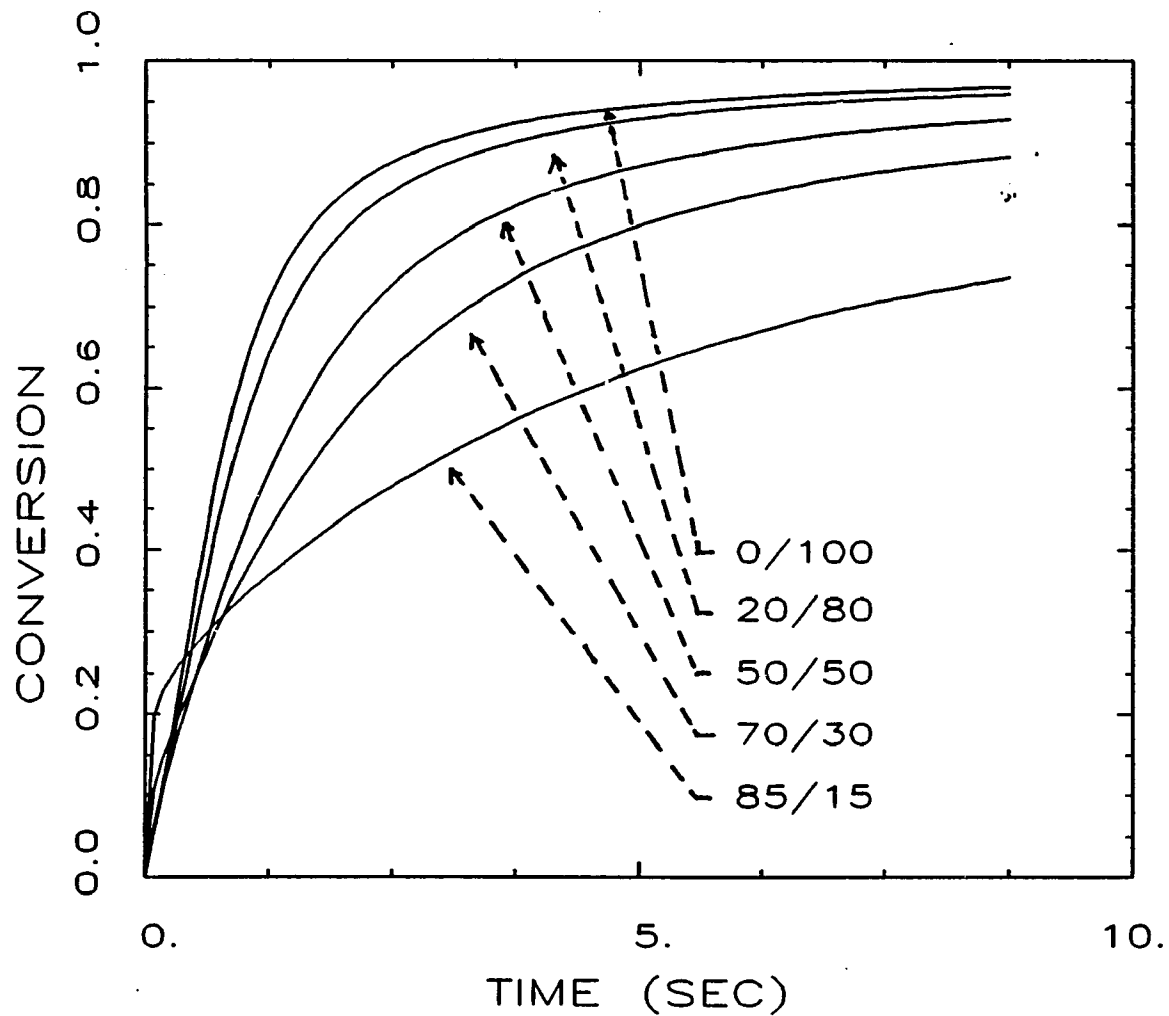


Figure 5.34 Predicted adiabatic conversion profiles of polyurea III in bulk with various compositions (85/15 ~ 0/100).

temperature. The reaction exotherm from the reaction of hard segment can help to promote the overall polyurea reaction.

From the results of this study, we conclude that the effect of aromatic amine chain extender in polyurea reaction is (A) to provide reaction exotherm to promote the polyurea reaction, (B) to cause physical crosslinking by forming hard segment, and (C) to compete with the reaction of aliphatic amine, which in turn, may affect the chemical crosslinking of soft segment.

CHAPTER VI

CONCLUSIONS AND RECOMMENDATIONS

6.1 CONCLUSIONS

This study was initiated to determine the processing characteristics of polyurethane/unsaturated polyester IPNs and polyureas by reactive polymer processing. The major points discussed in previous chapters are summarized as follows.

I. PU/PES IPN

1. The kinetics and heat transfer during curing of a PU/PES IPN were investigated experimentally and theoretically. A model based on the additivity rule of constituent ingredients was proposed to predict IPN's reaction kinetics and heat transfer. Predicted results were compared with the experimental results measured by the differential scanning calorimetry, the adiabatic temperature rise during reaction injection molding, and the temperature profiles measured during a casting process.

Generally speaking, the model gave a reasonably good prediction of temperature profiles for adiabatic reactions, but not for isothermal reactions. The prediction of casting was fairly well at high molding temperatures. The discrepancy might largely resulted from component interaction since the model proposed was based on the additivity rule of constituent components and without any consideration of interaction. These interactions could be categorized as either physical interactions or chemical interactions. The physical interactions mainly came from the "cage effect" of polyurethane on polyester and the "solvent effect" of polyester on polyurethane. Chemical interaction might happen between the isocyanate group of polyurethane and the hydroxyl and carboxylic groups of unsaturated polyester.

2. The property-structure-processing relationships of polyurethane/polyester IPNs were characterized from the morphological study by transmission electron microscopy, the dynamic mechanical analysis using a Weissenberg Rheogoniometer, and the tensile test using an Instron tensile tester. The measured physical properties were related to processing variables such as molding temperature and degree of mixing, material variables such as the type and concentration of initiator, and the chemical structures of constituent components.

The results showed that the RIM processed IPN had a more homogeneous morphology, indicating that phase interpenetration was better achieved in RIM process. On the other hand, the transfer-molded IPN showed phase separation, with distinguishable T_g 's in DMA spectra. Processing temperature was found to have a profound effect on IPN's morphology since higher molding temperature allowed the two polymerizations in an IPN to occur simultaneously. Morphology of IPNs might also be affected by the compound composition. As polyurethane content in IPN was increased, the T_g 's of both soft and hard domains in polyurethane increased and approached the T_g 's of pure polyurethane; while the T_g of polyester decreased, deviated more from the T_g of pure polyester. The increase of T_g 's in polyurethane and the decrease of T_g in polyester as the polyurethane content in IPN was increased was an indication of phase interpenetration. The domain size of polyester was greatly reduced as the redox initiator MEKP/amine/Co-3 concentration was increased three times. The earlier polymerization of polyester in IPN, due to high concentration of redox initiator, prevented polyurethane phase from forming continuous matrix. IPN's morphology could also be controlled by the physical structure of polyurethane. When the linear thermoplastic polyurethane was replaced by a crosslinked

thermosetting polyurethane, the particle size of polyurethane became smaller, tighter, and well dispersed.

The results of tensile strength measurements showed that PU/PES IPNs could improve the mechanical properties (e.g., tensile strength) of generally soft polyurethane, but the processing of IPN was more complicated than that of polyurethanes because of strong interaction between the two polymerizations. At a molding temperature of 80 °C, which was a typical molding temperature of polyurethane RIM process, incomplete reaction was found in all IPN samples, which resulted in a low tensile strength. This problem could be solved by postcure treatment or by using a higher molding temperature. A higher molding temperature was more beneficial for IPN with a higher polyester content, and the postcure treatment is more efficient for IPN with a higher polyurethane content.

Both the reaction sequence and the crosslinking nature of the constituent polymers were important in determining the tensile properties of IPNs. This study showed that, in addition to reaction kinetics, morphological characteristics such as degree of chain interpenetration, network structure, and crystallinity structure, play influential roles in governing the mechanical properties of IPN.

II. POLYUREA

Both experimental observations and theoretical modelling of processing of polyurea were studied. The experimental part includes the processing of polyurea by a lab-RIM machine, the solution polymerization to study the rheology and kinetics of polyurea. The theoretical part includes a kinetic and heat transfer model which can apply solution polymerization data to predict the bulk polymerization of polyurea in RIM process.

1. Experimental results of polyurea bulk polymerization in RIM indicated that about 90% of the adiabatic temperature rise took place within five seconds. The polyurea reaction in RIM was so fast that no existing analytical instrument could follow the entire reaction course. This necessitated the study of solution polymerization of polyurea in which the reaction rate was substantially reduced.
2. In the rheological measurement of 80% and 85% nitrobenzene-diluted polyureas, it was found that the viscosity rise of polyurea I (i.e., aliphatic amine and isocyanate only) took place much earlier than that of polyurea II (i.e., aromatic amine and isocyanate only), indicating that aliphatic amine reacted much faster with isocyanate than aromatic amine. However, in polyurea

III where both aliphatic and aromatic amines were presented and reacted with isocyanate, there existed a critical soft segment concentration at 8.2% in nitrobenzene. The viscosity rise of polyurea (i.e., III) reaction was primarily aliphatic amine-dominated above this critical soft segment content. Below 8.2%, although the reaction of aliphatic amine with isocyanate was still faster than the reaction of aromatic amine and isocyanate, the amount of soft segment was not high enough to cause viscosity build-up. The measured viscosity rise was mainly due to the reaction between aromatic amine and isocyanate. This was why that in the 80% and 85% nitrobenzene-diluted polyurea reactions, increasing the amount of aromatic amine in polyurea resulted in an earlier onset of viscosity rise, since all reaction systems had a soft segment content lower than the critical point.

3. The reaction kinetics of polyurea was measured using FTIR to obtain the conversion profile during polyurea reaction. Combining viscosity data from Haake viscometer and conversion data from FTIR, viscosity vs. conversion plots were constructed. The gel conversions of 80%, 85%, and 90% diluted polyureas were between 40% and 60%, which were below the gel conversions predicted by Flory's gelation theory. The low gel conversions measured might be attributed to the following reasons: First, the aliphatic amine had a higher reactivity than the aromatic amine, which

violated the equal reactivity assumption of Flory's theory. Secondly, the reaction between aromatic amine chain extender and isocyanate, although did not greatly increased the molecular weight of polymer chains, might form hard domains in solution. These hard domains might cause a physical crosslinking in the reaction and resulted in a sharp increase of system viscosity. For a given composition, the more the polyurea was diluted, the higher the gel conversion was. This can be attributed to the extent of intra-molecular reaction which increases when the reaction system is diluted with more solvent.

4. A kinetic and heat transfer model for polyurea reaction was proposed. This model assumed no interaction between soft and hard segments in polyurea. The kinetic parameters used were determined using data from solution polymerization of polyurea at 92.5% dilution of polyurea I and 90% dilution of polyurea II. The predictions of polyurea III at 90%, 85%, and 80% dilution levels were very good. The predictions of the adiabatic temperature rises in polyurea RIM both in bulk and 15% dilution were very good. The slight deviation was due to the model assumption that reactions of aliphatic and aromatic amines with isocyanates were independent of each other. In polyurea formation, the reaction of aliphatic and aromatic amines with isocyanate were parallel and competitive. The deviation could also result from

the physical interaction from domain formation. In addition, the extrapolation from solution to bulk polymerization could also result in some errors in prediction.

The predicted conversion profiles in adiabatic condition showed that the reaction of soft segment was much faster than that of hard segment at the beginning of reaction. The overall conversion profile, however, was similar to that of hard segment except at the initial stage. In the prediction of adiabatic temperature rises, increasing the hard segment content increased the maximum adiabatic temperature rise. The temperature rise of 50/50 polyurea was actually faster and higher than polyurea I. These suggested that a major function of aromatic amine was to affect the reaction temperature. The heat released from the reaction of hard segment helped to promote the polyurea reaction, although the reaction rate of hard segment was much slower than that of soft segment.

5. From the results of this study, it is concluded that the effect of aromatic diamine chain extender in polyurea reaction is (A) to provide reaction exotherm to promote the polyurea reaction, (B) to cause physical crosslinking by forming hard segment, and (C) to compete with the reaction of aliphatic amine.

6.2 RECOMMENDATIONS

Based on the results from this study, the following recommendations are suggested for future work:

I. PU/PES IPN

1. To improve model prediction of kinetic and heat transfer of PU/PES IPN, an interaction term should be included, which describes the physical and chemical interactions.
2. In the PU/PES IPN RIM, present work of curing should be extended to include mixing and molding filling.
3. Modelling of storage modulus G' and $\tan\delta$ is recommended. Several theoretical models for multicomponent polymers have been proposed in the literature, including the models of Takayanaki (1964) and Davies (1971).
4. Since IPN is the only way to combine two thermosetting resins in a polymer blend, its applications should be extended. At present, there are only a few commercially available IPN compounds (for example, Acrylamates of Ashland Chemical, polyester-polyurethane Hybrids of Amoco Chemical). Other thermosetting polymers such as

epoxies, polyureas, and thermoplastic polymers such as polymethyl methacrylate (PMMA) should be tried.

II. Polyurea

1. To further check the accuracy of the model proposed, different aliphatic and aromatic amines should be tried.
2. In the kinetic and heat transfer model proposed, the heat of reactions of soft segment and hard segment were obtained from that of a three-component polyurea according to the molar ratio of aliphatic to aromatic amine. However, it was found from this study that the reactions of soft and hard segment were parallel and competitive. To improve the model, it is suggested that individual heat of reaction should be experimentally measured separately. Also, the unequal reactivities of aliphatic and aromatic amines should be considered in the kinetic model.
3. Studies on the mechanical properties and the morphology of polyurea should be conducted.
4. More rheological measurements and theoretical modelling should be done in order to identify the roles of aliphatic and aromatic

amine chain extender in the formation of polyurea, including the chemical and physical crosslinking.

5. To investigate the processibility of polyurea RIM, research work should be extended to the flow analysis of mold filling and curing of polyurea.

REFERENCES

- Alberino, L.M., Gilmore, D.S., and McClellan, T.R., Proceeding of Annual Conference of Amer. Chem. Soc., Div. of Polym. Proc., PP. 409-413, August (1983).
- Allen, G., Eowden, M.J., Blundell, D.J., Hutchinson, F.G., Jeffs, G.M., Vyvoda, J., and White, T., Polymer, 14, 597 (1973).
- Allen, G., Bowden, M.J., Blundell, D.J., Jeffs, G.M., Vyvoda, J., and White, T., Polymer, 14, 604 (1973).
- Allen, G., Bowden, M.J., Lewis, G., Blundell, D.J., Jeffs, G.M., Polymer, 15, 14 (1974).
- Allen, G., Bowden, M.J., Lewis, G., Blundell, D.J., Jeffs, G.M., Vyvoda, J., and White, T., Polymer, 15, 19 (1974).
- Allen, G., Bowden, M.J., Todd, S.M., Blundell, D.J., Jeffs, G.M., Davies, W.E., and White, T., Polymer, 15, 28 (1974).
- Bamford, C.H., Barb, W.G., Jenkins, A.D., and Onyon, P.R., "The Kinetics of Vinyl Polymerization by Radical Mechanism," New York, Academic press (1958).
- Barone, M.R. and Caulk, D.A., Int. J. Heat Mass Transfer, 22, 1021 (1979).
- Baumann, W.M., Scott, D.W., Klempner, D., Frisch, K.C., Xiao, H.X., and House, R.V., J. Elast. Plast., 18, 233 (1986).
- Billmeyer, Jr., F.W., "Textbook of Polymer Science," 3rd Ed., John Wiley & Sons, Inc., New York (1984).
- Biesenberger, J.A. and Capinpin, R., Polym. Eng. Sci., 14(11), 737 (1974).
- Biesenberger, J.A. and Capinpin, R., Polym. Eng. Sci., 16(11), 101 (1974).
- Bird, B., Stewart, W.E., and Lightfoot, E.N., "Transport Phenomena," John Wiley & Sons, Inc., New York (1971).

- Blundell, D.J., Longman, G.W., Wignall, G.D., and Bowden, M.J., Polymer, 15, 34 (1974).
- Braudrup, J. and Immergut, E.H., "Polymer Handbook," Inter-Science (1967).
- Broyer, E. and Macosko, C.W., AICHE Journal, 22, 268 (1976).
- Broyer, E., Macosko, C.W., Critchfield, F.E., and Lawler, L.F., Polym. Eng. Sci., 18, 382 (1978).
- Camargo, R.E., Macosko, C.W., Tirrell, M., and Wellinghoff, S.T., Polym. Eng. Sci., 22, 719 (1982).
- Camargo, R.E., Gonzalez-Romero, V.M., Macosko, C.W., and Tirrell, M., Rubber Chemistry and Technology, 56, 774, (1983).
- Camargo, R.E., Macosko, C.W., Tirrell, E., and Wellinghoff, S.T., Proceeding of Annual Conference of Amer. Chem. Soc. , Div. of Polym. Proc., PP. 422-426, August (1983).
- Casey, J.P., Milligan, B., and Fasolka, M.J., J. Elast. Plast., 17, 218 (1985).
- Castro, J.M., Lopez-Serrano, F., Camargo, R.E., Macosko, C.W., and Tirrell, M., J. Appl. Polym. Sci., 26, 2067 (1981).
- Castro, J.M. and Macosko, C.W., AICHE Journal, 28, 250 (1982).
- Castro, J.M., Lipshitz, S.D., and Macosko, C.W., AICHE Journal, 28(6), 973 (1982)
- Castro, J.M., "Development in Plastics Technology," Vol. 2, Ch. 2, Ed. Whelan, A. and Crafts, J.L., Applied Science, London (1985).
- Chang, A.L., Briber, R.M., Thomas, E.L., Zdrahala, R.J., and Critchfield, F.E., Polymer, 23, 1060 (1982).
- Cheever, G.D., J. Coating Technol., 50, 36 (1978).
- Chiu, W.Y., Garratt, G.M., and Soong, D.S., Macromolecule, 16(3), 348 (1983).
- Davies, W.E., J. Phys. (D), 4, 318 (1971).
- Djomo, H., Morin, A., Damyanidu, M., and Meyer, G.C., Polymer, 24, 65 (1983).

- Domine, J.D. and Gogos, C.G., Polym. Eng. Sci, 20, 847 (1980).
- Dominguez, R.J.G., J. Cell. Plast., Nov./Dec., 433 (1984).
- Donatelli, A.A., Sperling, L.H., and Thomas, D.A., Macromolecule, 9(4), 671 (1976).
- Donatelli, A.A., Sperling, L.H., and Thomas, D.A., Macromolecule, 9(4), 676 (1976).
- Donatelli, A.A., Sperling, L.H., and Thomas, D.A., J. Appl. Polym. Sci., 21, 1189 (1977).
- Ebdon J.R., Hourston, D.J., and Klein, P.G., Polymer, 25, 1633 (1984).
- Edwards, H.R., Soc. Plast. Tech. Conf., 1326 (1986).
- "Encyclopedia of Polymer Science and Technology," Vol. 11, P. 129, Interscience (1969).
- Ephrath, L.M., IEEE Trans. Electr. Dev. ED-281(11), 1315 (1981).
- Estevez, S.R. and broyer, J.M., Polym Eng. Sci., 24(6), 428 (1984).
- Ewen, J.H., J. Elast. Plast., 17, 281 (1985).
- Fan, J.D., Marinelli, J.M., and Lee. L.J., Polymer Composites, 7, 239 (1986).
- Fan, J.D. and Lee, L.J., Polymer Composites, 7, 250 (1986).
- Fara, R.A., Polymer, 13, 127 (1972).
- Feger, C., Molis, S.E., Hsu, S.L., and Macknight, W.J., Macromolecule, 7, 1830 (1984).
- Feger, C. and Macknight, W.J., Macromolecule, 18, 280 (1985).
- Ferber, G., General Motors Company, Private Communication (1986).
- Ferry, J.D., "Viscoelastic Properties of Polymers," 3rd Ed., John Wiley & Sons, Inc., New York (1980).
- Flory, P.J., "Principles of Polymer Chemistry," Cornell University Press, Ithaca, New York (1953).

- Fridman, I.D., Thomas, E.L., Lee, L.J., and Macosko, C.W., Polymer, 21, 393 (1980).
- Frisch, H.L., Klempner, D., and Frisch, K.C., J. Polym. Sci., Part B, Polymer Letter, 7, 775 (1969).
- Frisch, H.C., U.S. Patent 2,153,987 (1972).
- Frisch, K.C., Klempner, D., Frisch, H.L., and Ghiradella, H., "Recent Advances in Polymer Blend, Grafts, and Blocks," Sperling, L.H., Ed., Plenum Press, New York (1974).
- Frisch, K.C., Klempner, D., Migdal, S., and Frisch, H.L., J. Polym. Sci., Polymer Chemistry Ed., 12, 885 (1974).
- Frisch, K.C., Klempner, D., and Mukherjee, S.K., J. Appl. Polym. Sci., 18, 689 (1974).
- Frisch, H.C., Frisch, K.C., and Klempner, D., Polym. Eng. Sci., 14, 646 (1974).
- Frisch, K.C., Klempner, D., Migdal, S., Thomas, H.L., and Dunlop, A.P., J. Appl. Polym. Sci., 19, 1893 (1975).
- Frisch, H.L., Foreman, R., Schwartz, R., Yoon, H., Klempner, D., and Frisch, K.C., Polym. Eng. Sci., 19(4), 284 (1979).
- Frisch, K.C., Rubber Chem. Tech., 53, 126 (1980).
- Frisch, H.L., Frisch, K.C., and Klempner, D., Pure Appl. Chem., 53, 1557 (1981).
- Frisch, K.C., Klempner, D., and Frisch, H.L., SAE Paper 820,422, Int. Conf. & Expo., Detroit, Michigan, February (1982).
- Galina, et al., European Polym. J., 16, 1043 (1980).
- Gillham, J.K., Polym. Eng. Sci., 19, 676 (1979).
- Gonzalez, V.M. and Macosko, C.W., Polymer Composite, 4, 190 (1983).
- Grabes, J.A., Thomas, D.A., Hickey, E.C., and Sperling, L.H., J. Appl. Polym. Sci., 19, 1731 (1975).
- Grigsby, R.A. and Dominguez, R.J.G., in "Proceedings of the SPI 29th Annual Technical/Marketing Conference," Reno, Nevada, Oct. (1985).

- Gupta, V.B., Drzal, L.T., Lee, C.Y-C., and Rich, M.J., Polym. Eng. Sci., 25, 812 (1985).
- Han, C.D. and Lem, K.W., J. Appl. Polym. Sci., 28, 3207 (1983).
- Han, C.D. and Lem, K.W., J. Appl. Polym. Sci., 28, 3155 (1983).
- Han, C.D. and Lem, K.W., J. Appl. Polym. Sci., 28, 3185 (1983).
- Han, C.D. and Lem, K.W., Polym. Eng. Sci., 24, 175 (1984).
- Harbison, W.C., in "Encyclopedia of Polymer Science and Technology," 2nd Ed., Ed. by Mark, H.F., Bikales, N.M., Overberger, C.G., and Menges, G., John Wiley & Sons, Inc., New York (1984).
- Hatzakis, M., Solid State Tech., 24(8), 74 (1981).
- Hawkin, British Patent 1,197,794 (1970).
- Hayashi, T., Ito, J., Mitani, K., and Mizutani, Y., J. Appl. Polym. Sci., 33, 375 (1987).
- Herman, E.M., Morden Plastics, 59, Oct. (1978).
- Hirate., K., Ozaki, Y., Oda, M., and Kimizuka, IEEE Trans. Electr. Dev., ED-28(11), 1323 (1981).
- Horie, K., Mita, I., and Kambe, H., J. Polym. Sci., A-1, 6, 2663 (1968).
- Horie, K., Mita, I., and Kambe, H., J. Polym. Sci., A-1, 7, 2561 (1969).
- Horie, K., Mita, I., and Kambe, H., J. Polym. Sci., A-1, 8, 1357 (1970).
- Horie, K., et al., European Polym. J., 16, 1043 (1970).
- Hsu, T.J., M.S. Thesis, The Ohio State University (1984).
- Hsu, T.J. and Lee, L.J., Polym. Eng. Sci., 25, 951 (1985).
- Hsu, T.J. and Lee, L.J., J. Appl. Polym. Sci., 33, 793 (1987).
- Hsu, T.J. and Lee, L.J., 42nd Annual Conference, Composite Institute, The Society of Plastic Industry, Inc., Session 18-C, Cincinnati, Ohio, February (1987).

- Huang, Y.J., M.S. Thesis, The Ohio State University (1983).
- Huang, Y.J. and Lee, L.J., AICHE Journal, 31, 1585 (1985).
- Huang, Y.J., Hsu, T.J., and L.J., Lee, Polymer, 26, 1247 (1985).
- Huang, Y.J., Fan J.D., and Lee, L.J., J. Appl. Polym. Sci, 33, 1315 (1987).
- Huelck, V., Thomas, D.A. and Sperling, L.H., Macromolecule, 5, 340 (1972).
- Huelck, V., Thomas, D.A. and Sperling, L.H., Macromolecule, 5, 348 (1972).
- Hull, J.L., in "Encyclopedia of Polymer Science and Technology," 2nd Ed., Ed. by Mark, H.F., Bikales, N.M., Overberger, C.G., and Menges, G., John Wiley & Sons, Inc., New York (1984).
- Hutchinson, F.G., British Patent 1,239,701 (1971)
- Hutchinson, F.G., Henbest, R.G.C., and Leggett, M.R., U.S. Patent 4,062,826 (1977).
- Ishida, H. and Scott, C., J. Polym. Eng., 6, 201 (1986a).
- Ishida, H. and Scott, C., paper presented in the 2nd Annual Meeting of Polym. Proc. Soc., Montreal, Canada (1986b).
- Jans, R.W., in "Modern Plastics Encyclopedia," Vol. 63, McGraw-Hill Co., New York, October (1986 -1987).
- Jordhamo, G.M., Manson, J.A., and Sperling, L., ACS Div. Polym. Materials: Sci. and Eng., Preprint, 50, 362 (1984).
- Kamal, M.R. and Sourour, S., Polym, Eng. Sci., 13, 59 (1973).
- Kamal, M.R., Sourour, S., and Ryan, M., SPE ANTEC Tech. Papers, 19, 187 (1973).
- Kaplan, K. and Tschoegl, N.W., Polym. Eng. Sci., 15(5), 343 (1975).
- Kaplan, M., Meyerhofer, D., and White, L., RCA Revirw, 44, 135 (1983).
- Kato, K., Polym Eng. Sci., January, 38 (1967).
- Kelly, W.L., Plast. Eng., 39 (1986).

- Kendall, D.N., "Applied Infrared Spectroscopy," P5, Reinhold, London (1966).
- Kim, S.C., Klempner, D., Frisch, K.C., Frisch, H.C., and Ghiradella, H., Polym. Eng. Sci., 15(5), 339 (1975).
- Kim S.C., Klempner, D., Frisch, K.C., Radigan, W., and Frisch, H.C., Macromolecule, 9, 258 (1976).
- Kim S.C., Klempner, D., Frisch, K.C., and Frisch, H.C., Macromolecule, 9, 263 (1976).
- Kim, S.C., Klempner, D., Frisch, K.C., and Frisch, H.L., J. Appl. Polym. Sci., 21, 1289 (1977).
- Kircher, K., Die Angewandte Makromolekulare Chemie, 76/77, 241 (1979).
- Kircher, K., Mrotzek, W., and Menges, G., Polym. Eng. Sci., 24 (12), 974 (1984).
- Klempner, D., Frisch, H.L., and Frisch, K.C., J. Polym. Sci., Part A-2, 8, 921 (1970).
- Klempner, D. and Frisch, H.L., J. Polym. Sci., Part B, Polymer Letter, 8, 525 (1970).
- Klempner, D., Angew. Chem. Int. Ed. Engl., 17, 97 (1978).
- Klempner, D. and Frisch, K.C., "Polymer Alloys," Plenum Press, New York (1981).
- Knoop, H.E., in "Modern Plastics Encyclopedia," Vol. 63, McGraw-Hill Co., New York, October (1986 - 1987).
- Kresta, J.E. and Hsieh, K.H., Makromol. Chem., 179, 2779 (1978).
- Kuo, J.F. et al., Polym Eng. Sci., 24(1), 22 (1984)
- Lawrence Amos, J., Polym. Eng. Sci., 14, 1 (1974).
- Lee, L.J., Polym. Eng. Sci., 21, 483 (1978).
- Lee, L.J., Doctoral Dissertation, University of Minnesota (1979).
- Lee, L.J., Rubber Chem. Technol., 53, 542 (1980).

- Lee, L.J. and Macosko, C.W., Int. J. Heat Mass Transfer, 23, 1479 (1980).
- Lee, L.J., Polym. Eng. Sci., 21, 483 (1981).
- Lee, Y.M., Doctoral Dissertation, The Ohio State University (1986).
- Lin, B.J., Proc. SPIE, 174, 114 (1979).
- Lin, B.J. and Chang, T.H.P., J. Vac. Sci. Tech., 16(6), 1669 (1979).
- Lin, D.J., Ottino, J.M., and Thomas, E.I., Polym. Eng. Sci., 25(18), 1155 (1985).
- Lipatov, Y.S., Karabanova, L.V., and Sergeyeva, L.H., Polym. Sci. USSR, 19(5), 1237 (1977).
- Lipshitz, S.D. and Macosko, C.W., J. Appl. Polym. Sci., 21, 2029 (1977).
- Macosko, C.W., Plastic Engineering, 21, April (1983).
- Macosko, C.W. and Lee, L.J., Rubber Chem. Tech., 58, 436 (1985).
- Mallick, P.K. and Raghupathi, N., Polym. Eng. Sci., 19, 774 (1979).
- Manson, J.A. and Sperling, L.H., "Polymer Blends and Composites, Plenum Press, N.Y. (1976).
- Manziona, L.T. and Osinski, J.S., Polym. Proc. Eng., 1(2), 171 (1983-1984).
- Matsuo, M., Nozaki, C., and Jyo, Y., Polym. Eng. Sci., 9, 197 (1969).
- Matsuo, M., Kwei, T.K., Klempner, D., and Frisch, H.L., Polym. Eng. Sci., 10, 327 (1970).
- Meyer, G.C. and Mehrenberger, P.Y., European Polymer Journal, 13, 383 (1977).
- Mikhail, E.D. and Girgis, M.M., Proceeding of Annual Conference of Amer. Chem. Soc., Div. Polym. Proc., 536, August (1983).
- Mitchell and Gauthier, Assoc., Inc., "Advanced Continuous Simulation Language, User Guide/Reference Manual," Concord, Mass. (1981).
- Mones, E.T. and Morgan, R.J., Polym. Preprints, 22, 249 (1981).

- Morin, A., Djomo, H., Meyer, G.C., Polym. Eng. Sci., 23, 394 (1983).
- Nalepa, C.J. and Eisenbraun, A.A., J. Elast. Plast., 19, 6 (1987).
- Nelson, M., M.S. Thesis, The Ohio State University (1987).
- Neubauer, E.A., Deva-manjarres, N., Thomas, D.A., and Sperling, L.H., Amer. Chem. Soc., Coating in Plastics Preprint, 31, 252 (1977)
- Neubauer, E.A., Thomas, D.A., and Sperling, L.H., Polymer, 19, 188 (1978).
- Nguyen L.T. and Suh, N.P., Proceeding of Annula Conference of Amer. Chem. Soc. , div. of Polym., Proc., August (1983).
- Nguyen, L.T. and Suh, N.P., ACS Organic Coatings & Appl. Polym. Sci. Proc., 49, 599 (1983).
- Nguyen, L.T., Ph.D. Dissertation, Massachusetts Institute of Technology, Cambridge, Massachusetts (1984).
- Nguyen, L.T. and Suh, N.P., Polym. Proc. Eng., 3, 37 (1985).
- Nguyen, L.T. and Suh, N.P., Polym. Eng. Sci., 26, 799 (1986).
- Nguyen, L.T. and Suh, N.P., Polym. Eng. Sci., 26, 843 (1986).
- Nichols, J., in "Modern Plastics Encyclopedia," Vol. 63, McGraw-Hill Co., New York, October (1986 - 1987).
- Nielsen, L.E., "Mechanical Properties of Polymers and Composites," Vol. I and II, Marcel Dekker, Inc., New York (1974).
- Ninomi, M., Katsuta, T., and Kotani, T., J. Appl. Polym. Sci., 2919 (1975).
- Nissen, D. and Markovs, R.A., J. Elast. Plast., 15, 96 (1983).
- O'Brien, J.C. and Lenosky, T., in "Modern Plastics Encyclopedia," Vol. 63, McGraw-Hill Co., New York, October (1986 01987).
- Odian, G., "Principles of Polymerization," McGraw-Hill Book Co., New York (1970).
- Omega Engineering, Inc., "Temperature Measurement Handbook," (1986).

- Osinski, J.S., Manzione, L.T., and Larson, R.G., in Proceedings of Soc. Plast. Eng. Tech. Conf., 801 (1983).
- Osinski, J.S., Polym. Eng. Sci., 23, 756 (1983).
- Osinski, J.S., Manzione, L.T., and Chan, C., Polym. Proc. Eng., 3, 97 (1985).
- Pannone, M.C., M.S. thesis, University of Minnesota (1986)
- Paul, D.R. and Newman, S., "Polymer Blends," Vol. I and II, Academic Press, New York (1978).
- Pernice, R., Frisch, K.C., and Navare, R., J. Cell. Plast., 121 (1982).
- Pouchert, C.J., "The Aldrich Library of Infrared Spectra," Ed. III, Aldrich Chemical Co., Inc., Milwaukee, Wisconsin (1981).
- Prime, R.B., "Thermosets", in "Thermal Characterization of Polymer Materials," Ed. Turi, E., New York, Academic Press (1982).
- Pusatcioglu, S.Y., Fricke, A.L., and Hassler, J.C., J. Appl. Polym. Sci., 24, 937 (1979).
- Pusatcioglu, S.Y., Fricke, A.L., and Hassler, J.C., J. Appl. Polym. Sci., 24, 947 (1979).
- Pusatcioglu, S.Y., Fricke, A.L., Hassler, J.C., and Mcgee, H.A., J. Appl. Polym. Sci., 25, 381 (1980).
- Richter, E.B. and Macosko, C.W., Polym. Eng. Sci., 18 (13), 1012 (1978).
- Richter, E.B. and Macosko, C.W., Polym. Eng. Sci., 20, 921 (1980).
- Rosovizky, V.F., Ilavsky, M., Hrouz, J., Dusek, K., and Lipatov, Y.S., J. Appl. Polym. Sci., 24, 1007 (1979).
- Sangamo Control Ltd., "The Weissenberg Rheogoniometer Instruction Manual R.18," Bognor Regis, England.
- Saunders, J.H. and Frisch, K.C., "Polyurethane Chemistry and Technology," Vols 1 and 2, Wiley-Interscience, New York (1962).
- Schwartz, S.S. and Goodman, S.H., "Plastics Materials and Processes," Van Nostrand Reinhold Co., New York (1982).

- Schwarz, E.G., Cristchfield, F.E., Tackett, L.P., and Tarin, P.M., Soc. Plast. Ind., Tech. Conf., 14-C, 34 (1979).
- Sibal, P.W., Camargo, R.E., and Macosko, C.W., Polym. Proc. Eng., 1(2), 147 (1983).
- Silberberg, J. and Han, C.D., J. Appl. Polym. Sci., 22, 599 (1978).
- Sneller, J.A., Modern Plastics, 55, February (1986).
- Sperling, L.H. and Arnsts, R.R., J. Appl. Polym. Sci., 15, 2731 (1971).
- Sperling, L.H., Thomas, D.A., Govitch, M.J., and Curtius, A.J., Polym. Eng. Sci., 12, 101 (1972).
- Sperling, L.H., Chiu, T.W., and Thomas, D.A., J. Appl. Polym. Sci., 17, 2443 (1973).
- Sperling, L.H., Material Engineering, 66, September (1980).
- Sperling, L.H., Modern Plastics, 74, October (1981).
- Sperling, L.H., "Interpenetrating Polymer Networks and Related Materials," Plenum Press, New York (1981).
- Sperling, L.H., ACS Div. Polym. Materials: Sci. and Eng. Preprint, 50, 19 (1984)
- Sperling, L.H., Polym. Eng. Sci., 25, 517 (1985).
- Spurr, A.R., Amer. J. Botany, 55 (1968).
- Stanford, J.L. and Stepto, R.F.T., Br. Polym. J., June, 124 (1977).
- Staudinger, J.J.P. and Hutchinson, F., U.S. Patent 2,539,377 (1951).
- Stenile, E.C., Critchfield, F.E., broyer, J.M., and Macosko, C.W., J. Appl. Polym. Sci., 25, 2317 (1980).
- Stepto, R.F.T. and Waywell, Dir Makromolek. Chem., 152, 263 (1972).
- Stevenson, J.F., SPE ANTEC Tech. Papers, 26, 452 (1980).
- Stevenson, J.F., 2nd International Conference on Reactive processing of Polymer (1982).
- Stevenson, J.F., Polym. Eng. Sci., 26, 746 (1986).

- Sweeney, F.M., "Introduction to Reaction Injection Molding," Technomic Publishing Co., Inc., Westport, CT (1979).
- Tadmor, Z. and Gogos, C.G., "Principles of Polymer Processing," John Wiley & Sons Inc., New York (1979).
- Takayanagi, M., Uemura, S., and Minami, S., J. Polym. Sci., Part C, No. 5, 113 (1964).
- Thomas, D.A. and Sperling L.H., in "Polymer Blends," Vol II, Ch. 11, Plenum Press, New York (1976).
- Thomas, D.A., J. Polym. Sci.: Polym. Symp., 60, 189 (1977).
- Touhsaent, R.E., Thomas, D.A., and Sperling, L.H., J. Polym. Sci., 46C, 175 (1974).
- Tucker, C.L. and Suh, N.P., Soc. Plast. Eng., Tech. Conf., 24, 158 (1978).
- Vespoli, N.P. and Alberino, L.M., Polym. Proc. Eng., 3, 127 (1985).
- Vespoli, N.P., Alberino, L.M., Peterson, A.A., and Ewen, J.H., J. Elast. Plast., 18, 159 (1986).
- Voelker, T.H., Balling, P., 30th Annual Polyurethane Technical/Marketing Conference, 133, October, (1986).
- Wang, D.N.K., Maydan, D., and Levinstin, H.L., Solid State Tech., 23(8), 122 (1980).
- Wang, C.L., Klempner, D., and Frisch, K.C., J. Appl. Polym. Sci., 30, 4337 (1985).
- Wang, K.J., M.S. Thesis, The Ohio State University (1985).
- Ward, I.M., "Mechanical Properties of Solid Polymers," 2nd Ed., John Wiley & Sons, Inc., New York (1983).
- White, K.L. and Meyerhofer, D., RCA Review, 44, 110 (1983).
- Wigotsky, V., Plastic Engineering, 19, May (1986).
- Wilkinson, T.C., Borgnaes, D., Chappel, S.F., and Kelly, W.L., ACS Organic Coatings & Appl. Polym. Sci. Proc., 49, 469 (1983).
- Wood, A.S., Modern Plastics, October, 48 (1984).

Yang, Y.S. and Lee, L.J., Macromolecule (1987, to appear).

Yoon, H.K., Klemperer, D., Frisch, K.C., and Frisch, H.C., Amer. Chem. Soc., Coating in Plastics Preprint, 36, 631 (1976).

APPENDIX

Appendix A ACSL Program for Polyurea Reaction.

Appendix B ACSL Program for the PU/PES IPN Reaction.

Appendix A. ACSL Program for Polyurea Reaction

PROGRAM POLYUREA

INITIAL

```
CONSTANT CO=2.25E-3
CONSTANT CO11=3.86E-4
CONSTANT CO22=5.66E-5
CONSTANT DL=1.081
CONSTANT HU=22591.
CONSTANT CP=0.4
CONSTANT ES=4212.58
CONSTANT OS=2.E5
CONSTANT RS=2.15
CONSTANT EL=1600.0
CONSTANT OL=3.14E6
CONSTANT RL=2.10
CONSTANT R=1.9872
CONSTANT TEM=0.0
CONSTANT TEMP=328.5
CONSTANT IQ=4
CONSTANT D1=0.889
CONSTANT D2=0.111
YIC=TEMP
CU1=CO*D1*HU*D1/DL/CP
CU2=CO*D2*HU*D2/DL/CP
F1IC=0.0
F2IC=0.0
F11IC=0.0
F22IC=0.0
N=1
```

```
CINTERVAL    CINT=0.01
NSTEPS       NSTP=1
```

END

DYNAMIC

DERIVATIVE

```
CONSTANT ETIME=10.0
TIME=T
```

PROCEDURAL

```
YDOT=CU1*F1DOT+CU2*F2DOT
Y=INTEG(YDOT, YIC)
```

END

PROCEDURAL

```
N=N+1
F1DOT=OS*EXP(-ES/R/Y)*(CO*D1)**(RS-1.0)*(1.-F1)**RS
F11DOT=OS*EXP(-ES/R/Y)*CO11** (RS-1.0)*(1.-F11)**RS
F2DOT=OL*EXP(-EL/R/Y)*(CO*D2)**(RL-1.0)*(1.-F2)**RL
F22DOT=OL*EXP(-EL/R/Y)*CO22** (RL-1.0)*(1.-F22)**RL
F=(F1*D1+F2*D2)/1.0
F1=INTEG(F1DOT,F1IC)
F2=INTEG(F2DOT,F2IC)
F11=INTEG(F11DOT,F11IC)
F22=INTEG(F22DOT,F22IC)
IF(N.EQ.50) GO TO 200
GO TO 300
200..CONTINUE
TEM=TEM+1
WRITE(IQ,100)TEM,F1,F2
N=0
300..CONTINUE
100..FORMAT(2X,3(3X,E13.7))
END
```

TERMT(TIME.GE.ETIME)

END
END
END

Appendix B. ACSL Program for PU/PES IPN Reaction

PROGRAM HEAT TRANSFER

INITIAL

```

ARRAY Y(35), A(35), ADOT(35), YDOT(35), GA(35)
ARRAY YADOT(35), YBDOT(35), YIC(35), AIC(35), FIC(35)
ARRAY DK(35), PK(35), BY(35), BO(35), F(35), FDOT(35)
ARRAY GF(35), G(35), B(35), TZ(35), BC(35)
ARRAY GYIC(35), GY(35), GYADOT(35), GYDOT(35), GYBDOT(35)
CONSTANT ZA=0.99
CONSTANT COU=0.0031, COE=0.0031
CONSTANT CPU=0.4, CPE=0.4
CONSTANT LOU=1.14, LOE=1.1
CONSTANT AU=2.0E7, EU=10600.0
CONSTANT DA=2.8E16, DE=31000.
CONSTANT PA=4.6E5, PE=10000.
CONSTANT GK=0.00036, GLO=2.375, GCP=0.18
CONSTANT ADV=1.9872
CONSTANT HU=19906., HE=95.95
CONSTANT UK=0.00036, EK=0.00036
CONSTANT RD=1.125, GRD=0.2
CONSTANT Q1=0.50
CONSTANT S1=0.50
CONSTANT P1=0.50
CONSTANT HW=0.06
CONSTANT TEMP=393.5
CONSTANT TEM=0.0
CONSTANT RO=2.0
IQ=57
Q2=1.0-Q1
S2=1.0
P2=1.0-P1
ZK=1.0/(Q1/UK+Q2/EK)
ZLO=1.0/(Q1/LOU+Q2/LOE)
ZCP=Q1*CPU+Q2*CPE
ALPHA=ZK/ZLO/ZCP
XY=GK/GLO/GCP
CU=COU*HU/ZLO/ZCP
CE=HE*LOE/ZLO/ZCP
R2=GK/ZK/GRD
D=AU*COU
ZZ=100./5233.
DY=RD/20.

```

```

DYY=DY*DY
GDY=GRD/10.0
GDYY=GDY*GDY
LUM=GK/ZK*DY/GDY
NN=1
N=1
DO LL I=1,21
YIC(I)=293.5
AIC(I)=0.0
FIC(I)=0.0
BC(I)=0.0
TZ(I)=0.0
B(I)=0.0
LL..CONTINUE
DO LL1 I=1,10
GYIC(I)=293.5
LL1..CONTINUE
GYIC(11)=TEMP
GY(11)=TEMP
CINTERVAL    CINT=0.1
NSTEPS       NSTP=1
END

DYNAMIC

DERIVATIVE
CONSTANT ETIME=800.0
TIME=T
YADOT(1)=2.*((Y(2)-Y(1))/DYY)
YBDOT(1)=P1*S1*CU*FDOT(1)+P2*S2*CE*ADOT(1)
YDOT(1)=YADOT(1)*ALPHA+YBDOT(1)
PROCEDURAL
DO L2 I=1,19
YADOT(I+1)=((Y(I)-2*Y(I+1)+Y(I+2))/DYY+(Y(I+2)-
Y(I+1))/DYY/(I))
YBDOT(I+1)=P1*S1*CU*FDOT(I+1)+P2*S2*CE*ADOT(I+1)
YDOT(I+1)=YADOT(I+1)*ALPHA+YBDOT(I+1)
L2..CONTINUE
Y(21)=(Y(20)+LUM*GY(2))/(1.+LUM)
Y=INTVC(YDOT,YIC)
END
PROCEDURAL
DO L33 I=1,8
GYADOT(I+1)=(GY(I)-2*GY(I+1)+GY(I+2))/GDYY
GYBDOT(I+1)=GYADOT(I+1)+(GY(I+2)-GY(I+1))/GDYY/(I)
GYDOT(I+1)=GYBDOT(I+1)*XY
L33..CONTINUE
GY(10)=TEMP+EXP(-HW/GK*GDY)

```

```

GY(1)=Y(21)
GYDOT(1)=YDOT(21)
GY=INTVC(GYDOT,GYIC)
END
PROCEDURAL
DO L77 I=1,21
FDOT(I)=D*EXP(-EU/ADV/Y(I))*(1.-F(I))*RO
L77.CONTINUE
F=INTVC(FDOT,FIC)
END
PROCEDURAL
DO L10 I=1,21
FK(I)=FA*EXP(-FE/ADV/Y(I))
DK(I)=DA*EXP(-DE/ADV/Y(I))
L10.CONTINUE
END
PROCEDURAL
DO L101 I=1,21
IF(TZ(I).NE.0.0) GO TO L101
B(I)=B(I)+ZZ*DK(I)
BY(I)=EXP(-B(I))
IF(BY(I).LE.ZA) GO TO L102
TZ(I)=0.0
A(I)=0.0
ADOT(I)=0.0
GO TO L101
L102.CONTINUE
BO(I)=BY(I)*0.01518
TZ(I)=TZ(I)+100.
L101.CONTINUE
DO L61 I=1,21
IF(TZ(I).NE.0.0) GG=1.0
IF(TZ(I).EQ.0.0) GG=0.0
IF(TZ(I).NE.0.0) BC(I)=BC(I)+ZZ*DK(I)
ADOT(I)=2.*BO(I)*FK(I)*(1.-A(I))*(1.-EXP(-BC(I)))*GG
L61.CONTINUE
A=INTVC(ADOT,AIC)
END
PROCEDURAL
NN=NN+1
N=N+1
IF(N.EQ.900) GO TO L14
GO TO L15
L14.CONTINUE
G(2)=Y(2)

```

```
G(17)=Y(17)
GF(2)=F(2)
GF(17)=F(17)
GA(2)=A(2)
GA(17)=A(17)
TEM=TEM+1.0
N=1
PQQ=NN
WRITE(IQ,101)TEM,Y(1),Y(2),Y(3),Y(4),Y(5),Y(6),Y(7),Y(8),Y(9)
WRITE(IQ,102)Y(10),Y(11),Y(12),Y(13),Y(14),Y(15),Y(16),Y(17)
WRITE(IQ,103)Y(18),Y(19),Y(20),Y(21)
WRITE(IQ,104)GY(2),GY(3),GY(4),GY(5),GY(6),GY(7),GY(8),GY(9)
LL5..CONTINUE
101..FORMAT(1X,F7.1,9(1X,F6.1))
102..FORMAT(1X,8(1X,F6.1))
103..FORMAT(1X,4(1X,F6.1))
104..FORMAT(1X,8(1X,F6.1))
END

TERMT(TIME.GE.ETIME)
END
END
END
```